THE DESIGN AND COMMISSIONING OF A LABORATORY THICKENER TEST PLANT FOR MEASUREMENT AND CONTROL INVESTIGATIONS

by

Adrian Roebl

A thesis submitted to the

Department of Electrical Engineering
University of Cape Town

for the degree of

Master of Science in Engineering

2 October 2006

Supervisor: Professor J. Tapson

Declaration

I know the meaning of plagiarism and declare that all the work in the document, save for that which is properly acknowledged, is my own.

signature removed

Adrian Roebl

ABSTRACT

This thesis discusses the design, construction, and commissioning of a laboratory scale thickener test plant to carry out measurement and control tests under controlled conditions. The laboratory scale thickener simulates the settling conditions found in full scale high compression thickeners.

A review of thickener technology, applicable measurements and control strategies was carried out. Using the slurry feed flow rates and cross-sectional areas of the thickeners at the CTP and Orapa treatment plants, the clear water rise rates in the thickeners could be determined. The scale thickener diameter was determined by the space required for a pair of Vega vibrating probes to switch without interference from the sidewalls. The scale thickener plant flow rates were determined based on the full scale rise rates and the laboratory scale thickener diameter. The height of the thickener was determined by the available laboratory space. The remaining equipment sizing was all determined by the thickener dimensions, and the required flow rates.

A bench top test was carried out to determine whether the slurry could be re-circulated and re-flocculated, while still generating a suitable mud bed for measurement and control testing. This was confirmed, and it was found that the laboratory would be able to function for 4 – 5 days with a single slurry sample of approximately 1800 litres. Modifications were made to the thickener base during commissioning, where the conical base section was replaced with a flat bottom section requiring the installation of a raking mechanism. The dual tube Coriolis mass-flow meter at the thickener underflow was replaced by a single tube version due to slurry deposition problems. It was determined that Coriolis mass flow meters were suitable for measuring the density of kimberlite slurry samples, but that the flow measurements were inaccurate. The calibrated flow rates of the positive displacement pumps were found to be accurate, and were used instead.

Two commissioning tests displayed similar behaviour to that in the bench top test, and the scale thickener test plant was deemed to be commissioned at this point. The underflow rheology estimation measurement and thickener overflow clarity measurements have yet to be installed. Initial test work in the plant will commence with the testing of the Vega vibrating probes for mud bed level control. An overall control strategy will be sought that seeks to maximise the liberation of water from the mud bed while keeping the underflow rheology and density within limits.

CONTENTS

LIST OF FIGURES

LIST OF TABLES

CHAPTER 1 INTRODUCTION

1.1 GENERAL INTRODUCTION

This thesis discusses the design and construction of a scale thickener for the purposes of measurement and control testing. It is part of a larger project that extends from the design of the scale thickener through to the testing of measurement and control strategies on full scale high compression thickeners. This document contains a review of thickener operation, measurement and control, followed by scale thickener design, slurry characterisation, and finally, plant commissioning.

A survey was carried out in 2002 to determine the measurement and control needs across De Beers mines in Southern Africa. One of the topics that appeared on the list was the optimisation of thickener control, specifically, the case of high compression thickeners.

The purpose of thickeners is to separate solids and liquids for the purpose of recovering water for re-use in the processing plant. Typically the material to be settled contains very fine particles that will not naturally settle under gravity. This requires the addition of a flocculant so that the particles are able to aggregate into what are referred to as flocs. These flocs are able to settle under gravity against the rising clear water to be recovered.

High compression thickeners generate higher underflow densities than other types of thickeners. This means that more water is liberated at the thickener for re-use in the plant. With other types of thickeners the slurry is pumped to a slimes dam where further water is recovered, with a significant loss due to evaporation. Water recovery is an important issue in arid areas, and a lack of water during droughts could result in plant stoppages, and loss of production.

For some time work had been carried out by Vietti, Dunn, and Langefeld at De Beers Research in Johannesburg, on what is referred to as co-disposal. There is a worldwide trend toward this method of disposal, where a high density paste is created at the thickener underflow. This is mixed with coarser tailings and carried by pipeline to the disposal area so that a separate conveyor to a tailings dump is not required. The required paste is delivered by a high compression thickener.

There are a number of issues that arise with the operation of high compression thickeners.

One of the problems associated with generating this paste is that the viscosity must be high enough to carry the solids, but not too high so that it cannot be pumped to the disposal area. If the viscosity is too low the solids settle out resulting in pipeline blockages. Since a single pipeline to the disposal area serves multiple thickeners it means that all of the thickeners must be stopped if a blockage occurs, and the treatment of ore stops.

Water recovery is maximised when the underflow density is maximised. If the paste density and/or viscosity is too high it results in excessive load on the raking mechanism (if present). When this happens the underflow density must be reduced by reducing the mud bed depth in the thickener. The deeper the mud bed, the more mass is available to squeeze water out of the dense slurry. If the mud bed is too deep there is a risk of damage to the thickener internal structures such as the feed well, and structures designed to guide the flow of the settling slurry. Damage to the internal structures of the thickener would require extensive maintenance and removal from production.

A large portion of the cost of operating a thickener is accounted for in the cost of the flocculant, and optimisation of flocculant consumption is an important issue for all types of thickeners.

In order to address these issues a project was initiated to investigate the behaviour of high compression thickeners. This includes evaluation of measurement and control strategies so that operation costs and plant downtime can be reduced while maximising the volume and quality of water recovered. It was decided to create a laboratory where experiments could be carried out in a situation that mimics as close as possible the settling conditions encountered on full scale. This avoided the difficulties associated with attempting to carry out test work on production thickeners, and potentially adding to plant stoppages.

1.2 AIMS AND OBJECTIVES

While this is an ongoing project to improve high compression thickener operation, the objectives of this piece of work are limited to:

- A review of the operation of thickeners in general, followed by a discussion of current measurements in use and some control strategies.
- The design of a scale thickener laboratory to achieve similar settling conditions to those found in full scale high compression thickeners, with the flexibility to simulate other thickener geometries.
- Characterisation of the slurry obtained from Finsch mine in the Northern Cape to obtain an understanding of the settling behaviour of the material under flocculation, and at different solids concentrations.
- A small scale bench top test to ensure that the slurry can be re-circulated and re-flocculated while still developing a suitable mud bed for measurement and control testing.
- The commissioning of the scale thickener laboratory. Construction of the laboratory is not discussed.
- A discussion of the path that the project is expected to take in the future, including the approach that appears to be most likely at this point in order to achieve a unified thickener control strategy.

1.3 SCOPE AND CONSTRAINTS

The scope of this thesis is a discussion of the progress made from the design of a scale thickener test laboratory, with the following constraints:

- The laboratory test work discussed was limited in that it used only material from Finsch mine since this is known to be easy to settle. The intention was to limit the complexity of the laboratory until the foundations of the operation and control of these thickeners have been determined.
- The feed to the thickener was limited to a 10 % solids concentration by mass since this is the average experienced on diamond mining operations in southern Africa. This value is used in the design of thickener installations.
- Underflow densities as close to those achieved on full scale thickeners were used (in the region of 1.5 – 1.6 $kg.l^{-1}$).

- The slurry flow into the scale thickener was designed for a nominal flow rate of 10 $l.min^{-1}$, and can be varied from approximately 6 $l.min^{-1}$ (below this value solids begin to settle in the pipes) up to 13.5 $l.min^{-1}$.
- Tests were conducted by re-circulating and re-flocculating the slurry samples. While this is not experienced in practice, it enabled tests to be carried out for at least a week, where the slurry would otherwise have been consumed within a day.
- The scale thickener dimensions were determined by the laboratory space available, the dimensions of measurement instruments, and the quantities of slurry sample available.

1.4 LAYOUT AND PLAN OF DEVELOPMENT

This document discusses the design, commissioning and initial test work carried out for a scale laboratory thickener for the purposes of measurement and control testing. The document is broken down into sections according to the phased approach taken to the project. The project phases are as follows:

1. Thickener Technology Review (Chapter 2)
2. Laboratory Scale Thickener Design (Chapter 3)
3. Sample Slurry Characterisation (Chapter 4)
4. Scale Thickener Commissioning (Chapter 5)

Each of these phases is discussed in its own chapter, taking the reader through the progression of work as the project proceeded. It will be found that in some cases topics are discussed in more than one chapter. This is due to the fact that pertinent issues were uncovered along the way as the requirements progressed. Although portions of these topics under discussion do not feature in the final test plant and work completed at the end of this document, they have been left in place as similar problems may be encountered on full scale thickeners, and the work provides a useful reference to solving problems that may be encountered in the field.

Figure 1.1 shows a graphical representation of the project as a whole, with the portion discussed in this thesis boxed in the central column.

A brief discussion of each chapter follows:

The review section in chapter 2 contains an overview of conventional, high rate, and high compression thickener operation. The focus of the project is high compression thickeners, although results will be applied to high rate and conventional thickeners where appropriate. A discussion of available thickener instrumentation and then some thickener control strategies follows this. Finally this information is discussed with the thickener measurement and control laboratory in mind, and how this leads on to the relevant scaling parameter, namely the thickener internal rise rate. The thickener internal rise rate was determined from a review of the thickeners in use on De Beers' mines in South Africa and Botswana. The background material was used as the basis for the design, as well as the background for future testing.

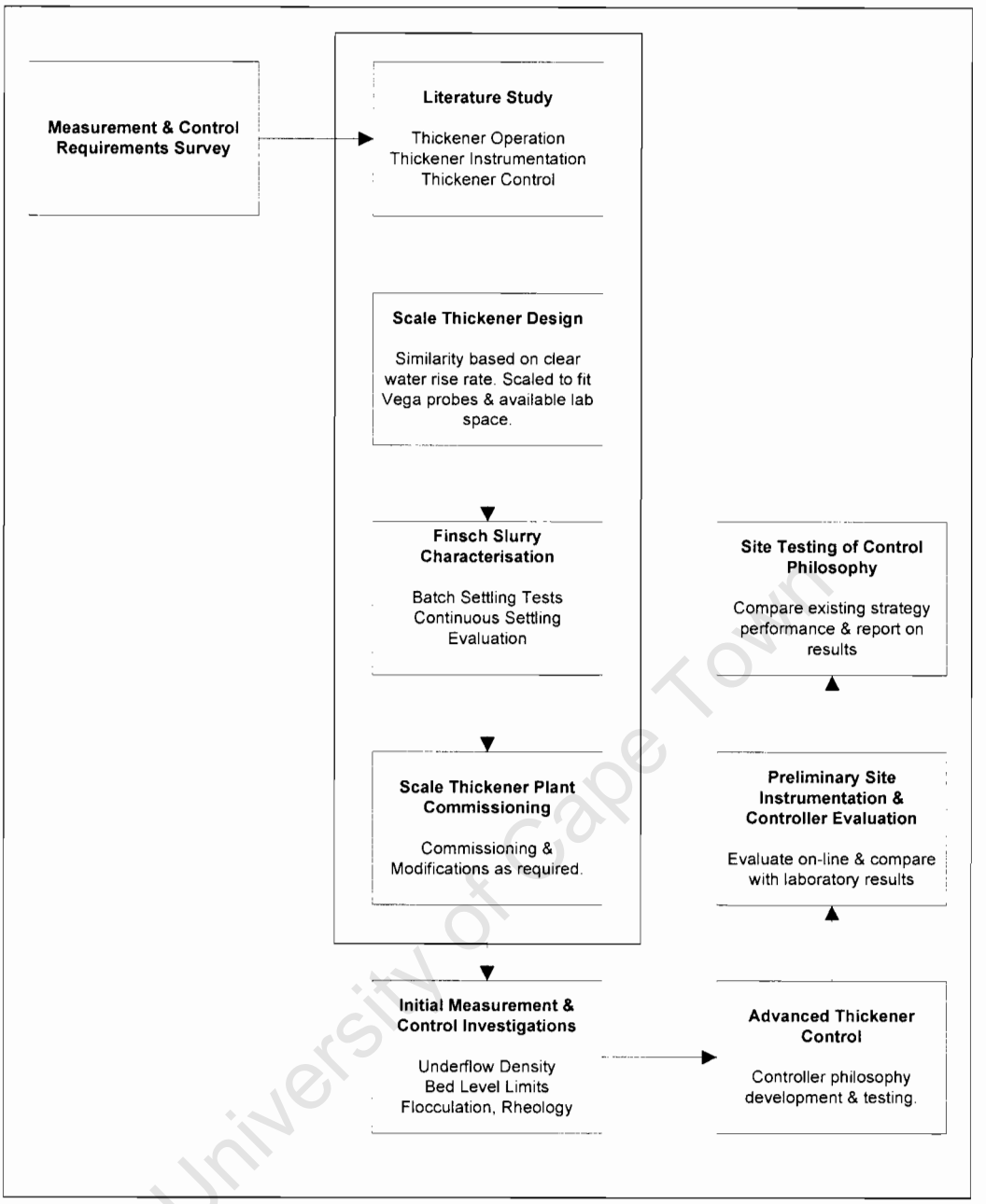

Figure 1.1 Thickener optimisation flowchart, showing the activities included in this thesis boxed in the centre column.

In chapter 3 the design of the scale thickener test facility on a laboratory scale for the testing of instruments and control strategies is discussed. The plant was designed to run in a closed circuit so that the slurry can be re-used. The required pumping capacity for slurry feed and the underflow were determined from the thickener dimensions to achieve the internal fluid rise rates experienced on full scale operational thickeners, and thus to create similar slurry settling conditions. A dilution circuit was designed to ensure a consistent feed concentration of 10 % solids by mass. Coriolis mass-flow meters were selected for density measurement in the laboratory. It was decided to manufacture the thickener from acrylic plastic so that the behaviour of the settling slurry can be observed while the plant is in operation. It was further decided to control the plant using Labview in conjunction with Fieldpoint hardware as the

interface to the drives and instruments. The Labview software package provides the necessary flexibility to reconfigure the system as required by the tests to be carried out. Finsch mine slurry was selected for use in the test plant, as it is known to settle easily when flocculated.

A series of tests characterisation tests are discussed in chapter 4, as carried out on the Finsch mine slurry sample. At the same time kaolin clay was tested as an alternative, since it is easy to obtain, eliminating the need for transporting samples from Finsch mine in the Northern Cape (approximately 650 km away). The initial intention was to run the plant without using flocculant, and instead to use a coagulant. Testing was carried out using batch settling tests, that showed that a coagulant was not sufficient to settle the slurry fast enough to be able to achieve the design feed rates. Further testing involved the selection of an optimum flocculant for the candidate slurry. Kaolin was eliminated as a possible candidate due to its tendency to form a sponge-like sediment that traps water and limits the underflow density to lower values than those achieved with kimberlite slurry. A continuous bench top test with recirculation and re-flocculation was carried out showing that it is possible to run the plant continuously for 4 – 5 days, for approximately 5 hours of testing per day.

Chapter 5 discusses the commissioning of the scale thickener test plant. After an initial slurry test a number of modifications were required. The dual tube underflow Coriolis mass-flow meter was replaced with a single tube version and evaluated, providing a stable density measurement. The dual tube meter was moved to the slurry feed. It was found that the calibrated flow rate for the positive displacement pumps was more accurate than that of the Coriolis meters, and this was used instead. The agitator in the slurry tank was upgraded to ensure proper suspension of solids. The thickener feed well was extended further into the thickener to allow for greater time for mixing of the flocculant with the slurry. The base section of the thickener was changed to a flat bottom from the original conical section as this hindered compression of the slurry. With the modification of the base a rake was installed to transport the dense slurry to the well where the underflow pump outlet is located. Two commissioning tests were carried out using two different slurries with significantly different settling behaviours. The results of both tests confirmed the commissioned status of the plant, making it ready for measurement and control tests.

Chapter 6 draws some conclusions regarding the final plant, listing the modifications carried out at commissioning, and finally some annotated images of the completed laboratory.

Chapter 7 briefly discusses the work which follows on with the completion of the test plant. It begins with a look at the available measurements at the CTP and Orapa treatment plants. This is followed by a discussion of the available manipulated variables and the relationships between these and the measured variables. The intention is to determine which are the key variables and relationships. The starting point for control testing is with Vega vibrating probes for measuring the position of the mud bed, and building on previous test work carried out in the laboratory. Measurement of the underflow rheological properties and overflow clarity will be included during this phase of the project.

CHAPTER 2 THICKENER TECHNOLOGY REVIEW

This chapter provides some background on the operation of thickeners with the laboratory test facility in mind. It begins by taking a look at the thickener classification scheme used in De Beers, and then explains the basic operation of a generic thickener, discussing the component parts and how thickening is achieved. The thickeners installed at De Beers operations are discussed here since they are a good example of thickeners typically used in industry, as well as being the target of this body of work. The operational parameters of the thickeners are dictated by the settling properties of the material being processed and the volume output by the processing plant. While this project is chiefly concerned with high compression thickeners, there may be results that are also applicable to high rate and conventional thickeners. It goes into some detail on the behaviour of slurry in the process of thickening and the important properties to be considered.

After explaining the basic thickener principles, a discussion of the instruments that might be applied to thickeners in order to measure their performance is provided. The instruments are not all applicable to every operation, and measurements are highly dependent on the slurry properties.

A brief discussion of some control strategies is presented, beginning with the traditional control strategies implemented at De Beers mines. These strategies have been implemented on most thickeners across industry at one time or another, unless superseded by more advanced control strategies. The implementation of control strategies is dependant on the desired result from the thickening process. For example, it may be more important to generate a clear overflow liquid than it is to maximise water recovery by achieving the maximum underflow density, or minimising flocculant consumption. The control strategy section includes a discussion of the Vega control strategy tested by Dunn [1,2] (for De Beers thickeners) that led to the inception of this project. A discussion of the thickener expert rules applied at Venetia mine follows, although this strategy was never successfully operated, most likely due to the lack of a reliable on-line mud level measurement. Finally a few strategies are discussed as implemented in industries other than diamond mining.

2.1 THICKENING FUNDAMENTALS & BACKGROUND

Thickening is based on the principle of sedimentation due to gravity. Sedimentation is used in three different ways: classification, clarification, and thickening. In classification two or more materials are separated by making use of the difference in specific gravity. Clarification and thickening are very similar processes where water is being separated from solids. In the case of clarification the goal is to achieve clear water, typically in water treatment processes that deliver potable water or water that will be returned to the environment. In the case of thickening, the aim is to remove water for re-use in a process, and to dewater the thickened slurry for transport to dumps. This does not require clear water since it will be re-used in the same process. The other key feature is that De Beers' diamond mining operations are often located in arid or semi-arid regions, where water recovery is an important issue.

The kimberlite treatment process revolves largely around the crushing and sizing or screening of ore. Typically the headfeed (i.e. the raw ore feed after passing through the primary crushers) is passed through scrubbers that wash fine material from the ore. After the scrubbers the ore is screened into three process streams, namely oversize (-30+15 mm), coarse (-15+8 mm), fines (-8+1.5 mm). The use of this size notation is standard practice with

plant metallurgists where '-' indicates less than, and '+' indicates greater than. The remaining undersize (-1.5 mm) material is sent to the thickeners. The oversize material is crushed in the secondary crushers and again screened into the same three size fractions. After processing, the coarse material is also re-crushed and screened and processed in the fines stream. In all of these screening processes the ore is washed by spray water that removes the undersize material. The undersize is collected in sumps and is then pumped to the thickeners. Kimberlite ores vary from site to site, and also within the same ore body, so that the thickening requirements at each site are different.

The undersize material is considered to consist of two portions, slimes and grits. When considering the thickener feed, the slimes are considered to be in the range of –0.3 mm, and the grits in the range -1.5+0.3 mm [3]. The grits are typically heavier quartz minerals, and the slimes are predominantly fine clay particles (sometimes referred to as fines). The thickener fines are not to be confused with the fines stream in the main treatment plant. The concentration of the slurry is usually in the region of 5 – 15 % solids by weight, with 10 % solids being an average concentration.

2.1.1 Thickener Types

The De Beers Group makes use of a thickener classification scheme based on the Outokumpu classification [3]. Table 2.1 gives an explanation of these classifications.

Table 2.1 Thickener Classification Scheme

Thickener	**Conventional**	**High Rate**	**High Compression**	
Approx. Max. Dia.	120 m	60 m	15 m (30 m)	
Cone Angle	Shallow	Shallow	Steep	
Typical Bed Depth	2 m	5 m	10 m	
Internal Rise Rate	< 3 $m.h^{-1}$	4 – 10 $m.h^{-1}$	> 10 $m.h^{-1}$	
Duty (dry solids tons)	Low 5–7 $t.m^{-2}.day^{-1}$	Medium 12–19 $t.m^{-2}.day^{-1}$	High 20-50 $t.m^{-2}.day^{-1}$	
Rakes	Yes	No	Yes	No
Underflow Density	1.3 – 1.4 $t.m^{-3}$	1.55 $t.m^{-3}$	1.6 $t.m^{-3}$	>1.7 $t.m^{-3}$

The data given in Table 2.2 are taken from information submitted in a review for the AMIRA P266 project – Improving Thickener Technology [4]. Conventional thickeners are typically constructed with concrete walls and base. The remainder of the thickeners are usually steel structures that stand above ground on legs. The defining difference between the types is the aspect ratio (ratio of width to depth). For conventional thickeners this value is high because the width is so much greater than the depth. This means that there is only a small depth available for settling and compression of the flocs. A floc is an aggregate of fine particles, held together due to the presence of flocculant (discussed further in section 2.2.2). The aspect ratio is decreased with high rate and high compression thickeners so that greater depth is available for the settling and compression of flocs. The final column in table 2.2 gives a classification according to that shown in table 2.1. The first three are high compression thickeners and this can be seen from the diameters, depths, and cone angles. The underflow densities are dependent on the specific site slurry properties, and depend on the material density and the ratio of fines to grits, so will not necessarily be in the range given in table 2.1.

Underflow density depends primarily on the mud bed depth, so that the deeper thickeners produce higher underflow densities than shallower ones for the same feed material.

Table 2.2 Some De Beers Thickeners

Mine	Type	Dia.	Depth	Cone Angle	Feed Rate	Underflow Density	Class
		(m)	(m)	(^{o})	($m^3.h^{-1}$)	($kg.l^{-1}$)	
Orapa	Bateman Ultrasep	10	16.4	60	600	1.300 - 1.450	HC
CTP	Alcan Deep Cone Paste	15	16.25	45	1000	1.500 - 1.650	HC
The Oaks	Bateman Ultrasep	6	13.5	60	100	1.350 - 1.500	HC
Venetia	-	60	6.4	6.47	1165	1.500	HR
Finsch	Conventional	45.7	6.21	7.23	750	1.150*	C
	Conventional	52.5	5.25	2.72	1300	1.150*	C
Koffiefontein	Conventional	45.7	6.59	9.51	1050	1.260	C

The Venetia thickeners are high rate, and deliver underflow density in the expected range. The remainder are considered conventional, although within the quoted diameters and underflow densities given in table 2.1. The Finsch underflow densities are marked with an asterisk since these values do not appear to be correct. In Carlaw's work, the underflow densities were closer to 1.3 $kg.l^{-1}$ [5].

High Compression thickeners are a more recent development (1985+) since the move toward co-disposal. Co-disposal consists of creating a thickened paste underflow that is able to carry coarse tailings (-8+1.5 mm) so that only a single tailings disposal site is required. The work in this project revolves primarily around high compression thickeners, although there may also be application to conventional and high rate thickeners.

Figure 2.1 shows high compression Ultraseps (Bateman) at Orapa No. 2 plant, and figure 2.2 shows a high compression thickener (left), Tasster (centre), and conventional thickeners at Orapa mine. The Tasster is a high compression device containing paddles to compress the thickened sediment, and was tested at Orapa mine.

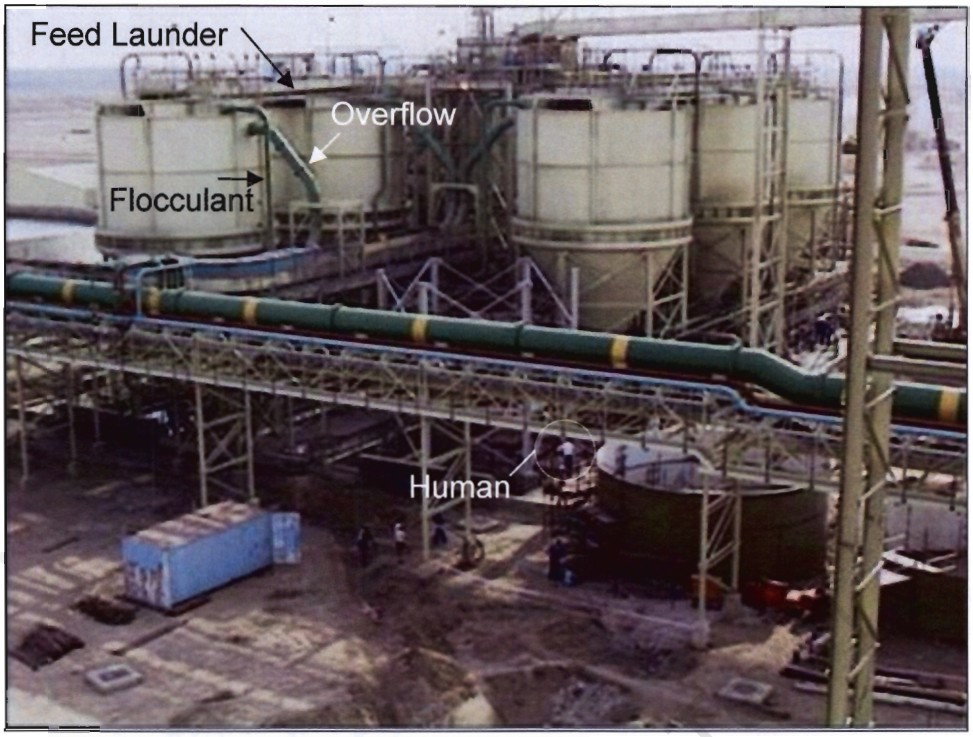

Figure 2.1 High compression thickeners (Bateman Ultrasep) at Orapa No. 2 Plant. Note the steep conical bases and the tall narrow cylindrical section. The feed is delivered to a central point via a launder, and then distributed to the thickeners.

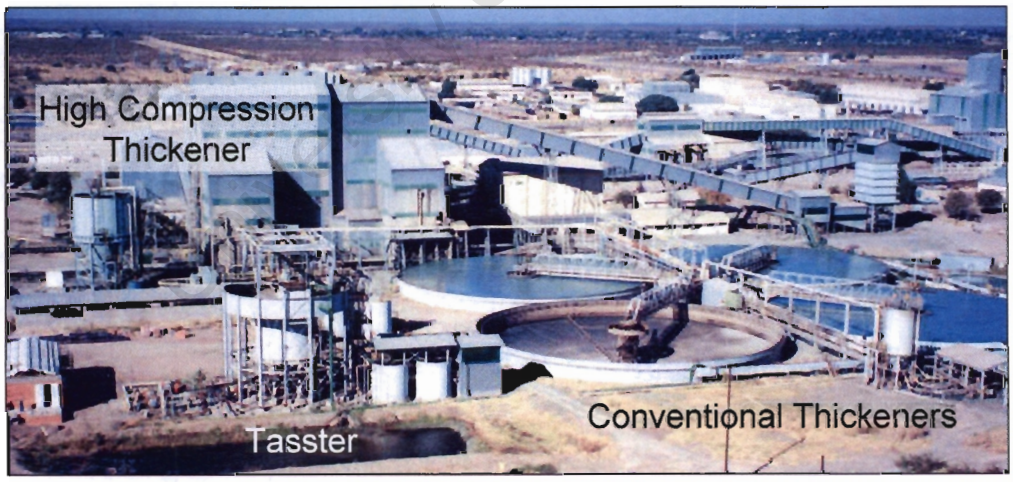

Figure 2.2 High compression thickener, Tasster, conventional/high rate thickeners at Orapa Mine. This shows the difference in aspect ratio between conventional and other thickener types.

2.1.2 Basic Thickener Configuration

Figure 2.3 shows a schematic of a generalised thickener comprising the following components:

1. A feed pipe or launder
2. Flocculant addition
3. A central feed well
4. A settling vessel
5. A clear water overflow weir
6. A rake, picket, or mud bed compression device
7. An underflow

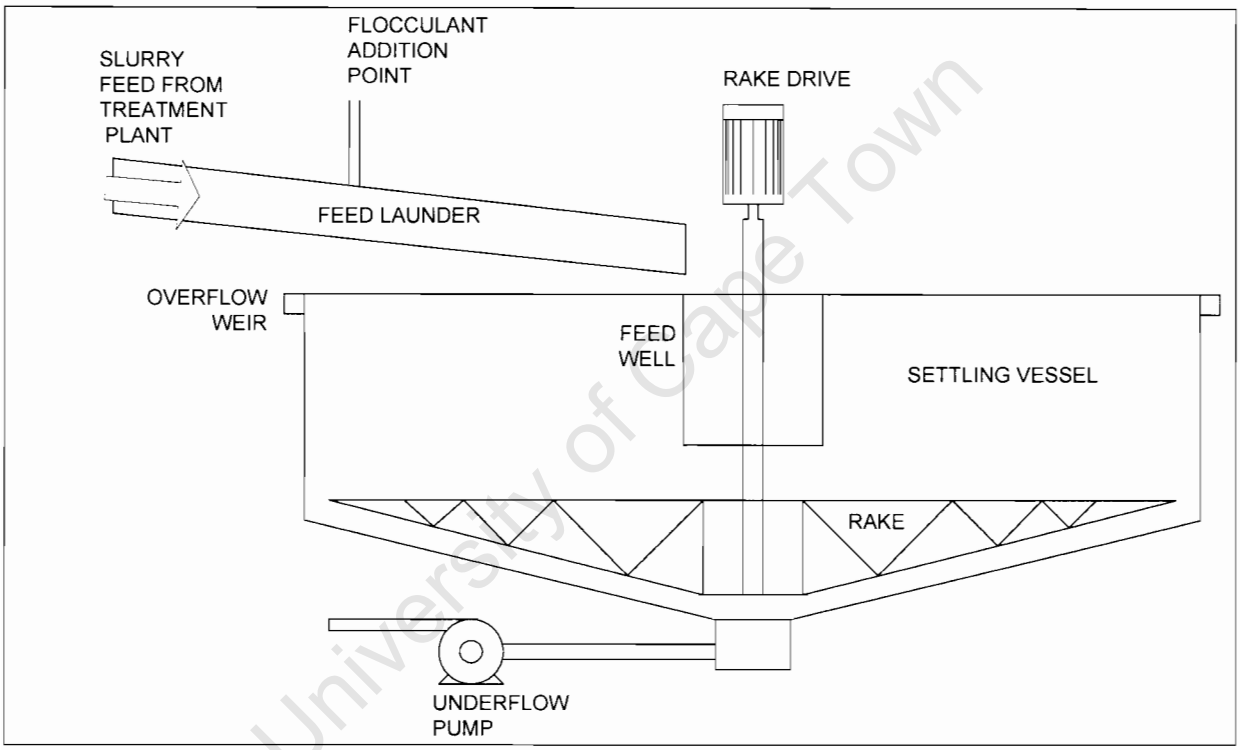

Figure 2.3 Generalised thickener schematic.

Each aspect is discussed briefly in the following sections.

2.1.2.1 Feed Launder or Pipe

The slurry is fed through a launder for conventional and high rate thickeners. This is either an open rectangular launder, or an enclosed pipe launder. In the case of the Ultrasep (high compression), the slurry is delivered via a full flowing pipe section. The launders deliver the slurry to the feed well from above via a gantry (see figure 2.5). In most high compression thickeners, the pipe into the central well runs beneath the surface of the thickener and delivers the slurry tangentially into the feed well to aid mixing. To improve settling the slurry is often mixed with some of the clear water from the upper layers of the thickener since a low concentration slurry will settle faster than a high concentration slurry (discussed further in

section 2.2.4). Outokumpu use the Floc-miser system that uses a flapper gate suspended by a float as shown in figure 2.4. This allows surface fluid to overflow into the well and dilute the slurry, without allowing concentrated slurry to flow back into the dilute water area. In the case of pipe fed thickeners a duct in the slurry feed line beneath the surface draws clear water in to reduce the concentration (see fig. 2.5). Suction is created in the ducts by the flow of slurry through the pump in much the same way that a jet pump works. There is a limit to the effectiveness of diluting the slurry, since too low a slurry concentration means that the flocculant does not undergo enough collisions with particles, and the flocculant effectiveness is reduced.

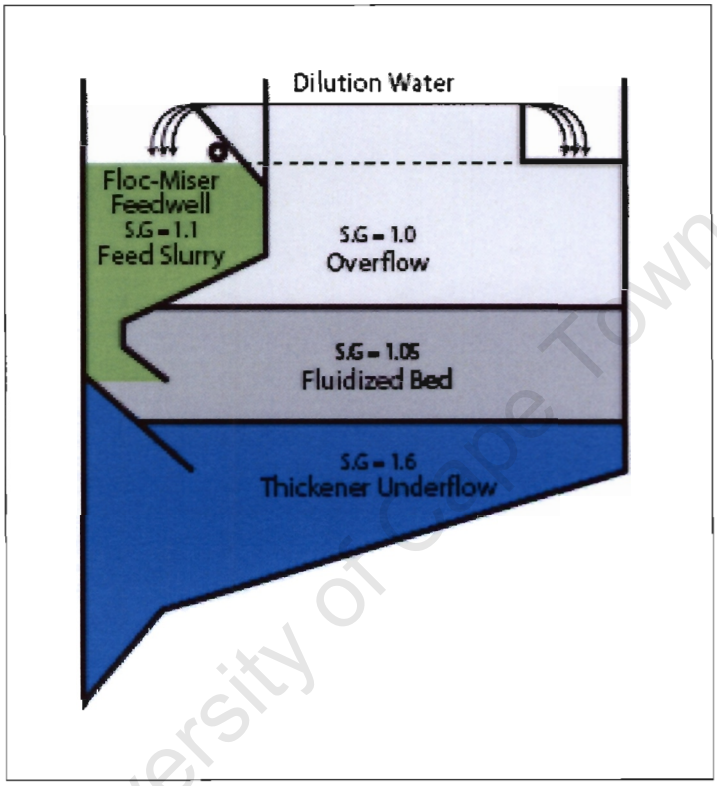

Figure 2.4 The Outokumpu Floc-Miser system [6]. Only the right half of the thickener is shown, with dilution water going over the flapper gate at the left, and going to the overflow at the right.

Figure 2.5 The GL&V E-Duc system for diluting feed slurry [7]. The pair of ducts is shown in the circle in this empty thickener.

2.1.2.2 Flocculant Addition

Flocculant is introduced some distance before entering the thickener to allow time for mixing with the slurry. For good mixing, turbulent flow is required and some launders feature baffles to ensure that this is the case. The flocculated slurry is delivered to the central well in the thickener where further mixing takes place and settling begins.

Flocculation is necessary because most of the particles in the slimes fraction do not settle naturally, and if they do it takes place very slowly. The particles remain in suspension in what is called a colloidally stable solution. In this state the inter-molecular charges dominate over the force of gravity. In order to settle the slimes it is necessary to aggregate them into larger particles called flocs that are able to settle under gravity. This is achieved using a flocculant.

Polymer flocculants consist of long polymer chains that attach themselves to the suspended solid particles. The longer the polymer chain, the more effective is the bridging and aggregation of suspended particles into flocs. It is important to have adequate mixing at the flocculant dosing point to ensure proper distribution of flocculant throughout the suspension, and to promote collisions between the suspended solid particles and polymer chains. It has been shown that the critical size fraction relating to flocculant dosage is the -20 μm fraction. The attachment is due to the charge on the clay particles. Kimberlite clays are plate-like particles with a negative charge on the flat surface, and a positive charge at the edges for pH less than 8. At a pH of 8 the overall charge is neutral (zero point of charge), and above a pH of 8 the edge charge becomes negative [3].

2.1.2.3 Feed Well

The purpose of the feed well is to allow the material to settle to the bottom of the thickener without spreading out and contaminating the clear water at the surface. From the base of the feed well the flocculated slurry spreads and settles while the clear water moves to the surface where it moves to the periphery for collection at the overflow weir. The slurry enters the settling vessel below the hindered settling zone, but above the mud bed. The settling zones in the thickener are discussed in the following section. In high rate and high compression thickeners the bottom of the feed well will often feature baffles and plates to assist spreading of the material at the bottom of the thickener, and to create desirable flow patterns (see fig 2.6 for an example).

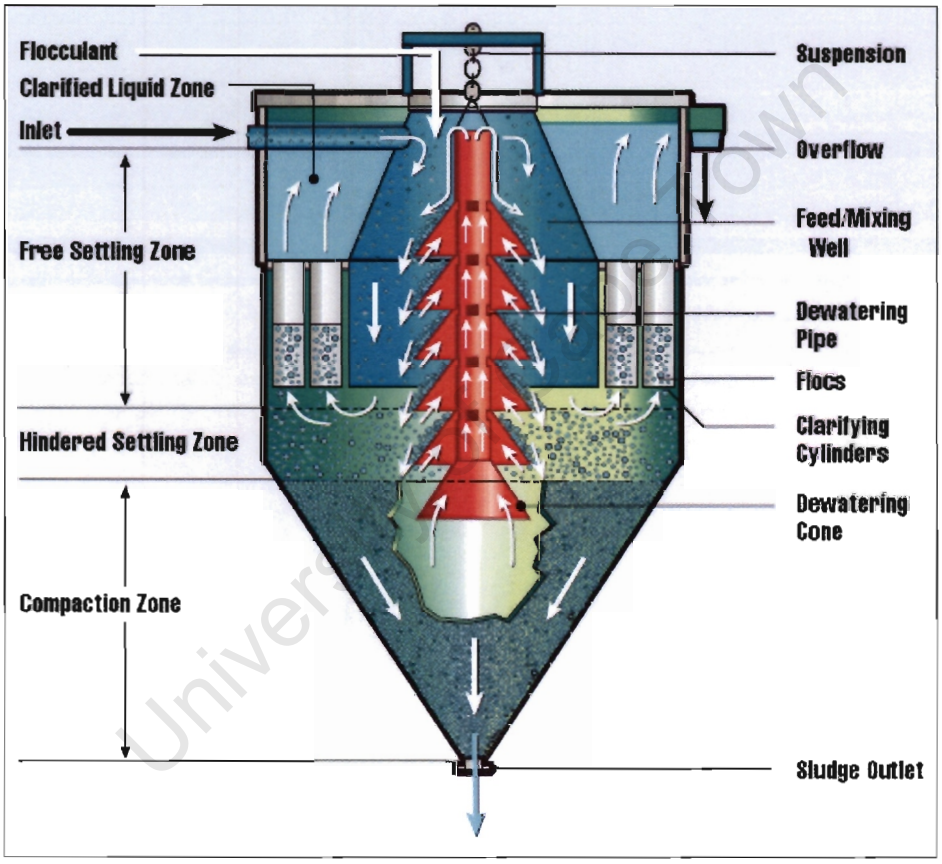

Figure 2.6 GL&V E-Cat high compression thickener showing flow directing mechanisms [8].

2.1.2.4 Settling Vessel

The main body of the thickener is the settling vessel where the water and flocculated slurry are separated. The settling vessel is also the area where the mud bed builds up and compresses under gravity to further liberate water. In order to understand the behaviour of the flocculated slurry it is necessary to introduce the four settling zones in the thickener as first described by Coe and Clevinger [9]. The zones in a thickener are shown in figure 2.7 as follows:

- Zone I: Clear liquid at the surface of the thickener
- Zone II: The hindered settling zone
- Zone III: Transition zone
- Zone IV: Compression zone

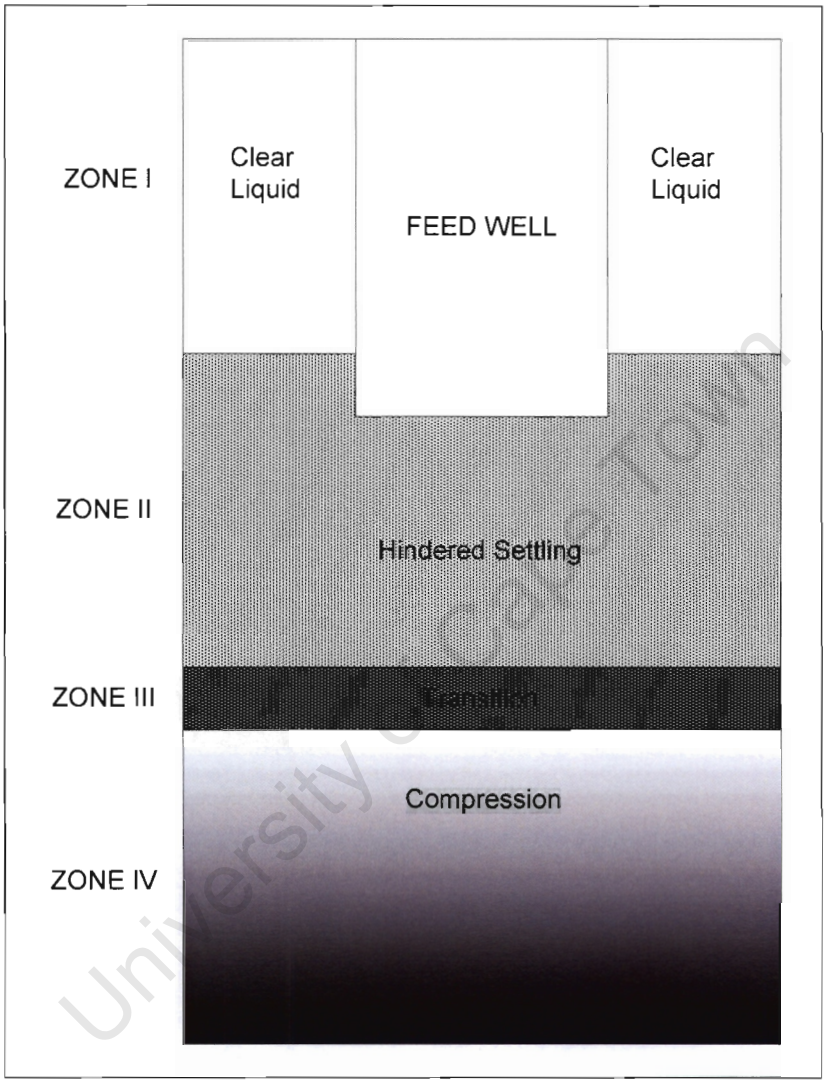

Figure 2.7 Thickener settling zones.

Zone 1: The clear liquid at the surface is the water recovered via the overflow weir, having been separated from the solids. The hindered settling zone can, under certain conditions, intrude into the clear water zone and enter the overflow. At this point the thickener is said to be overflowing, or sliming. Sliming is visible at the surface of the thickener as the flocs bubble to the top.

Zone 2: The hindered settling zone is the settling zone where the flocs are not yet in contact with each other. The terminal settling velocity of a single particle can be computed, and depends on the particle diameter, shape, density, fluid viscosity, and gravity. The terminal velocity is the relative velocity between the particle and the fluid. So it follows that if there is

a net upflow of fluid, the absolute velocity of the particle is reduced. When there are many particles present in the slurry the net upflow of water (due to displacement by settling particles) results in a reduced settling velocity. This is referred to as hindered settling. It follows that a lower concentration slurry will settle faster than a higher concentration slurry (of the same particle size distribution).

It is possible for the concentration in the hindered settling zone to be greater than the feed concentration. This concentration can be as high as the concentration at the beginning of the transition zone. If the particles are settling slowly, and hindered by interaction with each other then there is a build up of particles, and an increase in the population. At some critical population the flocs begin to overflow, i.e. the fluid rise rate exceeds the settling rate of the particles. The rise rate of clear water is approximated by the volume inflow to the thickener divided by the cross sectional area of the thickener (above the conical section). For the thickener to function the flocculated material must settle faster than this rise rate. This concentration is directly related to the slurry feed rate and to the size distribution of the slurry. If more slurry is delivered than can be settled out, the population increases. As the number of flocs increases and the settling rate decreases it is necessary to increase the flocculant dosage to increase the floc size, and decrease the population. The dilution of the feed assists by reducing the concentration and increasing the settling rate.

Zone 3: The transition zone is between the hindered settling zone and the compression zone. In this region the flocs transition from free falling separate particles to a bed. In some cases the transition zone will be very narrow, and will increase in height as settling is hindered.

Zone 4: In the final zone the flocs are all in contact with each other with water trapped in the inter-particle gaps. Compression under gravity is taking place, increasing the density of the mud bed and further liberating water in the process. As the compression zone (mud bed) rises, the compression increases and squeezes the water out so that the flocs are packed more closely together. There are two elements that determine the density at the bottom of the compression zone. The first is the mud bed depth, and the second is the residence time. The mud bed depth determines the amount of force available to squeeze water out. The residence time determines the amount of time available for the liberation of excess water as material moves from the top of the mud bed to the underflow. Pickets are often included in high rate and high compression thickeners to create channels in the mud bed that provide a path for the water to escape. Without pickets the force of the bed can lock the water in the inter-particle gaps.

2.1.2.5 Overflow Weir

The overflow weir collects the clear water at the periphery of the thickener from where it is returned to the plant for re-use. In the case of the Ultrasep the overflow weir is located at the periphery of the feed-well at the centre of the thickener.

2.1.2.6 Rakes and Pickets

In conventional thickeners a rake moves material toward the underflow by means of angled paddles where it is pumped out. Conventional thickeners have a shallow bottom so that the slurry must be moved to the centre. The rake is either powered by a central drive motor through a shaft, or in large diameter thickeners it is driven by a set of drive wheels at the periphery. In high rate thickeners the bottom of the thickener is steeper and less raking action is required, and rotating pickets might be fitted to assist in liberating water by providing flow channels. In high compression thickeners rakes and pickets may be present, although there are models with a very steep conical section that do not make use of rakes. Certain thickeners include angled paddles to assist in compressing the mud bed.

2.1.2.7 Underflow

The dense underflow is pumped from the base of the thickener to a disposal area. For conventional and high rate thickeners a centrifugal pump is used, and for high compression thickeners a positive displacement piston pump is used. The positive displacement pumps are used because the high density paste produced has a high viscosity, and requires significant force to pump. In addition to this, centrifugal pumps tend to shear thin the paste, so that it would no longer be able to carry the coarse tailings stream should co-disposal be considered.

2.1.2.8 Shear Thinning Ring

Flocculated kimberlite slurries exhibit Thixotropic (shear thinning) behaviour, which is non-Newtonian. The shear diagram or rheogram for a shear thinning material is shown in figure 2.8. The slope of the curve on the shear diagram gives the viscosity of the material. Newtonian materials exhibit a linear plot, and for non-Newtonian fluids the ratio of shear stress to shear rate is referred to as apparent viscosity to differentiate from Newtonian behaviour.

Referring to figure 2.8:

- The yield stress is the required shear stress before the slurry will begin moving. This is due to inter-particle forces, and the added bonding due to the flocculant.
- As the shear rate is increased, the shear stress increases (DA). At a fixed shear rate the material shear stress will decrease over time (path ABC), and as a result the apparent viscosity also decreases. When the shear rate is reduced, a different path is taken back to point D. At C a minimum is reached where no further shear will affect the shear stress of the material.
- When left to stand the bonds between the particles re-form so that the apparent viscosity will once again increase.

The above information is summarised from [3].

At CTP (Combined Treatment Plant, Kimberley) a shear thinning ring is fitted to the base of the thickener where the slurry is pumped using a centrifugal pump and returned to the thickener. The vanes of the centrifugal pump shear the inter-particle bonds in the slurry, so that its apparent viscosity is reduced. A pressure drop across this pipe section is measured, and this is related to the apparent viscosity of the slurry. Once the apparent viscosity is within range, the slurry is pumped to a holding tank before being pumped to the disposal site.

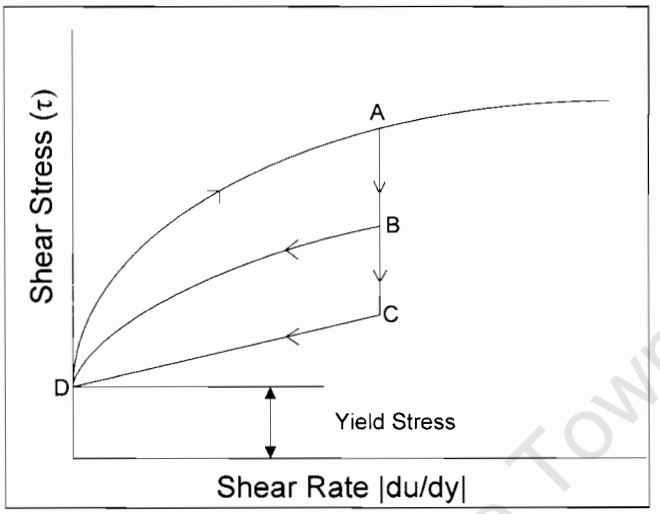

Figure 2.8 Shear diagram for a shear thinning material.

2.1.3 Discussion of High Rate and High Compression Thickeners in De Beers

The work in the thickener measurement and control project is based on high compression thickeners. Although there will be some applicability to high rate thickeners, less applicability to the older conventional thickeners is expected. In the De Beers group the high compression thickeners installed are the Alcan/Eimco Deep Cone Paste Thickener (CTP), and the Bateman Ultrasep (Orapa, The Oaks, Jwaneng). The move toward high rate and high compression thickeners comes from the desire to create denser underflow slurries. This is done by increasing the depth of the mud bed so that greater compression is possible.

In the Deep Cone Paste Thickener in figure 2.9 the combined rake/picket arrangement is evident in the bottom of the thickener. Figure 2.10 shows a schematic of a Bateman Ultrasep, showing spreaders that distribute the flocculated slurry beneath the feed well. No rake mechanism is installed in the Ultrasep, and this improves the feasibility of installing instrumentation inside the thickener* for measuring the properties of the mud bed.

* The work of Dunn [1,2] was initiated to investigate the measurement of mud bed level after the catastrophic collapse of thickener internals when the level became too high in several Ultraseps in the group.

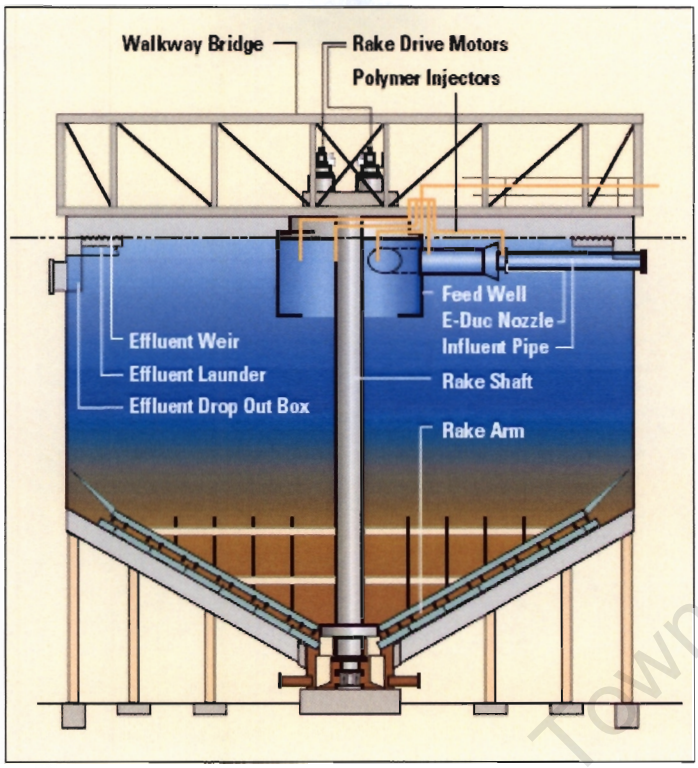

Figure 2.9 The Eimco Deep Cone Paste Thickener – note the rake arm including pickets, and the relatively shallow conical section [10].

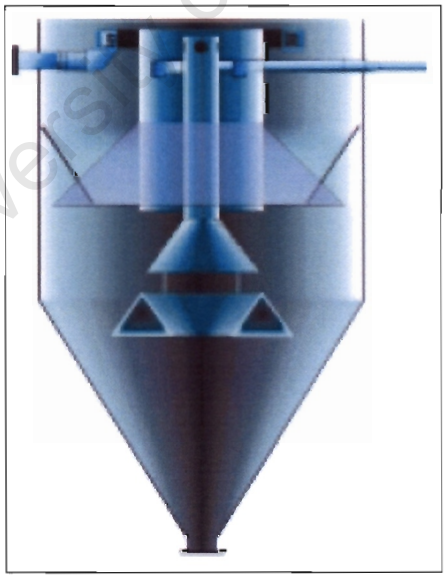

Figure 2.10 Bateman Ultrasep Geometry and Internal Structures – note the absence of a raking or picket mechanism and the steep conical base [11].

2.2 THICKENER INSTRUMENTATION

Having set out the basics of thickener operation it is now possible to consider the measurements that can be applied in order to determine the state of the system.

The instruments discussed here are taken from a number of sources. The first is a draft document compiled by Cragg et al. [12], titled 'Ultrasep Instrumentation, A Discussion Document'. This document contains information regarding the principles of operation and installation requirements for the instruments. Much of this information is not included since it can be found in the manufacturers' documentation. Information has been included where specific experience or lessons have been learned at De Beers. The second source is the AMIRA P266D 'Thickener Expert' [4]. This CD based resource contains the output of the AMIRA P266 project, 'Improving Thickener Technology', up to the end of 2002. De Beers was a sponsor of this project up to the end of 2003. The Vega vibrating probes, and some other instruments that were tested are discussed briefly from the work of Dunn [1,2]. An instrument from Solartron Mobrey was evaluated by Roebl [13], and a sludge blanket detector from Markland Specialty Instrumentation was evaluated in Canada using Finsch dust [14]. A few other instruments are also listed, either being brought recently to market, or being similar to others discussed in the references listed thus far. Additional instruments and suggested applications are based on the author's experience.

The instruments are discussed as they appear through the process, starting at the feed to the thickener, and finishing at the underflow of the thickener. Figure 2.11 shows a typical high compression thickener, and the instrumentation that may be installed. In the case of the thickener feed, the instrumentation can extend well beyond the thickener to the points where the slimes are generated, to determine the volume being generated at any one time, and to take pre-emptive action. These estimates fall into the class of virtual or derived measurements.

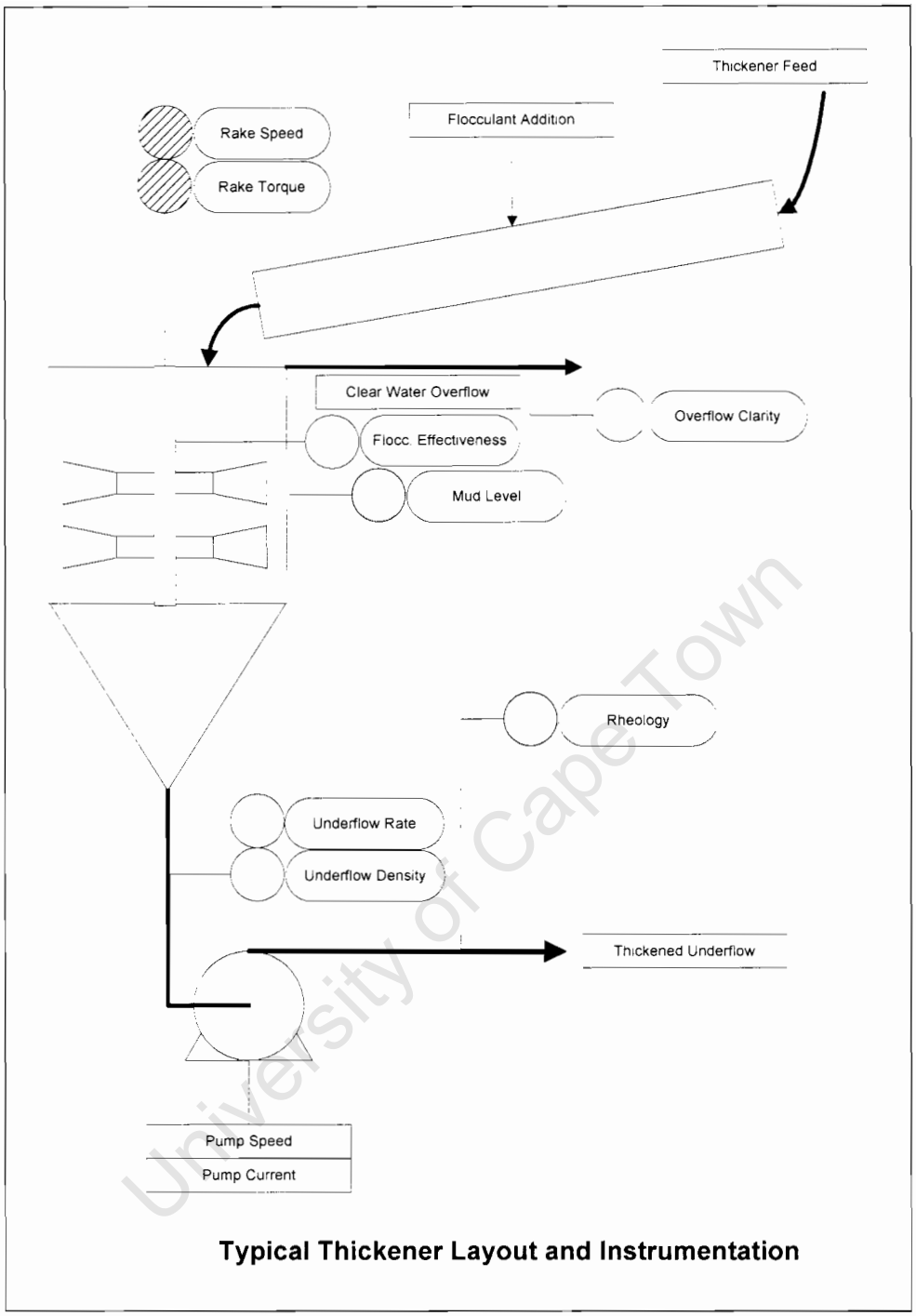

Figure 2.11 Typical high compression thickener layout and instrumentation.

2.2.1 Summary of Installed Instrumentation at De Beers Mines

Table 2.3 Summary of Installed Instrumentation at De Beers Mines

Mine	**Finsch**	**Venetia**	**CTP**	**Orapa**	**The Oaks**
Feed Concentration	PDS	PDS	NDG	NDG	
Feed Flow Rate			EMF	EMF	
Flocc Flow Rate		EMF			
Overflow Rate		OCF			
Overflow Conc		MCW			
Settling Rate	Clarometer	Clarometer			
Mud Bed Level	Manual - ST	UP	ST – NDG	VDP	VDP
Underflow Density	NDG	NDG	NDG	NDG	NDG
Underflow Rate		EMF	EMF	EMF	EMF
Underflow Viscosity			PDV		

Key:
PDS = Pulp Density Scale: Manual measurement with 1 litre sample (Marcy Scale)
NDG = Nuclear Density Gauge (Various Manufacturers)
EMF = Electromagnetic Flow Meter (Various Manufacturers)
OCF = Open Channel Flow Meter (KAB Sumpi Level Measurement)
MCW = Manual Clarity Wedge: Dip in probe (Pelichem)
ST = Siphon Tubes: Manual Inspection, or NDG
UP = Ultrasonic Probe: Endress & Hauser CUM 750
VDP = Vibration Damping Probes (Vegavib 52)
PDV = Pipe Differential Viscosity Measurement: Differential Pressure Viscosity Estimate

2.2.2 Thickener Feed

The thickener feed is the determining factor in how a thickener should be operated. The three features that have a critical impact, are the volume flow rate, the solids concentration, and the particle size distribution (PSD). The flow rate and concentration affect the loading of the thickener, and determine its operating point in terms of its design capacity. All three variables determine the required flocculant dosage, although high volume flow rates will also demand increased flocculant dosage due to the effects of hindered settling that result in the thickener overflowing.

2.2.2.1 Flow Rate

The conventional thickeners are fed through open rectangular launders, or closed pipe launders that feed into the top of the feed well. High compression thickeners such as the Bateman Ultrasep are fed via full flowing pipes that enter at the side of the feed well.

a) Electromagnetic Flowmeter

Electromagnetic flow meters operate on Faraday's principle of electromagnetic induction. A typical electromagnetic flow meter will measure accurately from around 1 $m.s^{-1}$ up to 10 $m.s^{-1}$, with a maximum of 12.5 $m.s^{-1}$ [15]. The accuracy is typically quoted as ±0.5 %, although potentially large errors (up to 20%) are present if the meter is not calibrated with the process medium [16]. Meters must be specified for slurry applications, and for Endress & Hauser meters the nominal pipe diameters range from 15 to 600 mm. The measurement is only suitable for full flowing pipelines. Where possible a calibration should be carried out to determine the accuracy of the meter.

b) Ultrasonic Flowmeters

Ultrasonic flowmeters are only applicable to slightly contaminated homogeneous fluids in full flowing pipes, and are not suitable for kimberlite slurries.

c) Level Inference

For measurements in launders, an alternative flow measurement is required. One means of doing this is by Manning's equation, which infers the flow rate based on the measured liquid level in the launder [17]. The launder level is inferred based on the channel level, the slope of the launder, and the launder geometry. No knowledge of the fluid density is required. The equation was developed empirically for use in irrigation and drainage channels where knowledge of the silt content was not available. A table of roughness factors are available and must be included in the equation. It would be appropriate to carry out a calibration to determine the accuracy of the technique. The surface of the fluid must be smooth at the measurement point, and any instability due to launder baffles must have settled. Baffles are typically included in the launders to assist in mixing of the flocculant, and will typically be installed prior to the measurement point. A KAB Sumpi FM [18] is installed at Venetia mine to estimate the flow into the thickener. This and many other devices include the required processing to characterise the shape of the channel, and provide a flow output.

d) Flumes and Weirs

Carlaw [5] installed a weir at Finsch mine to estimate the flow rate into one of the thickeners. This was hampered by the unevenness of the flow due to mixing baffles upstream of the measurement point. Weirs have the additional drawback that they provide a point where silt will be deposited, and hence impact on the flow patterns and the measurement principle. The flow rate is a function of the depth of flow through a structure of known dimensions.

e) Coriolis Mass Flow Meters

These are not suitable for flow rate measurement since they are designed for homogeneous mixtures or fluids. They are also limited to a maximum diameter of 150 mm for single straight tube designs [19].

f) Thickener Flow Estimation

This can be estimated from the points in the plant where the slurry is generated. The feed rate can be inferred here from the amount of water delivered to the scrubbers and screens in order to wash the ore. The amount of solids can be estimated from the weightometers on the various streams after screen sizing. The mass of ore is typically measured prior to entering a process, and then after sizing. Since plant feed is relatively constant it is not necessary to take into account the delay between the feed measurement, and the measurement after screening.

Flow Rate Discussion

In general it can be concluded that electromagnetic flow meters are appropriate solutions for closed full flowing pipes, and that a method such as Manning's equation is suitable in the case of open partially filled channels or launders. It is recommended that calibration be carried out in both cases. In practice this is a difficult task, which would be best accomplished by timing the fill of a known volume. This would have to be done by emptying or partially emptying the thickener on a maintenance day, and then measuring the time to fill when production resumes. There are not many opportunities for such an exercise in a production environment, but it is not impossible to arrange such a test.

2.2.2.2 Concentration

Concentration is expressed as a ratio of the slurry solids mass to the total mass of the slurry. If the solids and liquid densities are known the concentration can be converted to a slurry density, and the two quantities are equivalent. The fluid density is taken to be that of water, and the solids density is usually taken to be the bulk density of a sample containing clay and grits contents of different densities. The clay/grits content will vary as different parts of the ore body are mined.

a) Nuclear Density Gauges

The concentration is a difficult feature to measure considering the large diameter pipelines and launders. Nuclear density gauges are used at De Beers mines when density measurement is required. The feed pipes for Ultraseps and Deep Cone Paste thickeners are suitable candidates for nuclear density gauges provided the source can be mounted in a safe place and does not need to be excessively large. Having a sample line take-off from the main feed is a suitable means of avoiding the problem of large dimension feed launders. The one difficulty is that a take-off point might result in an inaccurate measurement due to stratification of the solids in the launder.

b) Coriolis/Vibration Density Measurement

The measurement of density using single line straight tube coriolis mass flow meters is improving, but not necessarily appropriate yet for the industrial measurement of slurries as they are designed for homogeneous mixtures [19]. The density measurement in the vibrating tube(s) is based on resonant frequency. As the mass in the tube(s) changes, the natural

frequency of the tube and its contents will change. The device does have difficulties if air inclusions are present. Maximum diameter for single straight tube devices is 150 mm.

Solartron Mobrey manufactures a vibration densimeter that excludes the Coriolis measuring portion. This is a single straight tube device, but the maximum diameter is limited to 25 mm [20].

The Solartron-Mobrey insertion vibrating density probe operates on a similar principle, where instead of vibrating the tube in which the slurry travels, a vibrating tuning fork is inserted into the pipeline to measure density. This instrument was found to be very accurate in the laboratory [12], and may have practical application for the measurement of concentration in thickener feed. The tuning fork takes the form of a slotted rod that is very robust. Mounting is via a flange fitting. The only important feature of the installation would be the location of the probe so that the probe is always covered with thickener feed material. Since the feed concentration is low, it is not possible that a build-up will take place if the instrument is mounted with the fork facing downward. Stratified flow might present a problem, unless the probe is mounted in a vertical pipe section. In a vertical pipe section it would be best to mount the probe so that it covers as much of the central portion of the pipe as possible. It is possible that wear on the probe will change the resonant properties of the probe and affect the readings. Non-contact measurements are preferred in a slurry with grits up to 1.5 mm diameter.

c) Turbidimeters (or turbidimetry)

Turbidimeters measure water clarity based on light backscatter. These instruments will typically be installed face down in the slurry feed stream. A light source is flanked by two or more sensors angled at 45 degrees or more to the side of the source (in the backscatter system). The amount of solids present will determine the amount of light scattered back to the sensors. Unfortunately the degree of backscatter is also dependent on the particle size distribution of the slurry solids. The water clarity is measured in NTU (nephelometry turbidity units), that are based on standard calibration samples. There is no direct means of calculating the concentration from the NTU measurement. The measurement window is usually fitted with a wiper to remove build up. Some models also output an estimate of TSS (total suspended solids) content in the range of approximately 0.001 – 150 $g.l^{-1}$ (Hach solitax [21], Endress CUM 740 [22]). This is 13.7 % solids by mass, or 1.09 $kg.l^{-1}$ for a slurry with a density of 2.60 $kg.l^{-1}$. This instrument is probably best used to evaluate the overflow clarity since it measures the fine suspended solids (in this case clay particles).

Similar devices are available that make use of optical or acoustic adsorption or transmission through the medium, although these do run the risk of having the transmitter completely obscured. There are devices that use infra-red on either a reflectance (from a target), or scatter, or transmission basis. The same is true for ultrasonic devices that measure adsorption (attenuation) of a signal, or backscatter. All of these devices suffer from the same problem, namely a sensitivity to the size frequency distribution of the slurry (particle size distribution). This was observed in the testing of the Solartron Mobrey MSM400 [23], which is a horseshoe shaped device with a transmitter on one face, and a receiver on the other (ultrasonic). Variations in the size distribution had significant impact on the reading when tested with kimberlite slurry, so that a useful repeatable measurement could not be taken. Hawk SSA [24] manufacture a device that features an acoustic transmitter and receiver in the same head, where the signal is bounced off a reflector. If the general properties of the feed material PSD

are known these devices can be used to determine whether to increase or decrease the flocculant dose, but not to obtain a specific measurement of the concentration.

The nuclear density gauge is the preferred measurement from an accuracy point of view although it must be very accurately specified since the range of feed density is typically between 1 and 1.1 $kg.l^{-1}$. The vibrating probe meter has a range of approximately 1 to 1.5 $kg.l^{-1}$, and may be better suited to this application. Both instruments would best be installed in vertical pipe sections.

2.2.2.3 Particle Size Distribution Information

Instruments that measure particle size distribution are available. These are based on a laser scanning through a sapphire window (referred to as FBRM: focused laser beam reflectance measurements). Lasentech produce such a probe [25] suited to laboratory scale measurements. The window will be prone to fouling due to the presence of flocculant. A Honeywell Microtrac X-100 desktop FBRM system is in use at the DBGS water laboratory for small sample analysis [26]. A larger industrial Lasentech probe is available [27], and requires the pumping of a sample through a pipe in which the probe is installed.

An instrument called the UltraPS [28, 29], a continuous on-line ultrasonic particle size analyser is available from CSIRO Minerals. The instrument uses ultrasonic velocity and attenuation over a range of frequencies to determine size information. An ultra-low activity radio-isotope source (exempt from licensing) is included for corrections due to variations in solids content. As a result the instrument also outputs the slurry solids content. The measurable size range is from 0.1 to 1000 microns which is greater than the 0.1 to 750 micron that the Honeywell Microtrac is capable of.

2.2.3 Flocculant Flow Rate

It is preferable to deliver the flocculant using a calibrated positive displacement pump so that an additional measurement of the flow rate is not required. Mono positive displacement pumps are available for low flow rates and are suitable for this application. Centrifugal pumps will shear and damage the flocculant prior to delivery to the feed stream. The positive displacement pump in conjunction with a VSD (variable speed drive) is able to deliver accurate flocculant dosage.

If some other pump is present, then a small bore electromagnetic flow meter will be adequate for the purpose, although it is unlikely (not suggested) that anything other than some type of positive displacement pump be used for the delivery of flocculant. There is also a possibility that a build up of flocculant will occur on the sensors across the measurement section.

2.2.4 Flocculant Dosage Measurement (Clarometer)

The Clarometer [30] is a flocculant dosage control system, but the measurement portion is of interest here. The measurement element consists of a glass measuring cylinder (approximately 500 ml). The measuring cylinder is filled with a sample pumped from the centre well of the thickener. Once filled, the flocculated sample is allowed to settle until it passes a fixed measuring point. The maximum level, and the settled level are determined using optical sensors. The time between these two points is measured, and compared with a

preset reference time. An alternative uses a turbidity meter to determine when the water reaches a specific clarity at a certain level in the cylinder. On this basis the amount of flocculant delivered to the feed slurry is adjusted. [29,5]. The glass must be kept clean so that the measurement continues to be accurate. The fine clays can tend to stick to the glass with time, reducing the reliability of the measurement.

2.2.5 Hindered Settling Zone Level

The top of the hindered settling zone is also referred to as the top of the sludge blanket in some cases. This is distinct from the mud bed level, and provides different information. Often this blanket will prevent accurate measurement of the top of the mud bed since it attenuates signals and provides a gradual transition through to the top of the mud bed, rather than a distinct measurable interface. The top of the hindered settling zone is important in that it provides information regarding the flocculation requirement. For a fixed flocculation level, the flow rate determines the level or thickness of the hindered settling zone. Since we have no control of the flow rate to the thickener, or of the particle size distribution, the flocculant dosage must be adjusted to maintain the hindered settling zone, and to prevent the thickener from overflowing or sliming. Instruments designed to measure the hindered settling zone have often been erroneously applied to the measurement of the mud bed level, and deemed inadequate when they don't work. The top of the hindered settling zone does not always present a distinct interface with the clear water zone. For this reason it is sometimes only possible to get an on/off indication when a specific concentration is reached.

a) Ultrasonic/Acoustic and Optical Measurements

There are many instruments to detect the level and concentration in the hindered settling zone using optical and ultrasonic techniques to measure the concentration. One drawback of these devices is that variations in the floc size and PSD do have an impact on the measurements. The ultrasonic devices are less sensitive to build-up on the sensors, since these typically take the form of a very fine slime, and will sometimes include some flocculant build-up. Generally the measurement technique makes use of the transmission of an optical or ultrasonic signal. The concentration is determined through attenuation of the signal, either through scattering by the particles, or by adsorption of the energy by the particles in the mixture. The measurement result can be affected by the size of the flocs and other particles in the fluid, where the degree of flocculation will determine the size of population of the flocs. There will be a significant difference between the dirty supernatant, and the hindered settling zone where large (mm order vs μm order) flocs have a larger impact on the measurement, depending on the wavelength and frequency of the transmitted signal. Due to the measurement technique, which is based on the area presented to the signal path, the resulting measurements are a volume concentration estimate.

b) Ultrasonic Devices

The Markland 502 TP device uses ultrasonic attenuation as the means of measuring the concentration. The transmitter and receiver are both located in the same head, and a target is used to reflect the signal back. The target can be screwed in and out of the head in order to adjust the sensing distance (depending on the density and population of the material being

measured). The sensor takes the form of a sensing head suspended in the fluid, providing a point measurement of the concentration. This device was tested in Canada by Markland using Finsch mine powdered slimes at various concentrations and was found to produce suitable results once converted to a solids concentration [14,31]. One of these devices has been purchased and will be tested in the laboratory at some time in the future.

The Solartron Mobrey MSM400 [23] consists of a remote transmitter and horseshoe shaped sensor, with the ultrasonic transmitter in one head, and the receiver in the other. It was difficult to calibrate this device and the measurements were found to drift significantly. The device was tested in thickened slurries, and was probably being used outside of its design range.

The Hawk SSA [24] operates on the same ultrasonic reflectance principle as the Markland 502 in a similar configuration, but has not been tested in the laboratory, or on site. The mounting is available with a lifting arm to move the sensing head out of the path of rakes or pickets.

d) Optical Devices

Markland supplies another instrument that makes use of optical technology, using a rail of optical sensors [32]. This instrument is not recommended since the water in the thickener is not of the quality of that found in clarifiers and is typically brown or grey coloured, depending on the type of ore being processed. Build-up on the sensor windows is an issue.

e) Turbidimeters

These have been discussed in section 2.2.2 c), and are not appropriate for the measurement since they are not immersion probes. The cable entry portion of the probe is not suitable for immersion below the water surface. The top of the hindered settling zone could be anywhere from the surface of the water to a few metres below.

f) Guided Microwave Measurement

These devices use a guide in the form of a rod that is suspended in the fluid [33], to transmit the microwave signal. The problem with this device is that the top of the hindered settling zone features a gradual increase in concentration. The same is true at the transition zone (in almost all cases), where the transition from hindered settling to compressed slurry is not distinct. In order to receive a reflected signal to detect the interfaces a sharp transition is required.

g) Ultrasonic Devices

An Endress & Hauser CUM 750 [34] ultrasonic measurement system is installed at Venetia mine. This device claims to be able to detect both the top of the hindered settling zone, as well as the top of the mud bed. The ultrasonic probe is attached to a cable that is wound onto a drum so that it can be winched into and out of the thickener, developing a profile of the hindered settling zone down to the mud bed as it travels. Typically the rake is fitted with a proximity switch so that the instrument can be raised out of the rake path as it passes. The

transceiver head operates based on the amount of energy reflected back, giving an estimate of the concentration.

A Royce Technologies instrument [35] was observed at Tweepad mine in Namaqualand. The transceiver is mounted at the end of a cable that is winched in and out of the thickener to avoid becoming trapped in the paddle mechanism.

Calibration of the above devices is difficult, since the hindered settling zone is in motion, and the PSD varies depending on flocculation. Further work may be required on analysing these devices, although it is possible that they would be used as a switch to indicate the level of the hindered settling zone.

2.2.6 Mud Bed Level

Mud bed level measurement entails either measuring the top of the mud bed, or measuring the density at some specific level within the mud bed. The density varies according to the PSD of the feed material and the size of the flocs. The intention is to attempt to measure the interface where there is a sudden change in concentration or density. At times it is difficult to draw a distinction between the hindered settling zone, the transition zone, and the compression zone. This makes it difficult to detect the beginning of the compression zone, and a specific density must be sought that can still be detected despite the lack of a clear interface.

Mud level detection was evaluated by Dunn specifically for the work carried out at Finsch mine described in [1]. Although the work of Cragg et al [11] is not dated, it appears that the work of Dunn is a direct follow on of this initial discussion document. A number of instruments were tested on a laboratory scale by Dunn in order to determine which would work best with Kimberlite slurry. It should be noted once again that the evaluations are specific to Kimberlite, and that the performance and results will vary from slurry to slurry.

a) Buoyancy/Float Methods

There are a few different implementations of float level measurements. These are point measurements taken by measuring with a float filled to the correct density to achieve a specific buoyancy. The correct density could be the top of the mud bed, or some concentration beneath the top of the mud bed. Laboratory tests are required to determine the best buoyancy for the float. All that remains is to determine the point at which switching takes place.

Guided Floats

Buoyancy floats tend to be located on a shaft that contains reed switches operated by a magnet located in the float. The alternative to using reed switches is magnetostrictive measurement. This requires a central rod of nickel or iron that is magnetized by a coil with an ac current and a dc offset. The varying position of the float magnet changes the natural frequency of the central rod. By finding the natural frequency of the rod the position of the float can be calculated.

These devices are simple, but suffer from a few drawbacks. The first is that solids are likely to settle on top of the float, and change the effective density, unless it is of a design that allows the solids to freely fall off (i.e. a steep conical top). It is also possible that the float will become locked in the slurry, and suction at the base might not allow it to float free. The final problem is that the float is located on a shaft that makes the level measurement. It is necessary that there is sufficient space for the float to move freely on the rod. It is very easy for the gap to become clogged with settling material so that its motion is halted. Physical contact with the bed is acceptable, but moving parts in a slurry are not recommended.

Cable Suspended Floats

Alternative devices are floats that are cable suspended. These contain an internal tilt switch, consisting of a mercury switch. The floats consist of a conical top portion, and a hemispherical bottom portion. The conical top prevents the build-up of material on top of the device when suspended vertically. These are typically made up to measure water levels in sumps, but could also be used to detect mud bed level if the buoyancy of the floats is in the correct range. Mellor supplied these floats in the past for use with submersible pumps, although no recent reference is available.

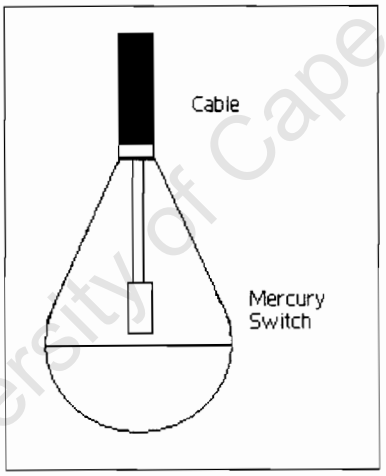

Figure 2.12 Mercury switch float.

On the upside, these devices do not have a problem with a gradually varying interface, since they will still switch at a point where the buoyancy force matches the density that the floats are designed for.

b) Natural Radioactivity

This technique makes use of natural radioactivity in the material that increases as the concentration of the material increases through the bed. The levels of natural radioactivity are too low in Kimberlite to make this technique feasible [12].

c) Nuclear Density

Measuring across the entire thickener is not practical since the attenuation is proportional to the square of the distance, and this would require a very large source. The technique becomes more feasible when only a portion of the thickener is measured. The preferred configuration is to mount the source on the outside of the tank looking inwards. The detector is suspended inside the tank. The source and detector are raised and lowered in the tank to develop a profile of the bed. This does require a particularly robust encapsulation of the detector in order to ensure water proofing. The third option is to pump out a sample from various taps on the side of the thickener. Potential difficulties involve the fact that the taps might preferentially draw material from lower density layers above since they have a lower resistance to flow. If this is compensated for, it is still possible to obtain a useful bed profile. It will also be necessary to pump enough slurry through the line to clear the material from the previous sampling point. [12]

d) Conductivity Measurement

Work carried out by Herholdt [36] showed that the settling profile could be determined using electrical impedance tomography, making use of resistance measurement which gives a current profile based on the bed make up.

Work conducted by Dunn with a point measurement showed that conductivity is highly temperature sensitive, and thus not suitable for a single point measurement [1]. Herholdt's work has the benefit of being a relative measurement between a number of sensing electrodes so that the temperature effect is reduced.

e) Mechanical resistance to movement.

Paddle

This device measures the resistance to motion, by the amount of force required to maintain a paddle in a specific position with a moving slurry, or to rotate a paddle, and measuring the force required to do so. The device did not switch under test conditions [1].

Damping

Vegavib 52 vibrating [37] probes were tested by Dunn [2] on a scale thickener and later on a pilot plant at Finsch mine for co-disposal tests. The technique has been shown to switch reliably without significant temperature effects, and a set of probes are installed at the Oaks mine. The probes resonate at a preset frequency with an adjustable amplitude. When the amplitude of the vibration is reduced to a factory set limit by damping due to the solids, switching takes place. The probes are specifically designed for sensing solids in liquids. These probes and the associated control philosophy provide the starting point for current laboratory tests.

f) Hydrostatic pressure measurement

In this instance, hydrostatic pressure measurement is used at various levels in the tank using sealed diaphragms mounted in the tank walls to determine the location of the interface. This is based simply on the principle of gravity head, and depends on the density of the material. By looking at the pressure difference between two probes the bulk density of the material between the two levels can be estimated, and thus the mud level can be estimated. Three or more probes are suggested.

2.2.7 Rake Torque Measurement

Rake torque is estimated by the current drawn by the rake/picket drive motor. The rake torque is determined by the resistance to flow presented by the dense slurry near the base of the thickener. Most VSDs (variable speed drives) can be configured to output the motor torque as a mA signal. The actual motor current is not equal to the current drawn by the VSD since there are losses involved in the inversion process, although it would still provide a reasonable estimate of the rake torque.

2.2.8 Underflow Flow Rate

Since the underflow is typically pumped using centrifugal pumps, it is necessary to measure the underflow flow rate. In the case of fixed volume positive displacement pumps the pumped volume is directly proportional to the rotational speed of the pump driver. The electromagnetic flowmeter discussed in section 3.2.1 a) is the most suitable measurement device provided it is specified for dense slurry due to the possible wear involved. This involves the use of a soft rubber lining and hard (typically Hastelloy) probes measuring the potential across the slurry. Calibration is suggested due to the possibility of errors involved in the measurement of dense slurry [15].

2.2.9 Underflow Density

Nuclear Density gauges are fitted as standard to all De Beers thickeners at the base of the thickener prior to the underflow pump.

2.2.10 Underflow Rheology

There are two types of viscometer installation, flow through (in-line), and immersion (insertion probe). The slurry to be measured must be treated as a non-settling slurry, otherwise viscometry cannot be applied. Flow conditions in the viscometer must be laminar for the calculation of viscosity. If this is not possible in the pipe, the installation of a sampling line becomes necessary. Most viscometers operate at only one shear rate (at a single flow rate). The dense underflow can be considered non-settling if it has the paste like consistency associated with high compression thickeners. The presence of grits in the kimberlite slurry eliminates the use of most of the devices presented by Alderman and Heywood [38]. The

following rule of thumb is provided: The smallest acceptable gap between coaxial cylinders, cone and plate, and parallel plates used in rotational viscometry, and the diameters of the tubes used in tube viscometry is 20 – 50 times the maximum particle size to avoid jamming. Only three options of the seven discussed by Alderman and Heywood appear feasible for measuring kimberlite slurries.

a) Rotating Bob

It would appear that the rotating bob device might be suitable – the torque on the rotating bob is measured to estimate the viscosity. The device is fairly complex with moving parts, and requires a process take off from which the sample must be pumped through the meter. It is very likely that wear and fouling will be a problem with these devices, although Alderman and Heywood state that it has been used in a wet grinding circuit [38].

b) Vibrational Viscometers

Vibrational viscometers consist of a stainless steel rod resonating along its length at its natural frequency – the loss of energy to the viscous drag of the slurry is related to the viscosity. Alternately a rod vibrating at a fixed amplitude is inserted into the slurry and the viscosity calculated from the force needed to maintain this amplitude. If the density of the slurry is varying with viscosity then an independent density measurement is required. This is not a problem since the underflow density is already measured. The instrument is fitted to the pipeline via a flange. Solartron Mobrey (7827, 7829) [39, 40] and Hydramotion (XL7 [41]) supply vibration meters of this type.

c) Full-bore Pipe Viscometer

The viscosity is estimated by measuring a pressure drop across a suitable length of pipe and applying the Hagen-Poiseuille equation [42]. This requires a measure of the flow rate through the pipe section, and knowledge of the pipe geometry. This has wide application including slurries containing coarse particles. It is a low cost option that requires the installation of two pressure transmitters and a flow measurement if not present on the line. This principle is used to estimate the viscosity in the shear thinning ring at CTP.

2.3 THICKENER CONTROL

In this section we begin by taking a look at the traditional control strategies typically applied throughout industry, and that have been applied in the De Beers group for a number of years. Also included is a discussion of the Vega control philosophy applied on pilot scale at Finsch mine. This is followed by a discussion of a series of rules of thumb that are typically applied on the mines, and the evolution of this into a set of expert rules applied at Venetia mine. Finally some strategies applied in industries outside of De Beers are presented, as these may have application for trial in kimberlite thickening. The focus of this project is to improve the performance of the thickeners installed at De Beers mines and the strategies that follow are considered with this in mind.

It is very important to note that although the physical dimensions of thickeners may be similar, the key to the performance of a thickener lies in the ground type that must be processed. This makes each thickener and the strategies that might be appropriate different. The settling behaviour varies between materials depending on the ground and water chemistry, and the flocculant used. Typically the flocculant in use is a compromise since the ground type will vary across an operation. This means that the thickener behaviour is not a constant and that this must be taken into consideration when applying a control philosophy.

2.3.1 Typical Control Strategies

There are three key variables in the conventional control of a thickener. These are:

- Mud Level
- Underflow Density
- Rake Torque

These are modified by adjusting the flocculant dosage, and the underflow pump rate.

2.3.1.1 Flocculant Dosage Control

The flocculant dosage is typically controlled based on the feed to the plant (headfeed). The spray water delivered to the scrubbers and screens is constant so that the flow to the thickener will not give an adequate indication of the concentration. A feedforward loop is used to adjust flocculant dosage to the thickener feed to be proportional to the headfeed. Flocculant dosage is estimated based on settling tests carried out in the laboratory using samples from the thickener feed. The dosage control is also sometimes based on settling data taken from the feed well, or from the thickener overflow clarity (turbidity). In the AMIRA project report [4] it is suggested that a single turbidity meter in the feed stream is adequate to estimate the degree of flocculation required based on concentration. Fine tuning of the dosage rate in a feedback loop can adjusted through the use of a Clarometer or similar device.

The flocculant dosage rate would be adjusted based on the overflow turbidity when the measurement indicates that more solids are reporting to the overflow. At this point the dosage would be increased, but must be decreased again after a period since there is no measure to indicate that the increased dosage is still required.

2.3.1.2 Mud Level Control

a) Manual Sampling

In some cases the flocculant dosage and underflow density are adjusted based on manual estimates of settling behaviour with a dip-in probe to determine the level of the top of the mud bed.

b) Vega Mud Level Control [1,2]

Dunn made use of the Vega vibrating probes in order to control the mud bed level in a scale thickener, followed by testing in a pilot plant thickener at Finsch Mine.

The initial tests are discussed in 'Ultrasep Mud Bed Interface Level Detection and Control' [1], and were carried out in Johannesburg. The work was motivated by failures of Ultrasep internal structures due to the pressure of the mud bed. This occurred in spite of the underflow density control philosophy, which consists of maintaining a fixed underflow density from the thickener. This is not a reliable approach since the density varies with the material properties (i.e. the bed depth can vary significantly for the same underflow density).

The solution to this problem is to detect and control the mud bed level so that this condition does not arise. After testing a number of instruments (see the section on mud bed level instrumentation) the Vega vibrating probes were selected by Dunn. Two probes are mounted at the end of pipe sections, and suspended in the thickener to give a low and a high level indication. When the probe vibration is sufficiently damped by the presence of mud, the probe switches on. The switching point is adjustable by varying the probe oscillation amplitude. The concept was tested with a basic on-off control philosophy where the pump was switched on when the high limit was reached, and switched off when the low limit was reached (bang-bang control).

One of the laboratory test results from Dunn's laboratory work [1] is shown in figure 2.13. The interface densities shown were achieved by taking samples at the probe points when switching took place.

Figure 2.14 shows the results from the tests carried out on a pilot plant at Finsch mine by Dunn [2]. Although there is significant variation in the underflow density when the pump is off, and this is due to the fact that some settling takes place in the vertical pipe section where the nuclear density gauge is mounted. The density in the measuring section increases as more solids move downward, and the water migrates upward.

The drawback of this approach is that it can be seen that the underflow pump spends a large amount of time in the off state. This is to be expected since the slime level takes longer to climb than it does to sink. During this time there is measurement, but it is not representative of the density at the base of the thickener. The suggested action is to run the pump at a nominal minimum until the high limit is reached or at least until the low level probe is no longer on. There is room to use the probes as limits and to control the thickener according to some other strategy until one of the limits is reached. When the high level is reached the pump would be set to maximum until it switches off again, and when the low level is reached the pump would be set to a minimum that is known to allow the mud bed to rise again until it switches off.

c) Other Methods

This would be based on some other method such as pumping samples from siphon tubes located at various heights in the thickener, and measuring the density, or by means of the moving nuclear source arrangement discussed in the previous section. Regardless of the measurement technique, the action taken is the same. If the mud level is too high, the underflow pump rate is increased, if it is too low the underflow pump rate is decreased – provided no other variable takes precedence at this point (e.g. rake torque or underflow density).

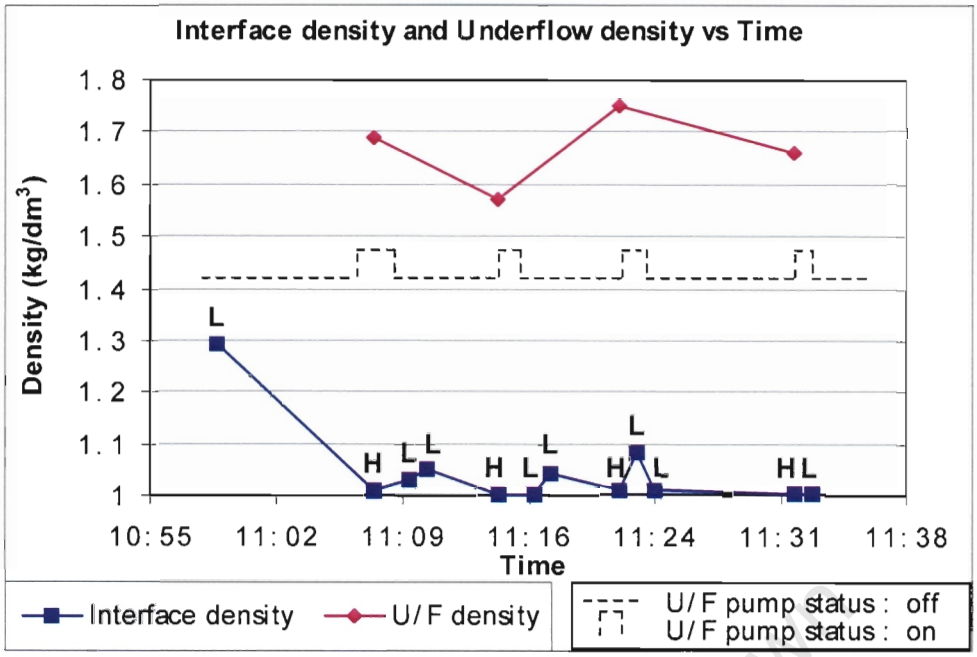

Figure 2.13 Laboratory level control test results [1].

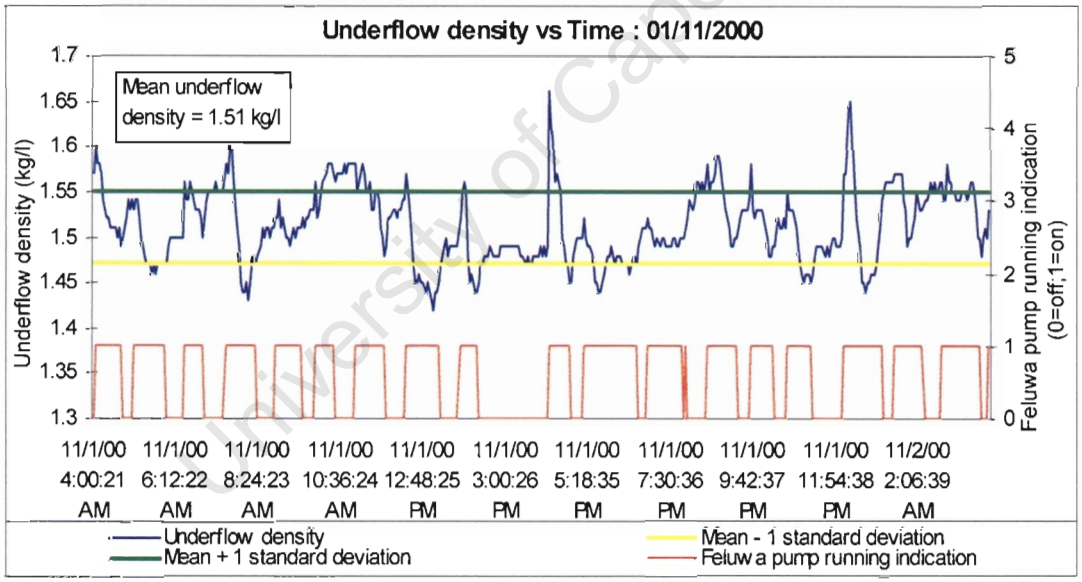

Figure 2.14 Finsch Mine mud level control results [2].

2.3.1.3 Rake Torque Control

Rake torque is based on the current drawn by the rake drive. If the density or viscosity of the slurry in the region of the rake is too high, then the underflow is increased until the torque returns to within safe operating limits. In extreme cases the flocculant dosage is also decreased since this contributes to the viscosity of the slurry.

2.3.1.4 Underflow Density Control

The density of the underflow is measured with a nuclear density gauge as the slurry exits the thickener. When the underflow density exceeds the setpoint value, the underflow pump speed is increased to remove the most dense material at the base of the thickener, and to reduce the mud bed level. Reducing the mud bed level decreases the compression of the bed due to gravity. When the density is below setpoint the pump speed is reduced so that the mud level increases, increasing the compression on the bed, and hence the underflow density.

Underflow density can be misleading since it is not always linked with the underflow rheology due to the influence of the particle size distribution of the material. A large grits component increases the underflow density (due to compression); a lower grits fraction means that a greater mud bed level is required to achieve the same underflow density. As a result the rheological characteristics of the slurry may vary considerably, and have a significant impact on downstream processes such as pumping and transport. Thus underflow density control is effective when rheology is not at a critical value.

2.3.1.5 Underflow Rheology Control

One form of underflow rheology control (as applied at CTP), takes advantage of the fact that kimberlite slurries are shear thinning. A shear thinning ring is fitted at the base of the thickener, where dense slurry is pumped through the loop (with a centrifugal pump) until the estimated viscosity reaches the setpoint. The viscosity is inferred through measuring the pressure difference across a length of the shear thinning ring – as the shear rate is increased, the apparent viscosity decreases. The underflow discharge pump is turned off if the viscosity is too high (high viscosity means that the positive displacement pump will not be able to pump the material without pipe blockages arising).

2.3.2 Thickener Operating Instructions

The thickener operating instructions shown in figure 2.15 were obtained from Venetia Mine where they are used by the operators for manual conventional thickener control. The chart in figure 2.15 summarises the basic strategy for thickener control based on slime level (mud bed level), rake torque, and underflow density. In order to modify these variables, the underflow pump rate and flocculant dosage are increased or decreased as shown, based on operator experience. The slime level is typically measured manually with a dip-in probe. Torque is measured based on the current drawn by the rake drive motor, and the underflow density is measured immediately below the thickener discharge by a nuclear density gauge mounted prior to the underflow pump.

The control action with the most impact is the underflow pump rate. The dominant affected variable in underflow pump rate is the underflow density. When there is no change in the underflow density, the mud bed level becomes dominant. Although there is no direct link with the rake torque here, the rake torque will typically increase because of the increase in underflow density due to the increased drag. If the rake torque becomes too high the underflow pump will be run at maximum until the condition clears.

There are only 5 instances where the flocculant dosage is modified, and 12 instances where the underflow pump rate is modified, so clearly the most effect is achieved by varying the underflow pump rate. The system responds faster to changes in underflow pump rate than it does to changes in flocculant dosage. Settled slurry must make its way from the top of the mud bed to the thickener outlet before the effects of a flocculant dosage change will be noticed, whilst the density is easily reduced by increasing the underflow pump rate.

The 'THEN NEXT' instructions in the chart are superfluous, as the thickener will naturally migrate to one of the conditions that result in the 'THEN NEXT' action. Note that this chart covers only 13 of the 27 possible combinations of the variables, although some combinations are highly unlikely. These rules lend themselves to implementation in a rule based expert system as discussed in the following section.

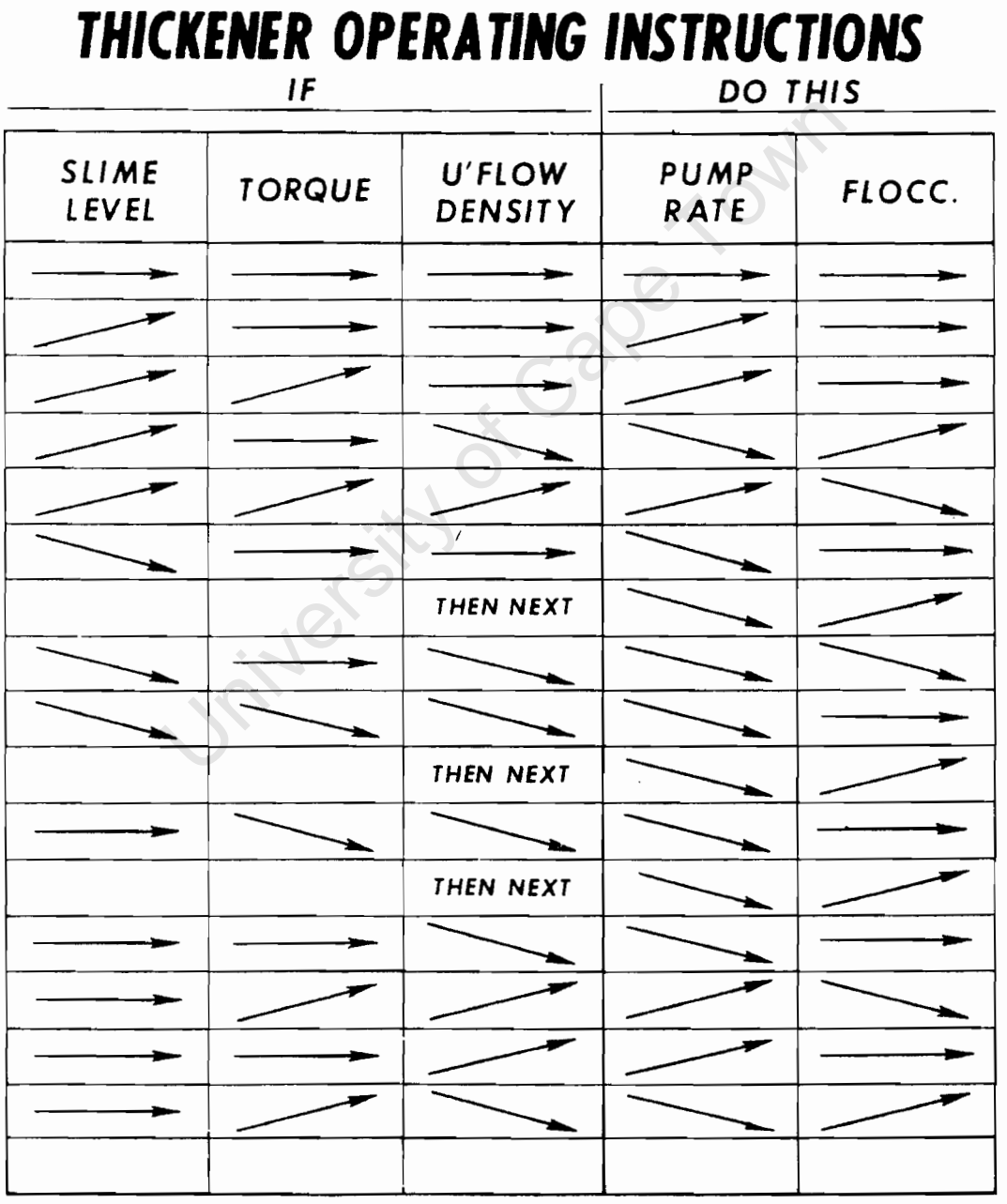

Figure 2.15 Thickener operating instructions from Venetia Mine.

2.3.3 Venetia Thickener Expert Rules

The control approach presented in this section is taken from the Expert System Controller Rulebase for Venetia [43].

The expert system operates by passing normalised input variables to rule blocks that will determine the necessary change to the setpoints of the underflow pump and flocculant dose. The calculations are performed once every minute (calculation interval), and setpoint changes are made at 5 minute or longer intervals (control interval). The output scaling includes rate limiting although this is made large, with the rate limiting being applied at the outputs to the pumps.

The input variables to the system are underflow density, slime level (mud bed level), and rake torque. Each input variable is filtered and then normalised and combined with its normalised gradient to provide a single variable that includes rate of change information. Both the normalised variable and the normalised gradient are rated on a scale from Very Low (-3), Low (-2), Somewhat Low (-1), OK (0), Somewhat High (1), High (2), up to Very High (3). The normalised variables are scaled between +1.5 and -1.5 before being passed to the rule blocks or interrupt actions, where the region outside of +1 and -1 is reserved for emergency or exception conditions. Exception conditions trigger interrupt rules to take actions to prevent damage to equipment, otherwise the signals are passed on to the rule blocks.

Table 2.4 shows the rule blocks for the underflow pump, and table 2.5 shows the rule blocks for flocculant dosage. The rule block inputs are given as LO (-1), OK (0), and HI (1), and the resulting change in setpoint as a percentage.

The change in underflow pump flow rate is given as a percentage of the maximum permissible change per control interval. ±100 % corresponds to a ±10 $m^3.h^{-1}$ change in underflow flow rate. The maximum pump speed is limited to 500 $m^3.h^{-1}$, and the output is clipped if the setpoint exceeds this value.

The change in flocculant flow rate is given as a percentage of the maximum permissible change per interval. ±100 % corresponds to a ±1.875 units change in flocculant dose. The maximum flocculant dosage is clipped to 25 units. The flocculant dosage is based on the plant headfeed, and is typically specified in grams of flocculant per ton of dry solids. The units are not specified in the document, but it is assumed that 25 units is equivalent to the flocculant dosing pump running at 100 %.

The underflow and flocculant rule blocks are shown for comparison with the previous 'Thickener Operating Instructions'. The highlighted blocks are common with those from the instructions, and those marked with an asterisk indicate that the nature of the control action is identical.

Table 2.4 Underflow Pump Rule Block

Slime Level	Rake Torque	Underflow Density	Underflow Change (%)	
HI(↑)	HI(↑)	**HI(↑)**	**100(↑)**	*
		OK(→)	**100(↑)**	*
		LO(↓)	100(↑)	
	OK(→)	HI(↑)	50(↑)	
		OK(→)	**33(↑)**	*
		LO(↓)	**33(↑)**	
	LO(↓)	HI(↑)	33(↑)	
		OK(→)	-33(↓)	
		LO(↓)	-33(↓)	
OK(→)	HI(↑)	**HI(↑)**	**100(↑)**	*
		OK(→)	33(↑)	
		LO(↓)	**33(↑)**	
	OK(→)	**HI(↑)**	**50(↑)**	*
		OK(→)	**0(→)**	*
		LO(↓)	**0(→)**	*
	LO(↓)	HI(↑)	33*(↑)	
		OK(→)	-66(↓)	
		LO(↓)	**-66(↓)**	*
LO(↓)	HI(↑)	HI(↑)	66(↑)	
		OK(→)	0(→)	
		LO(↓)	0(→)	
	OK(→)	HI(↑)	50(↑)	
		OK(→)	**-50(↓)**	*
		LO(↓)	**-50(↓)**	*
	LO(↓)	HI(↑)	33(↑)	
		OK(→)	-100(↓)	
		LO(↓)	**-100(↓)**	*

Table 2.5 Flocculant Feed Rule Block

Slime Level	Underflow Density	Floc Feed Rate Change (%)
HI	HI	33
	OK	50
	LO	100
OK	HI	-66
	OK	0
	LO	33
LO	HI	-100
	OK	-75
	LO	-50

If the rake torque becomes very high, then the underflow pump speed is increased to maximum until the torque returns to normal. If the torque continues to increase the flocculant addition is reduced to a minimum until torque returns to normal, at which point the previous operating point is restored. This is the only interrupt action in the system.

The operator is able to make manual adjustments to the flocculant dosage and underflow pump and then return the system to automatic control. The slime level is measured manually with a dip in probe.

This strategy has not achieved great success, with the operators generally operating the thickeners manually. This is most likely due to the absence of a useful slimes level measurement and, the required manual input of the settling behaviour of the thickener which is judged visually.

2.3.4 Other Thickener Control Examples

2.3.4.1 Interactive Thickener Automation [44]

This strategy was implemented at the Exxon Minerals Company's Highland Uranium Operations. As with most thickener control strategies, the flocculant dosage and the underflow pump rate are controlled independently.

The underflow rate is based on slimes level, rake torque, and underflow density. The slimes level is measured with a floatable ball exactly weighted with solution to float on the top of the slimes bed. The ball travels on a rod to give an indication of the level. This control strategy is different in that the rake torque takes precedence over the slime level and underflow density. If the rake torque is high then the underflow pump rate is increased until it is within limits again. If the rake torque is within limits then the slime level is brought within limits, and finally the underflow density is adjusted within a range of 55 – 58 % solids. It is unlikely that the rake torque will be high when the other two variables are in range. Each variable is linked to a PID controller that adjusts the underflow pump depending on the dominant variable. If all variables are in range then no change is made to the underflow pump speed.

Flocculation rate was previously based on Exxon's "Settle-O-Meter", that measures pulp settling rate in the centre well of the thickener, but later based purely on the slime level. Flocculant is pre-mixed with a portion of the overflow before being delivered to the centre well where it mixes with the thickener feed. The flocculant controller attempts to keep the slime level in the range 4.25 to 4.65 (no units provided), while the underflow pump attempts to keep it in the range of 3.5 to 4.8.

The key variable for this control strategy to work is the slime level measurement. For kimberlite slimes the float arrangement would quickly become jammed with slurry. This highlights again that thickener measurements are highly dependent on material properties and settling behaviour.

2.3.4.2 Dominion Mining [4]

The aim of this strategy is to keep the mass of solids in the thickener constant. A pressure transducer was installed in the base of the thickener to measure solids inventory or hold-up. While the slime level is constant, variations in the pressure measurement are proportional to variations in the average density of the sediment column. The pressure is proportional to the mass of solids in the thickener, and underflow pump rate is directly controlled by changes in the solids hold-up. To maintain constant solids hold-up, slurry flow in × concentration in = slurry flow out × concentration out (averaged over time). The bed level signal was measured using a weighted float as in the interactive thickener automation approach discussed in the previous section, and used to control flocculant dosage.

2.3.4.3 Autofloc [45]

The Autofloc controller is produced by the Nalco Chemical Company. The controller is available in three variations.

- One type monitors thickener bed level, and adjusts flocculant dosage accordingly.
- Another monitors water clarity in ponds and thickeners (overflow clarity).
- A third measures floc size in the thickener centre well, and adjusts flocculant dosage.

These measures are used in a feedback loop to make adjustments to the flocculant dosage rate that is typically a ratio of the ore feed to the plant, or some other measure that allows the amount of solids reporting to the thickeners to be estimated.

A similar Anichem unit was tested at the Oaks mine, but without success [46]. A major problem was fouling of the glass cylinder used to measure the flocculation effectiveness. In addition to this it was found that the disturbances in the feed i.e. in flow rate and concentration led the control output (flocculant dosage) to oscillate. It is expected that this may have been as a result of insufficient controller damping.

2.3.4.4 Alcoa [4]

This is a bauxite process as operated by the Alcoa corporation. Solids concentration in the feed to the thickeners is fairly constant, and flocculant flow is proportional to feed slurry flow in a feed forward loop. The ratio is manually adjusted periodically to maintain an overflow clarity target (which could possibly be measured with a turbidity meter if the slurry lends itself to this measurement). The underflow pump is controlled based on underflow density, and mud level is kept low and not monitored. Rake torque is monitored, but only used to determine maintenance intervals to remove scale.

2.4 DISCUSSION

This chapter summarises the current state of thickener technology in industry, with a particular focus on the equipment installed on De Beers group mines. While the equipment is identical across many industries, the behaviour of the thickener is determined by the material to be processed. Thickener performance is determined by:

- The volume of slurry to be processed.
- The concentration of the feed.
- The particle size distribution of the feed.
- The settling behaviour of the material.

The focus of this work is on high compression thickeners, and in particular the Bateman Ultrasep, and the Eimco Deep Cone Paste thickener. The aim of the scale thickener test laboratory is to provide a platform for testing of measurement and control strategies without the pressures of a production environment. The laboratory provides a settling vessel that provides the conditions to create a mud bed similar to that found in full scale thickeners. The intention was not to create a vessel with the same geometry as found in full scale, and rather to create a simulation of a portion of one of these thickeners where the concentration, rise rates, and settling conditions are similar.

The list of instruments discussed is by no means exhaustive, and there are many manufacturers of the instruments using the same techniques discussed. For laboratory trials the following instruments were selected as a starting point:

- Vega probe for mud level detection.
- The Markland 502-TP for hindered settling zone detection.
- Coriolis mass-flow meters for density measurement (nuclear meters are too large for laboratory scale).
- Positive displacement pumps so that separate flow measurement is not required.
- Full-bore pipe viscometer for underflow rheology measurement.

It is expected that something like the expert system control approach will be followed. With this approach, setpoints are adjusted to modify the state of the plant. The limitations of the installed measurements will be evaluated during the implementation of the control strategies. Some of these have already been discussed in the discussion regarding the initial control testing in the laboratory.

With this information in mind, the design of a laboratory test facility can now be discussed.

2.5 REFERENCES

1. F. Dunn, "Ultrasep Mud Bed Interface Level Detection and Control", De Beers Consolidated Mines Ltd, Debtech, Report Number R1999-09-01, August 1999.
2. F. Dunn, A. J. Vietti, and S. Ramulai, "The Concept of Co-Disposal of Processed Kimberlite Products on a Pilot Plant Scale – Part 1", De Beers Consolidated Mines Ltd, Debtech, Report Number R2001/06/03, July 2001.
3. A. J. Vietti and F. Dunn (Editors), "Paste and Thickened Tailings Disposal Handbook", De Beers Consolidated Mines Ltd, Technical Support Services, Technology, 2003.
4. AMIRA, "P266D, Improving Thickener Technology, Thickener Expert v2.0, Knowledge Base and Process Model", CSIRO, 2002.
5. R. C. Carlaw, "Instrumentation, Evaluation, and Control of a Conventional Thickener at Finsch Mine", De Beers Diamond Research Laboratory, Mineral Processing Division, Report Number E81/010/001, August 1992.
6. Outokumpu Supaflo Brochure 3008EN. Libris, Helsinki, Finland, May 2004. Available: http://www.outokumputechnology.com/.
7. Dorr-Oliver Eimco. E-Duc Feed Dilution System. Product Brochure, EMC 3365, 2003. Available: http://www.glv.com/.
8. Dorr-Oliver Eimco. E-Cat Clarifier-Thickeners. Product Brochure, EMC 3273, 2003. Available: http://www.glv.com/.
9. H. S. Coe and G. H. Clevenger, "Methods for Determining the Capacity of Slimesettling Tanks", Transactions of the AIME No. 55 (1916), pp356-385.
10. Dorr-Oliver Eimco. Eimco Deep Cone Paste Thickener. Product Brochure, EMC 3280, 2003. Available: http://www.glv.com/.
11. Bateman Process Equipment. Bateman Ultrasep 2000, Bateman Globe, Issue #20, January 2001, Available: http://www.bateman.co.za/.
12. G. L. Cragg, R. Gush, and A. J. Vietti, "Ultrasep Instrumentation, A Discussion Document", Preliminary Draft, Unpublished, 1999.
13. A. Roebl, "Test Results for the Solartron Mobrey 7826 Insertion Liquid Density Transducer with Finsch Dust Sample", De Beers Consolidated Mines Ltd, Technical Support Services, Technical Note No. 2004-01-17, January 2004.
14. A. Roebl, "Test Results of the Markland 502-TP Suspended Solids Meter with Finsch Dust Sample", De Beers Consolidated Mines Ltd, Technical Support Services, Technical Note No. 2004-01-16, January 2004.
15. Endress & Hauser, "Electromagnetic Flow Measuring System Promag 35", Technical Information TI 035D/06/en, No. 50075884, Issue 09/98. Available: http://www.endress.com/.
16. N. P. Brown and N.I. Heywood, "The Right Instruments for Slurries", Chemical Engineering, September 1992, pp106-114.
17. V. T. Chen, "Open Channel Hydraulics", McGraw-Hill, 1959.
18. KAB Instruments. Sumpi Instruction Manual. Version SM2704, 2005. Available: http://www.kabinstruments.com/KAB RANGE/Manuals/KAB SUMPI MANUAL 2005.pdf
19. Endress & Hauser, "Coriolis Mass Flow Measuring System PROline Promass 80/83 H,I", Technical Information TI 052DEN/06/en, No. 50098278, Issue 12/05. Available: http://www.endress.com/.
20. Solartron Mobrey. Type 7835 Densitometer. Technical Specification Sheet B1016, September 2005. Available: http://www.mobrey.com/downloads/datasheets/b1016.pdf.

21. Hach. Solitax SC. User Manual. Catalogue No. DOC023.54.03232 (Edition 3), October 2005. Available: http://www.hach.com/.
22. Endress & Hauser, "CUM 740 Transmitter for Turbidity and Solids Content", Technical Information TI 2320/07/en, No. 51504297, Issue 05/01. Available: http://www.endress.com/.
23. Solartron Mobrey, "MSM400 Ultrasonic Suspended Solids Density Monitoring and Control". Specification Sheet IP257, September 2005. Available: http://www.mobrey.com/downloads/datasheets/ip257.pdf.
24. Hawk Measurement Systems. SSA Series Sonar Point Density Transmitter. Data Sheet HMS SS Series 8/01. Available: http://www.hawklevel.com/DataSheets/SSA_Series_Data_Sheet.pdf
25. Mettler Toledo/Lasentech. S400A FBRM Particle Size Analyzer. Technical Data 005-6017 Rev. B, ECN 2677, 03/2006. Available: http://www.lasentech.com/.
26. Honeywell. X100 Particle Size Analyzer. Operation and Maintenance Manual, 70-82-25-02 Rev. 0, 9/96.
27. Mettler Toledo/Lasentech. M600P FBRM Particle Size Analyzer. Technical Data 005-6030 Rev. A, ECN 2345, 03/2006. Available: http://www.lasentech.com/.
28. CSIRO Minerals, UltraPS – Ultrasonic Particle Size Analyser Brochure, CSIRO Minerals, On-line Analysis and Control, Available: http://www.minerals.csiro.au/, Products
29. P. J. Coghill, M. J. Millen, and B. D. Sowerby, "On-line Measurement of Particle Size in Mineral Slurries", Minerals Engineering, Vol. 15, No. 1, January 2002, pp83-90
30. Oscillation Pty Ltd. Clarometer Description, October 2000. http://www.clarometer.com.
31. CSIRO Minerals UltraPS – Ultrasonic Particle Size Analyser Brochure, Markland Specialty Engineering Pty Ltd. Series 502 Suspended Solids Meter. Brochure. Available: http://www.sludgecontrols.com/502_brochure.html.
32. Markland Specialty Engineering Pty Ltd. Series 602 Suspended Solids Meter. Brochure. Available: http://www.sludgecontrols.com/602_brochure.html
33. Vega Controls, "Level Measurement in Liquids, Guided Microwave, Vegaflex 61,63,65,66",. Product Information 29657-EN-060407. Available: http://www.vega.com/downloads/PI/EN/2967-EN.pdf.
34. Endress & Hauser, "CUM 750 Ultrasonic Measuring System for Sludge Level and Interface Detection", Technical Information TI 225C/24/ae, 2002.
35. Royce Technologies, "Interface Level and Point Level Analyzers and Sensors", Bulletin No. Level-2R, December 2005. Available: http://www.roycetechnologies.com/ProductListing/Interface/InterfaceLevel.pdf.
36. S. Herholdt, "Image Reconstruction on Electrical Resistance Tomography Measurements in a Settling Process", University of Cape Town, Department of Electrical Engineering, MSc. Thesis, October 2004.
37. Vega Controls. Vegavib 52. Operating Instructions. Order No: 1099828_1, 17496-EN-030305.
38. N. J. Alderman and N. I. Heywood, "Selection of On-line Viscometers for Slurry Applications", Presented at the 14th International Conference on slurry Handling and Pipeline Transport: Hydrotransport 14, Maastricht, The Netherlands, 1999. pp373-399.
39. Solartron Mobrey. 7827 Digital Viscosity Analyser. Technical Specification Sheet IP 7827, September 2005. Available: http://www.mobrey.com/downloads/datasheets/ip7827.pdf.

40. Solartron Mobrey. 7829 Visconic Industrial Viscosity Transmitter. Literature Reference Number IP 700, September 2005. Available: http://www.mobrey.com/downloads/datasheets/ip7001.pdf.
41. Hydramotion. XL7 Process Viscometer. Available: http://www.hydramotion.com/xl7_data.html.
42. B. G. Liptak (editor), Instrument Engineers' Handbook, 3rd ed, Process Measurement and Analysis, Butterworth-Heineman, 1995, pp1247-1251
43. G. Metzner, "Expert System Controller Rulebase for Venetia", De Beers Consolidated Mines Ltd, MPD Engineering Documentation, Document Number P05-100000-805, Rev 1.0, March 1998.
44. J. A. Otto, "Interactive Thickener Automation", Hydrometallurgy Research, Development, and Plant Practice, Osseo-Assare, K. and Miller JK (Eds), AIME, 1983. pp419-428.
45. Nalco. Autofloc. Available: http://www.nalco.com/ASP/industries_served/mining_minerals/mining_minerals_innov.asp
46. G. Langefeld, Private Communication, April 2006.

CHAPTER 3 LABORATORY TEST THICKENER DESIGN

This chapter discusses the design of the laboratory thickener test facility on a laboratory scale for the testing of instruments and control strategies. The initial intention was to operate the plant with a Finsch mine kimberlite sample without the use of flocculant. The pre-commissioning slurry characterisation tests discussed in chapter 4 showed that the use of flocculant is essential to achieve similar settling conditions. The slurry characterisation was carried out after the completion of the design due to time and budget constraints, but there is sufficient flexibility in the design range, that a range of suitable operating points can be selected. The plant runs in a closed circuit so that the slurry can be re-used, extending the available testing time to approximately 1 week. This is due to the limited quantities of Finsch dust that can be obtained and which must be transported from the Northern Cape (165 km NW of Kimberley, 670 km from Johannesburg). The thickener dimensions were determined by the available space in the laboratory, and the size of the slurry tank that can be accommodated. Further, the diameter of the thickener was based on the dimensions of the Vega probes to be evaluated, providing sufficient room so that the walls do not affect the measurement. A dilution circuit was included to maintain the concentration of the feed slurry, and to remove the overflow water that contains expired flocculant that is no longer active.

The design process begins by determining the thickener capacity, and then choosing the desired pumping capacity based on the basic thickener dimensions. The remainder of the design follows on from this point.

The equipment installed in the laboratory is presented at the end of the chapter.

3.1 THICKENER TEST PLANT DESIGN

It was decided to manufacture the scale thickener from clear Perspex to aid in visualization of the settling process. A portion of a high compression thickener is modeled by taking a section out of the full scale thickener as shown in Figure 3.1. In a full scale high compression thickener the density at the underflow is typically between 1.4 and 1.6 $kg.l^{-1}$ [1]. The laboratory test thickener's similarity with full scale thickeners is achieved by designing for similar fluid rise rates in the clear water zone of the thickener. The main thickener dimensions are based on the height of the ceiling in the laboratory, and the side clearance that the Vega vibration probes require. The design of the entire system is integral with the thickener dimensions, and this will become clear in the discussion in the following sections.

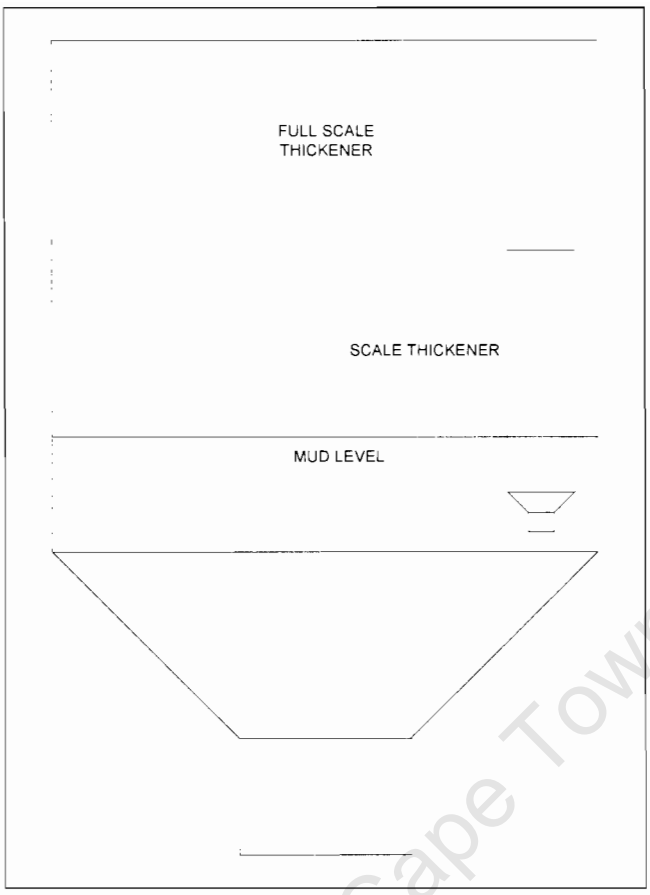

Figure 3.1 Laboratory thickener as a portion of a full scale thickener.

3.1.1 Basic Thickener Dimensions

The ceiling of the laboratory is 2.9 m high, and the roller-door entrance to the laboratory is 2.7 m high. In order to facilitate easy access to the laboratory the test thickener had to be less than 2.7 m high. A clearance of 0.4 m below the thickener was selected to allow easy access for piping connections, and to allow space for the future installation of rakes should this be required. Rakes were not included in the initial design since a steep conical section at the base was expected to eliminate the need. A clearance of at least 0.5 m was catered for above the thickener so that instruments, hoses, and a rake drive could be installed as required. This left 1.8 m for the thickener.

The Vega probes are 332 mm long, with an active probe length of 160 mm as shown in figure 3.2. The probe head containing the electronics is mounted external to the thickener, and connected via cable. It was decided to allow a vertical spacing of 0.5 m between the probes to allow a sufficiently deep mud-bed to get realistic results. To adjust the mud-bed depth, the probe heights within the thickener are manually adjusted by raising or lowering them.

It has been found that a suitable clearance between the Vega vibration switches and the thickener sidewall is 150 mm [2]. It was found that the measurement was free from interference effects due to the sidewalls at this distance. A thickener diameter of 350 mm was selected by doubling this distance and adding 50 mm to account for the body of the probe. The head of the probe has a diameter of 43 mm, but this portion is static. The active portion

of the probe has a diameter of 18 mm (fig. 3.2). It is important to attempt to keep the diameter of the thickener as low as possible since the slurry volume requirement increases with the square of the diameter.

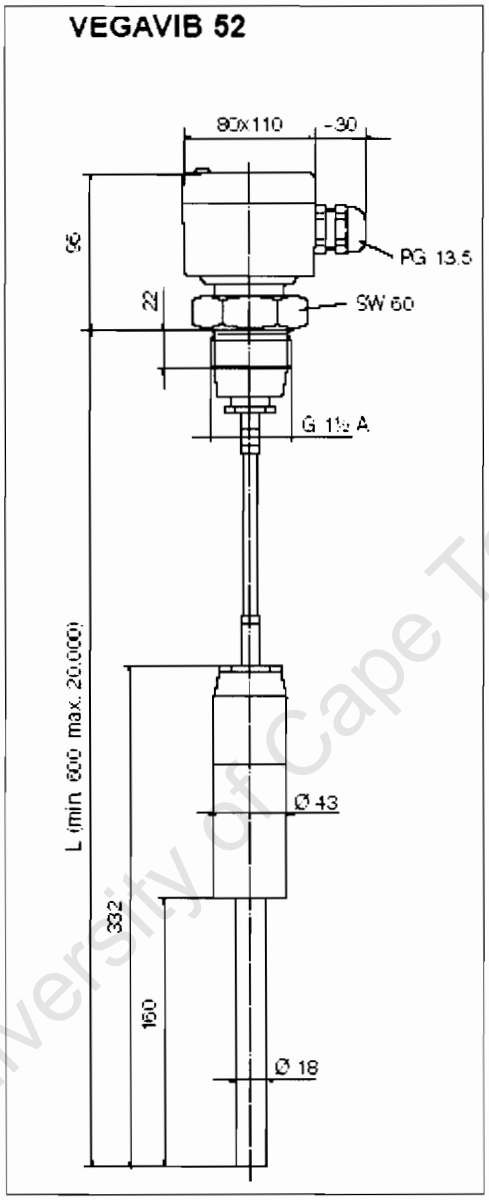

Figure 3.2 Vega probe dimensions [3].

3.1.2 Rise Rate and Mass Balance

Having selected the thickener diameter and hence area means that the rise-rate and the flow rates into and out of the thickener can be determined. Table 3.1 gives the fluid rise rates in the De Beers thickeners discussed in the review chapter. The aim of the test thickener is to be able to create similar rise rates to those in the Orapa and CTP high compression thickeners. The Oaks mine is not considered because it is known to be lightly loaded. It follows that the similarity with full scale thickeners is thus catered for not in a physical dimensional sense, but to achieve similar conditions under which flocculation and deposition take place.

Table 3.1 Fluid Rise Rates for Various De Beers Thickeners

Mine	Dia. (m)	Feed ($m^3.h^{-1}$)	RR ($m.h^{-1}$)	Class
Orapa No. 2 Plant (Botswana)	10.0	600	7.64	HC
CTP (Kimberley, RSA)	15.0	1000	5.66	
Oaks Mine (RSA)	6.0	100	3.54	
Venetia (Musina, RSA)	60.0	1165	0.41	HR
Finsch (Lime Acres, RSA)	45.7	750	0.46	C
	52.5	1300	0.60	
Koffiefontein (RSA)	45.7	1050	0.64	

The rise rate is calculated by taking the volumetric flow rate into the thickener (Q), and dividing this by the thickener cross-sectional area to give the rate or velocity at which fluid will rise inside the thickener in metres per hour ($m.h^{-1}$) [2]. The rise rate is given by

$$RR = \frac{4Q_{fsl}}{\pi D^2} \tag{1}$$

where D is the thickener diameter, and Q_{fsl} is the feed slurry flow rate to the thickener.

The subscripts shown in Table 3.2 are used throughout this document.

Table 3.2 Subscripts and their meaning

Subscript	Meaning
s	solid
l	liquid
sl	slurry
f	feed
o	overflow
u	underflow
d	dilution

The settling rate is typically assumed to be twice the rise-rate for a particular sample of slurry [2]. Batch settling tests are carried out prior to the design in order to determine the settling rate of the slurry. This makes sense since the slurry must settle at a higher speed than the upward velocity of the water in the vessel otherwise it will be carried over into the clear water overflow. The settling rate is then simply

$$SR = 2RR = \frac{8Q_{fsl}}{\pi D^2} \tag{2}$$

Consider a range of flow rates and rise rates as shown in Table 3.3:

Table 3.3 Rise Rate and Slurry Flow Rates

RR	**1**	**2**	**3**	**4**	**5**	**6**	**7**	**8**	$m.h^{-1}$
SR	2	4	6	8	10	12	14	16	$m.h^{-1}$
Q_{fsl}	0.096	0.192	0.289	0.385	0.481	0.577	0.673	0.770	$m^3.h^{-1}$
Q_{fsl}	1.6	3.	4.8	6.4	8.0	9.6	11.2	12.8	$l.min^{-1}$
			The Oaks		Orapa & CTP				

Given these flow rates a mass balance for these values can now be calculated. The mass balance will provide the required flow rates of the overflow and underflow for each slurry feed flow rate.

The slurry is made up to have a composition of 10 % solids by mass (a typical slurry feed density) using Finsch primary dust. The slurry density is calculated from the equation

$$\rho_{sl} = \frac{\rho_s \rho_l}{\rho_s - C_M(\rho_s - \rho_l)} \tag{3}$$

where

ρ_s = typical kimberlite solids bulk density = 2.650 $kg.l^{-1}$
ρ_l = liquid density = 1.000 $kg.l^{-1}$
C_M = solids concentration by mass = 10 % or 0.1

This equation is derived from the equation for the solids concentration (the ratio of solids mass to total mass), and the density formula for the bulk sample. A table of slurry density and concentration relationships are given in Appendix A.

The carrier liquid is water and the solids are kimberlite dust. The overflow concentration is assumed to be 0 %, and the underflow 40 % solids by mass, and the densities of the various components at these concentrations are shown in table 3.4.

The mass balance is calculated by evaluating the portions of the slurry that report to the overflow and the underflow at a particular slurry flow-rate. Litres per minute ($l.min^{-1}$) are used to represent the flow rates on small laboratory scale. On large scale thickeners $m^3.h^{-1}$ is used.

Table 3.4 Component % Solids and Density

Component	% Solids	Density (kg.l^{-1})
Overflow	$C_{Mo} = 0$	$\rho_{ol} = 1.000$
Feed	$C_{Mf} = 10$	$\rho_{fsl} = 1.066$
Underflow	$C_{Mu} = 40$	$\rho_{usl} = 1.332$

A useful method of evaluating the macroscopic mass balance in a thickener was presented in 1912 by Mishler [4]. Using Mishler's approach, a solid and water mass balance yield:

Solid: $\dot{m}_{fs} = \dot{m}_{us}$ (4)

Water: $\dot{m}_{fs} D_f = \dot{m}_{us} D_u + \dot{m}_{ol}$ (5)

The solids content in the feed is all assumed to report to the underflow. The quantity D is the dilution, a measure of concentration. Dilution is the ratio of the mass of water to the mass of solids, and is given by

$$D = \frac{1 - C_M}{C_M} \tag{6}$$

The relevant fractional value for C_M is substituted depending on whether the feed or underflow dilution is required. The volume flow-rate of water at the overflow is

$$Q_{ol} = \frac{\dot{m}_{ol}}{\rho_l} = \frac{\dot{m}_{fs}(D_f - D_u)}{\rho_l} \tag{7}$$

Notice that the overflow volume flow rate, and all other quantities can be written in terms of the feed solids flow rate. The slurry underflow volume flow rate is given by

$$Q_{usl} = Q_{fsl} - Q_{ol} \tag{8}$$

This method provides a neat compact means of computing the required flow rates. The mass balance for a range of flow rates is shown in Table 3.5. On the scale of the laboratory thickener it makes more sense to work in l.min^{-1} for the small flow rates under discussion, and this convention is followed throughout this document.

This gives a slurry feed range of 8 – 13 l.min^{-1} for Orapa and CTP, extending the range to 4.8 – 13 l.min^{-1} if The Oaks mine is included. A design range of 0 – 20 l.min^{-1} was selected to provide some additional capacity for clearing the tank when required. Using these figures the pump capacities for the slurry feed, and underflow could be selected. After this the size of the weir required at the overflow was addressed. First let us look at the required pumping capacity for the slurry feed.

Table 3.5 Thickener Mass Balance

RR	**1**	**2**	**3**	**4**	**5**	**6**	**7**	**8**	$m.h^{-1}$
SR	2	4	6	8	10	12	14	16	$m.h^{-1}$
Q_{fsl}	0.096	0.192	0.289	0.385	0.481	0.577	0.673	0.770	$m^3.h^{-1}$
Q_{fsl}	1.604	3.207	4.811	6.414	8.018	9.621	11.225	12.828	$l.min^{-1}$
Q_{ol}	0.077	0.154	0.231	0.308	0.385	0.462	0.539	0.616	$m^3.h^{-1}$
Q_{ol}	1.282	2.565	3.847	5.130	6.412	7.695	8.977	10.260	$l.min^{-1}$
Q_{usl}	0.019	0.039	0.058	0.077	0.096	0.116	0.135	0.154	$m^3.h^{-1}$
Q_{usl}	0.321	0.642	0.963	1.284	1.605	1.926	2.247	2.568	$l.min^{-1}$
			The Oaks		Orapa & CTP				

3.1.3 Slurry Feed Pumping Capacity

A Howden C32M Mono pump was located at the old thickener test plant in Johannesburg and evaluated for suitability. This is a positive displacement pump (progressive cavity) with a linear characteristic. The speed can be controlled well enough using a variable speed drive (VSD) that it is not necessary to measure the flow rate at the output of the pump. Siemens VSDs (standard equipment at De Beers operations) can operate from 10 Hz up to 650 Hz. This is providing that the installed motor can deliver sufficient torque at the low end to drive the load. It was expected that operating from 10 Hz to 100 Hz would be more than adequate to get the required flow range from the pump. All of the pump curves discussed in this chapter are shown in Appendix B. Since the head was only a maximum of 2 metres, and the pump curve is very flat at this point, the head was assumed to be 0 metres. This allows the flow rate to be read off directly on the y-axis on the pump curve.

Table 3.6 shows the pump flow rates versus shaft speed. From the table it is evident that the pump needs to be run between 100 and 700 rpm to achieve the desired flow range.

Table 3.6 C32M Pump Flow Rates for Pump Shaft rpm (n_p)

n_p	Q (0 m head)	
rpm	$m^3.h^{-1}$	$l.min^{-1}$
0	0.000	0.00
100	0.185	3.09
200	0.370	6.17
300	0.535	8.92
400	0.700	11.67
500	0.885	14.75
600	1.070	17.83
700	1.260	21.00
800	1.450	24.17

To deliver the required shaft rpm to the pump a geared motor was chosen that runs at 1450 rpm at 50 Hz. In table 3.7 the motor output speed at the shaft (n_m), and the output speed after a 2.91:1 reduction gearbox (n_{gb}) are shown together with the slurry flow rate. This provides the required pump shaft speeds shown in table 3.6, giving approximately 15 $l.min^{-1}$ at 50 Hz. To allow for further flexibility the gearbox output and pump input are coupled via dual vee

belts and pulleys. This allows the minimum speed to be adjusted without further reducing the VSD frequency. Within the available space the pulley arrangement allows the pump shaft drive speed to be reduced up to a factor of 2 if required, although the current arrangement features a 1:1 pulley drive.

From the pump curve it can be seen that the power required at 0 m head is 0.5 kW. The worst case scenario for the pump at 100 m head requires 1 kW to drive the pump. A 1.1 kW motor does the job with spare capacity in the laboratory and provides more than enough torque to run continuously at low speed. The pump efficiency is low, but acceptable. The minimum required starting torque for the pump is 12 Nm. A 1.1 kW motor with a 2.91:1 ratio gives 22 Nm torque at the gearbox output shaft. This is more than adequate for the low density feed that does not have a viscosity much greater than that of water.

Table 3.7 Motor Output Speed at Shaft (n_m), and Gearbox (n_{gb}), and Slurry flow rate(Q_{fsl})

f	**%**	n_m	n_{gb}	Q_{fsl}
Hz		rpm	rpm	$l.min^{-1}$
10	20	290	100	3.09
20	40	580	199	6.17
30	60	870	299	8.92
40	80	1160	399	11.67
50	100	1450	498	14.75
60	120	1740	598	17.83
70	140	2030	698	21.00
80	160	2320	797	24.17
90	180	2610	897	
100	200	2900	997	

An SEW Eurodrive 1.1 kW motor/gearbox combination (2.91:1 reduction) is used together with a 1.1 kW Siemens MM440 VSD to drive the pump. The VSD provides a constant torque mode that is used at low speeds in order to ensure that the pump speed remains consistent. A 3 phase 230 V VSD is wired in delta to the 380 V SEW motor.

3.1.4 Underflow Pumping Capacity

The underflow slurry is pumped using a C22M Mono pump (Appendix B), also found at the old thickener test site. For this pump a variation in the pump head has very little effect on the flow rate. The desired pumping range is 0.9 to 2.6 $l.min^{-1}$ under ideal thickener operating conditions. Since this pump is a crucial feature in the control of the thickener mud bed it was necessary to broaden this flow range. The pump flow rates for various speeds are shown in Table 3.8.

Table 3.8 C22M Pump Flow Rates

n_p	Q (0 m head)	
(rpm)	($m^3.h^{-1}$)	($l.min^{-1}$)
0	0.000	0.00
100	0.035	0.59
200	0.070	1.17
300	0.110	1.84
400	0.150	2.50
500	0.190	3.17
600	0.230	3.83
700	0.275	4.58

The underflow pump is driven with the same VSD/motor/gearbox combination as the slurry feed pump discussed in the previous section. In this instance the pulley reduction of 2:1 is used to reduce the flow rate as far as possible when operating at 10 Hz. This gives a flow range starting at about 0.3 $l.min^{-1}$, going up to 3.17 $l.min^{-1}$ at 500 rpm.

The required starting torque for the C22M is only 7.5 Nm, and the motor/gearbox combination is able to deliver this with ease, even with the viscous underflow, delivering 44 Nm (less losses) to the pump.

3.1.5 Pipeline Slurry Settling

To ensure that the slurry does not settle out in the feed line it is necessary to calculate the required velocity and hence the feed pipe diameter. Taking the maximum particle size (1.5 mm), and ensuring that it will not settle out requires the following analysis.

The flow rate is given by

$$Q = VA = \pi \frac{D^2}{4} V \tag{9}$$

Where V is the fluid velocity, and A the line area. The line diameter D will be selected by plotting the actual velocity for a particular line size against the critical velocity. The critical velocity is given by

$$V_c = 3.48 \sqrt[3]{C_V} \frac{\sqrt{gD(s-1)}}{\sqrt[4]{C_d}} \tag{10}$$

This is the velocity at which the particles will remain suspended in the flow without settling out [5]. Where

C_V is the concentration of solids delivered by volume (also referred to as the discharge coefficient), discussed further in this section

s = 2.65, the specific gravity of the solids

g = 9.81 $m.s^{-2}$, the gravitational constant

C_d is the drag coefficient, related to Reynolds number Re, discussed further in this section

D is the pipe diameter (a range of diameters will be considered)

The discharge coefficient $C_{l'}$ is given by

$$C_{l'} = \frac{C_M \rho_l}{\rho_s - C_M(\rho_s - \rho_l)} \tag{11}$$

Where C_M is the percentage solids, and is 10 % or 0.1 for the feed slurry. The resulting concentration is 4 % or 0.04 by volume.

The D in equation (10) is the pipeline diameter, and the particle diameter d is accounted for in C_d, the drag coefficient. From Perry [6], the following values for particles flowing in liquid are given for the drag coefficient on spherical particles (the particles in this analysis are assumed to be spherical). A table of drag coefficients is shown in table 3.9.

Table 3.9 Values for the Drag Coefficient C_d

Cd	***Re***	**Regime**
$\frac{24}{\mathrm{Re}}$	< 0.1	Given by Stoke's Law at low Re
$\frac{24}{\mathrm{Re}}(1 + 0.14\,\mathrm{Re}^{0.7})$	> 0.1 < 1000	Intermediate
0.445	> 1000 $< 350\,000$	Newton's Law

The particle Reynolds number Re_p is given by

$$\mathrm{Re}_p = \frac{dV_c\rho_m}{\mu_l} \tag{12}$$

With

d = 1.5 mm, the maximum particle diameter

V_c is the critical velocity - to be calculated

ρ_m = 1066 kg.m^{-3}, the density of the feed slurry

μ_l = 0.001 Pas, the viscosity of the carrier medium (water @ 23 °C)

The approach to calculating V_c is iterative since the Reynolds number (Re) must be checked at each value of V_c to ensure that it is valid. A maximum particle diameter of 1.5 mm and the fluid velocity (V) at the lowest feed flow rate for a range of pipeline diameters gives the curves shown in Figure 3.3.

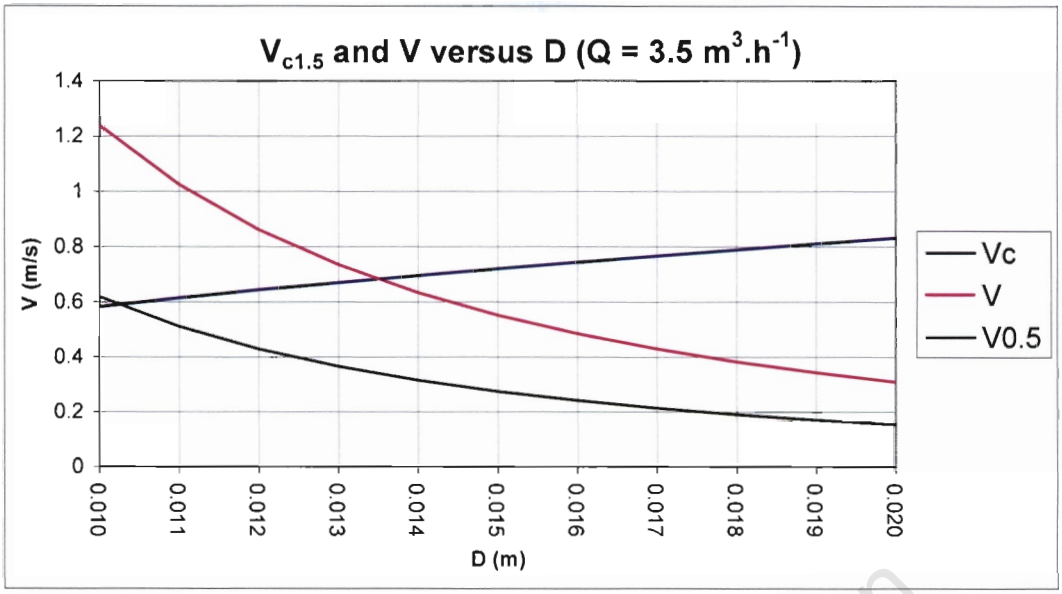

Figure 3.3 Critical velocity and velocity for Q = 3.5 $m^3.h^{-1}$.

The curve for V0.5 shows the velocity in the pipeline should the flow rate be halved. The velocity is clear of the critical velocity at a diameter of 0.0125 m or 12.5 mm (½"). There are two ways around this if it is found that a lower flow rate is required. Firstly the deposition of material in the line will reduce the cross-sectional area, and the velocity will increase, so that an equilibrium is reached where no more material is deposited. For particles smaller than 1.5 mm, the critical velocity also decreases so that it is sufficient to look at the largest expected particle diameter. The final delivery line to the thickener consists of flexible reinforced PVC hose, and the diameter can easily be reduced if deposition becomes a problem. The bulk of the delivery line is vertical and this also reduces the tendency of the material to settle in the pipeline. The suction line to the slurry tank was kept as short as possible by mounting the pump at the base of the tank.

If the density of the slurry increases the drag coefficient also increases, and the critical velocity decreases, so that a ½" line is also suitable for the underflow pump. All piping in the plant is ½", with the exception of the overflow, discussed in the following section.

3.1.6 Overflow Weir

The flow rate for the clear water overflow is 0.3 - 0.923 $m^3.h^{-1}$. Designing for a maximum overflow of 1 $m^3.h^{-1}$ provided sufficient capacity. The weir required an outlet that can manage this flow rate to avoid spillage. The equation for the flow rate through an orifice is given by [7].

$$Q = C_d A \sqrt{\frac{2\Delta P}{\rho\left(1-(d/D)^4\right)}} \qquad (13)$$

where d is the diameter of the outlet, and D the diameter prior to the outlet. An equivalent diameter D will equate to the area above the outlet. The outlet diameter d is much smaller than the diameter D and d/D is a small fraction, which when raised to the fourth power becomes very small and is neglected. In this case C_d is the discharge coefficient for the orifice. A value of $C_d = 0.7$ is used for a simple sharp edged orifice [7], giving

$$Q \approx C_d A \sqrt{\frac{2\Delta P}{\rho}} \tag{14}$$

The pressure differential is determined by the depth of the water in the weir and is given by

$$\Delta P = \rho g h \tag{15}$$

where h is the height of the fluid in the weir, and g (as usual) is the gravitational constant.

Substituting this into equation (14), and rearranging gives

$$A = \frac{Q}{C_d \sqrt{2gh}} \tag{16}$$

Rewriting the orifice area A in terms of the outlet diameter

$$d = \sqrt{\frac{4Q}{\pi C_d \sqrt{2gh}}} \tag{17}$$

With a weir height of 50 mm an outlet diameter of 22.6 mm was required. A standard hose size of 25 mm was chosen. To provide flexibility in the laboratory two 25 mm outlets were provided on opposite sides of the weir so that either hose (or both) could easily be taken to the overflow tank (depending on its location), whilst the other was blocked off, or used as a sampling point to measure turbidity. To allow sufficient space for hose and clamp attachment the width of the weir was chosen to be 50 mm, with the outlets mounted as near to the outer edge as possible. The outer edge of the weir was raised 20 mm above the top of the thickener to avoid spillage.

Looking back, the cross sectional area of the weir is sufficiently large that the assumption regarding the ratio d/D raised to the fourth power tending to zero holds.

Nine V shaped notches were made at the top of the inner wall of the weir. This allows the water to flow into the weir more smoothly and evenly. The notch details are shown in the final thickener design.

3.1.7 Feed Well

The purpose of the feed-well arrangement is to induce turbulence and provide time to allow for mixing of the slurry with the flocculant. After leaving the feed pipe the velocity begins to reduce, allowing further time for the formation of flocs, and allowing them to begin settling out.

A feed well with a diameter of 150 mm, and a length of 300 mm was selected on the advice of Vietti [8]. The feed-well is fitted so that it can be removed and modified should this be necessary. It is likely that the feed-well will be extended in future in order to deliver the flocculated slurry closer to the top of the mud bed. The feed-well is supported at the top of the thickener with 3 radial arms.

The slurry is introduced into the feed-well tangentially to aid in mixing with the available feed water by inducing swirl in the water column [8,9]. This is achieved by coiling the flexible PVC feed hose inside the top of the feed-well so that the slurry is delivered along the wall.

A spreader with an adjustable gap is included so that the material does not fall to the centre of the thickener and is evenly dispersed [8]. The spreader consists of a conical section supported at the base of the feed well. The initial spacing between the bottom of the feed-well and the spreader is 100 mm, and will be adjusted as required.

3.1.8 Final Thickener Design

The final thickener dimensions are shown in Figure 3.4. From the beginning of this chapter the maximum allowable height of the thickener is 1.8 m. The length of the thickener body is made up as follows:

- Feed-well: 300 mm
- Feed-well/spreader gap: 100 mm
- Spreader/probe spacing (min. settling gap): 300 mm
- Mud bed depth: 500 mm

The Vega probe length is 332 mm. A height of 1.5 m is adequate for the main body of the thickener (excluding the conical section and the pumping well at the base).

A window section was included on the front of the thickener to allow the installation of side probes without the need to modify the main body of the thickener. When replacing, or relocating probes it is only necessary to manufacture and drill another acrylic plastic pane. The width is based on the hole spacing on the Solartron Mobrey vibration density transmitter flange [10]. The flange is 150 mm wide, and a 160 mm wide window provides adequate clearance for nuts and bolts.

The bottom of the thickener features a conical section that tapers to a diameter of 150 mm (the same diameter as the feed-well). The angle of this section is 60 degrees, and this results in a conical section length of 170 mm. The slope is designed to minimise any slurry hold-up on the side of the cone in the absence of a raking mechanism.

The bottom section consists of a straight walled section allowing for the fitment of the underflow valve. This was included at the suggestion of Vietti [8], and assists in the

prevention of rat-holing. Rat-holing occurs when lower density slurry is preferentially drawn from high layers in the mud bed due to its lower resistance to flow. This section also allows for the fitment of an additional valve on the axis of the thickener for the clearance of blockages should they occur. This also provided a useful mounting point for a rake shaft.

The spreader contains a 25 mm hole in its centre to allow for the passage of instrument cables, and also caters for a rake shaft.

The mounting arrangement was determined by the manufacturer, based on the material strength, and the thickness of the material used. The volume of the thickener is approximately 144 litres. Including the conical section and the draw-off section brings the volume up to about 150 litres. Assuming that the entire thickener is filled with slurry at a specific gravity of 1.3 $kg.l^{-1}$, means that the slurry has a mass of approximately 188 kg. The clearance below the thickener is 400 mm.

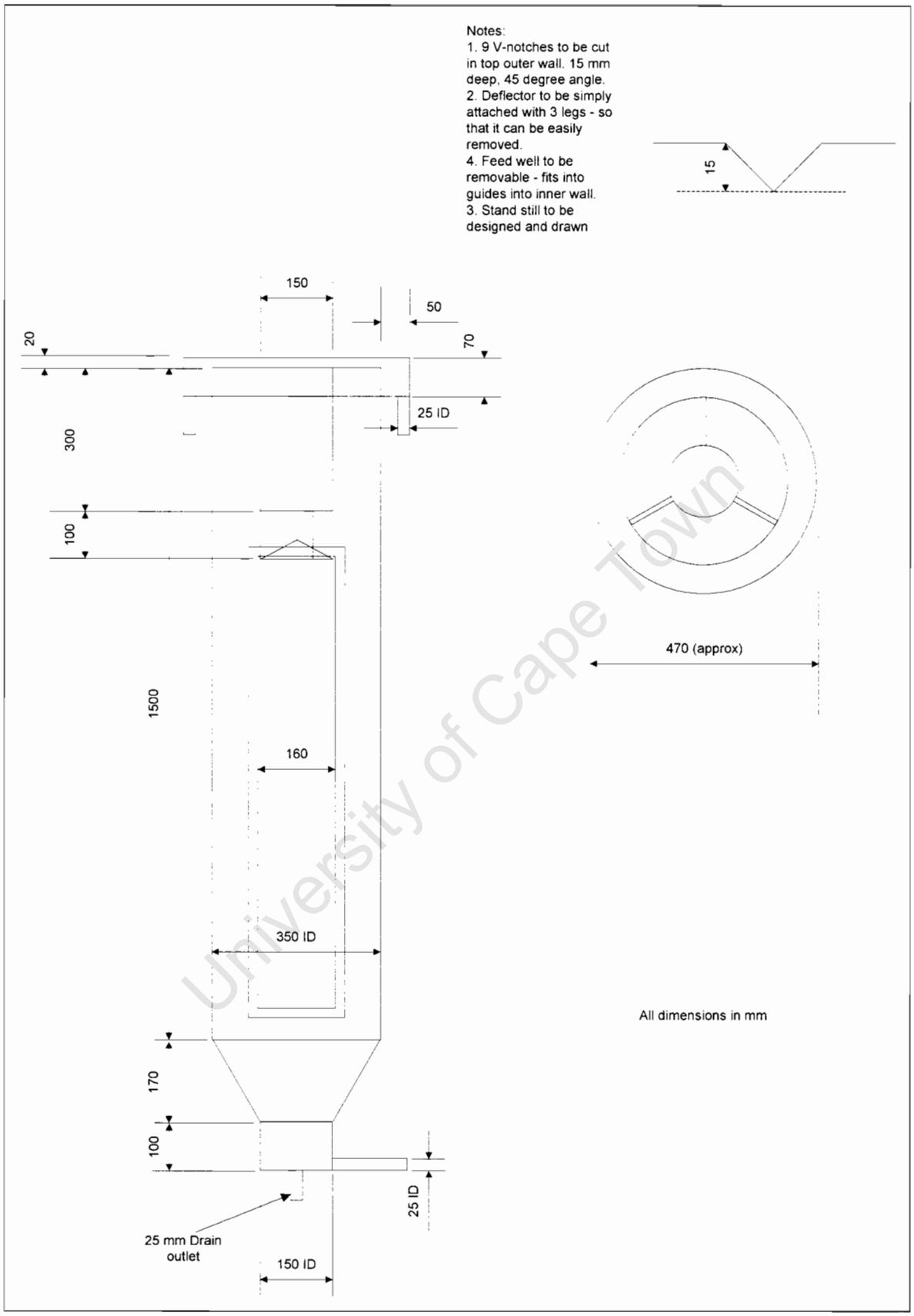

Figure 3.4 Final thickener dimensions.

3.1.9 Dilution Circuit

A dilution circuit was required to dilute the dense underflow slurry to the original concentration in the slurry tank, to maintain the feed slurry concentration. The underflow is pumped back into the slurry tank, and overflow and fresh make-up water are added to maintain the overall slurry concentration. The circuit also allows water containing expired flocculant to be discarded from the clear water tank.

In order to implement the circuit it was necessary to have a measurement of the underflow density. Nuclear density gauges are not available for line sizes of less than 50 mm, so an alternative was sought. After discussion with Endress & Hauser [11], it was found that a Coriolis mass flow meter would be suitable, but not as accurate as provided in the specification since the slurry is not a homogeneous fluid. A 15 mm Promass 83F dual tube coriolis meter was specified [12], but later found to exhibit large errors due to preferential flow in one or the other tube (see commissioning section). This was later replaced with a 15 mm single tube device.

Taking the maximum underflow density to be 1.5 kg.l^{-1}, and the flow rate ranging from 0.6 to 3.5 l.min^{-1}, the required amount of dilution water to achieve a concentration of 10 % can be calculated. The equation giving the modified concentration is

$$C_{Mf} = \frac{\dot{m}_{us}}{\dot{m}_{usl} + \dot{m}_{dl}} \tag{18}$$

Rearranging for the dilution water mass flow rate

$$\dot{m}_{dl} = \frac{\dot{m}_{us}}{C_{Mf}} - \dot{m}_{usl} \tag{19}$$

since

$$\dot{m}_{us} = C_{Mu}\,\dot{m}_{usl} \tag{20}$$

We have that

$$\dot{m}_{dl} = C_{Mu}\frac{(1 - C_{Mf})}{C_{Mf}}\dot{m}_{usl} \tag{21}$$

And

$$Q_{dl} = C_{Mu}\frac{(1 - C_{Mf})}{C_{Mf}}\frac{\rho_{sl}}{\rho_{l}}Q_{usl} \tag{22}$$

A dilution water flow rate of 4 to 20 $l.min^{-1}$ was catered for with the selection of a Howden/Mono GF pump (Appendix B) driven via a 1:1 pulley arrangement with an 0.75 kW WEG motor. In this instance the pulley arrangement allows for a ±10 % adjustment in the speed of the motor. Once again the motor is over-rated, where the pump specification requires an 0.37 kW motor to operate the pump with water. This allows for the pump to be run at low speeds via the VSD without overheating. The GF pump is a smaller version of the positive displacement pumps used for the feed and the underflow.

The design flow rate corresponds to the required dilution water for an underflow pump rate of 0.6 to 2.7 $l.min^{-1}$ at an underflow density of 1.5 $kg.l^{-1}$.

A 15 mm Yokogawa electromagnetic flow meter was chosen to measure the flow of water to the slurry tank [13].

A control valve was added to ratio the dilution water by providing a return path to the clear water tank to cater for conditions when very low flow rates are required. This is discussed further in the commissioning section.

A summary of the components for the dilution circuit is given below

Manufacturer	Model Number	Description
E&H	83F15	Promass 83F Coriolis mass flow meter
Emerson	15 mm/ES 25/F20/PT2	Ball valve with actuator and I2P module
Howden	Mono GF	20 $l.min^{-1}$ positive displacement pump

3.1.10 Circuit Layout

Figure 3.5 shows the complete layout of the system. The slurry tank has a 2 m^3 capacity, and the clear water tank is 1 m^3. The tanks both have a level measurement to ensure that the liquid does not drop below the level of the agitators. The clear water tank has an agitator since it is inevitable that some solids will carry into the overflow, and these must be returned to the slurry tank. The slurry is pumped into the thickener, where the overflow reports via gravity to the clear water tank, and the underflow is pumped back to the slurry tank. Dilution water is pumped to the slurry tank to maintain the feed density, and a dump valve is provided at the dilution pump to remove water containing expired flocculant. Two Vega vibration switches and the vibration density meter are shown on the thickener. The underflow slurry pipeline shows a Coriolis mass flow meter, and two pressure measurements for estimation of the underflow viscosity. A Watson-Marlow peristaltic pump featuring a remote 4-20 mA flow control input was loaned from the water laboratory. A 20 litre bucket is used for flocculant, with the flocculant strength being adjusted according to the slurry requirement. Flocculant addition is very small compared to the slurry flow rate into the thickener so that this does not have a significant impact on the slurry concentration.

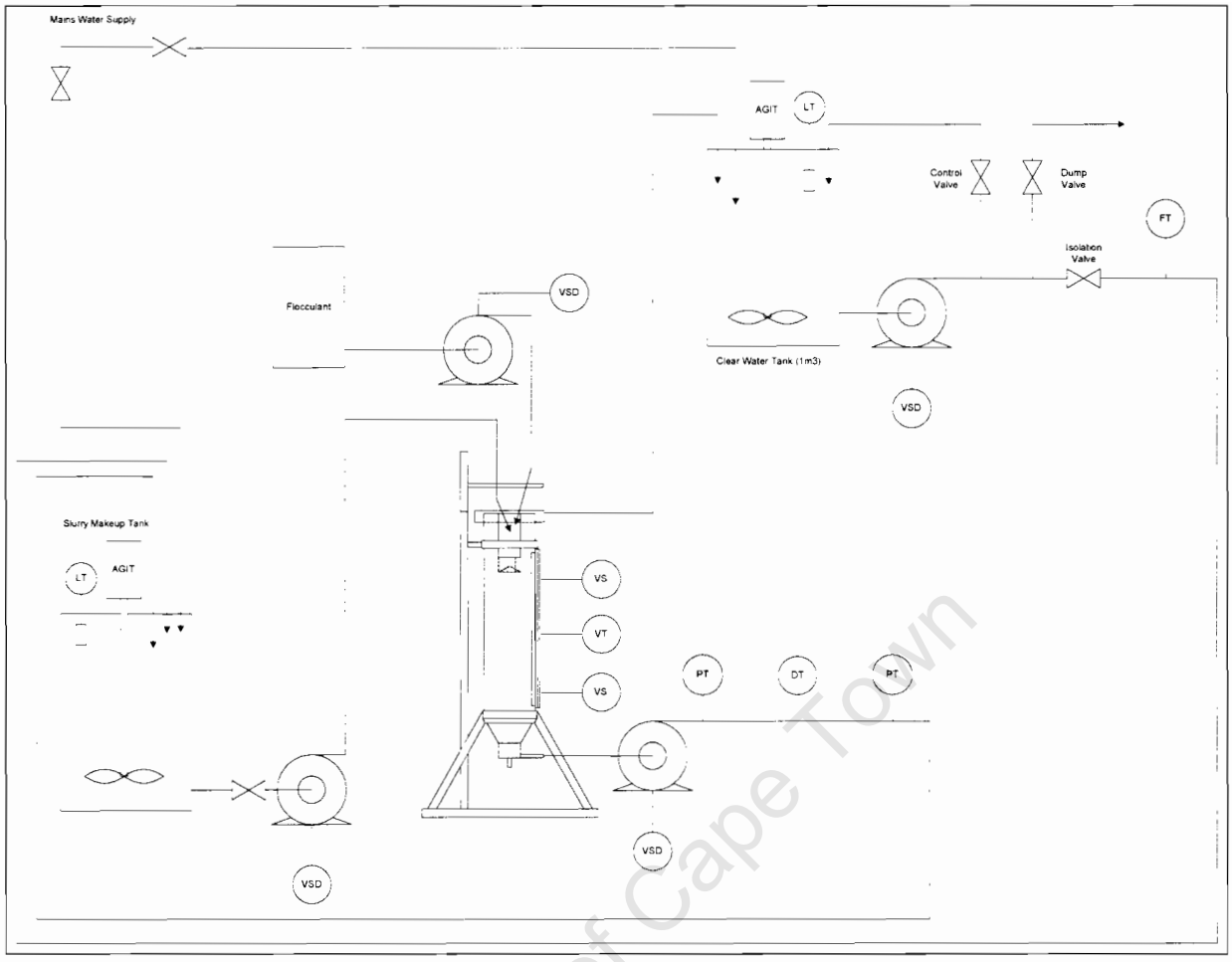

Figure 3.5 Process layout. The slurry and clear water (overflow) tanks are shown with their agitators. Slurry is pumped into the thickener feed well, the underflow is returned to the slurry tank. The overflow runs into the clear water tank, and is used to dilute the feed slurry to the correct concentration. The control valve shown, featured in the original dilution controller (discussed in Appendix D).

3.2 EQUIPMENT SUMMARY

The final list of instruments for the process layout shown in Figure 3.5 is shown in Table 3.10. The underflow density transmitter was replaced during commissioning, and the control valve removed during the initial control tests. These are discussed in the relevant chapters.

Table 3.10 Instrument List

Qty.	Instrument	Mnfr.	Model	Type
2	Level Transmit.	Endress&Hauser	FMU860	Ultrasonic
4	½" Ball Valve	Festo	QH-DR-1/2-B	Pneumatic
1	1" Ball Valve	Festo	QH-DR-1-B	Pneumatic
5	Valve Position	Festo	SM-M2 Armatic	Cam operated
1	Density TX.	Endress&Hauser	83F15	Coriolis
1	Control Valve	Emerson	15 mm/F20/PT2	Pneumatic
2	Vibration sw.	Vega	Vegavib 52	Probe
1	Flow Meter	Yokogawa	Admag SE-115	Electromagnetic

The electrical equipment list is shown in Table 3.11. In addition to the equipment below, an additional d.o.l. starter was included to operate an additional pump for emptying the tanks, or for a shear thinning loop was provided. The slurry agitator and its VSD were upgraded during commissioning, and are discussed in that chapter.

Table 3.11 Electrical Equipment List

Qty.	Item	Mnfr.	Model	Description
2	1.1 kW VSD.	Siemens	MM440	Feed & Underflow Pumps
2	1.1 kW motor	SEW Eurodrive	RX57 DT90S4	
2	0.75 kW VSD	Siemens	MM440	WEG Motor +Spare
1	0.75 kW motor	WEG	Mono GF	Dilution Pump
1	Flocc. Pump	Watson-Marlow	630-UR	Peristaltic Dosing Pump
2	0.75 kW VSD	Siemens	MM400	
1	0.75 kW motor	Stallion		Slurry Agitator
1	0.75 kW motor	Mixtec		Clear Water Agitator

Fieldpoint control hardware was selected based on an estimate of the number of inputs and outputs. Table 3.12 shows the I/O estimate, and the selected hardware modules.

Table 3.12 Control Hardware List

Qty.	I/O	No.	Module
2	Digital Input	19	FP-DI-301, 16 Ch. 24 V
1	Digital Output	12	FP-DO-401, 16 Ch. 24 V
1	Analogue Input	9	FP-AI-111, 16 Ch. 4-20 mA
1	Analogue Output	3	FP-AO-200, 8 Ch. 4-20 mA
1	Comms. Module	-	FP-1001 (RS-422/485)
5	Terminal Bases	-	FP-TB1

3.3 DISCUSSION

A scale thickener was designed to simulate a portion of a full scale thickener to create similar settling conditions. There are some aspects of the scale thickener that are not similar to full scale thickeners. These are:

- The ratio of the diameter of the scale feed well to the scale thickener diameter is large compared to that found on full scale thickeners. This means that the fluid flow patterns are quite different because there is an interference effect by the walls.
- The depth of the feed well is not scaled in any way, and is adjusted to achieve the best settling conditions through observation.
- The aspect ratio – the ratio of the width to the height or depth of the thickener – is large in comparison with full scale thickeners. Again, this results in different fluid flow patterns in the thickener.

- The scale underflow well is large in relation to the thickener diameter, and the underflow outlet pipe is large in comparison with the scale underflow well.

Despite these differences it is still possible to settle slurry and create a mud bed similar to that found on full scale thickeners, although not of the same depth. As will be shown later, it was possible to achieve similar underflow densities, although this depended on the type of slurry being processed.

During construction and installation in the laboratory a series of tests were carried out on Finsch mine slurry to evaluate its properties, and confirm operation of the plant by recycling the slurry.

3.4 REFERENCES

1. A Roebl, "Instrumentation R&D 2003: 2nd Quarter Status Report, Thickener Instrumentation and Control", TN 2003-07-01, 2 July 2003.
2. F Dunn, "Ultrasep Mud Bed Interface Level Detection and Control", Debtech Report R1999-09-01, 20 March 2003.
3. Vega Controls. Vegavib 52. Operating Instructions. Order No: 1099828_1, 17496-EN-030305.
4. F. Concha and A. Barrientos, "A Critical Review of Thickener Design Methods", Presented at KONA No. 11 (1993), pp79-104.
5. A G Bain and S T Bonnington, The Hydraulic Transport of Solids by Pipeline, Pergamon Press, 1970.
6. R H Perry and D W Green, "Perry's Chemical Engineer's Handbook 7th ed", McGraw-Hill International, 1998.
7. T Baumeister, E A Avallone, L S Marks (editors), "Marks Standard Handbook for Mechanical Engineers", 10th ed (1996); Mechanical Engineering Series (1996).
8. A J Vietti, personal communication.
9. G Langefeld, personal communication.
10. Solartron Mobrey. Type 7835 Densitometer. Technical Specification Sheet B1016, September 2005. Available: http://www.mobrey.com/downloads/datasheets/b1016.pdf.
11. K Meadway, Business Driver (Mining & Primaries), Endress & Hauser, South Africa, personal communication.
12. Endress & Hauser, Coriolis Mass Flow Measuring System PROline promass 80/83 F,M, Technical Information TI 053D/06/en, 50098280
13. Yokogawa, General Specifications ADMAG SE, GS 01E-10A01-01E, 13th Edition, October 2005, Available: http://yokogawa.com/fld/pdf/ADMAG/GS01E10A01-01E_013.pdf.

CHAPTER 4 FINSCH MINE SLURRY CHARACTERISATION

The overall objective of this portion of the project was to determine how best to settle the slurry in the test thickener in order to create similar settling conditions to those experienced on full scale. The aim was to find an operating point at which control tests can be carried out for a period of approximately one week. Four days is a suitable duration, since time is also required to fill and flush the plant. To complete this objective a number of intermediate steps were carried out as follows:

- To determine whether a coagulant is sufficient to achieve useful settling.
- To determine whether some alternative to Finsch Kimberlite slurry could be used whilst still providing similar behaviour to reduce reliance on the manual collection of dry solids on site, and transport to Johannesburg.
- To determine the optimum flocculant dosage and the best solids concentration for control testing.
- To determine the duration over which tests can be carried out under continuous flocculation, and the best concentration at which to do this.

The full tests results can be found in [1], including all test data. The chapter provides a summary of the important results.

The target underflow density of the laboratory system is in the region of 1.6 $kg.l^{-1}$, although this was not achieved on these small scale bench top tests. It was expected that this range would be achieved using the laboratory scale thickener with a significantly deeper mud bed.

There is a benefit to using coagulant over flocculant, and this is that the coagulant need only be applied once to a slurry, and continues to perform its task with time. Unlike flocculant, coagulant does not break down with time. In this case an inorganic salt (calcium chloride) was used, but was shown to be ineffective compared with the flocculant results. In fact the calcium chloride did not provide settling characteristics that agreed with the scale thickener design and they were far too low.

At the same time as the coagulant testing was carried out, two alternatives were tested. kaolinite clay was selected since it is not a swelling clay like kimberlite. The kimberlite clay adsorbs water, swells, and then breaks down into smaller and smaller size fractions. This would mean that the dose of coagulant would have to be increased over time. The kaolin was tested, and was found to be unsuitable since it is a pure clay, and does not settle well due to the high population of very fine material. To rectify this, a batch of white quartz was milled and sieved together with the kaolin to make up a slurry with a similar size frequency distribution to that of the kimberlite. Although this improved the settling, it was still not as good as the Finsch kimberlite. After initial flocculation tests with the raw kaolinite, and the kaolinite mix it was decided that it would be best to continue with the kimberlite slurry. The kaolinite slurry settling did not improve with flocculation, and the sedimentation behaviour was worsened, i.e. the mud bed was deeper than that achieved with kimberlite, resulting in a lower underflow density. The swelling of the kimberlite was no longer an issue since continuous flocculation would take care of this problem.

After determining that 7.5 % and 10 % solids concentrations would be tested further for final use, the optimum flocculant dosage was measured. Following this, the continuous tests were

carried out to determine if it is possible to continuously flocculate a slurry sample as required, and how well this could be expected to perform.

4.1 BACKGROUND

4.1.1 Settling, Coagulation, and Flocculation

4.1.1.1 Settling

The kimberlite test sample was sieved down to below 1 mm in order to avoid blocking the tubes in the Coriolis mass flow meter, which has 8.5 mm diameter tubes. The grits settle under gravity, and these typically consist of quartz minerals [2]. The smaller slimes fraction (-75 μm) requires the addition of coagulant or flocculant in order to settle. These typically remain in suspension due to the fact that the electrical forces between the molecules and the water are greater than the inertial forces which would settle them under gravity.

In kimberlite slurries, the colloidal particles are typically clays (smectite), which carry an overall negative charge. The clay solution is a homogeneous dispersion of very small particles, known as a colloidal solution or sol. These small particles are in the μm range. Particles with a Stokes radius smaller than 1 μm are considered to fall in the colloidal size range [3]. The Stokes diameter is given by [4]

$$r_{St} = \frac{d_{St}}{2} = \frac{1}{2}\sqrt{\frac{18\eta u}{(\rho_s - \rho_l)g}} \quad (1)$$

Where

η is the viscosity

u is the settling velocity

ρ_s is the solid density

ρ_l is the liquid density

g is the gravitational constant.

Taking a look at the settling velocity for a Stokes radius of 1 μm

$$u = \frac{4r_{St}^2(\rho_s - \rho_l)g}{18\eta} \quad (2)$$

With the viscosity for water being 0.001 Pa.s, the solid and liquids densities being 2390 and 1000 kg.m^{-3} respectively, and the gravitational constant g as 9.81 gives a settling velocity of

$$u = 3.03 \times 10^{-6}\, m.s^{-1}$$

Which is very slow indeed, and anything smaller than this will travel still slower. At the velocity given above, it would take in the region of 90 hours for a particle to settle one meter, at 10 μm radius the settling is still too slow (1 metre per 55 minutes) to be useful. The target settling rate is better than 10 m.h^{-1}, and preferably above 16 m.h^{-1}. In addition to this, the

particles that are settling at significantly higher rates give rise to a net upflow of water as they displace fluid in their path. This further hinders settling. The presence of Brownian motion, and electrical forces hinder settling further so that the colloidal particles remain in suspension, or move out of the thickener with the overflow. Note that the electrical forces are not likely to be a problem if the overall charge of the particles is neutral (such as kaolin). Kimberlite carries an overall negative charge, and hence some mechanism is required to ensure that these particles settle.

4.1.1.2 Coagulation

Coagulants come in two forms, electrolytes (inorganic salts), and poly-electrolytes (low molecular weight polymers). The Finsch Mine slurry was tested using calcium chloride (full name, calcium chloride dihydrate or $CaCl_2.2H_2O$, an inorganic salt) on the advice of Vietti [5].

The following explanation of coagulant behaviour is summarised from the Paste and Thickened Tailings Handbook [6].

When the kimberlite clay particles are immersed in water an electrical double layer forms around the particle to balance the overall negative surface charge. The electrical double layer consists of a layer of bound counter ions adjacent to the particle surface, known as the Stern layer, which is surrounded by a more diffuse ionic "cloud" that extends into the bulk solution. The repulsive forces around the particles prevent them from colliding and forming larger particle aggregates that could settle. Coagulants are used to destabilise the suspension by reducing the particle surface charge so that they can move closer to one another. With electrolyte coagulants, the inorganic salts separate into cations and anions in solution, and the negative surface charge of the particles is reduced through selective adsorption of multi-valent cations on the particle surface. The removal of repulsive forces between suspended particles is not always enough to allow aggregation to take place fast enough to significantly increase the settling rate. It may be necessary to further stimulate aggregation and settling through the addition of flocculant.

4.1.1.3 Flocculation

The following explanation of flocculant behaviour is summarised from the Paste and Thickened Tailings Handbook [6].

Polymer flocculants consist of polymer chains that attach themselves to the suspended solid particles. The longer the polymer chain, the more effective is the bridging and aggregation of suspended particles into flocs. It is important to have adequate mixing at the flocculant dosing point to ensure proper distribution of flocculant throughout the suspension, and to promote collisions between the suspended solid particles and polymer chains. It has been shown that the critical size fraction relating to flocculant dosage is the -20 µm fraction. Although flocculant dosage may be based on the mass-flow rate of slurry, the particle size distribution may change as different parts of the pit are mined, and the flocculant requirement will change accordingly. The same will be true due to variations in the solids concentration. Too high a solids concentration means that particles in suspension hinder each other in terms of settling, since the larger aggregates create a net upflow of water. Too low a concentration means that the particle collision rate is reduced, and both flocculation and settling become

inefficient. Most De Beers mines make use of the Ciba 'Magnafloc' range of flocculants from Pelichem [7]. For the testing of the Finsch slurry, Magnafloc 156, and Magnafloc 5250 were used at the suggestion of Vietti and Langefeld [2,5].

4.1.2 Slurry Density

In order to make up slurry solutions at various concentrations, it is necessary to know the density of the solids sample. The density was measured by adding a sample to a known volume of water in a measuring cylinder. The densities are as follows:

Kimberlite : 2.39 $kg.l^{-1}$

Kaolinite : 2.48 $kg.l^{-1}$

These densities were verified as accurate when added to the calculated volume of water in order to make up slurries of the required concentrations. Due to variations in ground type, each new sample must be tested to determine its density prior to use in the plant.

4.1.3 Sample Preparation

In order to calculate the solids mass and liquid volume, the slurry density must be calculated from the percentage solids by mass. The liquid volume is known, since 1 litre of slurry is required (although any required slurry volume could be inserted in the equation). The percentage solids value is fractional, and must be divided by 100 if given as a whole number percentage.

The volume of water required is calculated by

$$V_l = (1 - C_M)\frac{M_{sl}}{\rho_l} \tag{3}$$

And the mass of solids required is calculated by:

$$M_s = C_m M_{sl} \tag{4}$$

The measuring cylinder is first filled with the required volume of liquid, and then the solids are gradually added to ensure that they are completely wetted. Adding the liquid to the solids results in a dry zone at the base of the cylinder. This means that additional agitation is required in order to wet all of the solids powder, and to ensure that all lumps are removed. The intention is to keep the tests as similar as possible and excessive mixing is to be avoided. The previously estimated densities were confirmed in the process of mixing the sample, and found to be accurate in making up a 1 litre sample in a measuring cylinder.

4.1.4 Batch Settling Tests

Other than the qualitative tests used to get an idea of the behaviour of coagulant or flocculant with the slurry, the standard test to determine settling performance is the batch settling test which is carried out as follows:

1. A 1 litre sample is made up in a 1 litre measuring cylinder to the desired concentration.
2. A strip of masking tape is stuck down the length of the measuring cylinder.
3. Half of the optimum flocculant dose is added to the sample.
4. The cylinder is inverted 3 times, the second half of the flocculant dose added, and then inverted 3 times once again.
5. A stopwatch is started as soon as the cylinder is placed upright on the bench-top.
6. Marks are made on the masking tape to indicate the top of the liquid surface, and the bottom of the cylinder.
7. The mud/clear water interface is tracked by making marks on the tape at suitable intervals, and noting the time on the tape.
8. At the completion of the test, the masking tape is removed and stuck to a piece of paper where the interface level is measured using a ruler (measuring from the liquid surface).
9. The settling curve is plotted, and the settling rate determined from the curve.

Figure 4.1 shows an example of a settling test result. The initial region in the figure is the linear settling region from which the settling rate is computed. There is sometimes a knee at the top of this portion when the heavier grits settle quickly and the aggregated fines are smaller and settle more slowly. This is due to the fact that the grits settle rapidly, and create a net upflow of water as they displace it on their way down. Once the aggregates approach the size of the grits, this effect is no longer seen, although the aggregates still settle slower than the grits due to their lower density. In the second region shown, the initial compression of the mud bed is taking place. Some compression will already have taken place, since while the interface is moving downward material has already collected at the base of the vessel. There is typically a distinct knee between the linear region and the compression region, and this is easily seen when a linear trend is applied to the linear portion. After the initial rapid compression has taken place there is a more gradual compression that can take up to three days, until it reaches a point where no further compression takes place. Compression involves the removal of water between the particles through gravitational forces, until the particles are in contact with each other, and no further water can be released. This may not be strictly true since compression also slows, due to the fact that it becomes more and more difficult for water to escape through the layers above as the escape path becomes blocked.

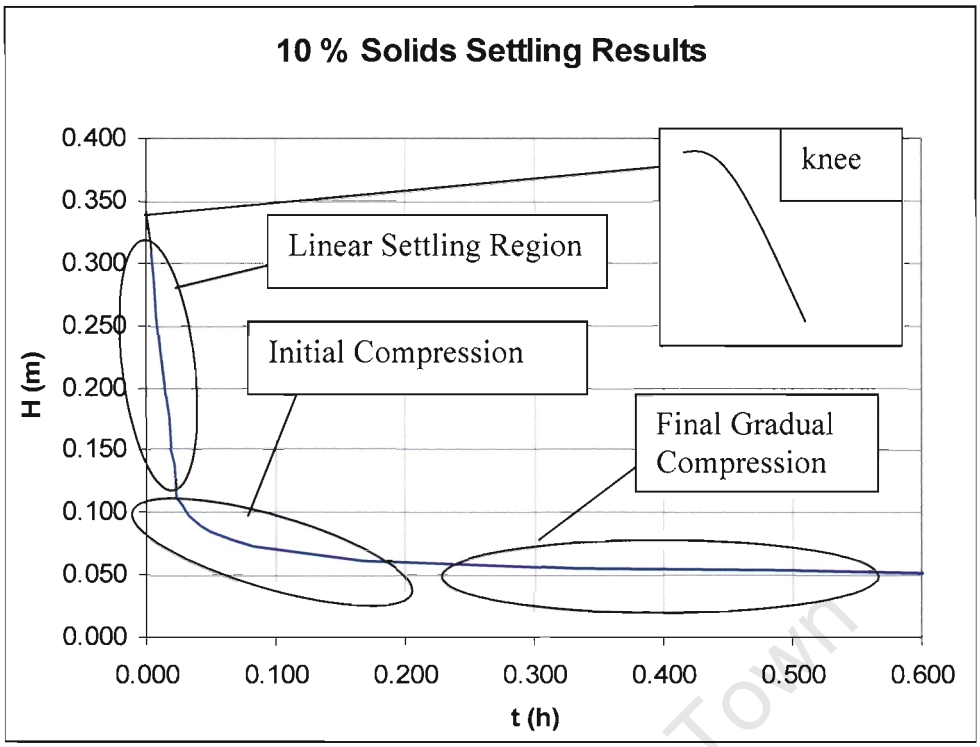

Figure 4.1 A sample 10 % solids settling result.

4.2 SLURRY TESTING

The slurry tests carried out on the Finsch slurry are taken directly from Appendix A of the Thickened Tailings Disposal Handbook [6], with the exception of the final hydraulic loading test which was modified to evaluate the results of continuous flocculation of the slurry. Continuous flocculation means that the sample is re-flocculated in order to extend the available testing period. The modifications to this test still yield the same results as the original hydraulic loading test, as well as giving insights into slurry behaviour when continuous flocculation is applied.

4.2.1 Coagulant Trials

The coagulant trials consist of a coagulant selection and demand test. Coagulation performance is rated on the scale shown in table 4.1.

Table 4.1 Coagulation Performance Rating

Rating	Behaviour
-	No coagulation
+	Partial coagulation
++	Complete coagulation

The point at which the rating goes from + to ++, is referred to as the critical coagulant concentration (CCC).

No coagulation means that the slimes remain in suspension and do not settle (the grits will be seen to collect at the bottom of the test-tube), even when left overnight there will still be some slimes in suspension if the settling is very slow.

Partial coagulation means that some of the slimes coagulate and settle out, generally the remainder will gradually settle overnight.

Complete coagulation means that most of the slimes coagulate and settle out. Note that in a small test-tube, the supernatant (the clear liquid above the settled slimes) will appear clear, while in practice it will still appear cloudy or milky in a larger vessel such as a 1 litre measuring cylinder. This is acceptable, since the goal remains to create a useful mud bed, and the overflow slimes will be returned to the thickener during dilution.

The test is carried out by filling a series of test tubes with 10 ml of slurry, and adding a stock coagulant solution of 1 % by mass working strength to each tube. Each tube is dosed with 0.2 ml of the solution incrementally, leaving the first tube as a control. The first tube is dosed with 0 ml of coagulant, the second with 0.2 ml, the third with 0.4 ml etc.

The tests were carried out at concentrations of 5, 10, 15, and 20 % solids by mass for kimberlite and kaolinite slurry.

Results

Being charge neutral, it was found that coagulant had no impact on the settling behaviour of the kaolin. The critical coagulant concentration for kimberlite was found to be 600 $mg.l^{-1}$ at 5 % solids by mass, and at 800 $mg.l^{-1}$ for the remainder.

Having selected coagulant concentrations, settling tests were carried out to determine the resulting settling rates. The settling test results for kimberlite slurry with coagulant are summarised in the table 4.2, below. Note that the magnitude of the settling rate is given, where it takes place in the downward direction with the base of the measuring cylinder as the datum.

The kimberlite settling rates ranged from 1.222 – 0.601 $m.h^{-1}$ at concentrations of 5 – 20 % respectively. The kaolin settling rates ranged from 0.749 to 0.076 $m.h^{-1}$ at concentrations of 5 – 20 % respectively.

The settling rates for pure kaolin were noted to be significantly worse than those for the kimberlite. At the same time it should also be noted that the kaolin creates a mud-bed of greater volume than the kimberlite. This is a very important factor, since the lower the volume of the mud bed, the greater the density of the expected underflow. With the raw kaolin clay it was found that the clay tends to build up a sponge-like network at the base of the cylinder that traps water in the gaps. This is not a desirable characteristic, since it is not possible for this water to escape easily under gravity. The water pockets become a part of the structure, so that they carry the load of the solids above. The network is strong enough that the water is held in the interstices, so that no further compression takes place.

It was also realised at this point that using pure kaolin clay to simulate kimberlite, whilst avoiding the potential problems presented by swelling clay, was not representative. In order to make the kaolin representative it was necessary to give it a similar size frequency distribution to kimberlite. To do this, a sample of kimberlite powder was washed to separate the clay from the quartz minerals. The two portions were sieved to get their particle size distributions (PSD).

To mimic this distribution, 1 kg of white quartz (-3 mm) was milled in a 0.4 m diameter ball mill with 8 steel balls of 50 mm diameter for a period of 3 hours. This produced a fine powder that was sieved to make up a sample to match the quartz minerals in kimberlite. This was mixed with the kaolin clay to get a test sample.

The kaolin settling rates ranged from 1.429 to 0.203 $m.h^{-1}$ at 5 to 20 % solids respectively.

The settling rates and sediment volumes are summarised in tables 4.2 and 4.3.

Table 4.2 Summarised Settling Rates ($m.h^{-1}$)

% Solids	5	10	15	20
Ki + CaCl2	1.310	1.016	0.745	0.606
Ka	0.749	0.239	0.159	0.077
Ka mix	1.429	0.737	0.384	0.203

Table 4.3 Summarised Sediment Volume (ml)

% Solids	5	10	15	20
Ki	75	140	210	285
Ka	100	200	300	480
Ka mix	110	220	310	400

As can be seen from the figures, lower concentrations lead to faster settling times but also lead to less sediment. There is a trade-off between the settling time and the amount of sediment or bed produced at different concentrations. At this point the kaolin, mixed or raw was not looking very promising. The kimberlite results were better, but still well outside the range for the plant design (> 16 $m.h^{-1}$). The logical next step was to proceed to flocculant evaluation to improve the settling rate.

4.2.2 Flocculant trials

The flocculant trial tests consist of two sub-tests, followed by an additional series of tests to determine which is the best operating concentration.

The operating concentration is determined by the amount of sediment produced and the settling rate achieved, although the settling rate is the dominant feature in order to fulfil the requirements of the plant design. The two tests carried out are

- The flocculant selection test
- The flocculant demand test

In the first test, two flocculants were tested to determine which would work best with the available slurries. In the second test, the dosages at different concentrations are determined to provide good flocculation and supernatant clarity.

4.2.2.1 Flocculant Selection Test

This test is conducted on a slurry sample which closest represents the actual feed conditions in a thickener. In the case of high compression thickeners this is usually in the region of 10 % solids by mass [6].

Flocculant is judged visually according to the degree of flocculation (size and definition of flocs), and degree of clear water produced (clarity of supernatant). The flocculant performance is judged according to one of the following four categories:

Table 4.4 Flocculant Performance Categories

Performance	Description
Poor	No flocculation, no clear water
Fair	Some flocculation, unclear water
Good	Good flocculation, unclear water
Excellent	Good flocculation, clear water

Three flocculants were chosen for testing based on the experience of Vietti [5] and Langefeld [2]. These are:

- Magnafloc 5250
- Magnafloc E10
- Magnafloc 156

The flocculant selection test is carried out by dosing a series of test tubes filled with 10 ml of slurry with a flocculant made up to a concentration of 0.025 %. Each test tube is dosed with a candidate flocculant drop-wise (approx. 0.1 ml) until the first signs of flocculation is observed. The results are recorded, and the optimum flocculant is selected. The best flocculant is selected based on:

- Supernatant clarity - clearer is better.
- Dosage requirement – lower dosage means lower flocculation costs.
- Bed compaction – the better and more quickly the bed compacts, the greater the underflow density, and the less time the dense slurry must spend in the thickener. Bed compaction is equivalent to dewatering, since the aim of the thickener is to remove water from the slurry.

The results of this test are shown in table 4.5.

Table 4.5 Flocculation Selection Results. Block text indicates flocculant performance according to table 4.4

Flocculant	E10	5250	156
Kimberlite	Excellent	Excellent	Good
Kimberlite coag	Excellent	Excellent	Excellent
Kaolinite	Excellent	Good	Good
Kaolinite mix	Excellent	Excellent	Excellent

Key:

Slightly worse settling than E10, but compacts better - seems to form smaller flocs that can get closer together, although the water is less clear

Very spongy, holds up water

Slightly spongy, holds up water

From these results, the 5250 and E10 results were selected for further testing, since it was uncertain which would produce the better results. It is difficult to choose between two tests when carried out in test-tubes, since the supernatant water appears reasonably clear with such a small sample.

Coagulated sample was no longer considered due to its nature of forming sponge-like beds that are not easily compressed. Kaolin in all its possible forms was abandoned as an alternative to kimberlite because of the tendency to form sponge like beds, when coagulated or flocculated, that resist compression and trap water.

4.2.2.2 Flocculant Demand Test

The two flocculants chosen in the previous section were tested to determine what dosage would be required for a range of concentrations.

This test is carried out by adding flocculant at a concentration of 0.025 % to a 200 ml stirred slurry sample in 0.5 ml doses until the first signs of flocculation are observed. The result is recorded, and confirmed by adding the recorded dose to a fresh 200 ml stirred slurry sample.

Flocculant concentration is calculated as

$$C_f = \frac{M_f}{V_l \rho_l} \times 100\% \qquad (5)$$

Where M_f is the flocculant mass, and V_l and ρ_l the volume and density of the liquid in which it is dissolved (water). So for the above case, we consider 2.5 mg of flocculant dissolved in 100 ml of water (100 g of water), giving

$$C_f = \frac{0.0025}{100} \times 100\% = 0.0025\%$$

The flocculant dosage in grams is easily calculated by

$$M_f = \frac{C_f}{100} V_f \qquad (6)$$

With the flocculant concentration C_f in %, and the flocculant dose volume V_f in ml. These calculations were used later when making up flocculant for use in the plant.

Optimum flocculant consumption is best determined by evaluating the amount of flocculant required in grams per ton of dry solids. The mass of dry solids per test is simply M_s, divided by 1000 to go from kg to tons. The flocculant dosage in $g.t^{-1}$ is thus M_f/M_s. This makes it possible to compare the dosages at different slurry concentrations.

The flocculant dosing results are summarised in Table 4.6. It was found that the required dosage for 5250 was consistently lower than that required with E10 to produce the same settling results, and 5250 was selected for the next series of tests.

Table 4.6 Flocculant Dose

		Dose ($g.t^{-1}$)	
C_M (%)	**ρ ($kg.l^{-1}$)**	**5250**	**E10**
5.0	1.030	3.24	4.85
7.5	1.046	3.51	5.84
10.0	1.062	3.06	7.85
12.5	1.078	2.94	9.58
15.0	1.096	2.84	10.14
17.5	1.113	3.31	13.05
20.0	1.132	3.92	16.57

It was found that the 5250 flocculant resulted in a more compact mud bed due to the formation of smaller flocs. Although 5250 results in a murkier supernatant, the benefits of the improved bed compression and lower overall flocculant consumption outweigh the benefits of a clearer overflow.

The optimum flocculant dose of 5250 is shown in table 4.7 for each concentration, along with the density, and mass of solids present at each concentration. While these tests are qualitative, the results were quantitatively arrived at in more detail in the following section through settling rate envelope tests. These flocculant doses were used as a starting point for the settling rate envelope tests.

Table 4.7 5250 Optimum Flocculant Dose

C_M (%)	ρ (kg.l^{-1})	Dose (mg)	M_s (kg)	g.t^{-1}
5.0	1.030	0.033	0.010	3.24
7.5	1.046	0.055	0.016	3.51
10.0	1.062	0.065	0.021	3.06
12.5	1.078	0.079	0.027	2.94
15.0	1.096	0.093	0.033	2.84
17.5	1.113	0.129	0.039	3.31
20.0	1.132	0.178	0.045	3.92

4.2.3 Settling Rate Envelope Tests

The following tests were conducted by means of settling tests to establish the settling rate envelope for the flocculated slurry:

- Settling rate as a function of solids concentration (at a given flocculant dose).
- Settling rate as a function of flocculant dose (at a given solids concentration).

4.2.3.1 Settling Rate as a function of feed solids concentration

The settling rate of a flocculated thickener feed slurry is determined primarily by the solids content of the feed (the higher the solids content, the lower the settling rate). This test is used to determine the shape of the settling rate curve at increasing solids concentration but at a fixed flocculant dose. The tests were run at 2.5 % intervals from 5 % solids up to 20 % solids, using batch settling tests. Each settling test was carried out using the flocculant doses given in table 4.7.

Results

Table 4.8 shows the results of the settling tests.

Table 4.8 Optimum Flocculant Dose Results

C_M (%)	SR (m.h^{-1})	m_s (kg.l^{-1})	RR (m.h^{-1})	Q_f (l.min^{-1})	$\dot{m}_s$ (kg.min^{-1})
5.0	31.96	0.010	15.98	25.6	0.256
7.5	27.00	0.016	13.50	21.6	0.346
10.0	16.71	0.021	8.36	13.4	0.281
12.5	11.90	0.027	5.95	9.5	0.258
15.0	6.74	0.033	3.37	5.4	0.178
17.5	5.33	0.039	2.67	4.3	0.167
20.0	3.20	0.045	1.60	2.6	0.115

For the desired plant operating range of 10 – 16 $m.h^{-1}$ and better, the values between 5 % solids and 12.5 % solids appear to be suitable. Figure 4.2 shows the ideal mass of solids that would be delivered to the thickener for each settling rate. The rise rate (RR) is the rate at which the clear water rises due to the delivery of feed slurry by halving the settling rate. In other words this allows the maximum feed rate at each concentration to be determined. The feed flow rate (Q_f) multiplies the cross-sectional area of the thickener by the rise rate to get a value in $m^3.h^{-1}$, and this is converted to $l.min^{-1}$. Since the mass of solids per litre is known, this can be multiplied by the flow rate to determine the amount of solids that would be delivered to the thickener per minute. With the aim of maximising solids delivery, the following conclusions were drawn

- At 5 % solids, the required feed rate to achieve this maximum is outside the design range of the plant. With a lower feed rate this performance would not be achieved.
- At 12.5 % solids the settling rate is close to the design limit for the plant, and since preliminary test work showed that the settling performance declines over time under continuous flocculation, this concentration was eliminated.
- This left 7.5 and 10 % solids concentrations to be evaluated for further testing.

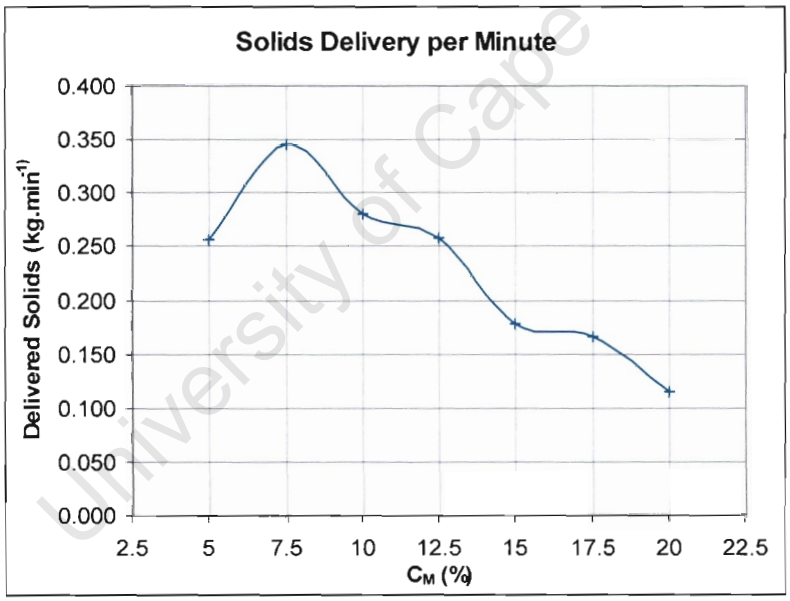

Figure 4.2 Solids delivery per minute.

The flocculant dosages were fine-tuned, having selected the candidate solids concentrations.

4.2.4 Settling rate as a function of flocculant dose

In this test the impact of varying the flocculant dose was tested on the two selected concentrations to determine if there could be any improvement either side of the previous optimal flocculant dose. The settling test results are shown in tables 4.9 and 4.10.

Table 4.9 7.5 % Solids (Concentration 0.0025 %)

Dosage ($g.t^{-1}$)	SR ($m.h^{-1}$)	Flocc (ml)	Water Clarity
0.5	12.67	1.56	Very murky, incomplete flocculation
1.0	16.19	3.12	Very murky, incomplete flocculation
1.5	17.29	4.68	Murky brown water - silt on top of bed
2.5	22.81	7.80	Better, but water still murky and brownish
3.0	24.56	9.36	Water becoming milky, but still brownish
3.5	26.69	10.92	Better clarity, water appears milky
4.0	28.52	12.48	Not much change in clarity, water milky
4.5	26.43	14.04	Same clarity
5.0	26.73	15.60	Same clarity

Table 4.10 10.0 % Solids (Concentration 0.0025 %)

Dosage ($g.t^{-1}$)	SR ($m.h^{-1}$)	Flocc (ml)	Water Clarity
0.5	8.78	2.12	Dirty brown supernatant
1.0	10.78	4.24	Dirty brown supernatant
1.5	9.57	6.36	Dirty brown water - fine silt on top of bed
2.0	14.62	8.48	Clearer water, but not quite milky yet
2.5	14.58	10.60	Milky water
3.0	16.36	12.72	Clearer water, better than previous
3.5	15.78	14.84	Not much change in clarity, water milky
4.0	16.19	16.96	Same clarity
4.5	18.86	19.08	Same clarity

Flocculant dosage was selected at each solids concentration at the point where the settling rate levelled out, and where there was no further improvement in the clarity of the supernatant. The selected dosages (highlighted in the tables) are 12.48, and 14.84 $ml.l^{-1}$ for 7.5 and 10 % solids respectively. Note that these dosage rates are per litre, so that this is easily applied to the plant based on the feed flow rate. There was a slight reduction in the settling rate for 10 % solids above a dosage of 12.72 $ml.l^{-1}$ flocculant.

It was decided to carry both of these forward to an adaptation of the hydraulic loading test.

4.2.5 Modified Hydraulic Loading Test

Having determined the optimum flocculant dosages and the desired concentrations at which to operate, it was now necessary to confirm that the thickener would operate as designed under continuous flocculation and recirculation of the slurry. The target period for testing with a slurry sample was one week.

The hydraulic loading test was conducted to determine the relationship between the hydraulic loading on the thickener (feed volumetric flow rate per unit area of thickener) and the density of the settled mud bed. This test provides the thickener sizing parameter which relates to mud bed residence time.

Two internal fluid rise rates are observed in the thickener under dynamic conditions. The first is the clarified fluid rise rate, which is determined by the feed to the thickener, and the cross-sectional area of the thickener. The second is the consolidated mud bed rise rate. This is determined by the rate at which the material is being deposited, and its density. The compaction of the bed under gravity is working in the downward direction, while material is continually being added via deposition. At the same time there is material being drawn from the underflow of the thickener. This is shown in figure 4.3.

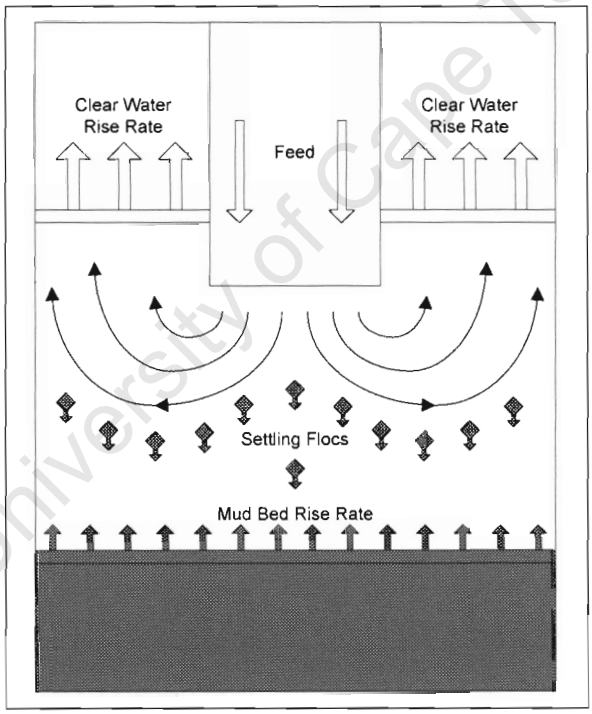

Figure 4.3 Thickener representation showing mud bed and clear water rise rates. The underflow outlet is not shown.

The hydraulic loading test was performed using the laboratory bench scale thickener from Outokumpu. An annotated image is shown in figure 4.4. The rake itself is not clearly visible in the thickener, but consists of three radial arms with plates mounted at 45°.

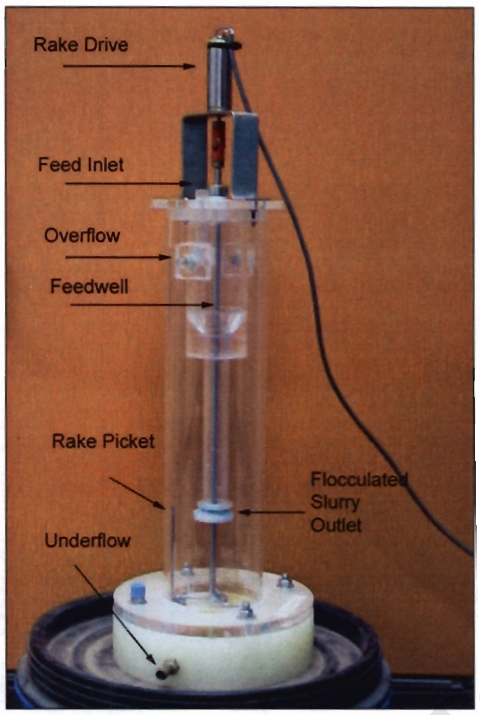

Figure 4.4 Outokumpu benchtop thickener. The height of the thickener vessel is 405 mm, and the diameter is 94 mm. Note that the feedwell outlet is roughly ¼ of the height from the base, and a three bladed rake is installed with a picket at the wall to eliminate sidewall effects.

In figure 4.5 a schematic of the experimental layout is shown. The layout is identical to that in the laboratory scale thickener, with the exception that no dilution circuit is included. Both the overflow and the underflow are returned directly to the slurry tank which has a capacity of 50 litres. Flocculant was introduced via a tee piece just before the slurry enters the thickener.

A series of feed rates were calculated for each concentration. Traditionally the experiment involves timing the rate of rise of the bed between two points. In this case the experiment was modified so that the mud bed level was maintained at a level 7 cm above the base of the thickener. This level is below the exit point for the flocculated feed stream so that the bed does not block the outlet. This also provides a leeway of at least ±1 cm above and below the desired bed position. The difference in this approach is that it permits the stabilisation of the bed at this level over time, before measurements are taken. The traditional method does not take this into account, so that the rise rate is not significantly affected by the extent of compression taking place in the bed. The rise rate of the mud bed is computed by looking at the underflow pump rate and the underflow density when the bed level is stable. From initial tests it was found that this method provided more reliable results, since it was noted that the bed height took some time to stabilise. It was decided to take five measurements of the underflow density and then to use the average to compute the rise rate (the underflow pump rate was static throughout these tests once the bed had finally stabilised).

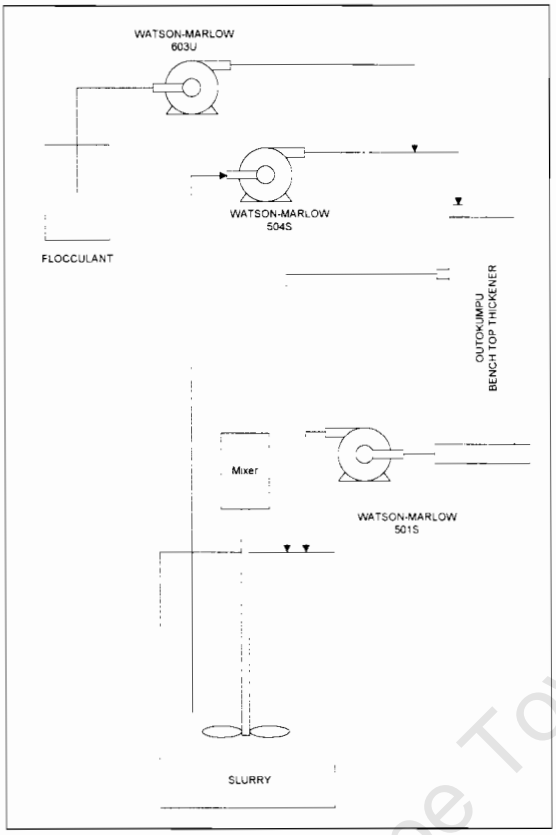

Figure 4.5 Experimental configuration.

The cross-sectional area of the thickener is 0.00694 m^2 (A) at the base. Excluding the lower section of the feed well from the area results in an area of 0.00632 m^2 (A') (the feed well internal diameter is 24 mm, plus the wall thickness of 2 mm). The base of the thickener is filled with sediment, so that the area where the slurry particles are likely to be drawn upward is above the mud bed – hence the use of the smaller area. In full scale thickeners, the feed well is a smaller percentage of the overall area, and does not penetrate as deep into the thickener.

A nominal best settling rate of 25 $m.h^{-1}$ for 7.5 % concentration, and 16 $m.h^{-1}$ at 10.0 % solids concentration were used to arrive at the slurry feed flow rates. In both cases a worst case of 10 $m.h^{-1}$ was used. Using the rise rate and the thickener area the maximum and minimum flow rates were calculated as shown in tables 4.11 and 4.12.

Table 4.11 7.5 % Solids Test Feed Rates

SR ($m.h^{-1}$)	**RR ($m.h^{-1}$)**	**Qi ($l.min^{-1}$) A**	**Qi ($l.min^{-1}$) A'**
25	12.5	1.446	1.318
10	5	0.578	0.527

Table 4.12 10.0 % Solids Test Feed Rates

SR ($m.h^{-1}$)	RR ($m.h^{-1}$)	Qi ($l.min^{-1}$) A	Qi ($l.min^{-1}$) A'
16	8	0.925	0.843
10	5	0.578	0.527

The flocculant dosing rates are taken from the previous section as 12.5 $ml.l^{-1}$ (4 $g.t^{-1}$) and 15 $ml.l^{-1}$ (3.5 $g.t^{-1}$) for 7.5 % and 10.0 % concentrations respectively. The flocculant concentration was 0.0025 % (2.5 mg per 100 ml water), and 2 litres were made up for each day of testing.

The required volume rate of flocculant was

$$V_F = \frac{M_s d_F}{C_F} \times 100 \qquad (7)$$

For a given flocculant dosage at a specific flocculant concentration and feed solids concentration in $ml.l^{-1}$.

It was assumed that all of the solids report to the underflow (not true in practice), and that the underflow concentration is a nominal 50 % solids by mass. The nominal flow rates for the underflow were used as a starting point in each test. The feed and flocculant pump rates were fixed and the underflow pump rate varied to achieve a stable mud bed. The density of the underflow was measured by taking a sample in a 100 ml measuring cylinder, and determining the mass.

Results

Figures 4.6 and 4.7 show the underflow pump rates versus the slurry feed rates at 7.5 and 10 % concentrations respectively. Note that the feed flow rate is equivalent to the hydraulic loading since they are related by the thickener area, and the same is true of the underflow flow rate. These two graphs illustrate that for the purposes of achieving consistent behaviour in the thickener underflow, 10 % solids concentration is the preferred operating value. At 7.5 % solids concentration the underflow flow rates are closer to the nominal but show a greater spread in behaviour over the four days of testing. At 10 % solids concentration the values remain very similar over time even though they are never near to the nominal value, only departing from the norm on the fifth day of testing.

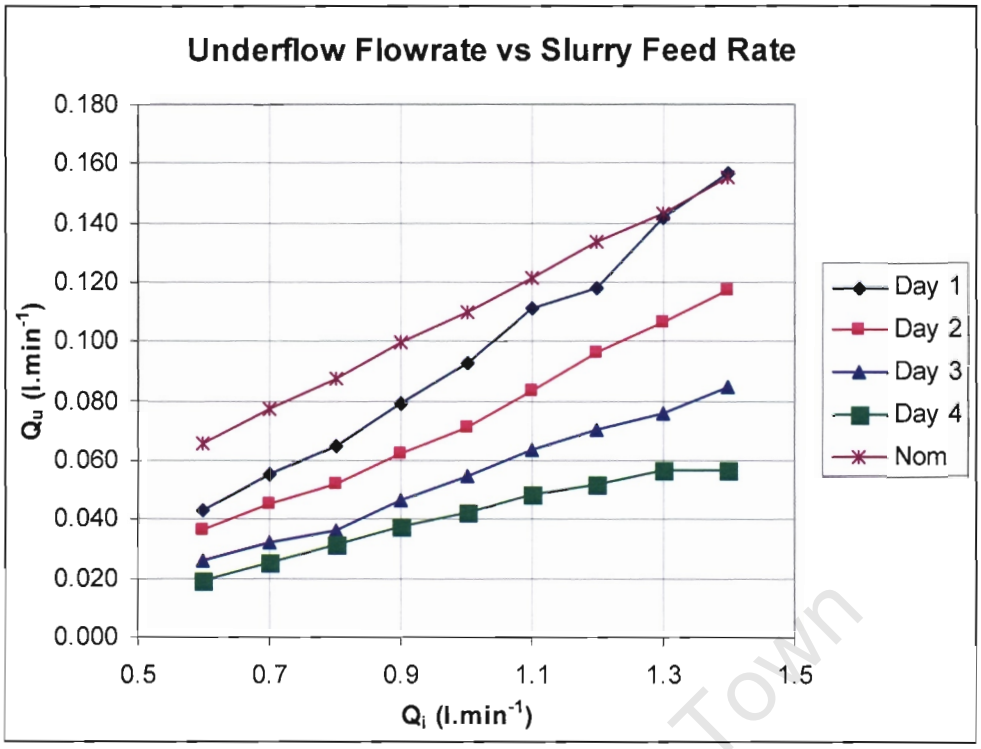

Figure 4.6 Underflow flowrate vs slurry feed rate at 7.5 % solids concentration, showing the spread in underflow flow rates to achieve a stable mud bed over 4 days of testing.

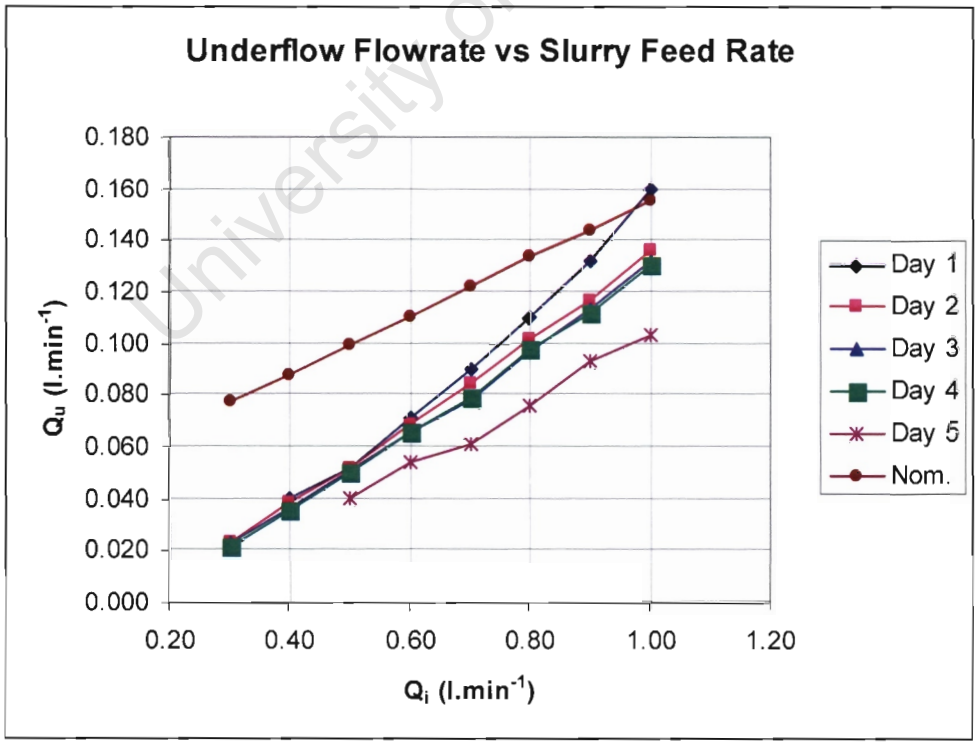

Figure 4.7 Underflow flowrate vs slurry feed rate at 10 % solids concentration, showing consistent underflow flow rates for a stable mud bed over 5 days of testing.

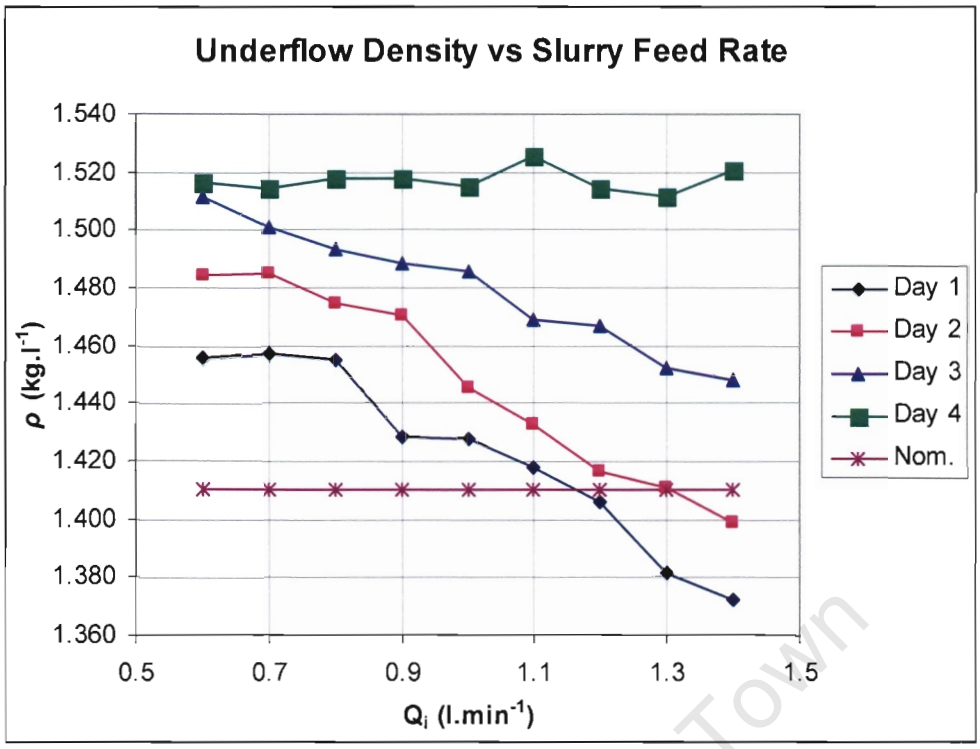

Figure 4.8 Underflow density vs slurry feed rate at 7.5 % solids concentration, showing the spread in underflow density over 4 days of testing.

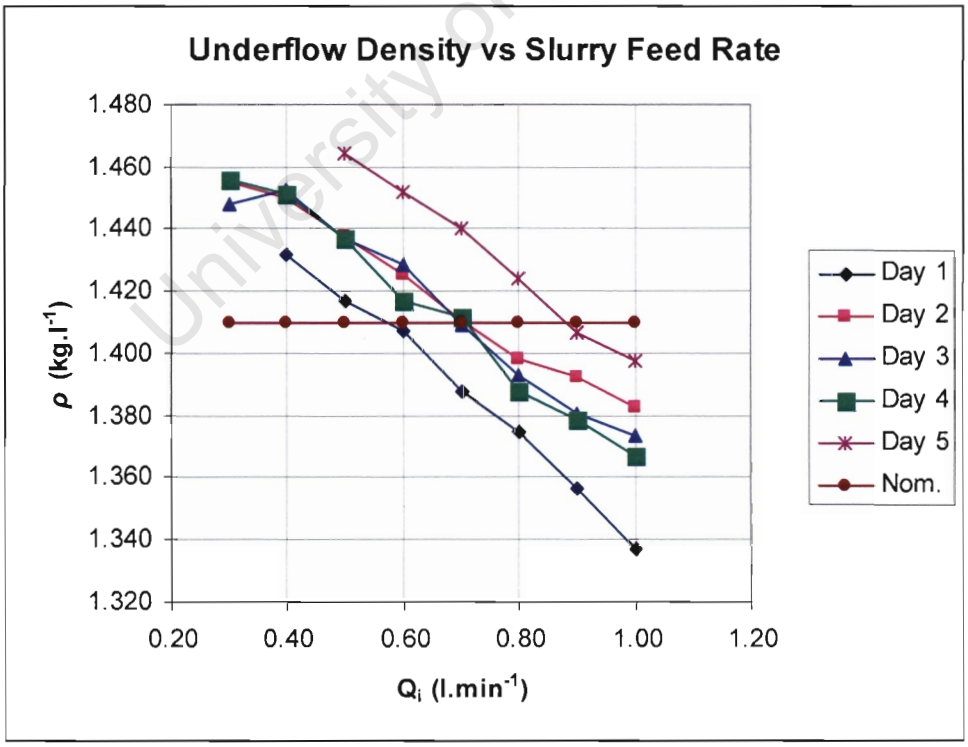

Figure 4.9 Underflow density vs slurry feed rate at 10 % solids concentration, showing consistent underflow densities over five days of testing.

In figures 4.8 and 4.9, the underflow density is presented versus the slurry feed flow rate. The 7.5 % solids concentration results show greater variation, and are further from the nominal values than in the 10 % solids case. To ensure consistent operation over a week of testing the choice of 10 % solids concentration was once again shown to be the better option, and was chosen as the nominal operating point for the laboratory scale thickener. Variations in slurry behaviour over the 4/5 day period are due both to the swelling and breaking up of the clay particles in the slurry, as well as the continual flocculation. Note also that the underflow density saturated during the 7.5 % solids test on the last day of testing.

4.3 DISCUSSION

During the course of the test work carried out it was shown that coagulation is not a suitable means to assist the settling of Finsch Mine kimberlite slurry. The kaolin alternative did not prove to be suitable due to its tendency to form a network that traps water, and its behaviour did not improve under either coagulation or flocculation.

Under flocculation, the kimberlite settled better than required for the thickener test plant design. A design concentration of 10 % solids by mass was shown to be best suited when operated in the bench top thickener, with a flocculant dosage of 12.8 $ml.l^{-1}$ of flocculant at 0.0025 % concentration. The objective of the tests was achieved, since it has been confirmed that the plant can be operated continuously under constant flocculation and still provide a useable mud bed with good underflow densities for control testing in the laboratory.

In order to confirm these results, a set of similar hydraulic loading tests were carried out on the laboratory scale thickener in order to complete the final commissioning. While a scale-up relationship has not been computed for the two cases (lab and bench scale), it was expected that the laboratory thickener would show similar results.

4.4 REFERENCES

1. A Roebl, "Finsch Mine Slurry Characterisation for use in the Scale Test Thickener Plant", De Beers Technical Note 2006-01-02, 16/01/2006.
2. G Langefeld, DBGS Research, Private Communication
3. H van Olphen, "An Introduction to Clay Colloid Chemistry 2nd ed", John Wiley & Sons, 1977
4. Perry RH, Green DW (editors), "Perry's Chemical Engineers' Handbook 7th ed", McGraw Hill, 1997
5. A J Vietti, DGBS Research, Private Communications (currently Patterson and Cooke Consulting Scientists)
6. A Vietti, F Dunn (editors), "Paste and Thickened Tailings Disposal Handbook", 2003 Environmental Technology Research, Technical Support Services – Technology, De Beers Consolidated Mines.
7. Pelichem, Stand 101, Schooner Street, Lazer Park Honeydew, 011 794 5902

CHAPTER 5 PLANT COMMISSIONING

This chapter discusses the commissioning of the Scale Thickener Control Laboratory for Thickener Measurement and Control. The plant has been commissioned according to standard phases of commissioning. These are as follows:

Table 5.1 Commissioning Stages

Phase	Description
C1	Construction, installation, loop checking
C2	Cold Commissioning: drive direction tests and operation.
C3	Wet Module Commissioning (commissioning with water, no slurry)
C4	Product Commissioning (commissioning with slurry)
C5	Completion Certification (complete plant)
C6	Final Certification (plant handover)

The C1 phase of the project was straightforward and is not discussed in this document.

Phase C2 consisted of drive direction testing, and the operation of any equipment that can be carried out without any product or water in the system. Drive direction testing was carried out in conjunction with the project electrical engineer as part of the final certification of the electrical panel. A basic Labview I/O panel was used at this point in order to read and write information to equipment to determine that all was functioning correctly. These aspects of the commissioning are not discussed further in this document.

Phases C5 and C6 are not relevant in this case, although the successful commissioning of the plant fulfils these requirements. They are not discussed further.

Phases C3 and C4 constitute the discussion in this chapter.

Phase C3 consisted of filling the plant with water, and operating it as though it contained slurry. In this phase the plant software was written so that a structure was present in order to design and implement the dilution controller, and then to operate the plant as a whole. With the addition of water it was also possible to check the tank level calibrations, and to ensure that the pumps were delivering the correct flow rates, and to confirm this against the rates measured by the available instruments.

In phase C4 slurry was added to the plant to determine that it operated as required and that there was not significant deviation from the operation of the plant with water. A brief initial test showed a number of problem areas.

- The underflow Coriolis mass-flow meter was moved to the slurry feed line, as its error at the low flows encountered at the underflow showed it to be erratic and inaccurate. It was replaced by a smaller diameter single tube meter that was shown to perform well in comparison with manual samples and with the water calibrated pump flow rate.
- The mass-flow meter at the slurry feed line showed that the agitation was insufficient to keep all of the particles in suspension, and to ensure that they are delivered to the pump inlet. A new agitator with an 800 mm diameter three blade impeller was installed, also requiring the installation of baffles in the tank.

- At the same time baffles were installed in the clear water tank since fines were reporting there from the overflow, and not being returned to the slurry tank.
- It was found that the conical shape of the base of the thickener hindered compression of the sediment under gravity, and was replaced with a straight section.
- Having modified the base of the thickener it was also necessary to install a rake to move the dense slurry to the well at the centre of the base of the thickener where the underflow outlet is located.
- The feed well outlet was located too high in the thickener so that flocs were easily captured and carried to the overflow. The feed well was lengthened, and the problem eliminated.
- The Vega vibrating probes did not always switch as required, and were adjusted to do so.

In the first commissioning tests, a sample used for the initial test and for the slurry characterisation work was run in a similar manner to the modified hydraulic loading test discussed in the previous chapter. In the second test a fresh sample was used that behaved very differently from the previous batch. After some modifications to the flocculation rate it was found that the plant could be operated continuously for a week.

Having operated the plant without dilution control, it was decided that the dilution controller would be used for control tests in the future due to the variations in the feed concentration as solids are held up in the thickener.

The completed software (as built) is discussed in Appendix C. The software is flexible and portions will be modified as future testing demands.

5.1 WET MODULE COMMISSIONING

The section begins with a discussion dealing with the commissioning of the individual instruments and drives where relevant, and any pertinent settings or calibrations. Following this is an explanation of the dilution computer, and dilution controller design.

5.1.1 Tank Level Commissioning and Calibration

The slurry and water tanks are fitted with Endress & Hauser Prosonic FMU 860 ultrasonic level sensors (LT-001 and LT-002). The sensors have a deadband near to the actual probe, so the upper level of the liquid was limited. The location of the outlet pipe does not allow the tanks to be drawn completely empty. A dipstick was used to measure the actual depth of the fluid, and the internal diameter of the tank was measured to complete the calculations. The calibration was carried out with the agitators off. The tank calibrations are given in table 5.2.

Table 5.2 Tank Calibrations

Slurry Tank (1400 m dia.)			Clear Water Tank (1080 mm dia.)		
%	H (mm)	V (l)	%	H(mm)	V(l)
0	97	150	0	24	22
100	1343	2068	100	984	902

5.1.2 Flowmeter Calibration

In order to calibrate the drives and the control valve it was necessary to have the flowmeters operational.

The Yokogawa ADMAG SE115 flowmeter (FT-001) was set up to have a range of 0 to16 $l.min^{-1}$.

The Endress & Hauser Promass 83H mass flow meter (FT-002) was set up to have a density range of 0.9 to 2 $kg.l^{-1}$. The flow range was set from 0 to 5 $l.min^{-1}$. When it was found that the meter had a tendency to block due to its dual tube design, it was replaced with a Krohne OPTIMASS single tube mass flow meter. This instrument was installed in the author's absence, and was found to be erratic and unreliable at low flow rates (below 1.5 $l.min^{-1}$). The diameter of the measuring tube is 15 mm (½"). It was replaced with an Endress & Hauser 83I single tube meter, calibrated to the same density range as before, with a flow range of 0 – 3.5 $l.min^{-1}$. Although the Endress & Hauser meter is specified as DIN15, or 15 mm bore, it is not a full bore version, and has an internal diameter of 8.55 mm.

The dual tube mass flow meter (FT-003) was moved to the slurry feed line and was calibrated for a range of 0 – 20 $l.min^{-1}$.

5.1.3 Drive Commissioning and Calibration

The slurry feed pump was calibrated using the dual tube mass flow meter (FT-003). The dilution water pump (PC-02) was calibrated by observing the flow measurement on FT-001 for various speeds. The underflow pump was calibrated in a similar fashion using the mass flow meter (FT-002). Although problems were encountered later measuring slurry flow, the meter was found to be highly accurate when operating with clean water. A 4 litre beaker was used to confirm the flow rates. This was carried out a number of times for different pump speeds until a calibration curve was created. Since all the pumps in the plant are MONO positive displacement type, the curves are all linear (minimal impact from a static head of 2 m).

The flow ranges and pump specifications are shown in the table below.

Table 5.3 Calibrated Pump Ranges

Pump	Description	Model	Flow ($l.min^{-1}$)
PC-01	Slurry Feed	C32M	0-18
PC-02	Dilution	GF	0-16
PC-04	Underflow	C22M	0-3.5

These calibrated ranges are flexible, and will be adjusted as required during test work. The lower bound on the speed is adjusted by changing drive pulleys or gearbox ratio, and the upper speed bound is adjusted by changing the VSD maximum frequency output.

5.1.4 DILUTION CONTROL

The dilution controller was set up at this point with clear water by providing a simulated underflow density. The intention was to return dilution water to the slurry tank in proportion to the density and volume of slurry being returned from the underflow. A controller allowing fine control of the dilution water was designed and implemented using the combination dilution pump and control valve. The control valve allowed a portion of the dilution water to be returned to the clear water tank to achieve low flow rates. This controller was discarded when the control valve failed, but the design is given in Appendix D.

With insufficient time on hand to replace or repair the control valve, it was decided to eliminate it from the design. At the time of the original design a mass flow meter was not present on the slurry feed line, but had been installed when the underflow mass flow meter was replaced. It was decided to return dilution water to the slurry tank based on the measured density of the slurry feed. This was found to be a better approach for three reasons.

- As the level in the tank varied, the flow patterns changed, so that the amount of solids collected at the bottom of the tank varied.
- As the thickener filled with a dense bed, the overall concentration in the slurry tank was reduced.
- As the slurry feed rate is varied, more or less solids are collected at the pump inlet.

Using a direct measure of the feed concentration was found to be a far superior means of ensuring consistent slurry feed concentration.

Now it was only necessary to have the dilution pump to control the addition of clear water. A new dilution water computer was implemented to generate the setpoint for the dilution pump, and a controller tuned for the purpose of tracking this setpoint. It was found that this circuit controlled within 9 – 11 % solids by mass, whereas it could drop to 7.5 % without the controller in place. Since the slurry tank showed a tendency for the feed concentration to decrease significantly as the dense mud bed builds up in the thickener, the thickener was initially loaded at a concentration of 120 % of the solids required for a 10 % by mass feed. Once the initial mud bed has built up, the slurry feed concentration remained within 9 – 11 % by mass.

5.1.4.1 Dilution Flow Computer

The dilution flow computer that was previously based on the underflow density was discarded, and a new algorithm implemented to generate the setpoint for the amount of water to be returned to the slurry tank.

The first step is to compute the amount of dilution water that must be added to the slurry tank to achieve the correct concentration at the thickener feed. The mass of dilution water required at any instant to correct the slurry tank concentration is:

$$M_d = \rho_{sl} V_{sl} \left(\frac{C_M}{C_{Msp}} - 1 \right) \qquad (1)$$

The entire volume of the slurry tank is assumed to be at the concentration measured at the feed to the thickener. Since the density in the dilution tank is assumed to be that of pure water it follows that the volume of dilution water required is:

$$V_d = \frac{M_d}{\rho_l} = M_d \tag{2}$$

Although the dilution water comes from the thickener overflow, and is at a slightly higher density than tap water, the controller takes care of this in the long run. Since the density is given in $kg.l^{-1}$, it follows that the calculated volume is in litres. To make the added water into a flow rate we must determine over what time period (in minutes) this volume of water will be added to the slurry tank. In this way a flow rate setpoint in $l.min^{-1}$ is generated. This is done as follows:

The dilution water addition is calculated by taking the overflow flow rate, and adding the dilution water flow rate to this. The overflow flow rate is simply the difference between the feed flow rate, and the underflow flow rate. The execution time T_e, is calculated by multiplying the number of execution cycles per minute by the number of minutes over which the action will take place. This becomes an additional gain in the system, since the smaller the time over which the action takes place, the greater the flow rate offset. The dilution water flow rate is thus:

$$Q_d = Q_{ol} + \frac{V_d}{T_e} = Q_{dsp} \tag{3}$$

Notice that in equation 1, the offset is negative if $C_M < C_{Msp}$, and positive if $C_M > C_{Msp}$. It was found that a time of 0.25 minutes provides a suitable dilution water flow rate that remains within the range of the dilution water pump. The range of the dilution water pump (PC-02) was increased to a maximum of 16 $l.min^{-1}$ by increasing the maximum frequency to 80 Hz.

5.1.4.2 Dilution Controller Design

A series of coarse step tests were carried out to characterise the underflow pump. Due to its linear characteristic it was not necessary to carry out a range of step tests over the full pump range. The step response is shown in figure 5.1.

The delay in the system was measured from figure 5.1 as 2.5 seconds, with a gain of 0.15, and a time constant of 4 seconds. This gives the following plant transfer function.

$$P(s) = 0.15\left(\frac{-s + \frac{2}{2.5}}{s + \frac{2}{2.5}}\right)\left(\frac{\frac{1}{4}}{s + \frac{1}{4}}\right) \tag{4}$$

The delay is given by the Padé approximation, and the plant response approximated as a first order system.

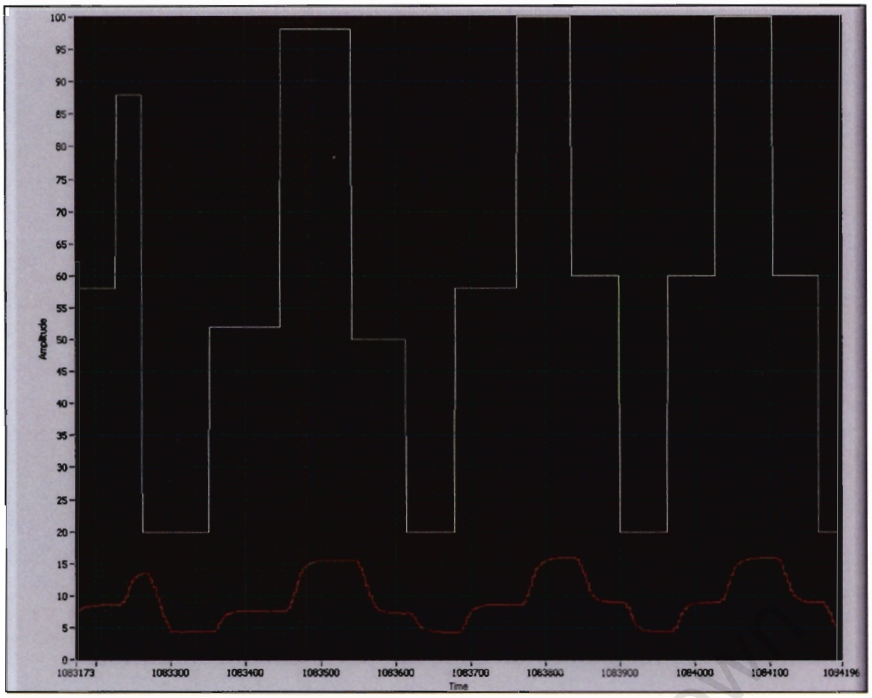

Figure 5.1 Dilution pump step responses. The x-axis shows execution intervals, where the software executes every 250 ms. The upper curve is the input, and the lower curve is the output.

In Labview the PI algorithm is implemented as follows:

$$C(s) = K_p\left(1+\frac{1}{T_i s}\right) = \frac{K_p}{T_i}\left(\frac{T_i s+1}{s}\right) \tag{5}$$

Using the Root Locus in Matlab SISOTool, and designing for a maximum overshoot of 5 %, with the fastest possible response, the following results were achieved.

$T_i = 4$ s
$K_p = 3.6$

Since the integration time in Labview is given in minutes, the value of T_i becomes 4/60 = 0.067. While implementing the controller it was found that the ramp-up time configured in the VSD was 10 seconds, and this applies rate limiting to the controller output. This time was reduced to 2.5 seconds before testing the controller. The controller was found to track the generated setpoint within ±0.5 % at 10 % solids concentration. This controller is not critical since the expected variations in setpoint later are not expected to be large.

5.1.5 Flocculation Pump Installation

To be able to complete the product commissioning it was necessary to install and calibrate the flocculation pump. The pump is the same Watson-Marlow 603U/R [1] used in the slurry characterisation tests. It was necessary to modify the system wiring so that it could be driven by a remote 4-20 mA signal, and then carry out a recalibration from the original front panel settings. The flocculant was introduced in a tee piece located just before the slurry enters the thickener. The slurry feed hose is snaked around the outside of the feed well so that the slurry is delivered tangential to the feed well wall. In conjunction with the spreader at the base of the feed well, this helps to mix the slurry and flocculant so that floc aggregates are able to form.

The present scaling of the output is 15.8 $ml.l^{-1}$ at 18 $l.min^{-1}$ slurry feed to give an output of 90 % to the pump. The 603U/R pump has an internal controller that allows it to run right down to 0 %. It becomes slightly non-linear below 10 % and above 90 % and is not used in this region. The flocculant flow rate is thus

$$Q_f(\%) = Q_t \frac{d_f}{1000} K\% \qquad (6)$$

Q_t = slurry feed rate ($l.min^{-1}$)

d_f = flocculant dosage ($ml.l^{-1}$)

K is the tuning parameter according to adjustments made to the range potentiometers on the 603U controller circuit board. This scales the software value from $l.min^{-1}$ to %, which is output to the Fieldpoint analogue output module which delivers the mA signal accordingly. The present value of K is 315.95. The pump can be recalibrated as required, although it is simpler to change the flocculant concentration. A 20 litre bucket is available for flocculant to be used for each day of testing. Fresh flocculant is made up each morning and then as required depending on consumption. Although the original intention was to make up only one bucket of flocculant, it was found that it was difficult to mix high concentrations effectively without clusters of undissolved flocculant forming.

5.2 PRODUCT COMMISSIONING

In the product commissioning phase a kimberlite sample was introduced at 7.5 % solids, and making up 1600 l. This was run through the plant with the intention of carrying out a final commissioning test, but it soon became apparent that there were a number of problems in the system. These are listed below:

1. The Vega probe switching did not always take place in the presence of the mud bed.
2. The conical base of the thickener appeared to hinder compression of the underflow so that densities above 1.3 $kg.l^{-1}$ could not be achieved.
3. The bottom of the feed well was located too high up in the thickener so that slurry reported easily to the overflow.
4. A rake or picket was required to prevent the slurry from rat-holing and reducing the underflow density further.

5. The slurry tank agitation was inadequate, and the desired feed slurry density was not achieved.

These issues are addressed in the following sections, prior to a discussion of the final commissioning tests.

5.2.1 Vega Probe Switching

The Vegavib 52 probes did not always switch reliably. It was found that as more flocculant was added to the slurry, the properties changed somewhat so that the required amount of damping was not present. These probes are specifically designed to switch according to a solids level within a liquid. This took place even when the sensitivity of the instrument was at its maximum. It was subsequently found that there is an additional factory-set potentiometer on the circuit board, and adjusting this permits a coarse adjustment of the sensitivity [2]. No further problems were encountered after having carried this out.

It was also noted that hysteresis is present in the switching behaviour. When the sediment reaches the top 1/3 of the probe it switches on, and when the sediment is at the lower third of the probe it switches off again. The switching in these regions is not precise, and will have to be accommodated for in the control design. In a full scale thickener this will be of little to no consequence when the size of the probes is compared with the depth of the thickener, but due to the scale of the test thickener it becomes a factor. The probes are 160 mm long and 18 mm in diameter [2]. This means that the difference between the 'on' and 'off' switching depths is approximately 55 mm.

5.2.2 Thickener Modifications

It was found that the underflow density increased to approximately 1.24 $kg.l^{-1}$ until the slurry reached the beginning of the conical section at the base of the thickener. As it began to rise in this region the underflow density began to decrease again. A number of pickets were attached to the rake drive described in the following section as it was expected that rat holing was taking place. Rat holing is where the pump preferentially draws lower density material from layers above because it has a lower resistance to flow. Pickets are vertical rods that are designed to assist in dewatering by providing a path for entrapped water to escape. The rotating pickets did not significantly improve the underflow density.

Looking at the thickener, it was thought that the conical section actually inhibits gravity compression of the slurry, and enhances the opportunity for rat-holing along the shaft of the picket drive. Figure 5.2 shows what was thought to happen, and figure 5.3 shows a photograph of the thickener as manufactured.

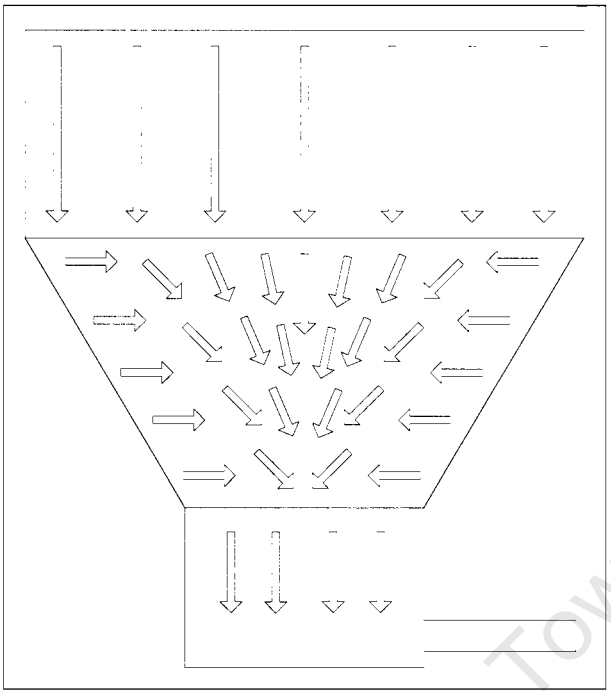

Figure 5.2 The badly behaved conical portion at the base of the thickener - where it appeared that compression of the mud bed was limited while the slurry was making its way to the well at the base. The arrows show the hypothesized path of the slurry.

It is obvious that the only portion of the thickener that has the full bed height for compression is that directly above the well. Unfortunately the contraction in the conical section also means that material is pushing inward toward the centre as it attempts to move down in the cone. It is surmised that this results in a locking effect that prevents material from moving down to the base, as well as preventing dewatering, since a network is formed that holds the water in. It would seem that there is some solid reasoning behind the Outokumpu bench top thickener having a flat bottom. Note that this issue may not be present on full scale thickeners, and may only appear on these small scales, although it is the opinion of the author that thickeners with steep conical sections at the base are not effective. One reason for this is that there is only a very small volume of slurry available to pump at the base where the compression would be the highest, since the conical volume is small.

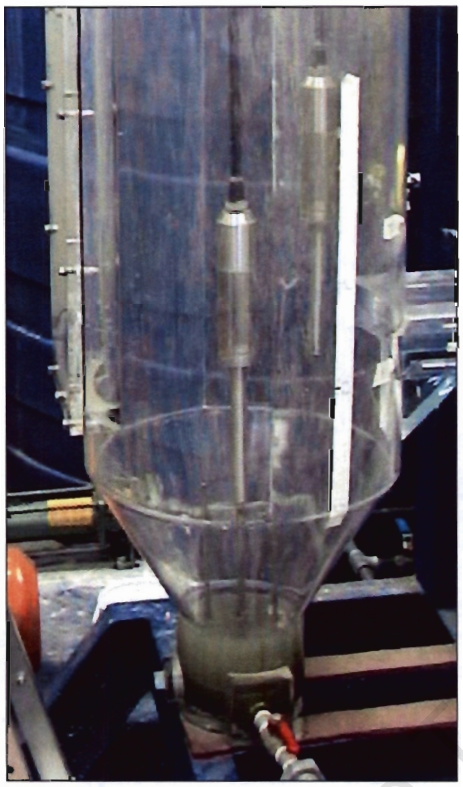

Figure 5.3 The conical portion at the base of the thickener, with the underflow outlet visible at the front of the image (pipeline featuring red hand operated flow valve). The two Vega probes and the pickets are visible in the thickener.

The thickener base was changed to make this section completely straight sided, but requiring a rake (rather than pickets) to move material towards the well. It may have been suitable to put a mild slope on the base, but this was not a cost effective solution. It is far easier (and less time consuming) to make modifications to the rake than it is to make further modifications to the thickener structure. Figure 5.4 shows the base of the thickener with the straight extension in place. The horizontal band is the point where the conical section was previously located.

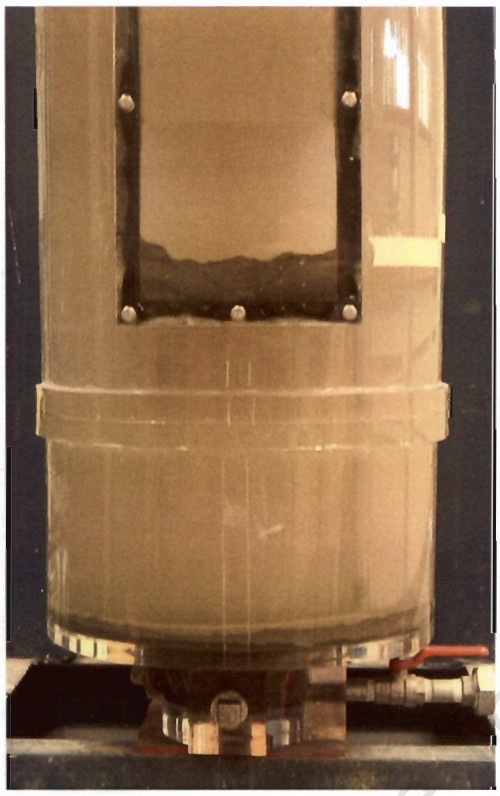

Figure 5.4 Modified thickener base showing flat bottom section replacement for the conical section originally mounted below the horizontal hoop.

An additional modification was made to the feed well. It was noted that the feed well was too close to the overflow, and that material easily reported to the overflow since there was not enough time for it to gravitate through the turbulent flow at the exit. The feed-well was extended by 400 mm to a total length of 700 mm. The base of the spreader is 100 mm below this so that material is delivered 800 mm from the top of the thickener. The total length of the thickener from the top of the feed well is 1700 mm. This places the feed well exit about halfway down the thickener. The location of the feed well exit can have significant implications. It was observed that some space is required below the exit since flocculation continues to occur between the exit, and the surface of the mud bed.

The feed well was easily modified by bonding an additional section of clear Perspex to the bottom of the existing feed well. The spreader below the exit is fastened with stainless steel tie rods so that all that is required is the drilling of three small holes to refit it to the new bottom section. Additional modifications will be made if necessary during the course of controller testing.

5.2.3 Rake Installation

A number of picket devices were tested to determine whether the dewatering in the underflow could be improved. After testing four devices it was concluded that the conical section was to blame for the lack of compression. Having modified the thickener to have completely straight sides meeting perpendicularly with the bottom, it was necessary to include a rake to move the dense slurry along the flat bottom to the central well where it is pumped out of the thickener.

According to the AMIRA P266C report, the optimum blade angle is 30^{o} – 40^{o} to the track along which it rotates. This is sensible in a larger diameter thickener where the angles to the track do not vary much from the outside edge of the blade to the inner edge. In order to achieve this in the scale thickener, the blades would have to be ridiculously small for such a small base diameter. A rake similar to that in the Outokumpu bench top thickener was designed, using three blades, and a picket at the end of the blade that extends furthest to the wall. The purpose of the picket is to remove any wall effects that might tend to hold the slurry up, and hinder compression. A brief exercise was carried out in an attempt to balance the torque on the three arms, but this resulted in a very small outer blade, and an overly large inner blade. The blades were set at 45 degrees to the arms, evenly spaced over the radius (see figure 12). A 50 % overlap was selected, with a 5 mm gap below the blades, and a 5 mm gap at the wall. The inner blade overhangs the well at the base by 10 mm. The rake assembly was made up with an adjustable collar so that the height could be varied, and fixed to a central shaft coupled to the drive motor with a Fenner jaw coupling. The jaw coupling eliminates any direct stress on the motor-gearbox combination. The bottom of the jaw coupling turns on a 5 mm Teflon washer so that the load of the rake and shaft are taken up by the mounting bracket. The bottom of the shaft locates in the central drain in the well at the base of the thickener. A rudimentary speed controller and transformer were supplied with the motor. The speed was set to approximately 2.5 rpm based on the setting used in the Outokumpu thickener. See figure 5.5 for a layout of the rake and the radii along which the blades travel. The blades are all the same size and fixed to the supporting arms at the top centre of each blade.

A rough torque requirement estimate was computed from:

$$F = \frac{1}{2}\rho \upsilon^{2} C_{D} A \qquad (7)$$

The drag coefficient C_D is taken to be 1 as a worst case (in other words it is assumed that the blade acts as though it is a flat plate when its area (A) is projected into the track of rotation). Each blade is 75 mm wide and 40 mm in height. The density of the slurry is taken to be 1600 $kg.l^{-1}$. The velocity was taken as that for the longest arm of 140 mm. The maximum design rotational speed of the rake is 3.5 rpm. The circumference at the maximum radius is 880 mm, giving a speed of approximately 3080 $mm.min^{-1}$ or 0.051 $m.s^{-1}$, which is very slow and unlikely to require a great deal of torque to move. The combined force on the three blades if they were all at the periphery is 0.037 N.

Coupling this with the shaft length of 140 mm gives a very low torque requirement of 0.005 Nm.

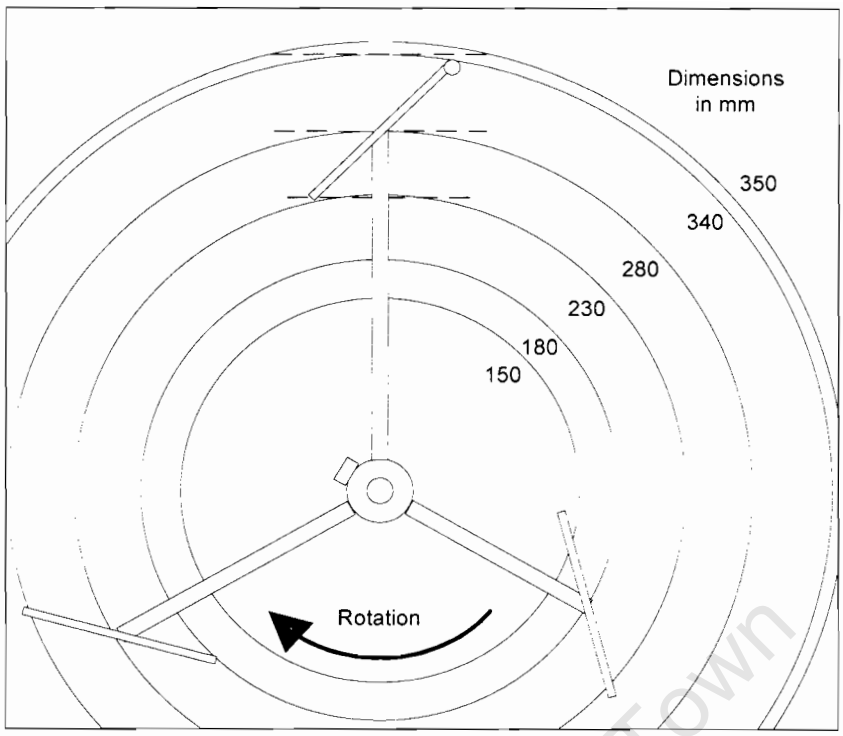

Figure 5.5 Rake blade configuration (diameters shown).

The motor selected was chosen because it is an industrial type with heavy duty metal gears. Other motors considered for this design torque have plastic or Teflon gears and are not expected to be very long lasting. The motor is required to run continuously.

The specifications for the selected SPG motor and gearboxes are tabulated below.

Table 5.4 SPG Motor/Gearbox Specifications

Item	**Model**	**Specifications**
Motor	S6D15-12/0B05	12 V dc, 1.9 A (max), 15 W, 0.13 N.m. torque, 1470 rpm
Gearbox 1	S6GX10B	10:1 ratio, efficiency 81 %
Gearbox 2	S6DA40B	40:1 ratio, efficiency 73 %

The speed of the motor is reduced through the two gearboxes bolted on at the shaft end, at the same time this increases the torque output at the gearbox shaft. The maximum output speed after the two gearboxes is 3.675 rpm. The torque is multiplied by the gearboxes, but must be multiplied by the gearbox efficiency at each stage. After the second gearbox the torque is 30.75 Nm, which is a great deal more than is required. This analysis does not include effects due to the viscosity of the slurry, but it was not expected to be a problem due to the significant excess torque available.

A Phoenix Contact MCR-S-1-5-UI [3] current measurement module was installed to monitor the load on the rake as the underflow properties are varied. It was not certain whether the large gear ratio will hide the effects of load change since the available torque is so high, although it was expected that the rake load only needs to be greater than the gearbox losses to

be visible in the motor current. An alternative was to mount the motor on a freely rotating gimbal and to measure the torque using a strain gauge or torque sensor.

A Phoenix Contact MCR-C-UI-UI-DCI [3] module was installed so that the motor voltage can be measured. This module is an isolation amplifier, and allows the measured voltage to be converted to a current signal.

A Turck MS25-UI [4] rotational speed transmitter delivers a speed output based on the frequency signal from a proximity switch mounted at the drive jaw coupling. There are four teeth on the jaws so that four pulses are generated per revolution. The transmitter includes averaging to smooth the signal since only 8 pulses are generated per minute when the rake rotates at 2 rpm. There is a possibility that some properties of the thickened slurry rheology can be extracted from this information.

5.2.4 Agitator Upgrade

When the underflow Coriolis meter was moved to the slurry feed line, it was found that the delivered slurry was below the concentration initially made up in the tank. This is not to be confused with the decrease in concentration when there is a large mass of solids in the thickener and the true concentration in the tank is reduced (which also took place). It was clearly determined that the agitation was inadequate when the tank was flushed, and the agitator was not able to lift the solids from the bottom of the tank so that they could be removed by the slurry pump. When the speed of the agitator was increased moving waves built up in the tank that were strong enough to move the tank with 1600 kg of water along the laboratory floor, so the speed was limited. Both agitator impellers had the same pitch, so that no counter motion was produced to generate enough turbulence to assist in keeping the particles in suspension.

To correct this two vendors were approached, namely Mixtec, and Lightnin' Africa. The two designs are summarised in table 5.5 along with the parameters for the existing agitator, and the clear water agitator.

Table 5.5 Agitator Specifications

	Stallion (existing)	**Mixtec**	**Lightnin'**	**Mixtec (clear water)**
Position	Vertical, centre	Vertical, centre	Vertical, centre	Vertical, centre
Rating (kW)	0.37	1.5	2.2	0.37
Speed (rpm)	147	118	286	173
Impellers	2	1	1	1
Dia. (mm)	300	800	559	400
Baffles	-	3 (117 mm wide)	3 (120 mm wide)	3
N_{Re}	14.5×10^6	83×10^6	98×10^6	30.5×10^6

The Mixtec solution was selected for a number of reasons.

- The bigger impeller running at slower speed was expected to reduce the break-up of clay particles swollen with water.
- The Lightnin' motor is large, and too heavy for the existing framework, and ceiling clearance was insufficient.
- The Lightnin' motor required the addition of a VSD two frame sizes larger than the current VSD, and there wasn't sufficient space in the panel to mount the larger VSD. The Mixtec motor required a VSD only 1 frame size larger, which is the same size as the current pump VSDs in the same row, and there was sufficient space.
- The Lightnin' agitator was more expensive, and the increased cost of the larger VSD meant the selection of the Mixtec was the best solution. The agitator in the clear water tank is also of Mixtec design.

A comparison of the two agitators in terms of the impeller Reynolds number shows that the two designs are similar. The impeller Reynolds number is given by [5]:

$$N_{\mathrm{Re}} = \frac{D_a^2 N \rho}{\mu} \tag{8}$$

Where the density, ρ, and the viscosity μ are the same in both cases. For similarity the product of the speed and the square of the impeller diameter should be similar. For the Mixtec agitator the product is 75.52, and 89.37 for the Lightnin' agitator. The resulting impeller Reynolds numbers with a density of 1100 $kg.m^{-3}$, and a viscosity of 0.001 Pa.s (water) gives approximately 83 x 10^6, and 98 x 10^6 for the Mixtec and Lightnin' agitators respectively. Flow in the tank is deemed to be turbulent when N_{Re} > 10 000 [8]. Using a slightly higher viscosity of 0.01 Pa.s only reduces the outcome by a factor of 10 so that conditions still remain well in the turbulent region.

Both manufacturers specified a centrally located vertical agitator with a single impeller, and the inclusion of baffles to eliminate swirling and increase turbulence to keep the particles in suspension. The Mixtec impeller is fitted with flow straighteners beneath the blades.

Estimates for baffle dimensions are given in Perry [5]. A common baffle width is $^1/_{10}$ to $^1/_{12}$ of the tank diameter (1.4 m). For agitating slurries, the baffles are often located ½ their width from the vessel wall to minimise the accumulation of solids on or behind them. This means that baffles of width 116 – 140 mm were required, with a wall spacing of 58 – 70 mm. A width of 120 mm was selected as suggested by Mixtec. A wall spacing of 30 mm was selected at the sides to provide extra clearance for the impeller and to reduce interference, with 100 mm at the bottom to prevent build-up. Three baffles were fitted to coincide with the three blades of the impeller. Three or four are usually fitted but it is good practice to match the number of baffles with the number of blades to avoid the build up of resonance due to the interference of the flow with the baffles and the impeller. This can result in vibrations in the agitator shaft, and ultimately in the premature failure of the seals at the base of the agitator gearbox resulting in oil leaking into the slurry.

Both of the tanks are plastic, and the available options were to purchase a fibre tank with moulded baffles, or a stainless steel tank with installed baffles. The moulded baffles do not provide wall or floor clearance so that build up will take place against the sides. Stainless steel tanks are expensive, and in either case replacement would have involved removing the supporting framework and piping in order to make the change. It was decided to design and

manufacture stainless steel cages supporting the baffles, and to construct these inside the tanks.

Appendix E provides details of the baffles for the slurry and clear water tanks. Baffles were also fitted to the clear water tank to reduce sloshing, which makes the tanks unstable as well as putting unnecessary axial loads on the shafts. The clear water tank agitator gearbox seals failed for this reason and had to be replaced. The cage designs show only the baffles, base arrangement, and the top arrangement. The slurry tank arrangement differs in that it includes a centre hoop to stabilise the baffles and prevent oscillations due to flexing. All components were manufactured from 4.5 mm stainless steel. The cages were designed to fit into the tanks snugly, and the addition of the bolts to secure the components at the wall increased the diameter slightly so that it became a tight fit sufficient to secure the cages in place.

Testing of both agitators with the baffles in place showed that there was no movement of the baffles, and that the surface of the fluid was almost completely calmed, eliminating the swirling problem, and improving the tank level measurements.

During the commissioning tests with slurry it was found that close to the correct concentration - at 10 % solids - 1.062 sg, an sg of 1.059 was measured (with the coriolis meters known to slightly under estimate the density) - compared with the previous measurement of approximately 1.040 sg. Flushing of the tanks showed that all solids could be removed from the tanks by pumping. It was also found that the agitator could be run at 35 – 40 Hz and still achieve excellent suspension of the solids at 10 % concentration, leaving room for the agitation of higher concentration slurries.

It was now possible to commence the evaluation of the coriolis mass flow meter and the commissioning tests.

5.2.5 Coriolis Mass Flow Meter Evaluation

To evaluate the mass flow meter with actual test results, the density and flow errors were compared for the two different samples. The measurements were taken once the mud bed level had stabilised at a level of 350 mm above the bottom of the thickener. The level was adjusted by changing the underflow flow rate, resulting in a change in density due to the change of residence time for the thickened slurry. A greater residence time (lower underflow flow rate) gives more time for compression of the bed and thus results in higher underflow density.

a) Density Evaluation

The sampled density is calculated from the mass M of a measured volume V, and the density is:

$$\rho = \frac{M}{V} \tag{9}$$

The absolute error in this measurement is given by [6]:

$$\delta\rho = \left|\frac{\partial\rho}{\partial M}\delta M\right| + \left|\frac{\partial\rho}{\partial V}\delta V\right| \quad (10)$$

This can be rearranged to give

$$\frac{\delta\rho}{\rho} = \left|\frac{\delta M}{M}\right| + \left|\frac{\delta V}{V}\right| \quad (11)$$

In the first commissioning test, manual samples were taken in a 6 litre plastic bucket, and in the second commissioning test a 1 litre measuring cylinder was used.

The following measurement errors apply

$\delta M = \pm 0.0005$ kg
$\delta V_6 = \pm 0.052$ l
$\delta V_1 = \pm 0.005$ l

Where V_6 applies to the 6 litre bucket, and V_1 to the 1 litre measuring cylinder.

The error in the Promass 83 I Coriolis mass flow meter density is stated as

$\delta\rho = \pm 0.02$ kg.l^{-1}

in the operating manual [7]. This error applies to the standard instrument calibration carried out with tap water, setting the density reading to 1 kg.l^{-1}. The error can be improved to ± 0.002 kg.l^{-1} through field commissioning with a second calibration point. To complete an accurate field commissioning an accurate calibration sample is required. Coriolis mass flow meters are designed for homogeneous liquids such as molten chocolate or syrup. This is not true for the kimberlite slurry. The fine clay particles behave like a homogeneous medium, but the larger solids do not oscillate with the medium due to their higher inertia. It was not expected that the high accuracy that is expected from homogeneous media would be obtained here. The error in single tube meters is higher than that in dual tube meters according to the specification in the manual. The stated error in density measurement is a fixed quantity whereas the volume measurement error is a function of the reading and range of the instrument.

Figure 5.6 shows the results for the first commissioning test (Day 4). The manual sample data is in reasonable accordance with the measured values, with the exception of the first reading at an underflow rate of 8 l.min^{-1}. The mean error in the sample measurement was found to be 0.0135 kg.l^{-1} with a standard deviation of 0.000159 kg.l^{-1}. For clarity the error on the sample measurement is shown as a dashed line, and the error on the meter is shown with error bars. 99 % of the error in the sample measurement is due to the uncertainty in the volume measurement. In the second commissioning test a 1 litre measuring cylinder with improved accuracy was used.

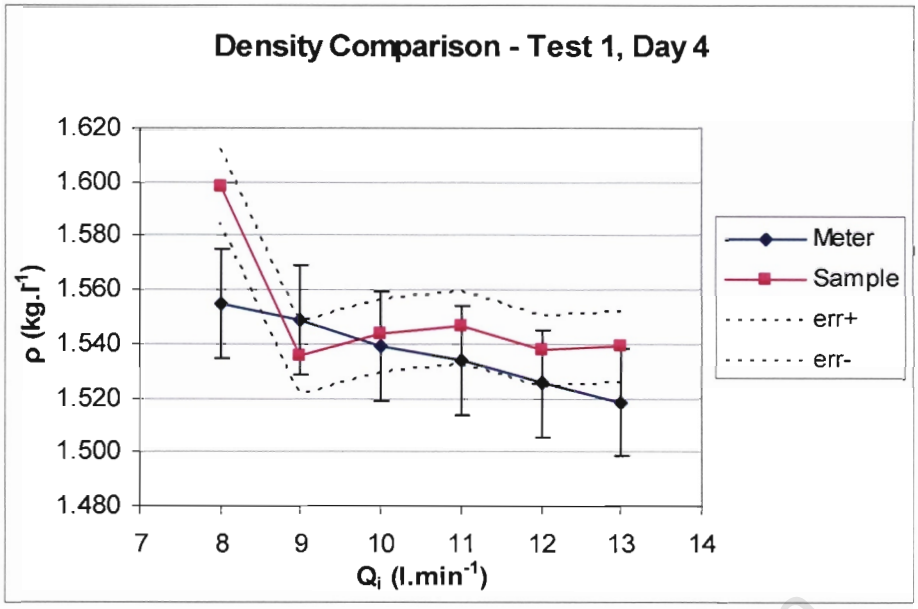

Figure 5.6 Density comparison for test 1, day 4.

Figures 5.7 and 5.8 show the results for the 3rd and 4th days of the second commissioning test carried out with the new sample. The data from day 2 was insufficient to draw any conclusions from as it was incomplete. The data for days 3 and 4 is encouraging and shows that with this particular sample the correlation between the sample measurement and the instrument is within the measurement error of the instrument.

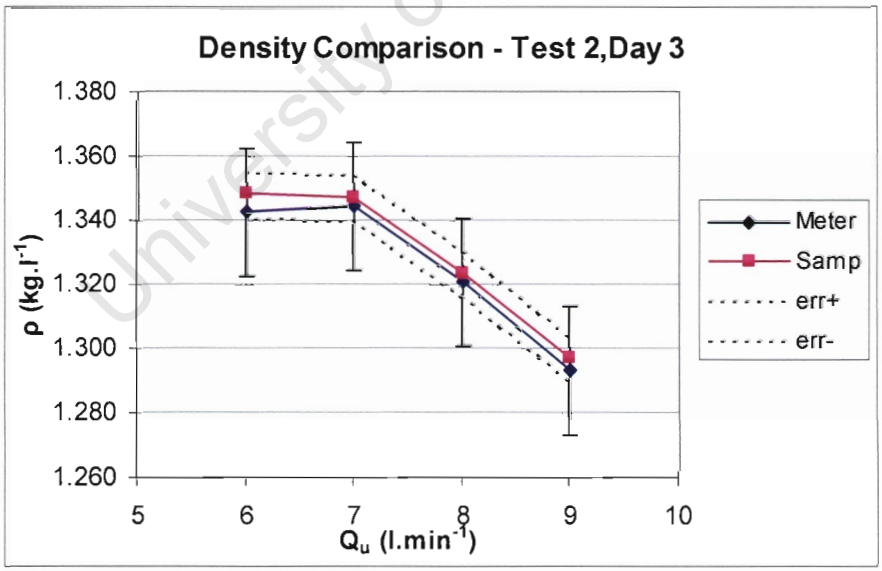

Figure 5.7 Density comparison for test 2, day 3.

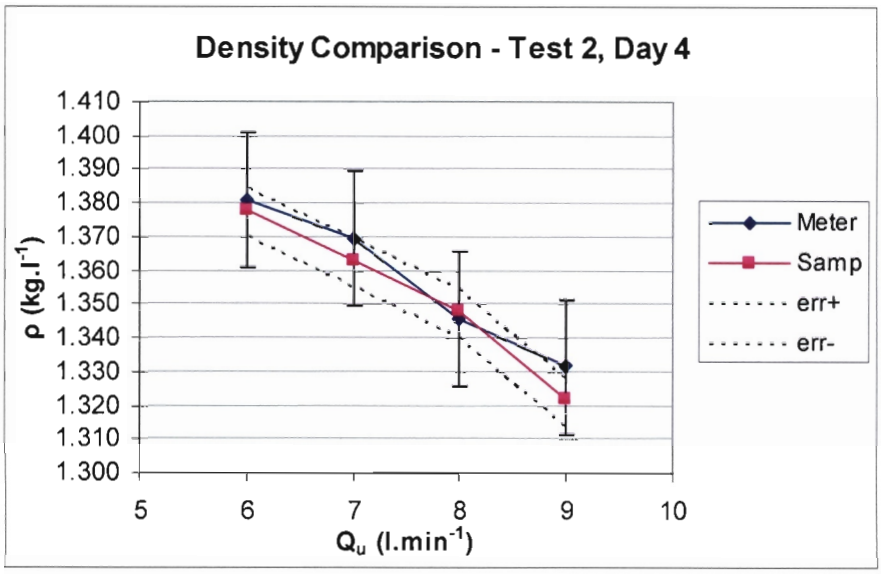

Figure 5.8 Density comparison for test 2, day 4.

The mean error between the measurements for the second commissioning test is 0.0072 $kg.l^{-1}$ with a standard deviation of 0.00016. The mean error is significantly better than that in the first test (0.0135 $kg.l^{-1}$), and the standard deviations are the same for the two tests. The difference in the mean errors are due to the difference in particle size distribution as shown in figure 5.9. The particle size distributions are measured using the Honeywell Microtrac X100 particle size analyser. The 'Old' trace refers to the first sample tested. Note that the 'New' sample contains almost double the amount of fines in the 10 μm range as the 'Old'. It was noted during sieving that the old sample contained more grits than the new sample.

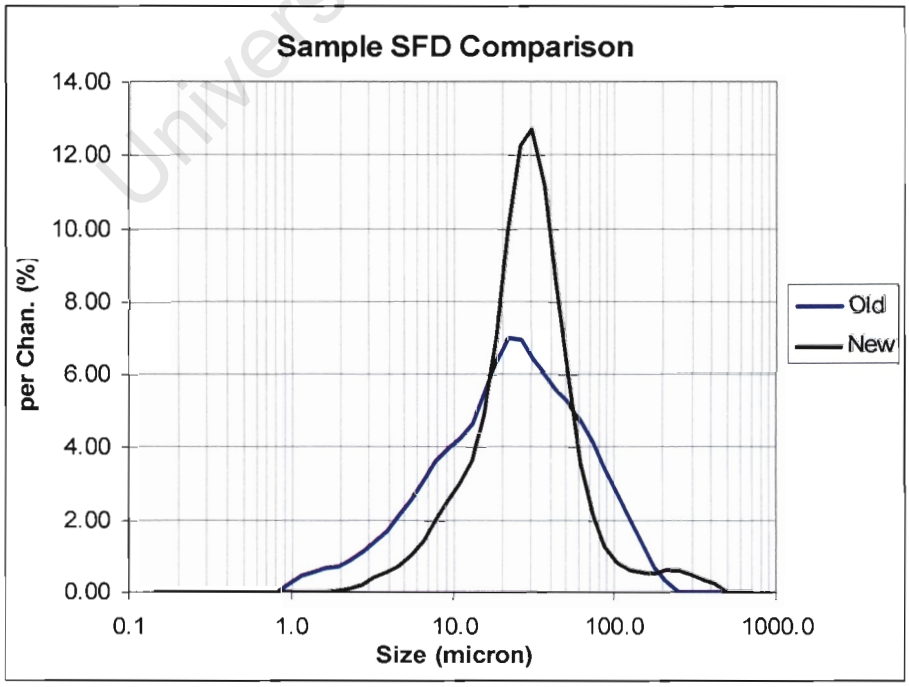

Figure 5.9 Sample SFD comparison.

The density measurement results are better than those obtained with the flow results (which follow) since density is the primary measurement of the instrument. The density is directly proportional to the amplitude of oscillation in the measuring tube which is maintained at a fixed level [7]. As the fluid density changes the amplitude is adjusted back to the preset level giving a direct indication of the density, hence the fixed error range for density.

The density measurement of the instrument is adequate for the purposes of the laboratory. Due to variations in the sample makeup it is not possible to give an absolute measure of the accuracy of the instrument with kimberlite slurry. It will be necessary to continue taking manual samples throughout the control tests to confirm the behaviour with each sample as the data shown above are somewhat limited.

b) Flow Evaluation

The errors in the flow are computed from

$$\frac{\delta Q}{Q} = \left|\frac{\delta t}{t}\right| + \left|\frac{\delta V}{V}\right| \tag{12}$$

Since the volume and time are correlated, only one contributes to the error, and the flow rate error reduces to

$$\delta Q = Q\left|\frac{\delta V}{V}\right| \tag{13}$$

With

$\delta V_6 = \pm 0.052$ l
$\delta V_1 = \pm 0.005$ l

as for the density calculations. Figures 5.10, 5.11, and 5.12 show the results for the flow rate comparison. In this case the calibrated pump flow values are also included since these were previously set for the desired flow rates. The error bands around the measurements are shown as dashed lines. As can be seen in the figures all three flow estimates follow the same trend, but offsets are present.

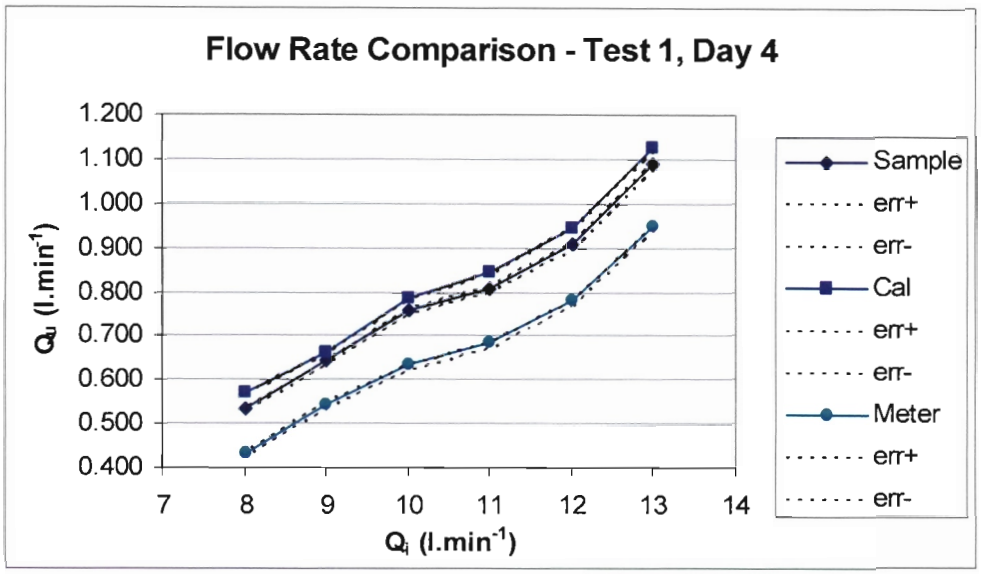

Figure 5.10 Flow rate comparison for test 1, day 4. The errors are small, and can just be seen above and below the respective traces.

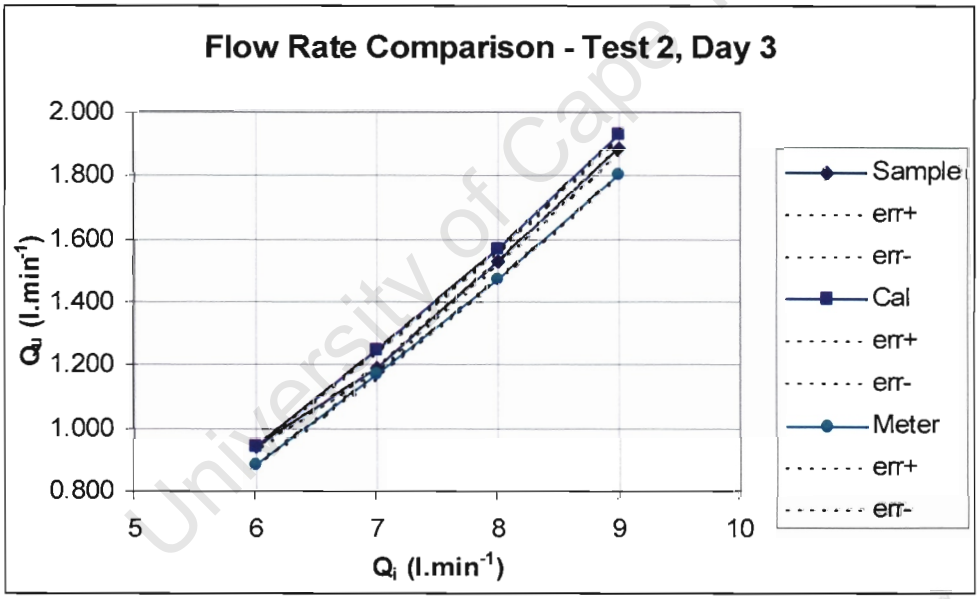

Figure 5.11 Flow rate comparison for test 2, day 3. The errors are small, and can just be seen above and below the respective traces.

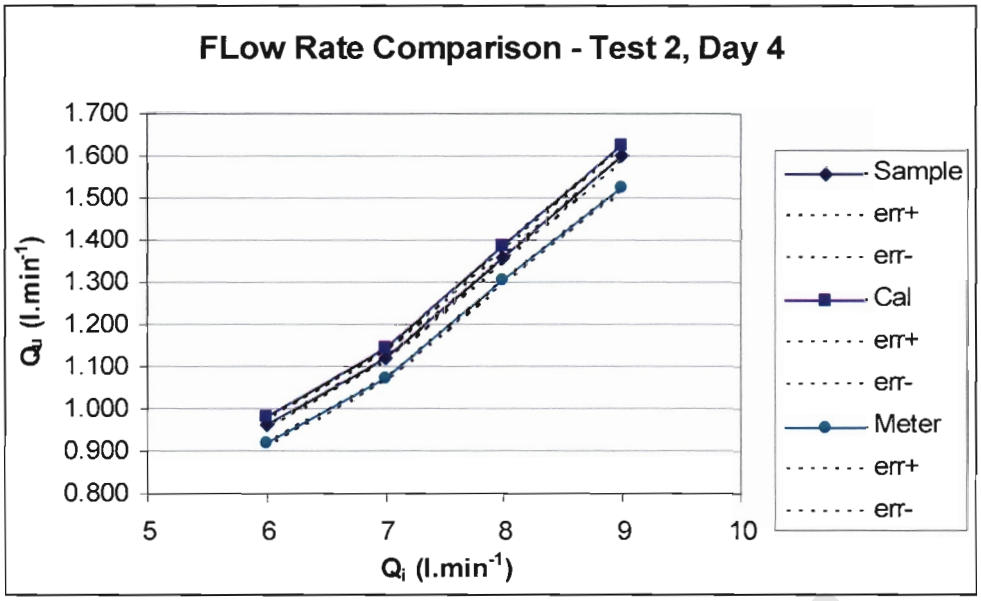

Figure 5.12 Flow rate comparison for test 2, day 4. The errors are small, and can just be seen above and below the respective traces.

The mean errors are shown in the following table

Table 5.6 Comparative Flow Errors

	Test 1		Test 2	
Error ($l.min^{-1}$)	**Mean**	**Std. Dev.**	**Mean**	**Std. Dev.**
Calibrated – Sample	0.032	0.0076	0.029	0.0129
Sample – Meter	0.120	0.0170	0.051	0.0176
Calibrated - Meter	0.152	0.0212	0.080	0.0207

The errors between the calibrated flow rate and the sampled flow rate in the underflow were lowest for both tests, with the lowest standard deviations. On this basis the calibrated flow was used for future measurements, along with the meter density. The same was applied to the slurry feed meter, and the feed controller already used the calibrated flow for its PV.

5.2.6 Commissioning Tests

Two tests were carried out over a two week period using the modified hydraulic loading test discussed in chapter 4. The first test was conducted using the sample used for the slurry characterisation tests, and for the initial plant test. The second test was conducted using a new sample from Finsch mine that showed quite different behaviour, but that still allows the plant to be operated successfully for the purpose of control testing. Manual sample measurements were taken to evaluate the performance of the Endress & Hauser PROmass 83 I coriolis mass flow meter,. The commissioning tests are discussed after the mass flow meter evaluation.

5.2.6.1 Commissioning Test 1

In the first test, 1600 litres were made up in the slurry tank at 10 % solids by mass using sample from the same batch as used for the slurry characterisation tests. 1600 litres corresponds to a tank level of 80 %. The modified hydraulic loading test was used to evaluate the slurry behaviour for control testing. To begin with a series of nominal feed and underflow rates were determined prior to commencement of the test as shown in table 5.7. The nominal feed and underflow rates are based on an idealised system that ignores compression of the mud bed over time i.e. it assumes a constant mud bed level density at the underflow outlet of 50 % solids by mass.

Table 5.7 Nominal Test Settings

Q_i (l.min^{-1})	Q_u (l.min^{-1})	Q_o (l.min^{-1})
6	0.904	5.096
13	1.958	11.042

The test consisted of creating a mud bed in the thickener until the interface reached a level of 350 mm from the thickener base. This level was selected so that both of the Vega vibrating probes were covered with mud and switched on. The underflow pump speed was manipulated to maintain the interface at this level, and once it had stabilised the operating point was noted. The interface took a while to stabilise each time the feed flow rate (Q_i) was changed. This was due to the fact that as the feed flow rate was reduced, the underflow rate also had to be reduced to maintain the same mud bed level. Because of this the mud now spent longer in the thickener, and had more time to compress so that a greater underflow density was achieved (resulting in a reduction in the bed height). The time that the slurry spends in the thickener between arriving at the mud bed interface, and leaving through the underflow is called the residence time. For this test the flow was started at maximum first thing in the morning, and reduced during the day, progressing through the above range of flow rates.

The flocculant dosage remained the same as for the characterisation tests at 3.5 g.t^{-1}. A 20 litre bucket was available to hold the flocculant for each day of testing, and the required flocculant concentration needed to be determined for the bucket to last the whole day. It takes 1 – 2 hours for the flocculant to hydrate properly depending on the preparation. It is preferred that this is done once in the morning, with enough flocculant to last for a full day of testing. It was assumed that the testing on each day would last for 5 hours. Since there were 8 tests per day, each test would last approximately 37.5 minutes. Table 5.8 estimates the volume of slurry to be processed for a 5 hour day of testing.

Table 5.8 Estimated Slurry Volume

Q_i (l.min^{-1})	V (l)
6	225.0
7	262.5
8	300.0
9	337.5
10	375.0
11	412.5
12	450.0
13	487.5
Total	2850

The volume of slurry that would pass through the system is 2850 litres, and this had to be flocculated at 3.5 g.t^{-1} of dry solids. At 10 % concentration, the density of the slurry is 1.062 kg.l^{-1}. So the mass of the total volume of slurry is 3026.7 kg, and hence the mass of solids that would pass through the system is 302.67 kg. The mass of flocculant required is 1.059 g in total. To have a small amount of remaining flocculant available at the end of the test so that the flocculant hose is not sucking air, the concentration is calculated based on 19 litres of water in the bucket, meaning that 55.74 mg of flocculant are required per litre, and this requires 1114 mg of flocculant mixed with 20 litres of water, or 5.57 mg per 100 ml water. This is still a reasonable amount of flocculant to mix without clusters of undissolved flocculant forming.

The flocculant dosage to be set on the front panel is

$$\frac{V_f(ml)}{V_{sl}(l)} = \frac{19000}{2850} = 6.67 ml.l^{-1} \tag{14}$$

The resulting concentration of the flocculant solution is

$$\frac{M_f}{M_w} \times 100\% = \frac{1.114}{20000} \times 100\% = 0.00557\% \tag{15}$$

Which is roughly double the previous dosage of 0.0025 % used for the characterisation tests.

The results are shown in figures 5.13 and 5.14. In figure 5.13 the pump calibrated flow is used, and in figure 5.14 the meter density is used based on the results of the density evaluation in the previous section.

The feed slurry density started out at 1.051 kg.l^{-1} when there is no material in the thickener. It is expected that the flow pattern in the tank keeps the entrained solids away from the pump outlet at the lower side of the tank. Once a bed was established the feed density ranged between 1.046 kg.l^{-1} at 13 l.min^{-1} and 1.043 kg.l^{-1} at 7 l.min^{-1}. Although the dilution circuit was available, it was not used at this point in order to maintain similarity with the bench top thickener testing.

The underflow flow rates are all reasonably consistent and do not exceed the nominal values. The density values show some variation, but tend to move toward limiting density on days 3 and 4. The lower limit of the underflow pump speed meant that it was not possible to run at 6 $l.min^{-1}$.

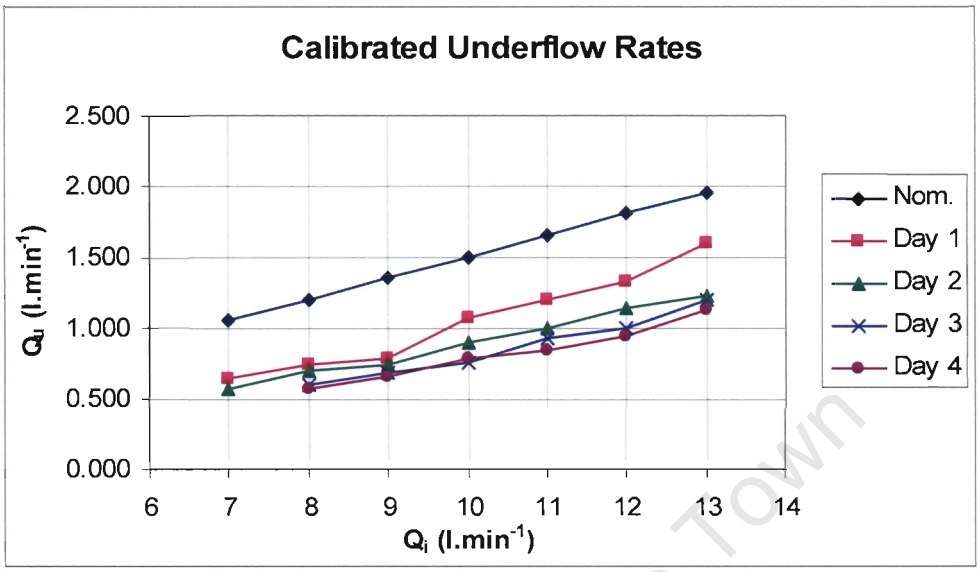

Figure 5.13 Calibrated underflow rates for a range of slurry feed rates.

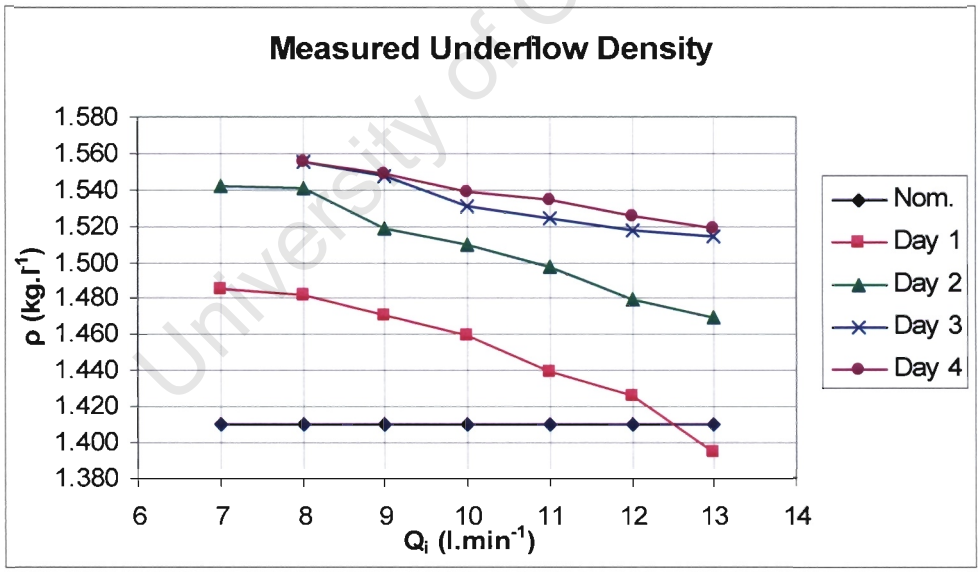

Figure 5.14 Measured underflow density versus slurry feed flow rate. Notice that the density increases over time due to re-flocculation of the slurry.

5.2.6.2 Commissioning Test 2

The new sample batch was made up in the tank to a concentration of 12.5 % solids, giving a total volume of 1600 litres (80 % level) of slurry. The intention was to ensure that the feed solids remained at 10 % solids after the bed had been established in the thickener. The sample was expected to behave in a similar fashion to the initial sample, and the same flocculant dosage used previously was assumed. This proved to be an error, and there was a significant difference between the behaviour of this sample and the previous sample tested. The first issue that was noted was that the population of flocs was significantly higher than before and that the thickener was overflowing or sliming (flocs were reporting to the overflow). The first step taken to counter this was to raise the flocculant dosage to 24 $ml.l^{-1}$ (four times greater) and then 50 $ml.l^{-1}$. This did not improve the situation at all – although it was later realised that the maximum calibrated flocculant flow rate was 17.5 $ml.l^{-1}$, and that the flocculant concentration needed to be increased. Reducing the feed flow rate to its minimum of 6 $l.min^{-1}$ didn't help either. The next step was to dilute the slurry back down to 10 % solids concentration by filling the tank with additional water to a level of 92 %. At this concentration, and at the lowest nominal feed flow rate the flocculation behaviour could be observed by adjusting the flocculant dosage.

The behaviour of the flocculated slurry is discussed with reference to the four settling zones in the thickener as first described by Coe and Clevenger [8], and presented in chapter 2.

Observations

At a fixed feed rate of 6 $l.min^{-1}$ the flocculant dose was varied from close to zero to a value where large flocs were produced.

- At very low flocculant dosage the feed remained the dirty brown of the slurry in the tank.
- Increasing the flocculant dosage resulted in very small flocs forming. These flocs were small enough that they did not settle in the presence of the fluid rising toward the overflow. Clearly the slurry was under-flocculated because a lot of brown slurry was still rising to the overflow – i.e. the water was not clarified.
- When the flocculant dosage was high enough that all of the slurry was being flocculated, the rising water became clearer, but the flocs were still too small to fall through the rising water. This resulted in a very high population of very small flocs that were travelling to the overflow. The presence of so many small flocs hinders settling further because of the interaction between them. Because they are not falling, the concentration rises as new flocs continue to arrive, until settling is hindered to the point where they all rise up and are carried to the overflow. At the same time, the distinction between the compression, transition and hindered settling zones is no longer visible. The entire thickener is filled with a multitude of small flocs. The bed can still be detected with the Vega probes, but the thickener is quite useless. The mud bed also becomes very light and fluffy, trapping a large amount of water and not forming an even compressed bed. The bed begins to look like sponge, with water cavities being clearly visible.
- Increasing the flocculant dose further resulted in there being sufficient excess flocculant that the very fine flocs were starting to be collected together into bigger flocs that could settle effectively. There are two mechanisms at play here. The

first is that settling is hindered less in the presence of fewer larger flocs, and the second is that the larger flocs settle faster.

- At this point there was still an excess of small flocs that were not being carried away toward the underflow. It was necessary to slightly over-flocculate in order to capture these flocs so that the overflow became clear once again. The top of the hindered settling zone gradually moved down until it was level with the exit at the base of the feed well.
- Once the excess particles had been captured and removed there was an excess of flocculant so that a few very large flocs are observed – these tended to be flat plate-like structures that started to settle more slowly as they drifted downward like feathers.
- The flocculant dosage could now be reduced to a level where the floc size was stable. The flocculant dosage at this point was found to be 16 $ml.l^{-1}$ at double the concentration of the previous test i.e. 0.0114 %.

The very fine flocs were approximately 0.5 mm in diameter and appear spherical. The well behaved flocs tended to be somewhere between 1 – 2 mm and appeared spherical. The large flocs were observed to be up to 4 mm in some cases, and looked like uneven flat plates.

A comparison of the two size frequency distributions was shown in figure 5.9. The concentration in the 10 μm zone was almost double that of the first sample. In the 'Paste and Thickened Tailings Handbook' [9], it is stated that the flocculant demand is determined by the amount of particles in the 20 μm size fraction. For both these samples the maximum concentration exists in the 10 μm fraction (near enough to 20 μm). Having observed the behaviour of the settling with the second slurry the flocculant dosage was expected to be approximately 3-4 times that of the first sample (in retrospect). The reasoning is as follows:

Double the amount of flocculant is required to create a series of flocs having the same size in both samples. Because the population of these small flocs is lower in the first sample, they are able to settle. In the second sample the population of small flocs is doubled, so that their settling is hindered. Additional flocculant is required in order to get these smaller flocs to aggregate so that the hindrance is removed by lowering the population and increasing the settling rate.

Test Results

The tests were carried out in the range of 6 – 9 $l.min^{-1}$. The underflow pump was unable (due to its calibration) to operate outside of this range. The results for the third and fourth days are shown as the first day was spent evaluating the flocculation behaviour. A portion of the second day was spent characterising the slurry followed by some follow up tests at 6 and 7 $l.min^{-1}$ to confirm that the thickener could be tested further. In this case the tests were started at the lower end of the nominal range as it was easier to stabilise flocculation and the mud bed at this setting. The flocculant dosage remained set at 16 $ml.l^{-1}$, with no problems encountered with overflowing of the thickener. The overflow clarity also remained good throughout the tests, although it did darken somewhat as the days progressed. The results shown are considered to be similar to those shown in the first test since flocculant was added on days 1 and 2 and this effect is thus included.

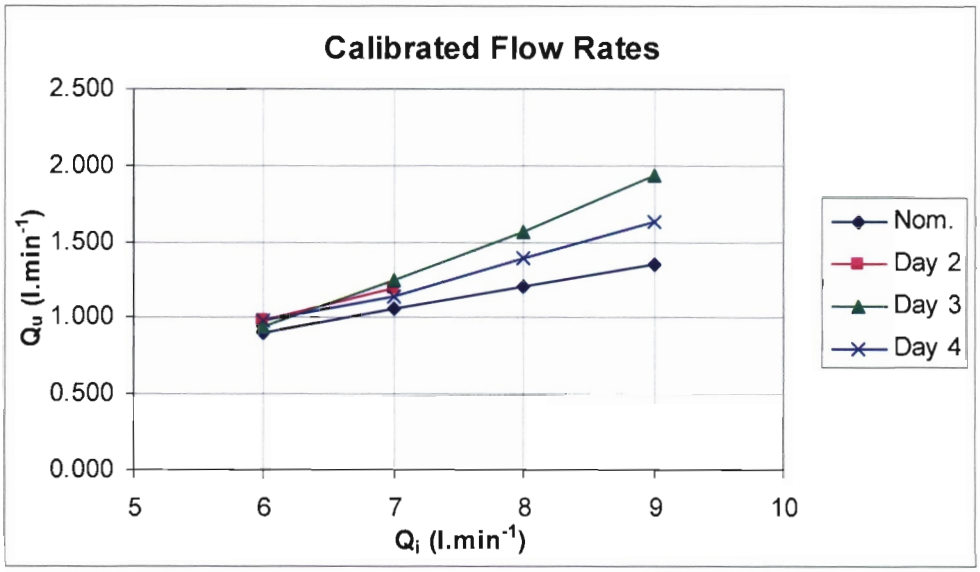

Figure 5.15 Underflow flow rate versus feed flow rate. This is equivalent to a plot of mud bed rise rate versus clear water rise rate since both are related to the flow rates by the cross sectional area of the thickener.

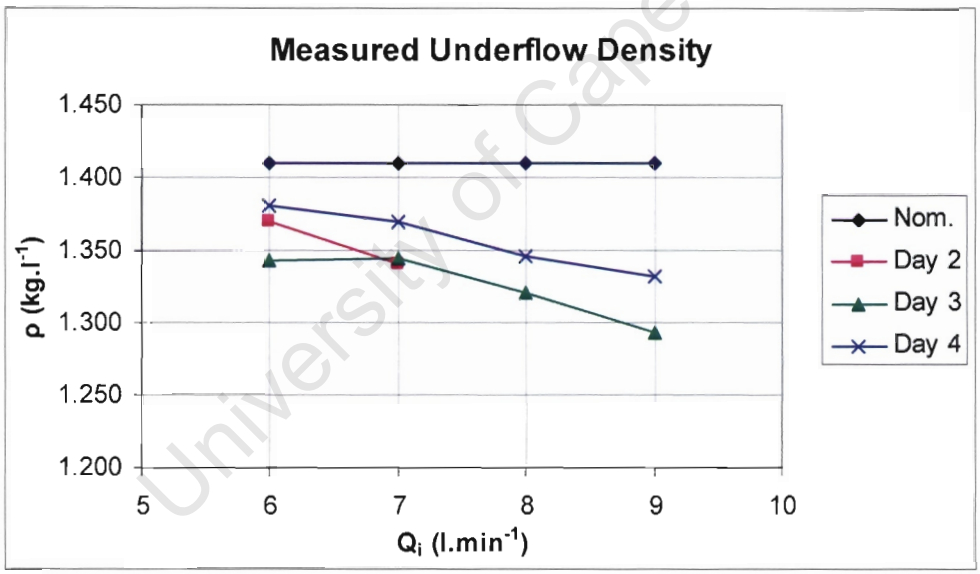

Figure 5.16 Measured underflow density - for a range of feed flow rates from 6 – 9 l.min-1 over a period of three days.

Notice that the underflow rate is above the nominal in all cases in figure 5.15, but otherwise is useful for future testing. The underflow densities in figure 5.16 are all below the nominal value, but still in the design range of 1.2 to 1.4 kg.l^{-1}. Despite the initial hiccups it was found that the plant could be run with a very different sample. The underflow pump range was increased by changing the drive pulleys to reduce the lower speed, and the frequency range extended so that a greater upper speed can be achieved. This assisted in coping with the possible future variations expected from sample to sample.

5.3 DISCUSSION OF COMMISSIONING RESULTS

At this point the plant commissioning was deemed complete, and ready for control testing. Despite the extensive work carried out during slurry characterisation, it was discovered that there is significant variability which can be expected in the test samples. It is possible to modify the test plant operating parameters to generate a bed for control testing and the objective of the design has been achieved. The commissioning exercise highlighted some of the practical difficulties experienced in real world thickener control, and these will be dealt with as they present themselves in future.

The single tube Coriolis mass flow meter at the underflow was found to give an accurate density measurement compared with manual samples. The flow measurement on the Coriolis mass flow meter was not found to be suitable, and the calibrated flow values from the progressive cavity pumps (feed and underflow) were used instead. The dual tube Coriolis mass flow meter on the slurry feed was found to perform adequately for density measurement since the flow rates are high enough that deposition does not occur in the tubes.

The dilution circuit was implemented and found to maintain the feed concentration within ± 0.5 % based on the density measurement from the Coriolis mass flow meter installed on the slurry feed line.

Some remaining instruments are required in the plant during the control tests that will follow. These are :

- The installation of pressure transducers on the underflow pump pipeline to estimate the slurry viscosity. The rake torque is to be evaluated as an indicator of underflow rheology.
- The installation of a device at the thickener overflow to evaluate the clarity and determine if flocs are being carried over into the overflow. The Markland 502-TP suspended solids meter (ultrasonic) will be included at this point (already installed, but not calibrated), and an Endress & Hauser suspended solids meter (optical) is being considered.

The two commissioning tests showed that it is possible to create a mud bed under conditions similar to those experienced in full scale thickeners. From this point on, the installation and modifications to the plant will be determined by the requirements of a phased approach to the measurement and control of the thickener parameters. After the experience gained during the commissioning of the plant it seems that mechanical issues are often responsible when measurements do not deliver the expected information. It is necessary, however, to rectify these issues in order to successfully control the thickener, and it may be that this feedback will assist in improving the measurements and control on full scale thickeners.

5.4 REFERENCES

1. Watson Marlow, 603u Peristaltic Pump Manual, 603ur-gb-01.pdf, Available: http://www.watson-marlow.de/wm-de/manuals.htm.
2. Vega Controls, Vegavib Operating Instructions, Vega Grieshaber KG, 17496-EN-030305, Order No:1099828
3. Phoenix Contact, Online Specification Sheets (pdf files generated on request), Products | Analogue Interface Products | Signal Conditioning, Available: http://phoenixcontact.com.
4. Turck Industrial Automation, Turck Compact Catalog, Interface Technology, Rotational Speed Monitors, Document no. D900210, September 2003.
5. RH Perry and DW Green (editors), "Perry's Chemical Engineers' Handbook 7th ed", McGraw Hill, 1997
6. T.J. Napier-Munn, An Introduction to Comparative Statistics and Experimental Design for Minerals Engineers, University of Queensland, 2nd Ed. V4.0, 2000
7. Endress & Hauser, PROline promass 83 Coriolis Mass Flow Measuring System, Operating Instructions, BA 059D/06/en/04.02, 50098470
8. H.S. Coe and G.H. Clevenger, Methods for Determining the Capacity of Slimesettling Tanks, Trans AIME, 55:356-385, 1916.
9. A. J. Vietti and F. Dunn (Editors), "Paste and Thickened Tailings Disposal Handbook", De Beers Consolidated Mines Ltd, Technical Support Services, Technology, 2003.

CHAPTER 6 CONCLUSIONS

A laboratory scale test thickener has been designed, constructed, and commissioned and fulfils the requirements set out at the beginning of the project. The scale thickener provides a platform where:

- Measurement and control testing can be carried out without full scale production pressure.
- Similar settling conditions to those experienced on full scale thickeners can be created.
- The construction of the scale thickener from acrylic plastic allows the flocculation behaviour and mud bed formation to be observed.
- Full size instruments can be tested under controlled conditions.
- Conditions can be controlled until fundamental principles can be understood before simulating more difficult conditions by varying the feed to determine how well the measurement and control strategies are able to cope.

Numerous changes were made over the course of the project thus far, in order to achieve the design performance. These include:

- The modification of the thickener base from a conical section to a flat base, and the installation of a raking mechanism to move slurry to the underflow.
- The extension of the feed well to deliver the flocculated slurry closer to the mud bed to prevent it from being carried to the overflow.
- The installation of a single tube Coriolis mass flow meter for density measurement at the thickener underflow to cope with the low flow rates required.
- The use of the calibrated flow rates from the progressive cavity pumps instead of the inaccurate flow measurement from the Coriolis mass flow meters.
- The upgrade of the slurry tank agitator to maintain solids in suspension, and the installation of baffles in both the slurry tank, and the clear water tank to prevent sloshing, and to aid in the suspension of solids.
- Simplification of the dilution circuit based on the slurry feed density after the failure of the dilution control valve.

Further instrumentation has yet to be installed to estimate the underflow rheology, and the overflow clarity. In both cases space has been provided for the installation, and these will be installed as required by the measurement and control testing schedule.

Annotated images of the plant are shown in figures 6.1 and 6.2.

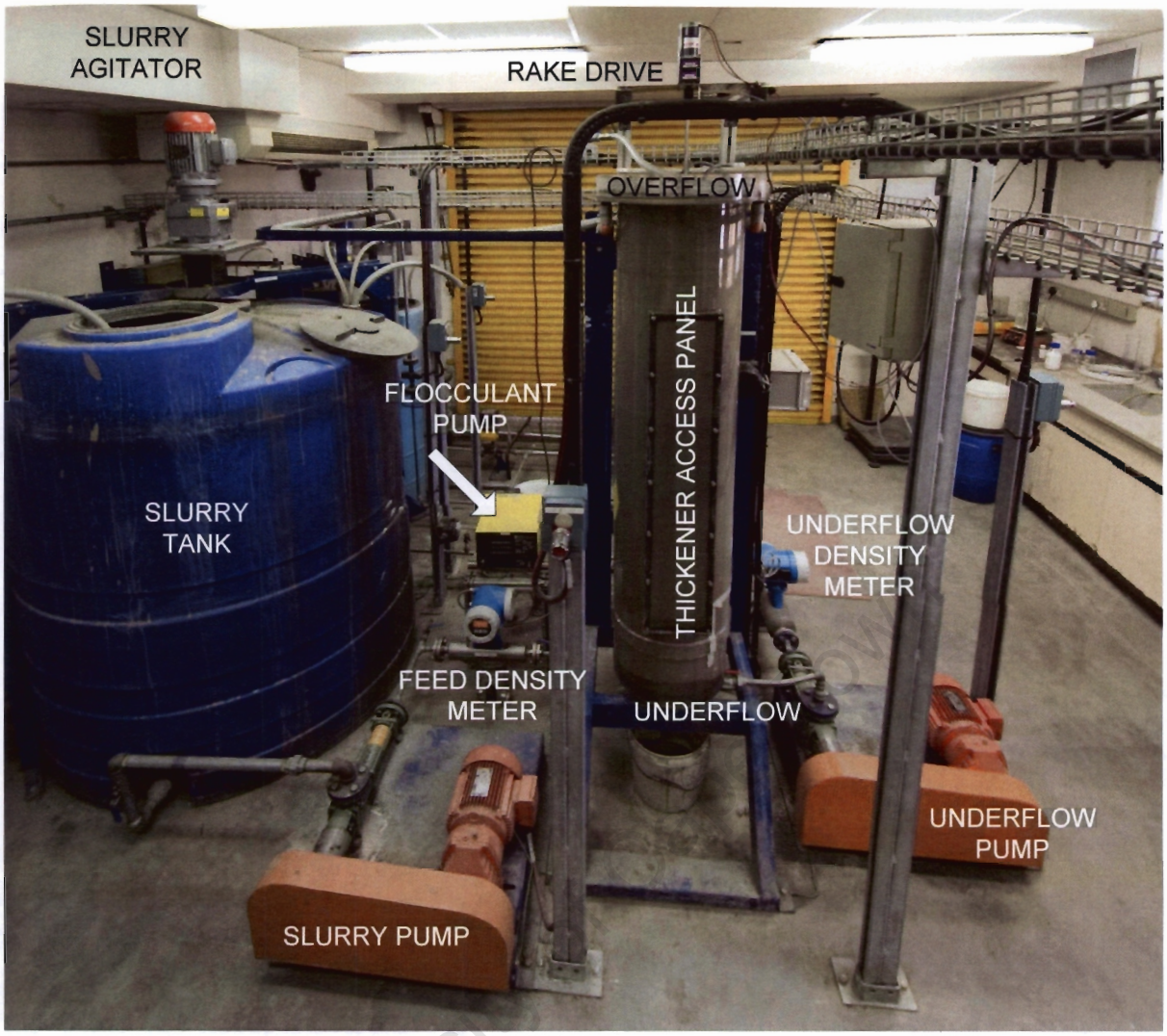

Figure 6.1 Annotated plant front view.

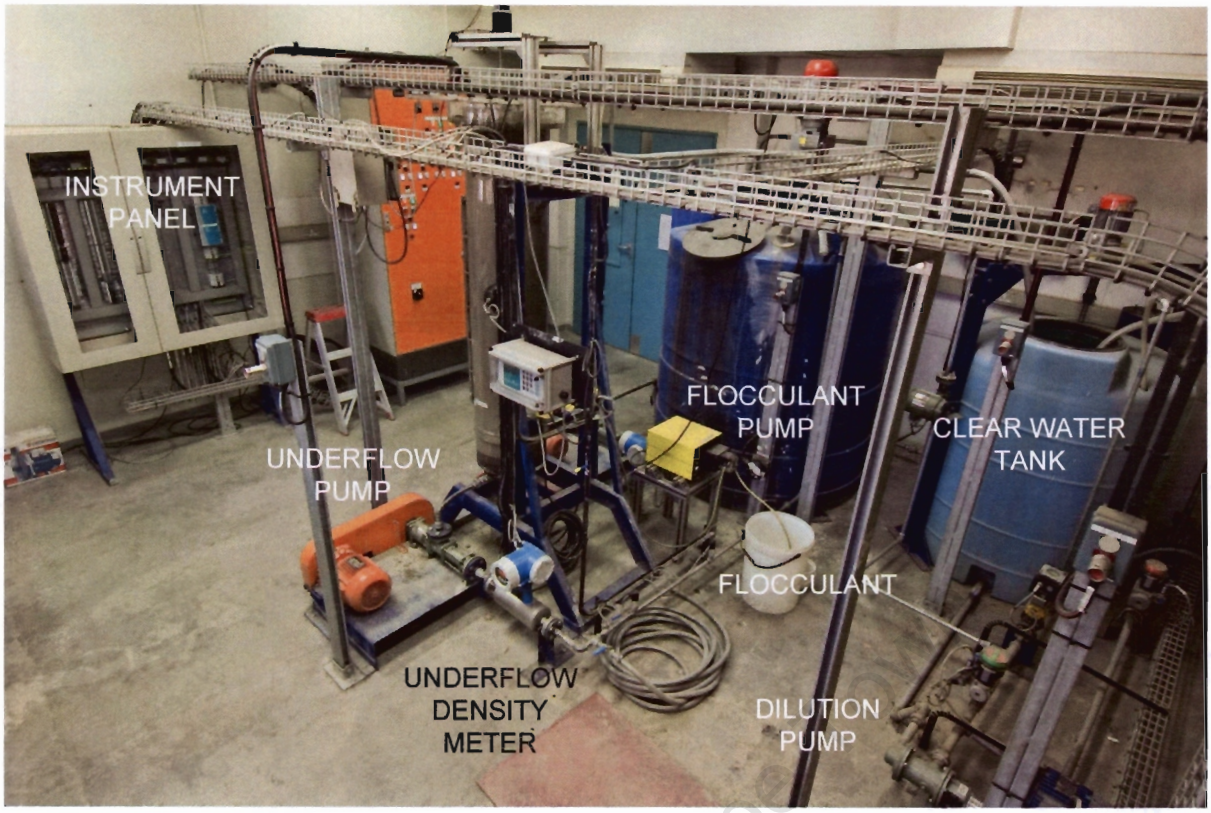

Figure 6.2 Annotated plant side view.

CHAPTER 7 FUTURE WORK

Future work entails formulating and testing a control strategy using a combination of the instrumentation installed at CTP (Combined Treatment Plant, Kimberley) and Orapa mine, where high compression thickeners are installed. The idea is to take the measured input variables, and to determine the limits for normal operation. The following are available input variables:

Table 7.1 Available Measurements at CTP and Orapa. Solid blocks indicate direct continuous measurements, while the empty blocks indicate inferred or manual measurements.

Measurement	CTP	Orapa
Feed concentration	■	■
Feed flowrate	■	■
Feed particle size distribution		
Flocculant Dosage (inferred from pump spd)	□	□
Mud bed level (not continuous measurement)	□	□
Rake Torque	■	■
Overflow clarity (installation in progress)		□
Underflow Density	■	■
Underflow Rheology	■	

There are a limited number of controllable variables that impact on more than one of these measured variables:

Table 7.2 Available Manipulated Variables. Solid blocks indicate the presence of the control variable.

Control Variable	CTP	Orapa
Flocculant Dosage	■	■
Underflow flow rate	■	■
Shear thinning pump speed	■	

The next stage is to determine which of these control variables impacts which of the measurements, and to determine when each of these is most important or has the greatest impact. The input/output relationships are shown in table 7.3. A single manipulated variable impacts on more than one of the measured variables, and under different conditions the most important variable to be adjusted may change. This is potentially where the thickener operating instructions in chapter 2, or expert logic, or fuzzy control may come into play.

There are further hidden variables that do not appear directly, but that could be estimated from the state of the process. One of these is the residence time, where the longer the slurry spends in the thickener the greater the underflow density will be, up to some maximum where water can no longer be liberated from the bed. This is most likely to be estimated based on a model of the bed dynamics.

Table 7.3 Input/Output Relationships

	Flocculant Dosage	Underflow flow rate	Shear thinning pump speed
Feed concentration	●		
Feed flowrate	●		
Feed PSD	●		
Mud bed level		●	
Rake Torque	●	●	●
Overflow clarity	●		
Underflow Density		●	●
Underflow Rheology	●	●	●

For each of the measured variables a set of limits must be put in place, as well as some ideal setpoint that each variable can be moved toward. This does not apply to the feed variables, since there is no control over these – although a feedforward controller is usually tied in with the flocculant addition so that the flocculant is varied according to the measured headfeed tonnage.

Thus each variable has an ideal setpoint, and the three controlled variables have their own controllers in place. It follows that these setpoints are modified in order to keep the measured variables within limits, while maximising them in some sense which has yet to be determined. There are two possible approaches to this problem. The first is to put a cost function in place in order to maximise water recovery, whilst minimising flocculant consumption. The second approach is to make use of fuzzy logic, and/or rule blocks in order to determine what control action should be taken. There may be further strategies worth investigating as work progresses, which will help to show the direction of the control action required. The intention is to work within a bounded space, where the most critical measurement is adjusted by creating a vector in that space that determines what control action is required. Perhaps a principal components type of approach will yield information on the optimum control action to take.

It is felt that the rake torque might provide more information than is presently extracted. One area that has yet to be investigated, is the relationship between the underflow rheology, and the load experienced by the rake. It is possible that the overall feed conditions can be determined by a combination of measurements so that feed measurement instruments become less important. Another feature to be investigated is that it should be possible to carry out the full set of measurements on one thickener in a group, and to share this measurement with other thickeners so that the overall instrumentation requirement is reduced.

The idea is to determine what the minimum number of measurements is, and which of these measurements are the most important. The key variable is likely to vary as the material properties change. From this basis it is possible to determine the possible improvements as more measurements are included, and how to quantify these, as well as under what conditions these additional measurements are required.

The starting point for control testing is the work carried out by Vietti et al. using the Vega vibrating probes for detecting solids in liquids. This will begin with some initial bang-bang control testing. In Dunn's work the pump was shut down when the lower limit was reached.

This will not be done here since no measure of the underflow density is available when pumping stops. Instead a nominal flow rate will be maintained in order to monitor underflow density.

The following step will be to implement a predictor that will attempt to maintain the mud bed level at some point between the two probes. This will be done by using the time taken for the mud bed level to move between the two probes, and will depend also on whether the bed is rising or falling.

The mud bed level will then be combined with the underflow density control in order to achieve some specified underflow density. Variations in the sample characteristics mean that an optimum underflow density will have to be determined in situ depending on the bed behaviour. Combining the predicted mud level and the underflow density should provide some measure of the sample properties if a suitable model can be created, and should also be able to predict a density profile in the bed itself.

The following steps are to determine the impact of varying bed properties on the rake torque, and to determine if something regarding the underflow rheological properties can be inferred. Further rheological properties will be estimated from the underflow differential pressure sensing. If this is successful then it will be incorporated into the control scheme in order to find optimum conditions for the operation of the thickener.

Finally it is envisaged that a mechanism to evaluate the clarity of the overflow will be included, although this has not yet been investigated. The continuous operation of the plant does result in decreased clarity as the days pass, although this was not significant with the second sample tested, which is expected to be the more typical Finsch sample. Regardless of this, the controller will have to be able to cope with variations in the sample properties, as this is a condition experienced in real thickeners.

A final option that may be considered in the future is to run a small scale thickener alongside full scale thickeners, and use this to generate scaled up control actions. This would be a similar concept to the idea of internal model control.

CHAPTER 8 APPENDICES

8.1 APPENDIX A: SLURRY DENSITY CONVERSION FACTORS

The following table gives a number of different representations for the density and concentration of slurries in terms of the solid and liquid densities. The solid and liquid densities are given by ρ_s and ρ_l, typically in $kg.l^{-1}$ although the units are not important provided they are the same in the calculations. The representations shown in the table are given by

ρ_{sl} Slurry density in the same units as the solid and liquid densities.
C_V Concentration by volume, the ratio of solids volume to total volume.
C_M Concentration by mass, the ratio of solids mass to total mass.

The conversions are provided for ease of reference, since some calculations are more easily performed with the solids concentration by mass, and others with the slurry density. Many references make use of slurry concentration by volume, and some instruments, such as those providing solids concentration, measure concentration by volume (typically optical, sonic, or ultrasonic).

To Get	Use	Given
ρ_{sl}	$\frac{\rho_s \rho_l}{\rho_s - C_M(\rho_s - \rho_l)}$	C_M
C_V	$\frac{C_M \rho_l}{\rho_s - C_M(\rho_s - \rho_l)}$	C_M
C_M	$\frac{C_V \rho_s}{\rho_l + C_V(\rho_s - \rho_l)}$	C_V
ρ_{sl}	$C_V(\rho_s - \rho_l) + \rho_l$	C_V
C_M	$\frac{\rho_s(\rho_{sl} - \rho_l)}{\rho_{sl}(\rho_s - \rho_l)}$	ρ_{sl}
C_V	$\frac{(\rho_{sl} - \rho_l)}{(\rho_s - \rho_l)}$	ρ_{sl}

8.2 APPENDIX B: PUMP CURVES

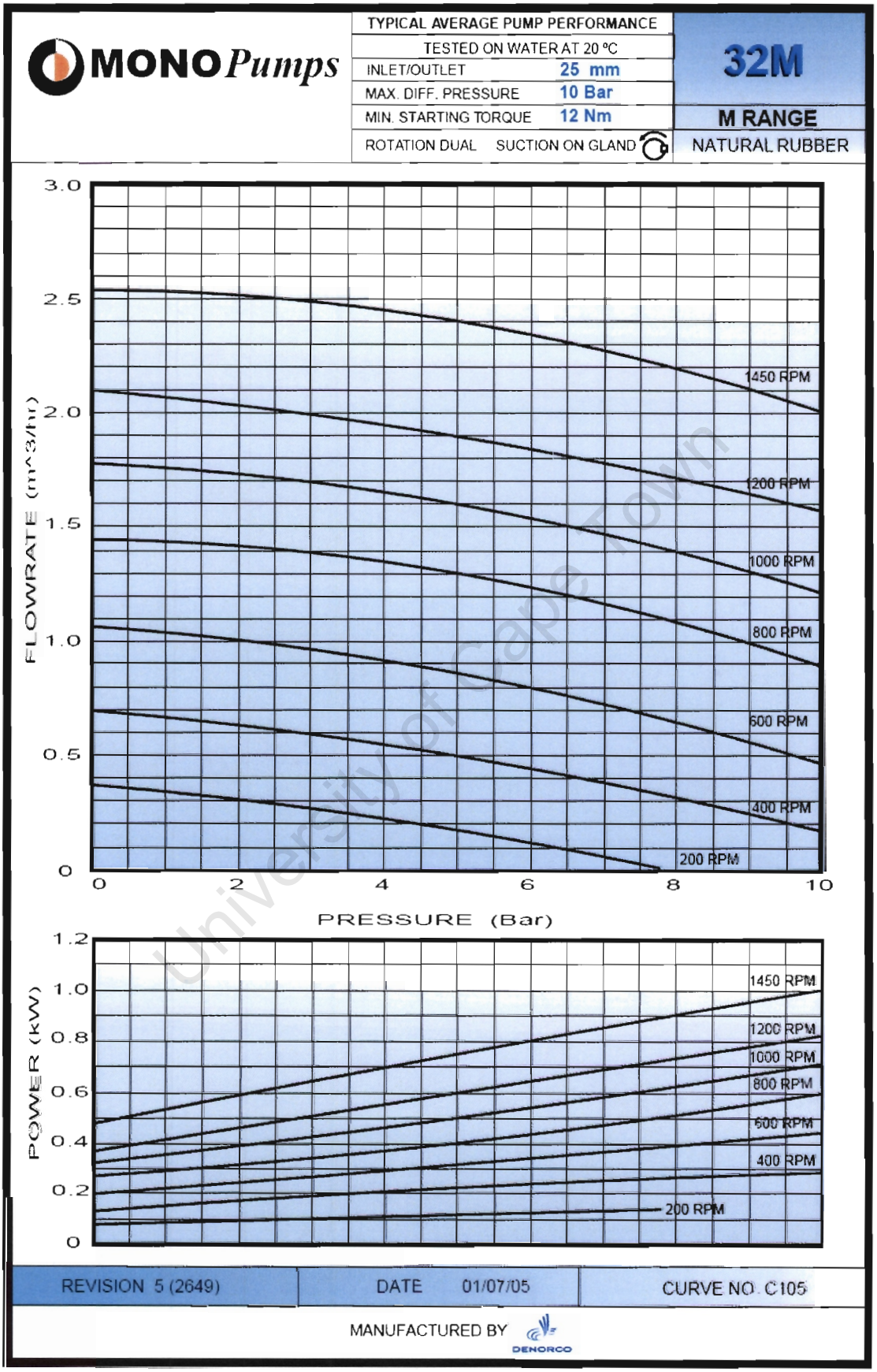

MONO Pumps

TYPICAL AVERAGE PUMP PERFORMANCE		22M
TESTED ON WATER AT 20 °C		
INLET/OUTLET	25 mm	
MAX. DIFF. PRESSURE	10 Bar	
MIN. STARTING TORQUE	7.5 Nm	M RANGE
ROTATION DUAL SUCTION ON GLAND		NATURAL RUBBER

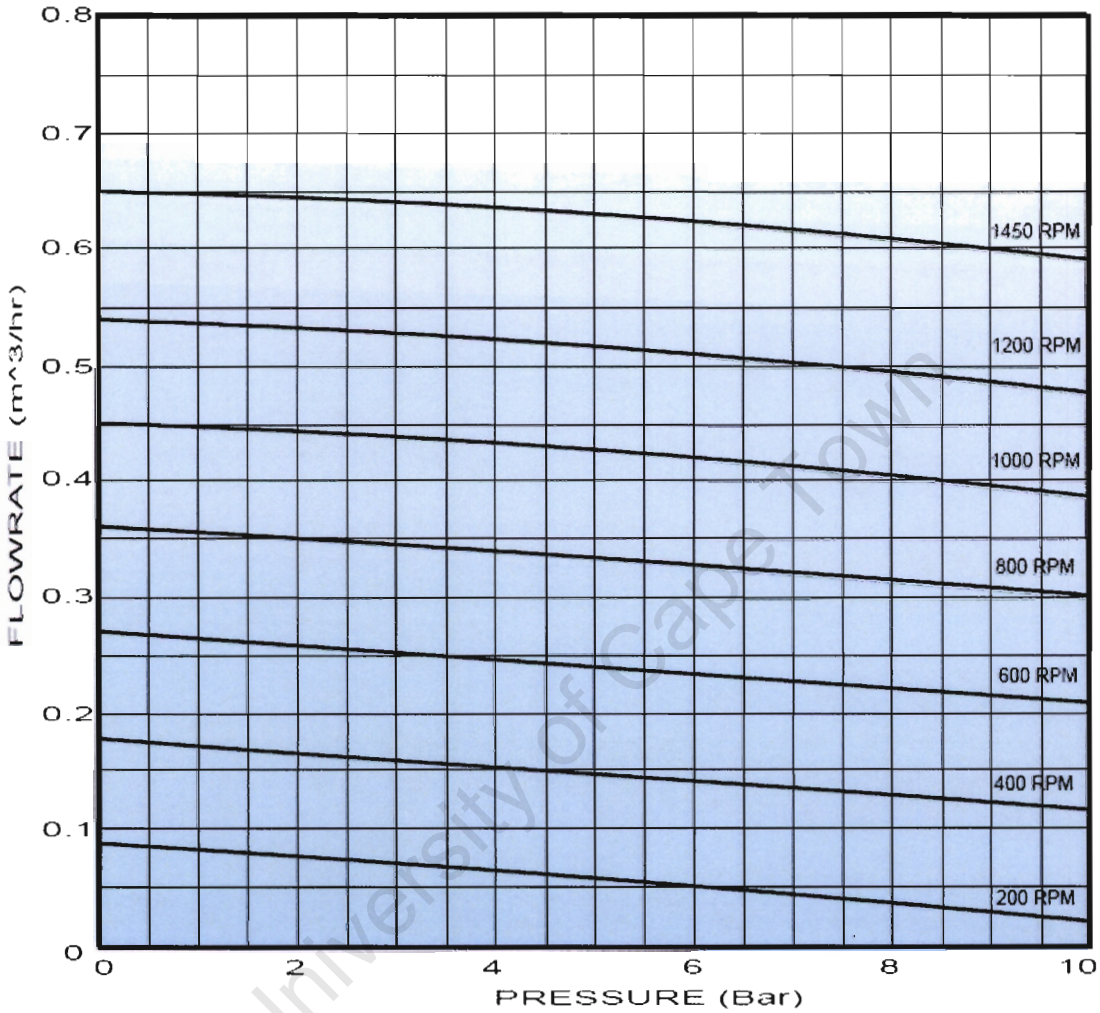

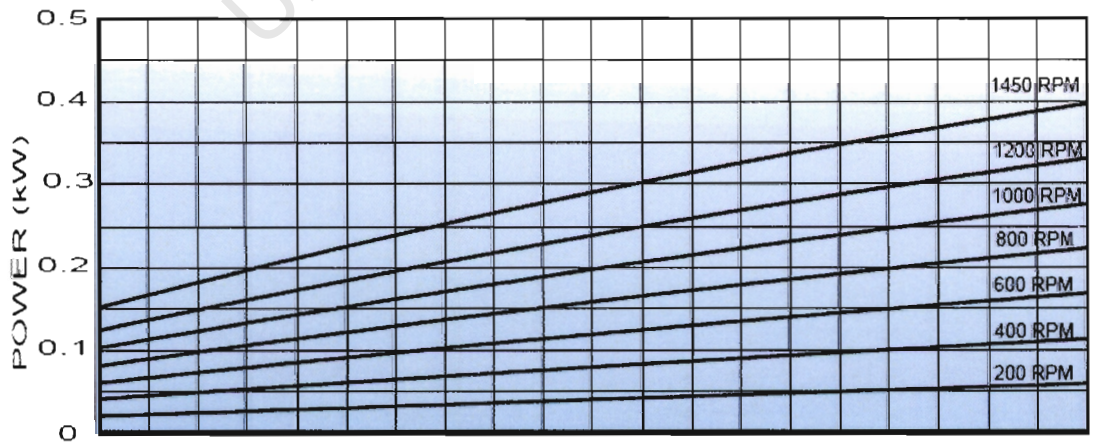

REVISION 5 (2649)	DATE 01/07/05	CURVE NO. C101

MANUFACTURED BY DENOROO

MONO Pumps

TYPICAL AVERAGE PUMP PERFORMANCE		GF
TESTED ON WATER AT 20 °C	ROTATION SINGLE DELIVERY ON GLAND	
INLET/OUTLET - Ø 25		
MIN. STARTING TORQUE 2.16 Nm		NITRILE RUBBER

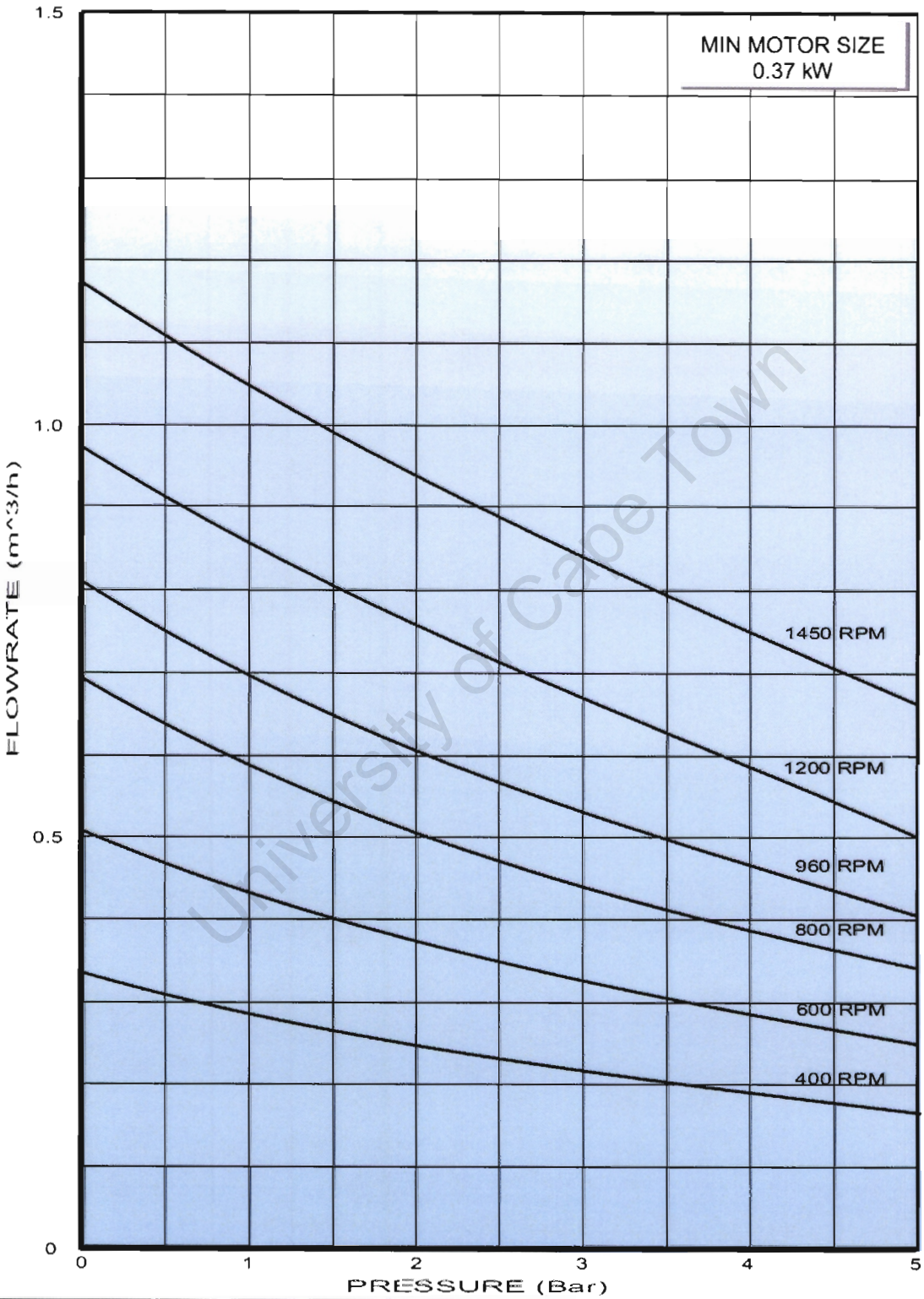

REVISION 4	DATE 01/07/05	CURVE NO. C399

MANUFACTURED BY DENORCO

8.3 APPENDIX C: SCALE TEST THICKENER LABORATORY SOFTWARE STRUCTURE VERSION 1.0 (AS BUILT)

TABLE OF CONTENTS

1. INTRODUCTION

This document provides a description of the as-built software for the scale thickener laboratory control system. A control philosophy was not generated for the plant, although the basic principles of operation are encapsulated in the design document for the plant [1]. The software is written using the Labview Developers Suite, and includes the user interface and control code. The software runs on a PC, linked to Fieldpoint I/O modules, connected via RS485 communications link. Figure 1 shows the hardware layout with the module addresses.

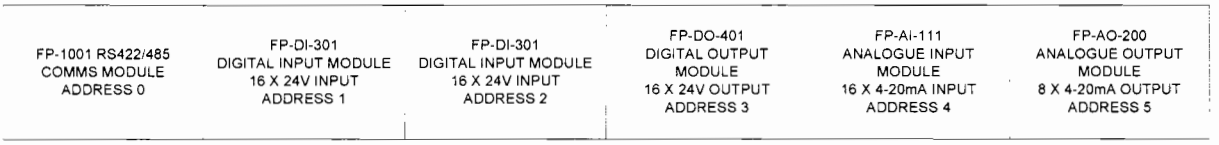

Figure 1 Hardware Modules

The software should be read in conjunction with the P&ID diagram [2] and loop diagrams [3] for the scale thickener plant.

This document is intended to capture the software state, as well as to provide a reference for use in future software modifications. To aid in this regard each section discussing a VI (Virtual Instrument) shows the icon that identifies it. These icons are also shown in the software hierarchy presented at the end of the document.

A high level overview of the Labview software implemented to control the thickener test facility is shown in Figure 2. The software code is contained in a single loop executed every 250 milliseconds. The flow is in a natural sequence across the page from left to right. A discussion of the high level functionality follows.

1.1 Initialisation

The first operations shown on the left hand side of the iterative loop (large grey block), are executed prior to execution of the loop itself. Before the loop begins to execute, the scaling values for the analogues, the display images, and any prior save values are loaded. These operations are executed once only when the software is started.

1.1.1 Load Scaling Values

The scaling values consist of a table containing the variable name, range, and units. These values are applied in pre-processing.

1.1.2 Display Images

The display images consist of small bitmaps of different colours. For example there are three images for a motor, one green (running), one red (stopped) and one orange (trip fault). The drive and valve blocks determine which image is displayed on the front panel.

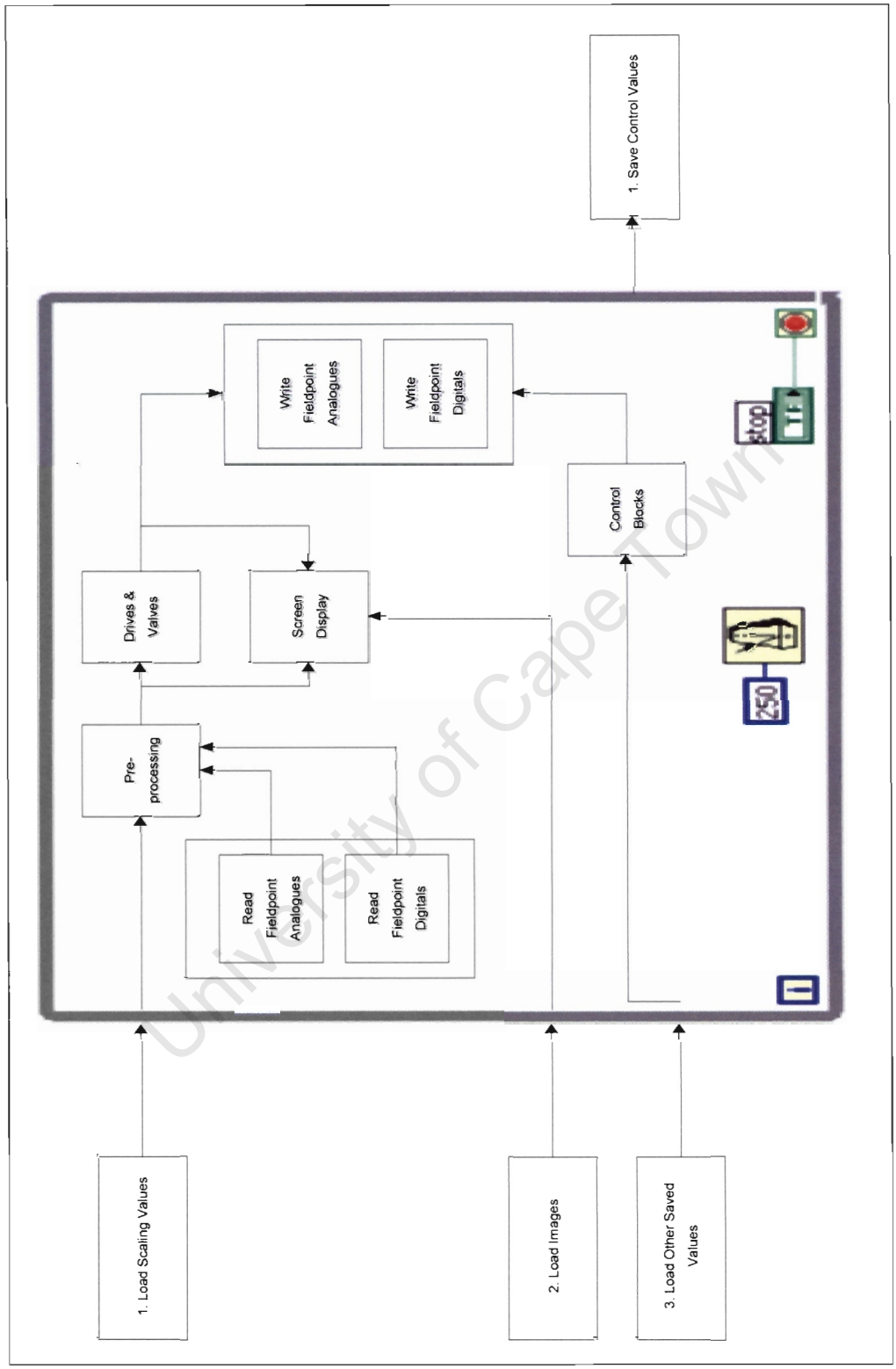

Figure 2 Software Structure

1.1.3 Save Values

Save values are used when values from calculations such as the slurry dilution control block should be reloaded when the software is restarted after shutting down after a power failure or similar event.

1.2 Pre-processing

1.2.1 Read Inputs

The next step, which is executed on every cycle, is to read the values from the Fieldpoint modules, and to place these into two arrays. The analogues and digitals are stored in separate arrays at this point.

1.2.2 Scaling

From here the analogues are first processed by computing and applying the scaling values. The computation to determine the offset and multiplier for each value is executed on each cycle. This is done so that the instrument ranges can be updated while the software is executing.

1.2.3 Alarms & Derived Values

Following this, the analogue alarms are generated, where digital tank levels such as high, high high, low and low low are created. Any other computations for derived values such as estimating a flow from an rpm value are also carried out here.

1.2.4 Interlocks

The drive and valve enable signals are generated using combinatorial logic using the alarms, derived values, and digital signals. Each of these signals is fed to each drive or valve block and determines whether it can be started/opened or not.

1.2.5 Grouping

The analogues and digitals are now combined into clusters so that there is a separate cluster for each drive containing the relevant drive status signals.

1.3 Drives & Valves

The drives and valves are treated separately on a higher level, since their operation is somewhat different. Each drive has a block that determines whether it is enabled (interlocks enabled), and contains the various inputs and outputs to start/stop and control speed. The flow control valve on the dilution control circuit is treated slightly differently, although it behaves more like a drive, than a valve. The valve blocks are fairly simple, but differ in that they have two feedback inputs, one for the open position and another for the closed position. Both the drives and valves feature a timeout mechanism so that if the requested operation is not completed within a given period an error is generated.

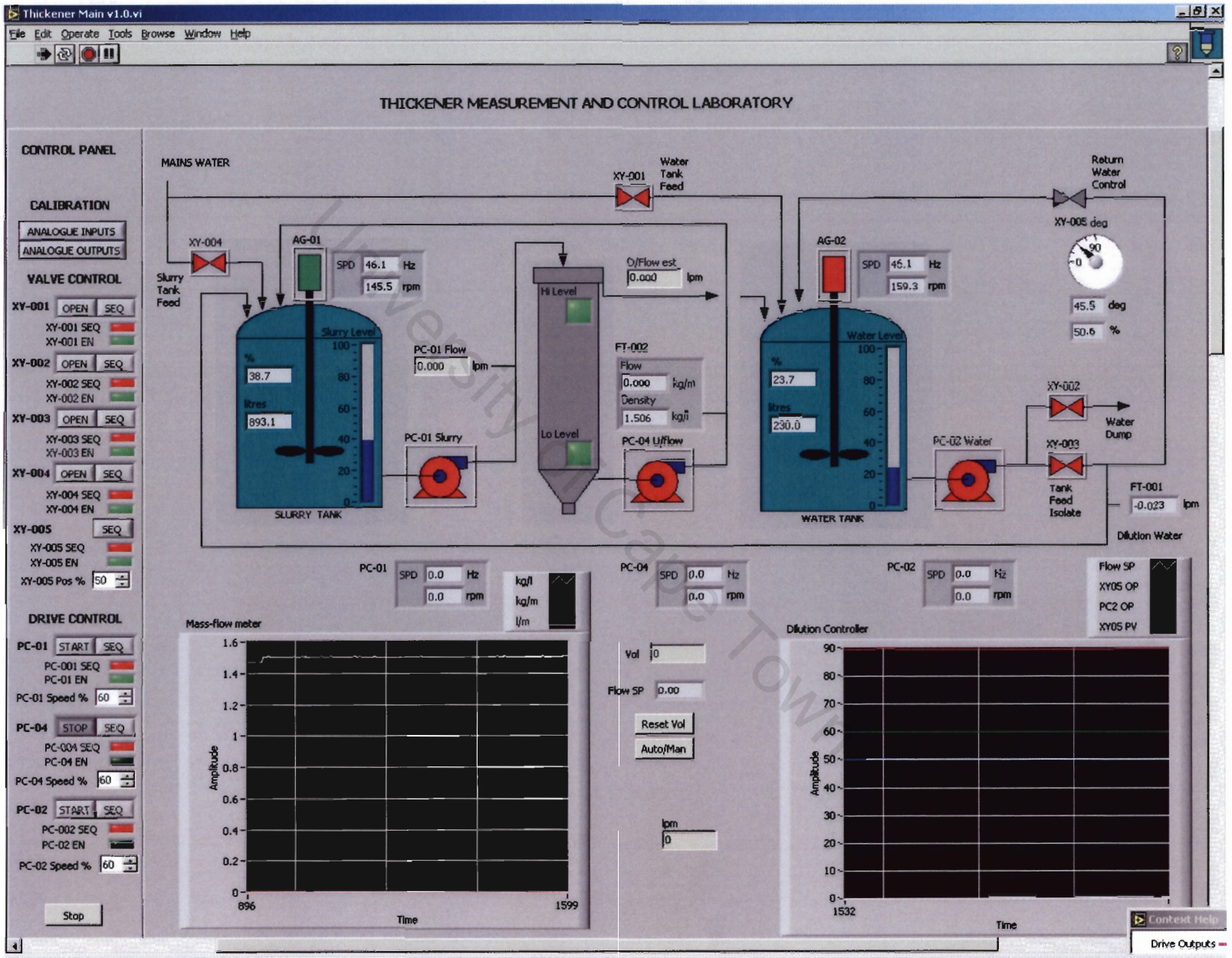

Figure 3 Thickener Main VI Front Panel

1.4 Screen Display

Although shown as one block here, the screen display is generated from many different locations. Screen display includes both the display of values and indications, as well as reading command inputs from the various buttons located on the control panel. The control panel is shown in Figure 3.

The control panel is fairly flexible, in that features will be added and removed as required. The left hand panel contains all of the automatic controls by which each piece of equipment can be controlled. Controls are broken down into three different types.

Manual control, where the device is controlled from the electrical panel.
Automatic control, where the device is controlled via the control panel.
Sequence control, where the device is controlled via a software sequence.

More about this later.

The central panel contains a mimic of the P&ID diagram [2], for the plant, and the lower portion of the central panel is reserved for graphs and similar indications that are implemented as required.

1.5 Control Blocks

Control blocks contains items such as the dilution water controller, and the mud-level controller which will be implemented at a later stage. It is also possible that control sequences will reside in this block. Control sequences implement a controlled start up through various states, until a controlled shut down of the plant is required.

1.6 Write Outputs

From here the outputs are written to the Fieldpoint modules.

1.7 Save Control Values

Any values that are required for computations when the software restarts are saved at this point. For example, if there is a residual value in the dilution calculation that must be reloaded on a restart it will be saved here. Although not yet implemented, this feature will definitely be required at a later stage. All important status values are saved at this point. Although this is shown as being executed after the loop is stopped (outside the loop on the right hand side of figure 2), this does not mean that status values cannot be saved from within the program. Any essential values can be saved by the program while the loop is executing so that they can be reloaded when the software is restarted.

1.8 Thickener Main V1.0 VI

The top level VI contains all of the sub-VIs discussed in the remainder of this document. The icon above is shown as the top level in the hierarchy and also includes the front panel from which the plant is controlled. The front panel was shown previously in Figure 3.

The left hand panel contains all of the panel controls for direct stop/start/open/close of drives and valves, as well as the speed or position controls. This panel also contains the sequence selectors, which take the drives into automatic sequence control.

The upper half of the main panel contains a replica of the P&ID diagram [2], with equipment labels, and any values and status as required. All of the drives are given as image containers, so that the colours of the equipment can be changed depending on their status. The other equipment images were generated as bitmaps, and then pasted into the front panel. These images are contained in the \Images subdirectory to the \Labview Applications directory, which contains the complete code for this application.

The lower half of the main panel contains graphs and other controls which are changed from time to time as the requirements of the project change. Presently the left hand graph shows the underflow density, and mass flow, and the right hand graph shows the status of the dilution controller. In-between these graphs are the Auto and Reset controls for the dilution water totaliser.

A discussion of the individual VIs that make up the application follows.

2. INITIALISATION

2.1 Load Calibration Values (LoadCal2.vi)

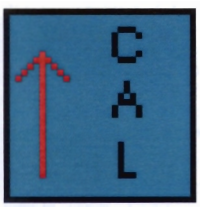

The calibration values are loaded directly from the directory named 'Labview Applications', located in the file 'AICalVal.txt'. The 'Labview Applications' directory contains all of the VIs and subVIs required to run the thickener application. The block marked 'CAL' is the subVI LoadCal2.vi. This VI takes the file path information, and loads the information from file.

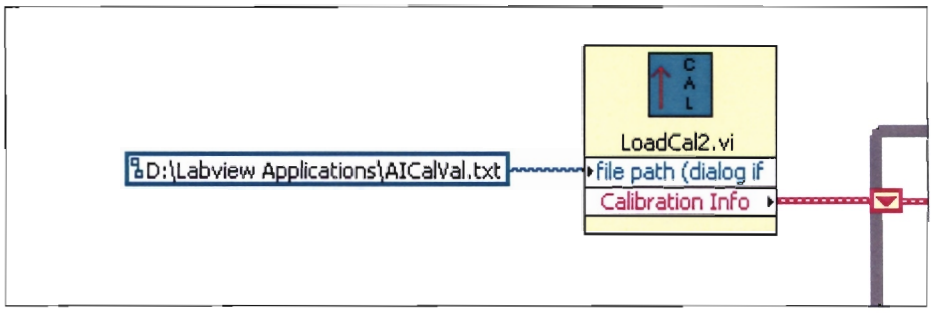

Figure 4 Load Calibration Values

The contents of the calibration file are shown below in Figure 5. The file contains the following information:

Channel : The data channel on the Fieldpoint analogue input module.
Tag : The tagname allocated on the I/O schedule
Description : The tag description
Min mA : Milliamp minimum value (default = 4 mA)
Max mA : Milliamp maximum value (default = 20 mA)
Min Range : Minimum value for the instrument range
Max Range : Maximum value for the instrument range
Units : Units of the actual value represented by the 4-20 mA signal

AICalVal - Notepad

File Edit Format Help

Channel	Tag	Description	Min mA	Max mA	Min Range		Max Range		Units
0	FT-001	Dilution Water Flow Rate	4	20	0	20	l/m		
1	LT-001	Slurry Tank Level	4	20	0	100	%		
2	LT-002	Dilution Water Tank Level	4	20	0	100	%		
3	DT-001	Column Density Meter	4	20	0	2	kg/l		
4	DT-002	Underflow Slurry Density	4	20	0.5	2	kg/l		
5	FT-002	Underflow Slurry Flow Rate	4	20	0	10	kg/m		
6	XY-005	Dilution Water Valve Position	4	20	-0.3	101	%		
7	PC-01	Slurry Pump Speed	4	20	0.3	50	Hz		
8	PC-04	Underflow Pump Speed	4	20	0.1	50.6	Hz		
9	PC-02	Dilution Water Pump Speed	4	20	-0.1	49.5	Hz		
10	PC-05	Spare Pump Speed	4	20	0	50	Hz		
11	AG-01	Slurry Agitator Speed	4	20	0	50	Hz		
12	AG-02	Dilution Water Agitator Speed	4	20	0	50	Hz		
13	PT-001	Underflow Pressure 1	4	20	0	2	kPa		
14	PT-002	Underflow Pressure 2	4	20	0	2	kPa		
15	PT-003	Underflow Pressure 3	4	20	0	2	kPa		

Figure 5 Contents of AICalVal

The LoadCal2.vi block parses this file, using two nested loops. The outer loop looks for the carriage return character, and the inner loop takes each item of information (tab delimited) as listed above, and populates an array. Figure 6 shows the output of this process.

The Channel information is loaded into a numeric array, while the Tag, Description and Units information are each loaded into a text array. The min and max values for both mA, and range are loaded into a single numeric array. The format for each line is:

Row 1: [(min mA) (max mA) (min Range) (max Range)]
Row 2: [(min mA) (max mA) (min Range) (max Range)]
Row 3: etc.

Each line is indexed by its location in the array – by channel number. One note here is that Labview indexes arrays starting at 1, whilst the I/O channels are indexed starting from 0. So there is an offset of 1 between the physical I/O location, and the location of the information in the array. The same is true of the data when the 'Read Fieldpoint' VI is implemented.

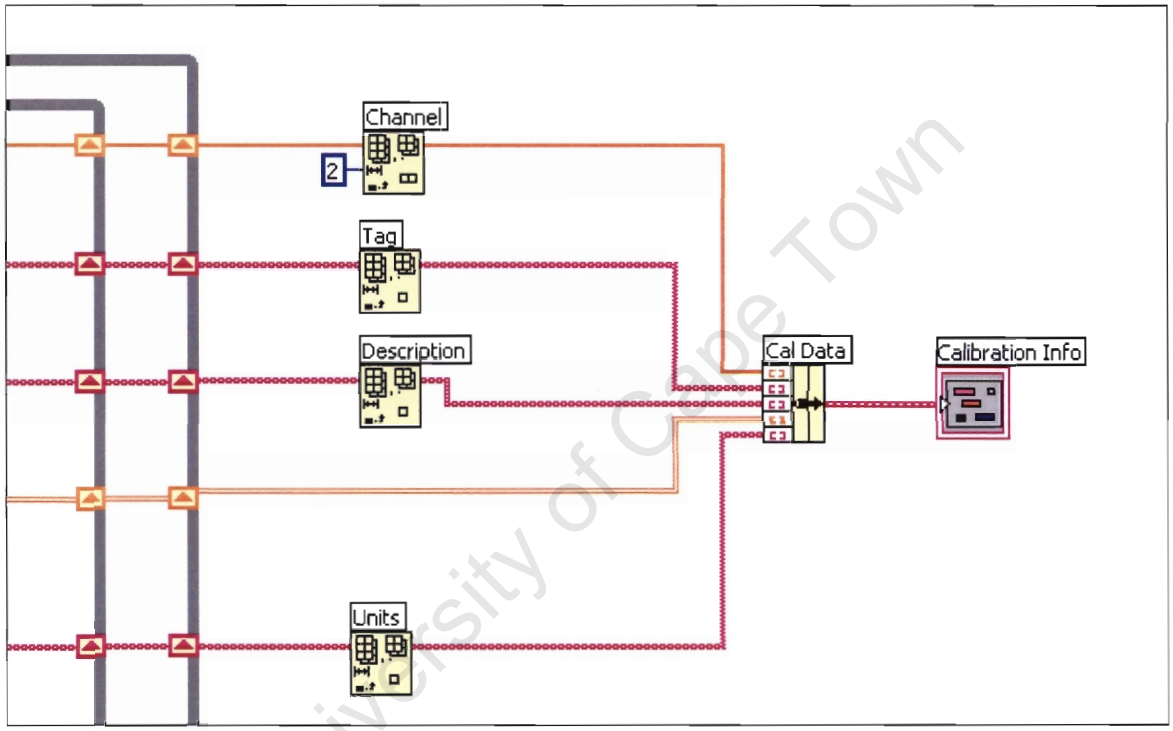

Figure 6 Outputs from the LoadCal VI

The individual arrays are now bundled together into a cluster as the output of the LoadCal2 VI, and passed to a shift register which is indicated by the small block containing the downward pointing arrow on the edge of the for loop. The shift register is used here, because the information is loaded back into the bundled array at the end of each cycle. This means that the array, and any changes which have been made to it are presented at the beginning of the next iteration. In other words the information is dynamic, and can be changed whilst the loop is executing. The static data case where a tunnel is used (in Image Loading) means that the static data is available on each iteration of the loop, but cannot be changed. The Image Loading section shows the use of the tunnel.

Parsing of the file is completed when the remaining file length is zero. This is done by discarding each line from the file once it is processed until a zero length line is found.

2.2 Image Loading (BMP Load.vi)

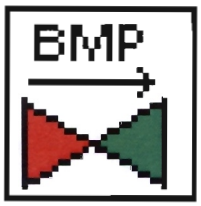

Three different blocks are used for the loading of graphical information. There is one block each for the agitators, pumps, and valves. These are done separately, instead of in one larger VI, to minimize the crossing of data lines within the main loop. The image files are all located in a subdirectory named *Images*. The images are passed through a tunnel in the loop, and are thus available as static data on each loop iteration. If the images were to be modified within the loop they would have to be passed via shift registers. The tunnel is indicated by a solid block on the edge of the loop structure.

Figure 7 shows the bitmap load VI for the agitators and pumps. The inputs are the path to the directory containing the images, and then the names of the image files in the order Orange, Green, Red. The output of this VI is a cluster containing the three images. Clusters permit the grouping of both similar and dissimilar objects. Unbundling of the clusters will be shown later where it is used.

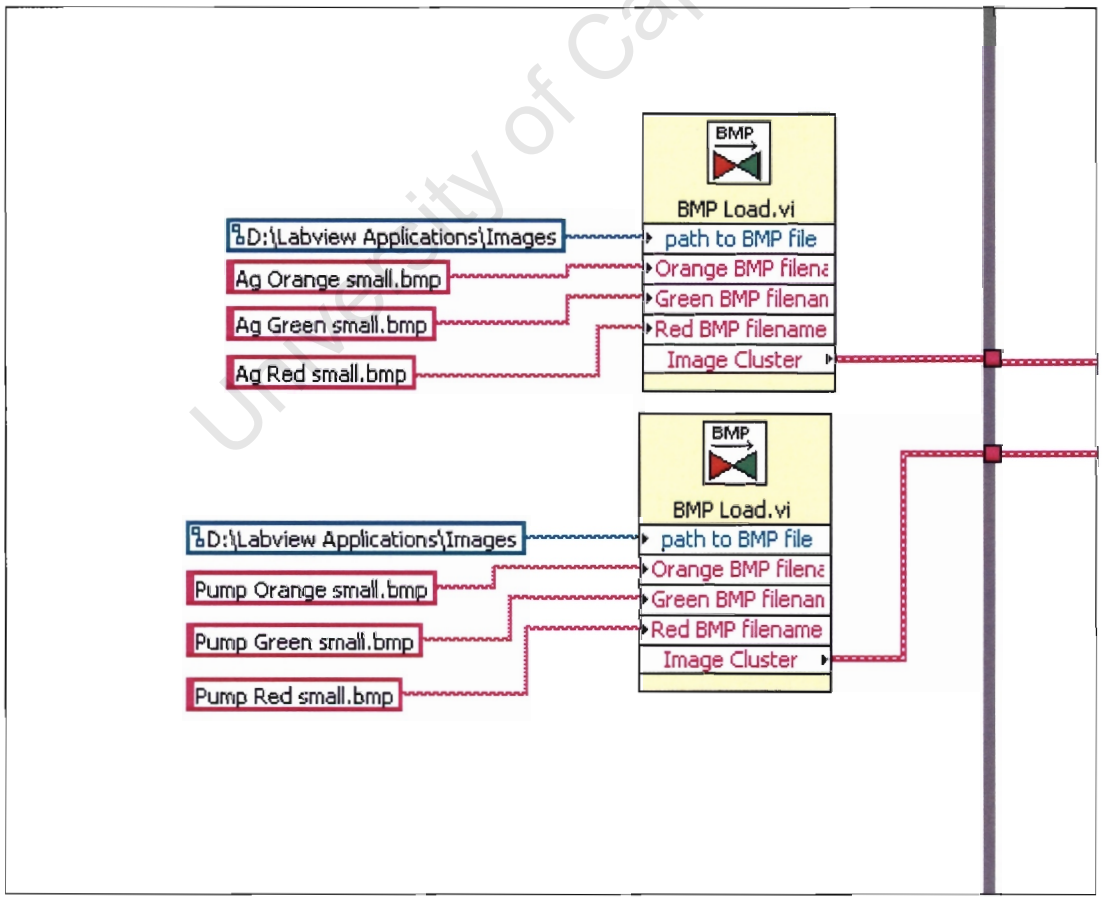

Figure 7 BMP Load VIs

The internal structure of the *BMP Load* VI is shown in Figure 8. Each of the images is loaded from disk using the 'Read BMP File' VI – this is a Labview VI which simply loads the bitmap from file into memory. The following block is also a Labview VI, 'Draw Flattened Pixmap', which takes the bitmap information, and creates a flat structure, that can be displayed in a Picture Container on the front panel. The three images are then bundled together into a cluster, and passed to the loop via a tunnel. The selection and display of the images is discussed later when the contents of the loop are dealt with. The images used on the front panel are shown below.

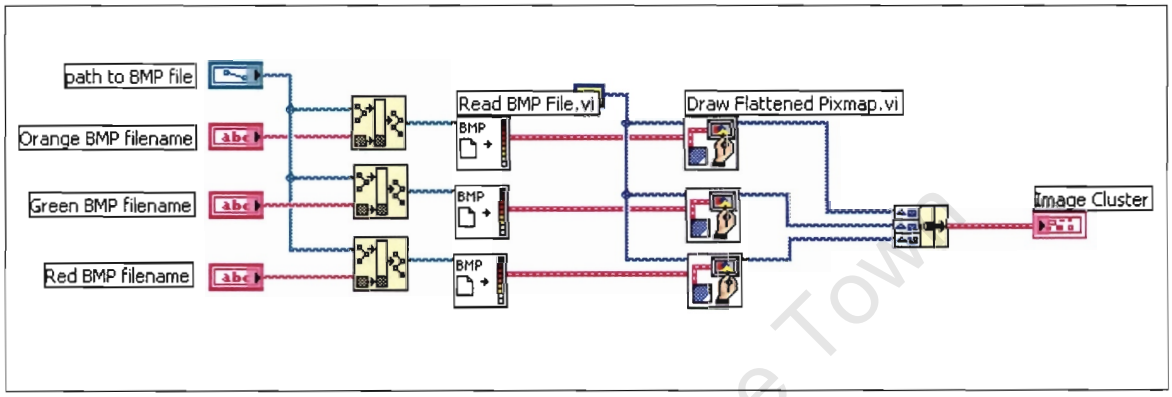

Figure 8 BMP Load Structure

Each image is a simple bitmap, created using MS Paint. The background colour of the image matches that of the background for the main panel. The images are sized according to the size of the picture container on the front panel. The drive, agitator, and valve blocks determine which image to output to the picture container on the front panel, depending on the status of the equipment.

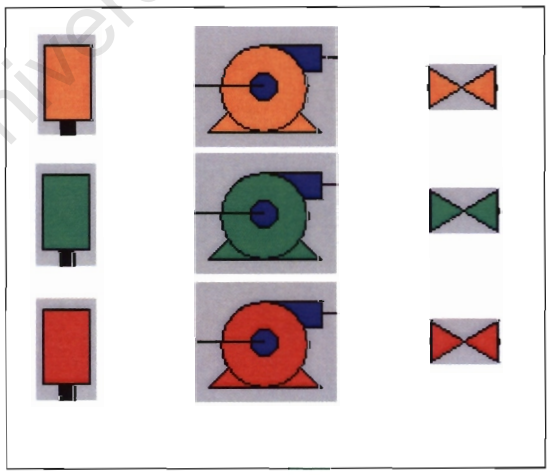

Figure 9 Agitator, Pump, and Valve Images

3. MAIN LOOP : PRE-PROCESSING

The pre-processing functions carried out in the main loop are dealt with here in the order that they take place. The main loop is executed every 250 ms.

3.1 Inputs (Inputs.vi)

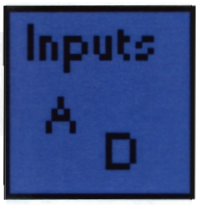

The *Inputs* VI is shown in Figure 10. The input to this VI is the scaling array taken from the unbundled Calibration Info from the LoadCal2 VI discussed previously. The Calibration Info cluster is unbundled inside the Inputs VI in order to keep the main loop tidy. Notice that the Calibration Info cluster is carried through above the Inputs VI, and meets with the output of the shift register at the far right hand side of the for loop. All shift registers come in pairs, one presenting the information at the start of the iteration, and another collecting the information (possibly updated) at the completion of the iteration. The information from the end of the iteration is presented at the input of the following iteration. The reason for carrying this information through in this fashion is that it can be modified, and saved back to the *AICalVal* file within the loop, so that the modified information is reloaded when the application is started again. The feature allowing on-line reconfiguration of the scaling information will be implemented in version 2 of the software.

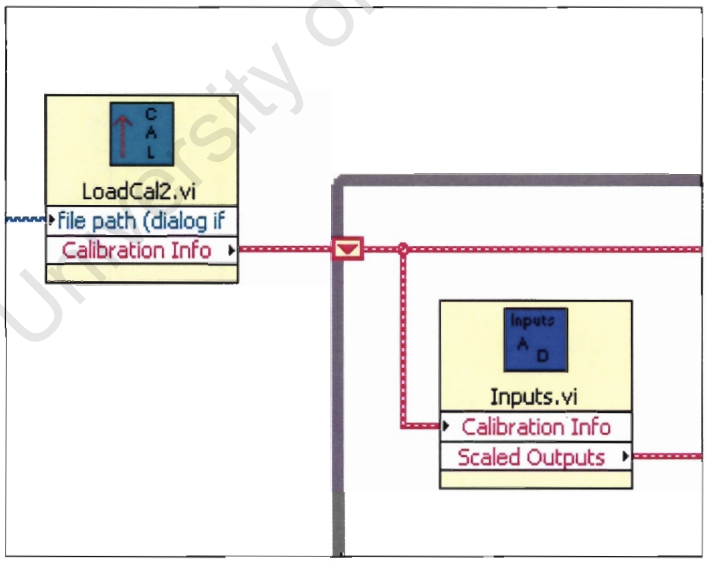

Figure 10 Inputs

The information in the following sections deals with the contents of the *Inputs* VI.

3.1.1 *Analogue Input Scaling (AIScaling.vi)*

The unbundled *Calibration Info* is shown in Figure 11 as the input to the *AIScaling* VI. Note that it is not necessary to make a connection to each terminal of the unbundle function. In this case only the Scaling array is taken as an input. The outputs of the AIScaling VI are the multiplier and offset for each analogue value, as well as the analogue scaled output values. From this it can be seen that the reading of the physical I/O is carried out within this VI. The multiplier and offset have been provided as outputs here as it was decided that they might be used in future for further computations.

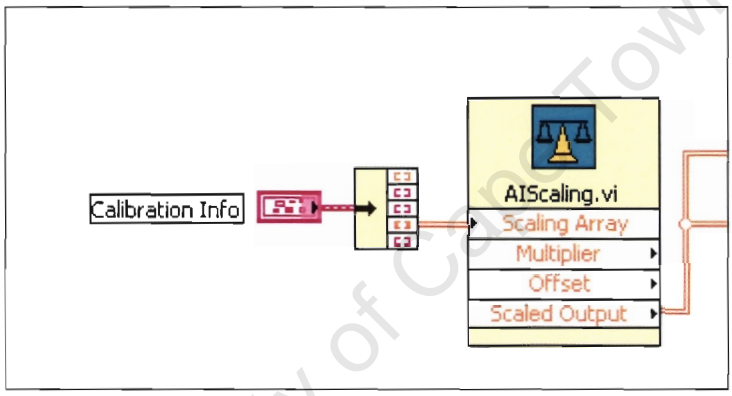

Figure 11 AIScaling

The following discussion deals with the contents of the AIScaling VI. This VI has three primary functions. The first is to compute the multiplier and offset from the scaling array, the second is to read the values from the analogue Fieldpoint module, and the third is to apply the multiplier and offset to the analogue values.

3.1.1.1 *Compute Multiplier and Offset*

In this portion of the VI, the multiplier and offset are simply computed based on the equation

$$y = mx + c$$

where

$$m = \frac{y_2 - y_1}{x_2 - x_1} = \frac{Max\_range - Min\_range}{Max\_mA - Min\_mA} = multiplier$$

and

$$c = y_1 - mx_1 = Min\_range - multiplier(Min\_mA) = offset$$

The computation is not shown here as it is quite expansive when shown in graphical terms. In this case the multipliers and offsets are each computed as a vector that is applied to the analogue input values. Labview does not carry out these computations in the way that matrix algebra is carried out. The operations are simply carried out on an element by element basis where mathematical operations are applied to elements with the same index.

3.1.1.2 *Read Fieldpoint Analogues*

The segment of the code which reads the analogue Fieldpoint module is shown in Figure 12.

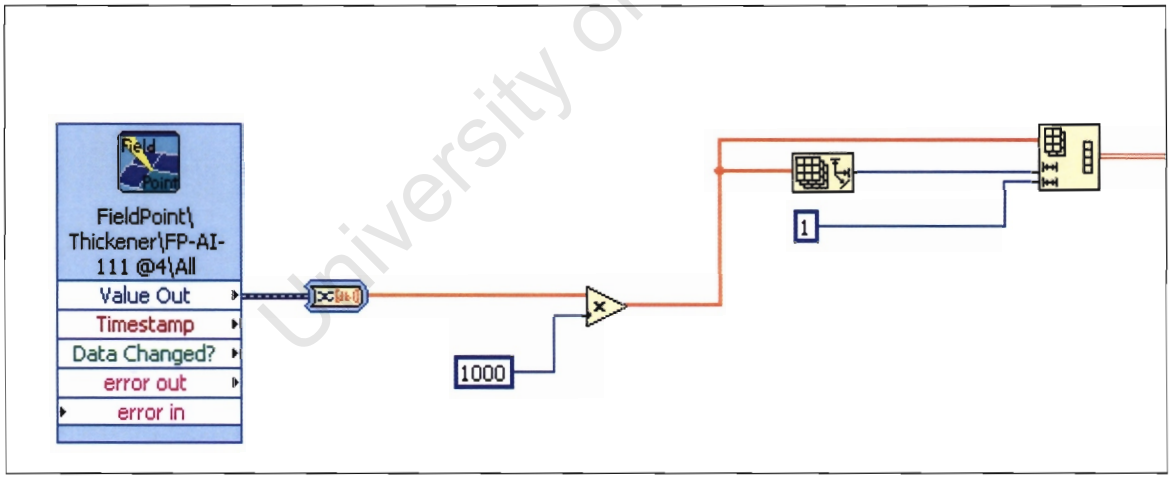

Figure 12 Read Analogue Fieldpoint Module

The Fieldpoint read operation is carried out using the Fieldpoint Express VI. This VI makes it very simple to select the module to read, and allows the user to either read a single point on the module or to read the entire module in as an array. For this to be carried out, the user must already have configured the IAK file which is generated by the Measurement & Automation Explorer (MAX). The explorer allows the user to configure the communications module, and auto-detects the modules connected. In Figure 9, the Fieldpoint VI contains the header:

Fieldpoint\Thickener\FP-AI-111@4\All

This gives the name of the IAK file – Thickener.IAK,
the module type – FP-AI-111 (analogue input module),
module address - @4 (4^{th} module connected to the communications module)
the input being read – All (all inputs are being read into an array)

MAX allows the user to allocate logical tag names to each channel, instead of referring to each element via channel number. The user must allocate this names within MAX, so that it is possible to pick an element by name using the Fieldpoint Express VI. The tag names are stored in the IAK file.

The remaining outputs from the Fieldpoint Express VI are not used in this case. Timestep information is not used here, and timestamps will be generated where appropriate as required from the system time. 'Data changed?' is not used since a complete read of the module is carried out on each cycle, regardless of whether data has changed or not. The system will generate an error if it is unable to communicate with the Fieldpoint modules, and times out.

The Value Out from this VI is a dynamic data type, and this must first be converted to a numeric data type (array of double). The data read from the analogue module is in its raw format, so that 4 mA is represented by 0.004. As a result the first step is to multiply this value by 1000 to get milliamp values. The following blocks in Figure 9 are required in order to force the array to a one dimensional vector. For some reason, the output after the type conversion is a one dimensional array, but any array operations which follow seem unsure of what the true dimension of the array are. This would appear to be a remnant of the dynamic data type. To rectify this the array is forced to be one dimensional, by reshaping it to have the same number of rows as before, but only a single column (despite the fact that the size function shows that it was only a single column before).

3.1.1.3 Apply Multiplier and Offset

At this point the multiplier and offset vectors are applied to the analogue input vector.

$$y = mx + c$$

As mentioned before, Labview carries this operation out on an element by element basis, and not as one would in matrix algebra. Now the outputs are available as a scaled output array (one dimensional).

3.1.2 *Digital Inputs (Digital Inputs.vi)*

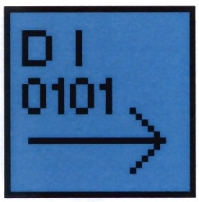

The digital inputs are read in the *Digital Inputs* VI, located within the *Inputs* VI. The VI is shown in Figure 13. The two indicators showing as Module1, and Module 2 are VI front panel indicators used when required for debugging and commissioning purposes.

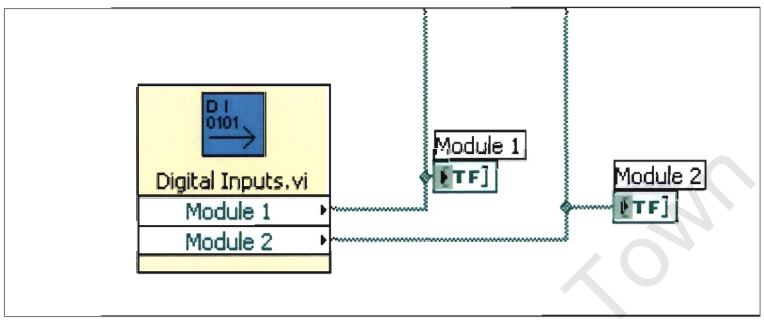

Figure 13 Digital Inputs VI

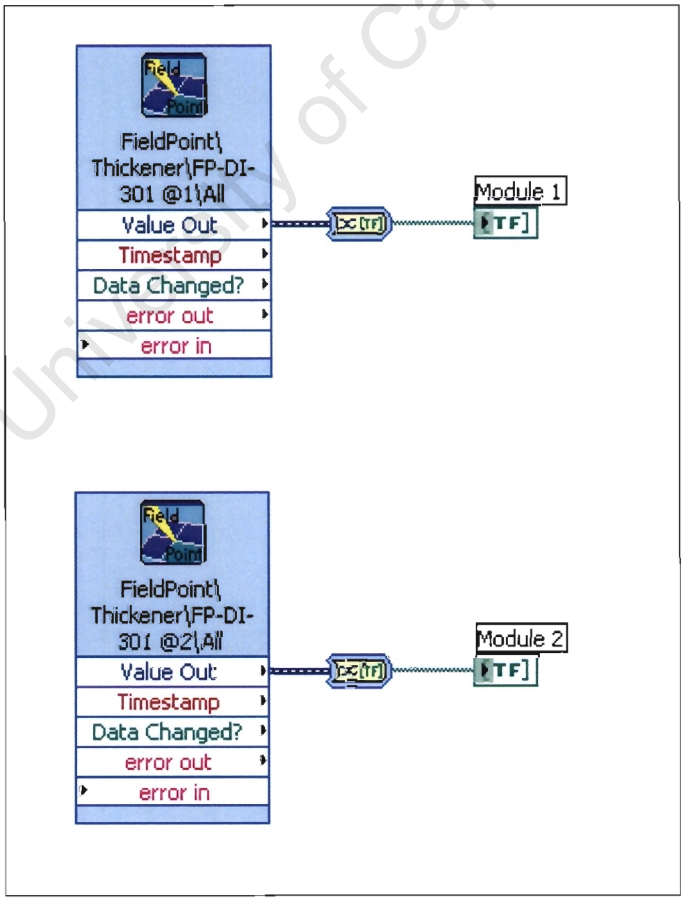

Figure 14 Read Digital Inputs

Inside the *Digital Inputs* VI, the two digital input modules are read as shown in Figure 14. As before, the Thickener.IAK file is used since it contains the configuration information. Each Fieldpoint Express VI is used to read one hardware module. There are two modules each containing 16 input channels, to give a total of 32 digital inputs. After the Fieldpoint read module there is a conversion from the dynamic data type to a Boolean array.

The final step in the *Inputs* VI is to bundle the analogue and digital signals together into a cluster titled Scaled Outputs. The order of the signals in the cluster is:

Scaled Analogues
Digital Module 1
Digital Module 2

Further in the program the information is rearranged as required so that it can be applied in a sensible fashion. This will become clear when the drive and valve blocks are discussed.

The output from the *Inputs* VI is the input to the following VIs:

Drive Clusters
Valve Clusters
Derived Tags
Analogue Displays

3.2 Derived Tags (Derived Tags.vi)

The Derived Tags VI takes the analogue and digital inputs, and creates level alarms where required, and this information is then used to create the interlock or drive/valve enable outputs that prevent equipment damage when it is not appropriate to operate the equipment.

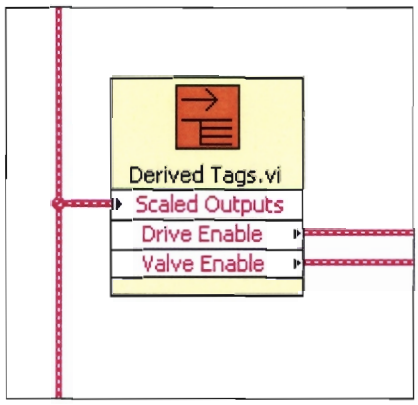

Figure 15 Derived Tags

The Derived Tags VI contains the Alarms VI (digital alarms from analogue values), and the Interlocks VI, as shown in Figure 16.

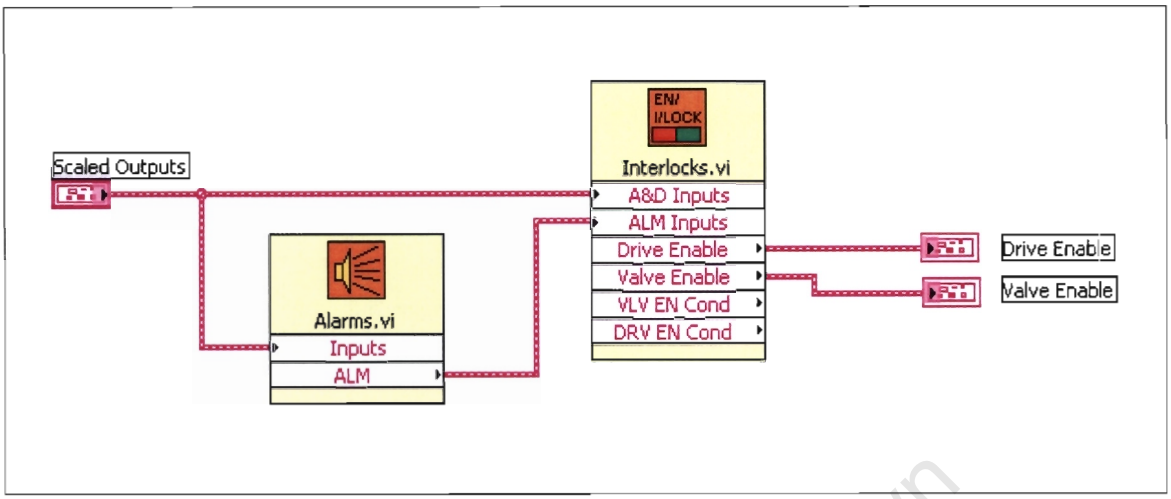

Figure 16 Alarms

3.2.1 Alarms (Alarms.vi)

Figure 17 shows a portion of the Alarms VI. Here the values for the LL, LO, HI, and HH alarms are input to the Deadbanding VI. For the present there are only two variables for which alarms are generated. These are the slurry tank level, and the water tank level, LT-001, and LT-002 respectively.

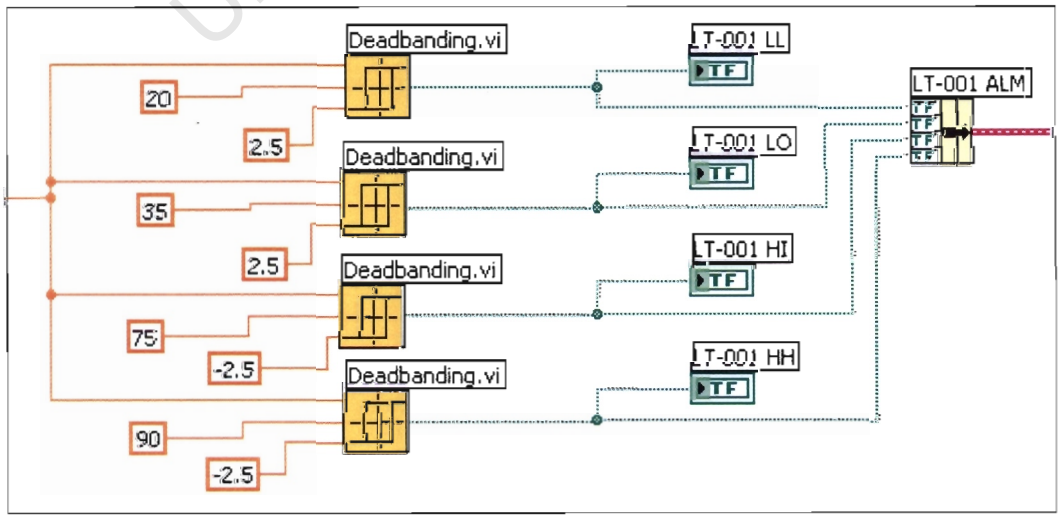

Figure 17 Alarm Generation

3.2.1.1 *Deadbanding (Deadbanding.vi)*

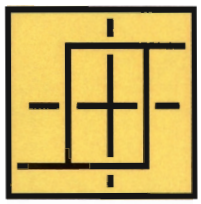

The Deadbanding VI prevents the alarms from chattering, and resulting in drives and valves starting and stopping as the enable signals go True and False. The Deadbanding VI was created from scratch as the Express VI provided by Labview to carry out this function was not found to be suitable. The first input value (topmost) to the Deadbanding VI is the analogue input value. The second is the value at which the alarm becomes active, and the third value determines when the alarm will be reset. For the LL, and LO alarms, the alarm becomes active when the analogue value is below the alarm value. The alarm is then reset when the analogue value is at e.g. 20 + 2.5. For the HI, and HH alarms, the alarm becomes active when the analogue value exceeds the alarm value, and is reset when the analogue value is at e.g. 75 + (-2.5). All values in the above blocks are given in percent. If there were more alarms to be generated from analogue values, it would make sense to store all of the alarm limits and their deadband values in a file, load these at startup, and allow them to be configured whilst the software is executing. This may be the case in future, at which point the functionality will be included.

The Deadbanding VI is fairly complex, without necessarily appearing so, and determines whether to switch on the positive side of the alarm value, or the negative side of the value, depending on the sign of the Deadband value. There are some special features to the Deadbanding VI which must be noted at this point. The while loop of the Deadbanding VI is shown in Figure 18.

The first important feature of this while loop is that it is configured to run once only. This is done by wiring a false indication to the run terminal of the while loop. Each time it is executed within the main loop, it will execute once, and then stop. The purpose of this is to make it possible to use shift registers to hold the state from the previous iteration. In order to make this possible the VI must be configured as re-entrant in the VI properties dialogue. This forces Labview to create a memory space for each instance of the Deadbanding VI, to store the previous state. This VI is a state machine, combining two case blocks with a while loop. To have used the main loop to implement shift registers would have made the code very messy indeed. Depending on the value of the deadband value, the VI decides which of the two case statements to execute. This decides which side of the alarm value the actual switching should take place. The state is then held until the main loop iterates once again. If the VI is not made re-entrant, a problem arises, since when the first instant of the VI is executed, it takes its state from the last instance of the VI that was executed. This will also happen in the Alarms VI, where each Deadbanding VI will take its state from the last one that executed. The result is that nothing works. This turns out to be one of those useful tricks that need to be applied in Labview, and the technique is also used elsewhere in the code.

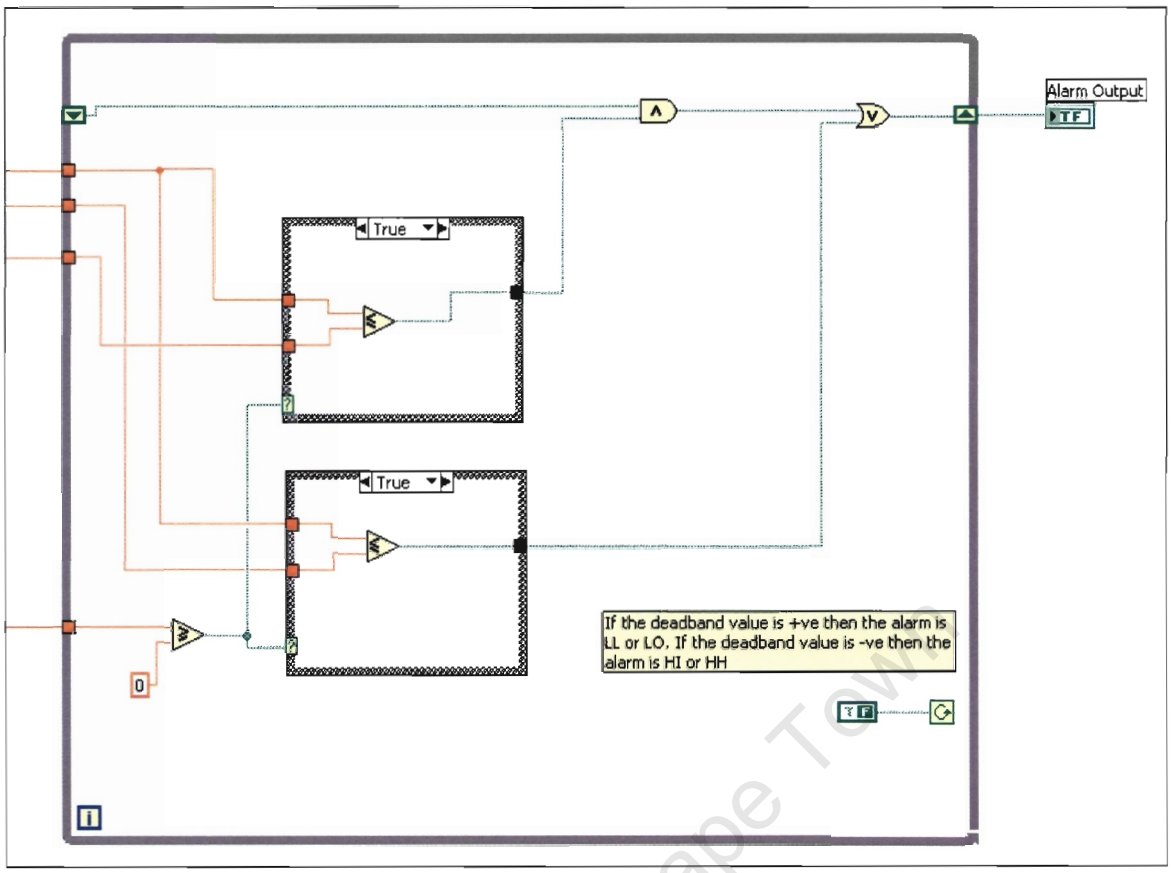

Figure 18 Deadband WHILE Loop

3.2.2 Interlocks (Interlocks.vi)

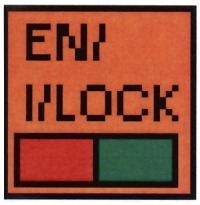

To avoid clutter, the valve and drive enable signals (interlocks) are dealt with separately within the Interlocks VI, as shown in Figure 19. The valve and drive enable condition outputs, are clusters containing all of the relevant signals used to derive the enable conditions for all of the valves and drives respectively. These outputs are to be used for the interlocks display page.

The interlocks display page has yet to be implemented, and is intended to show the user which conditions are responsible for the lack of an enable condition on any drive or valve. At present the means to open and close a separate page from the main loop, without affecting its execution has not yet been determined. The intention is that on the click of an Interlocks button, a separate page will pop up, without affecting the execution of the main loop, even though it must update itself from the main loop. The user must be able to view this page, and minimise or close it at will. Attempts to achieve this have resulted in the main block halting, and waiting until the interlocks page is closed before continuing with its execution. This is not acceptable, since any controllers running in the main loop will be halted, along with any

other dilution estimation calculations. The dilution and other controllers must continue to run regardless.

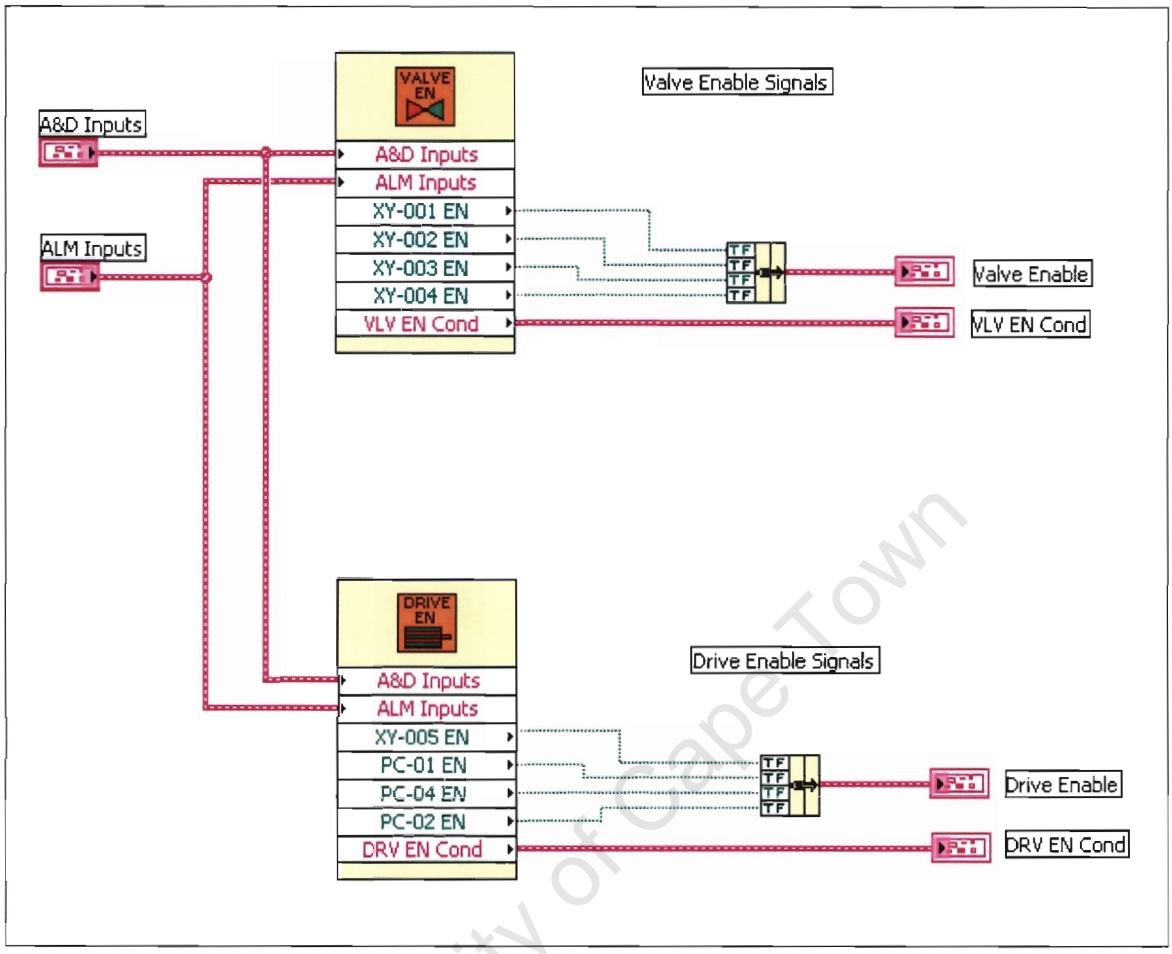

Figure 19 Valve and Drive Enable Blocks

3.2.2.1 Valve Enable (Valve Enable.vi)

The Valve Enable VI is shown in Figure 20. The figure shows how the necessary conditions are extracted from the PS-001 OK (air supply OK) signal, and the tank level alarms. The tank level clusters have been configured here so that hovering the mouse over one of the Boolean outputs will display the name of that alarm at the cursor. All clusters in the code have been configured in this fashion for clarity.

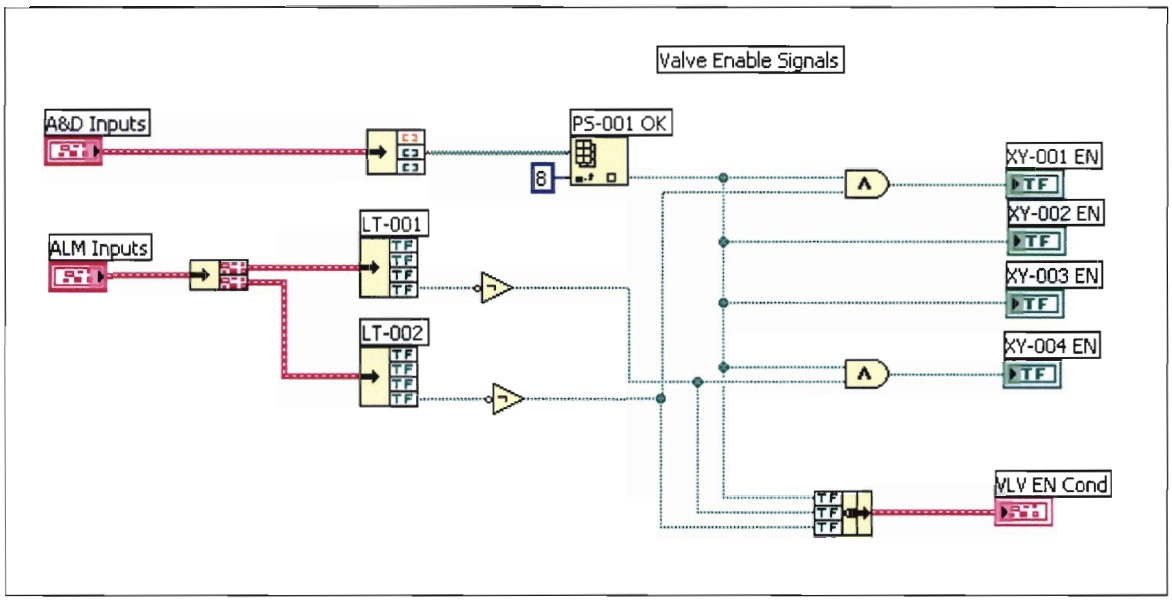

Figure 20 Valve Enable

The interlocks or enable signals for the valves are given in Table 1. To make sense of the table, it should be read in conjunction with the P&ID diagram for the Scale Thickener Test Plant [1].

Table 1 Valve Enable Conditions

Valve	**Description**	Condition
XY-001 EN	Mains Clear Water Feed	(PS-001 OK) AND (LT-002 NOT HH)
XY-002 EN	Clear Water Dump	PS-001 OK
XY-003 EN	Clear Water Isolate	(PS-001 OK) AND (LT-001 NOT HH)
XY-004 EN	Mains Slurry Water Feed	(PS-001 OK) AND (LT-001 NOT HH)

A brief explanation of the enable conditions follows:

XY-001 EN: This is the mains clear water feed, and the pressure supply must be present in order to operate. The second condition is that the tank is below its maximum level, otherwise the tank will overflow. This condition ensures that once the tank reaches its maximum level, the enable signal will fall away, and the valve will automatically close, thus preventing an overflow condition.

XY-002 EN: This is the clear water dump valve, and is used to dump water from the clear water tank if the system becomes unbalanced and there is too much water in the system. Air pressure supply must be healthy for this valve to operate.

XY-003 EN: This is the clear water isolate valve, and is used to shut the dilution line to the slurry tank, so that the water is forced to the clear water dump line. When this valve is open, dilution water is pumped to the slurry tank, and hence the slurry tank (LT-001), cannot be above its maximum level if this valve is to operate (open).

XY-004 EN: This valve supplies mains water to the slurry tank. This valve is used to fill the tank when making a slurry up. For this valve to operate, the tank must not be at its maximum

level. If the maximum level is reached, the valve will automatically close when the enable condition drops away in order to prevent flooding of the laboratory. The air pressure supply must be healthy.

3.2.2.2 Drive Enable (Drive Enable.vi)

Within the Drive Enable VI, the conditions required for the interlocking are first extracted in the Drive Enable Conditions VI, and bundled together into a cluster. This cluster is then unbundled for each drive, as well as being output for the interlocks display panel (to be implemented).

3.2.2.3 Drive Enable Conditions (Drive Enable Conditions.vi)

The Drive Enable Conditions VI extracts the necessary alarms and analogue values to be used in the Drive Enable VI, and bundles them into a cluster. Caution should be exercised when modifying these values, since the order of the outputs becomes rearranged, and the enable function ceases to work correctly. The order of the outputs in the cluster can be rearranged by right clicking on the cluster on the front panel, and selecting 'Reorder Controls in Cluster'. This allows the user to define the index of each control in the cluster. The Valve Enable VI does not feature a similar VI, although the caution regarding the ordering of controls in clusters still applies at the output of the VI, and any other VI for that matter.

The present cluster control is given as follows:

Table 2 Drive Enable Cluster Control Order

Cluster Index	Control Name	Description
1	XY-005 OP?	Is XY-005 Open? (i.e > 5 %)
2	LT-001 NOT LL	LT-001 above min. level
3	LT-001 NOT HH	LT-001 below max. level
4	LT-002 NOT LL	LT-002 above min. level
5	LT-002 NOT HH	LT-002 below max. level
6	XY-002 OP	XY-002 Open?
7	XY-003 OP	XY-003 Open?
8	PS-001 OK	Supply air pressure healthy?
9	PC-01 RN	Slurry pump running?
10	PC-01 AUTO	Slurry pump in Auto?
11	PC-04 AUTO	Underflow pump in Auto?
12	PC-02 AUTO	Dilution pump in Auto?
13	AG-01 RN	Slurry agitator running?
14	AG-02 RN	Water agitator running?

Any new enable conditions should be added to the end of this list for the index to be automatically incremented to the next value.

To be noted here is that the required signal is created within this block, and an example in the above table, is the negation of the level alarms. For XY-005 a comparison is carried out to determine whether the valve position is above or below 5 %. Below 5 % the valve is closed, since it does not always return fully to the 0 % position due to stiction in the valve seat. Above 5 % the valve is treated as open, or opening.

Returning to the drive enable block. The portion of the drive enable block is shown in Figure 21. The control valve XY-005 is also treated as a drive for the purposes of generating an enable signal, and is shown in the figure as an example. The signals from the DRV EN Cond cluster are unbundled, and used as necessary with logic gates to create the drive specific enable output. Any logic may be applied as necessary to create the enable signal. As mentioned on the previous page, negation is generally applied in the Drive Enable Conditions VI. To add to the existing enable conditions, the logical AND VI can be enlarged by dragging the lower end to create further terminals. Further drives can easily be added in the Drive Enable VI by appending them to the bottom of the block diagram.

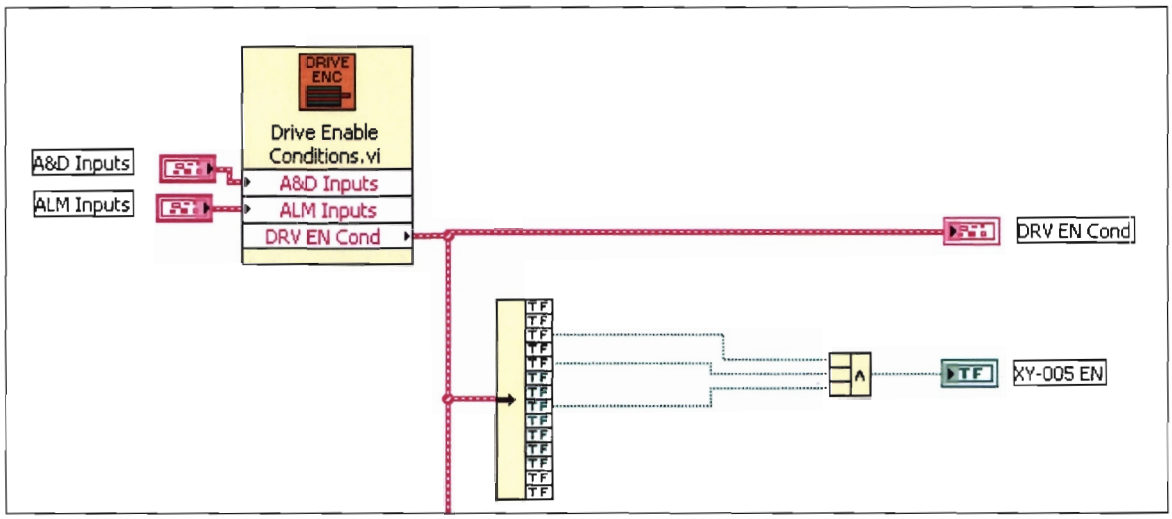

Figure 21 Drive Enable VI

Present drive enable conditions are shown in Table 3.

Table 3 Drive Enable Conditions

Drive	Description	Conditions
XY-005 EN	Dilution water control valve	(LT-001 NOT HH) AND (LT-002 NOT HH) AND (PS-001 OK)
PC-01 EN	Slurry feed pump	(LT-001 NOT LL) AND (LT-002 NOT HH) AND (PC-01 AUTO) AND (AG-01 RN)
PC-04 EN	Thickener underflow pump	(LT-001 NOT HH) AND (PC-01 RN) AND (PC-04 AUTO)
PC-02 EN	Dilution water supply pump	(LT-001 NOT HH) AND (LT-002 NOT LL) AND [(XY-002 OP) OR (XY-003 OP)] AND (PC-02 AUTO) AND (AG-02 RN)

A brief explanation of the drive enable conditions follows:

XY-005 EN: XY-005 is the dilution water control valve. In conjunction with the dilution water supply pump, this valve determines how much dilution water to add to the slurry tank to maintain the design solids concentration. The dilution water pump delivers a certain flow rate, and this control valve determines how much of that flow should go to the slurry tank, and how much is returned to the clear water tank. For this reason, neither the slurry tank (LT-001), nor the clear water tank (LT-002), can be at their maximum level for this valve to be operational. The air supply must be healthy.

PC-01 EN: The slurry feed pump delivers dilute slurry to the thickener. To protect the pump, the slurry tank (LT-001) cannot be below its minimum level. Running the pump drive will seize the rotor/stator in the positive displacement (progressive cavity) pump within minutes. Under normal operating conditions, the thickener runs full, and the overflow reports to the clear water tank. If the clear water tank reaches its maximum level then the pump will shut down to prevent flooding. The slurry pump must be in Auto mode (selector switch at the electrical panel) for the pump to be started from the control panel, or via automatic sequence. Finally, the slurry tank agitator (AG-01) must be running. If the agitator is not running, the

slurry will settle out in the tank, so that a high density slurry, rather than a dilute mixture will be pumped. The thickener will tend to overflow with dense slurry under these conditions, so that water containing thick slimes will report to the clear water tank.

PC-04 EN: The thickener underflow pump returns high density slurry to the slurry tank (LT-001). If the slurry tank is full for some reason (e.g. by the addition of dilution water), then this pump will be disabled. The slurry feed pump (PC-01) must be running for the underflow pump to run. This condition is present to ensure that the thickener is not pumped dry. If this were to happen then the pump will operate dry, and seize within a few minutes. PC-04 must be in auto mode (selector switch at the electrical panel) for the pump to be started from the control panel, or via automatic sequence.

PC-02 EN: Both the slurry tank, and the clear water tank must be below their maximum levels. PC-02 is the dilution water pump, and this water is split between the two tanks via XY-005. If either tank runs the risk of overflowing, the pump is disabled. Either of XY-002 (clear water dump valve) or XY-003 (clear water isolate valve) must be open for this pump to operate. If both are closed, the motor will attempt to burst its seals, possibly damage the rotor and/or stator, and finally trip the motor at the electrical panel due to current overload. The final condition is that the clear water agitator (AG-02) is running. Since the clear water overflow from the thickener contains fine particles the clear water tank does not contain perfectly clear water. The purpose behind the agitator is to ensure that the particles remain in suspension, and are pumped back to the slurry tank over time. Failure to do this results a gradual buildup of a fine sediment at the bottom of the tank. Ultimately this would be detrimental to the test work, since the balance of fine and coarse particles in the slurry must be maintained.

The two agitators do not appear in this list since they are manually operated from the electrical panel. In future it is possible that these will be wired in for automatic operation so that the system is able to recover on its own from a power failure. At present this mode of operation is suitable.

3.3 Drive Clusters (Drive Clusters.vi)

This VI groups the inputs according to the drive that they apply to. This simplifies the process later where the information required to control and display the status for each drive is easily accessed. Figure 22 shows this VI so that the icon is familiar to the user.

This block splits the analogue and digital signals from their individual arrays, and then recombines them into clusters for each drive. This will also be used later for the automatic sequencing. The drive order is as found on the electrical panel, and the output of the VI is the bundled combination of the drive clusters in the order given below:

PC-01 : Slurry Pump
PC-04 : Underflow Pump
PC-02 : Dilution Pump
PC-05 : Spare 0.75 kW drive
AG-01 : Slurry Agitator
AG-02 : Water Agitator
PC-03 : Spare drive (flocculant addition – for future use)

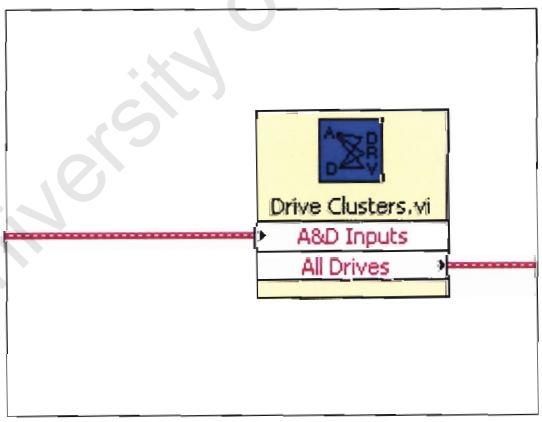

Figure 22 Drive Clusters

An example of the contents of this VI are shown in Figure 23.

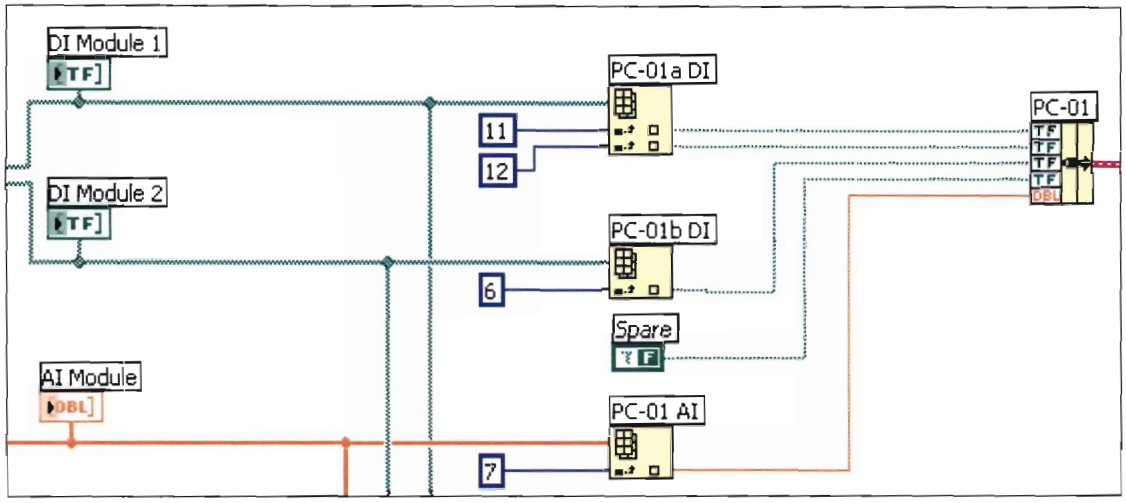

Figure 23 Drive Clusters Code

Although this may seem somewhat difficult to interpret it is actually quite simple. In each case the relevant digital inputs are extracted by indexing the digital array, and then combined with the indexed analogue input for the drive. The order of the inputs has been standardised, and is the same for each of these drives. The structure of each drive cluster is as follows:

Element 1:	Digital Input	:	RUN Indication
Element 2:	Digital Input	:	Auto/Man Indication (panel selector)
Element 3:	Digital Input	:	Drive Healthy (Trips OK)
Element 4:	Digital Input	:	Spare
Element 5:	Analogue Input	:	Speed in Hz

The Drive Healthy inputs for the two agitators are forced to a True state here, since they are not physically present on the electrical panel – this is an error on the panel manufacturer's part, and is to be rectified. The Auto/Man indication is also not present on the panel (by design), and is simply forced to a False state in this VI. The I/O schedule is shown in Appendix 1.

3.4 Valve Clusters (Valve Clusters.vi)

In this VI a similar function is carried out to that in the Drive Clusters VI.

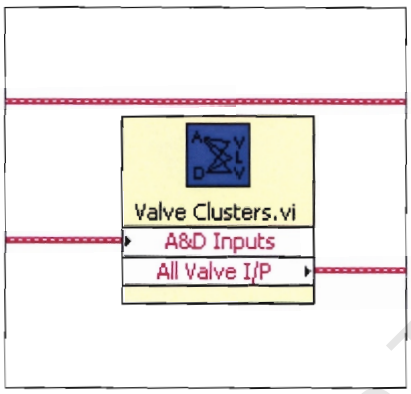

Figure 24 Valve Clusters

This block splits the analogue and digital signals from their individual arrays, and then recombines them into clusters for each valve. This will also be used later for the automatic sequencing. The valve order is:

XY-001	Water Tank Mains Feed
XY-002	Water Dump Valve
XY-003	Water Tank Isolation Valve
XY-004	Slurry Tank Mains Feed

The output is a cluster containing the status for all valves. Each cluster within this combined cluster contains only two status indications:

Element 1	:	Valve Open Indication
Element 2	:	Valve Closed Indication

These are taken in the order that they have been wired into the digital input module.

4. MAIN LOOP : DRIVES AND VALVES

The drives and valves have been grouped together into two separate high level VIs. The contents of each of these VIs, and the philosophy applied in their operation are discussed in the following two sections.

4.1 All Drive Control (All Drive Control.vi)

A portion of the main loop containing the *All Drive Control* VI is shown in Figure 25.

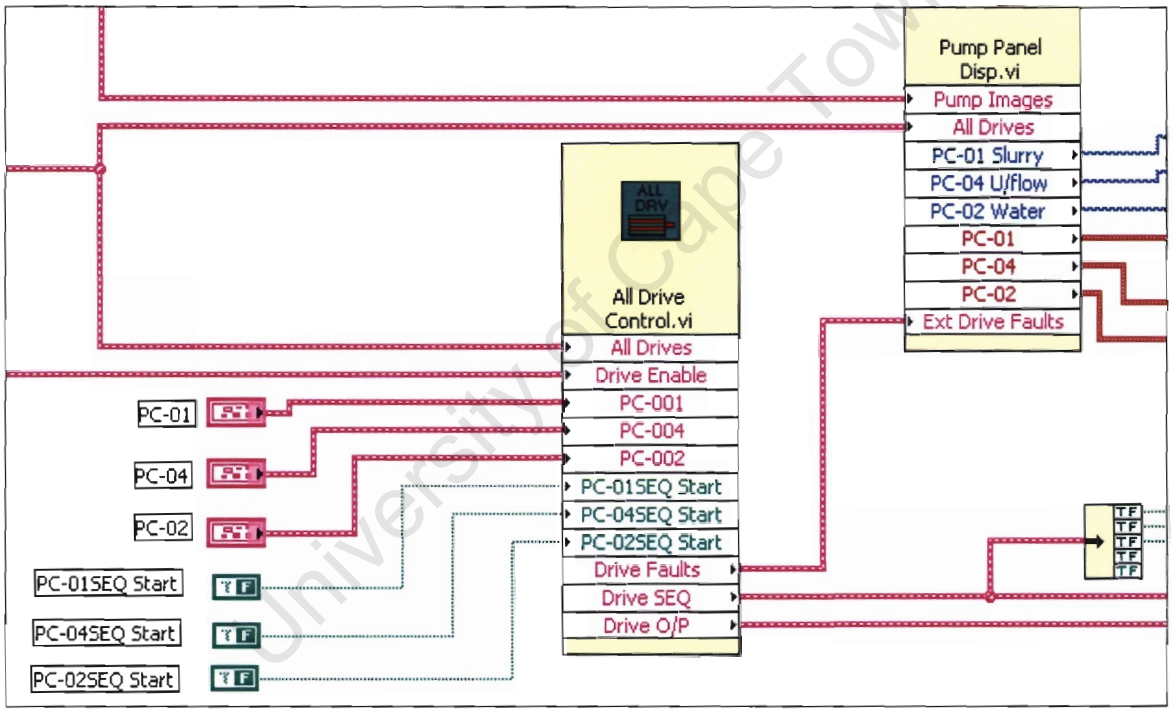

Figure 25 All Drive Control VI

This VI serves as the container for all for the drive control blocks. The contents of this VI are best explained by examining the contents of the *Drive Control* VI.

4.1.1 *Drive Control (Drive Control.vi)*

The contents of the *All Drive Control* VI are shown in Figure 26, and the contents of the *Drive Control* VI are shown in Figure 27.

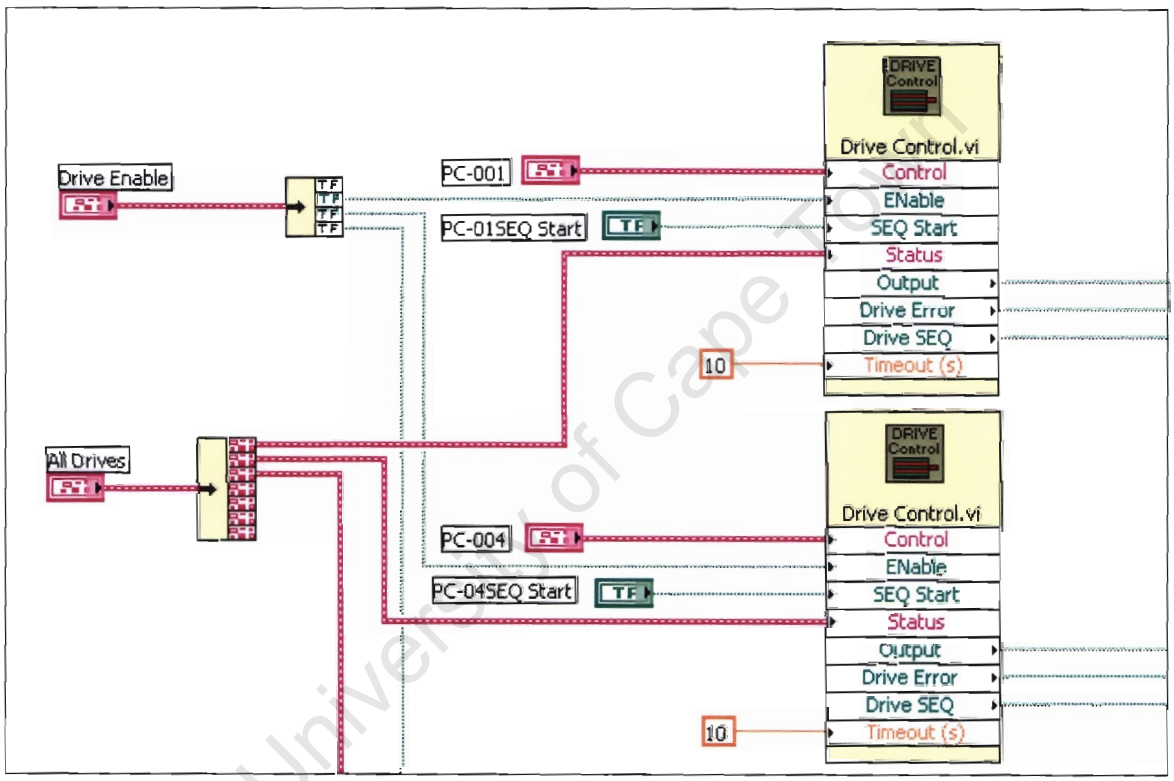

Figure 26 All Drive Control VI contents

The drive control philosophy is as follows:

It must be possible to start and stop a drive (or open and close a valve) from more than one location. As mentioned previously there are three possible ways to start or stop a drive. These are

Manual – Electrical Panel
Auto – Control Panel
Sequence – Automatic control sequence.

The first mode does not allow any action from the front panel, or from an automatic sequence, since the switch on the electrical panel is set to manual. In this mode it is not

possible to start the drive from the control panel or via automatic sequence (the VSDs are configured in this way). When the selector switch on the electrical panel is set to Auto, it is now possible to start the drive by pushing a button on the control panel, or via a pre-configured control sequence. In order to start the drive in sequence mode it must have been set to sequence mode on the front panel. The system has been configured so that even if the drive is in sequence mode, it can still be stopped and started by pressing buttons on the control panel. It is thus possible for the operator to carry out actions while an automatic sequence is in progress. The sequence will continue to run as long as the operator action doesn't violate any of the automatic sequence conditions. In order to facilitate the start/stop functionality from multiple locations, it is essential to start and stop the drives using pulses. If pulses were not used then one routine might be holding the drive output high, and would not allow another to reset it and vise versa. The drive output signal is configured in the same way as the electrical panel pushbutton start, so that the start signal is latched in by the running feedback from the drive. The stop signal breaks this circuit and the drive stops. What this means is that it may happen that a drive has stopped, even though the control panel button would seem to show that it is still running. To start the drive the button must be cycled to the stop position and then restarted in order to generate the output pulse. If the enable condition for a drive falls away, then the run circuit will also be broken.

If the drive enable signal is not present, then no panel start request, or sequence start request are passed through to the output. The timeout function determines the duration of the start or stop pulse. If the required action does not take place within this period, then an error is generated when the pulse goes back to zero. The following sections describe the *Pulsar* VI, and the *Drive Error* VI.

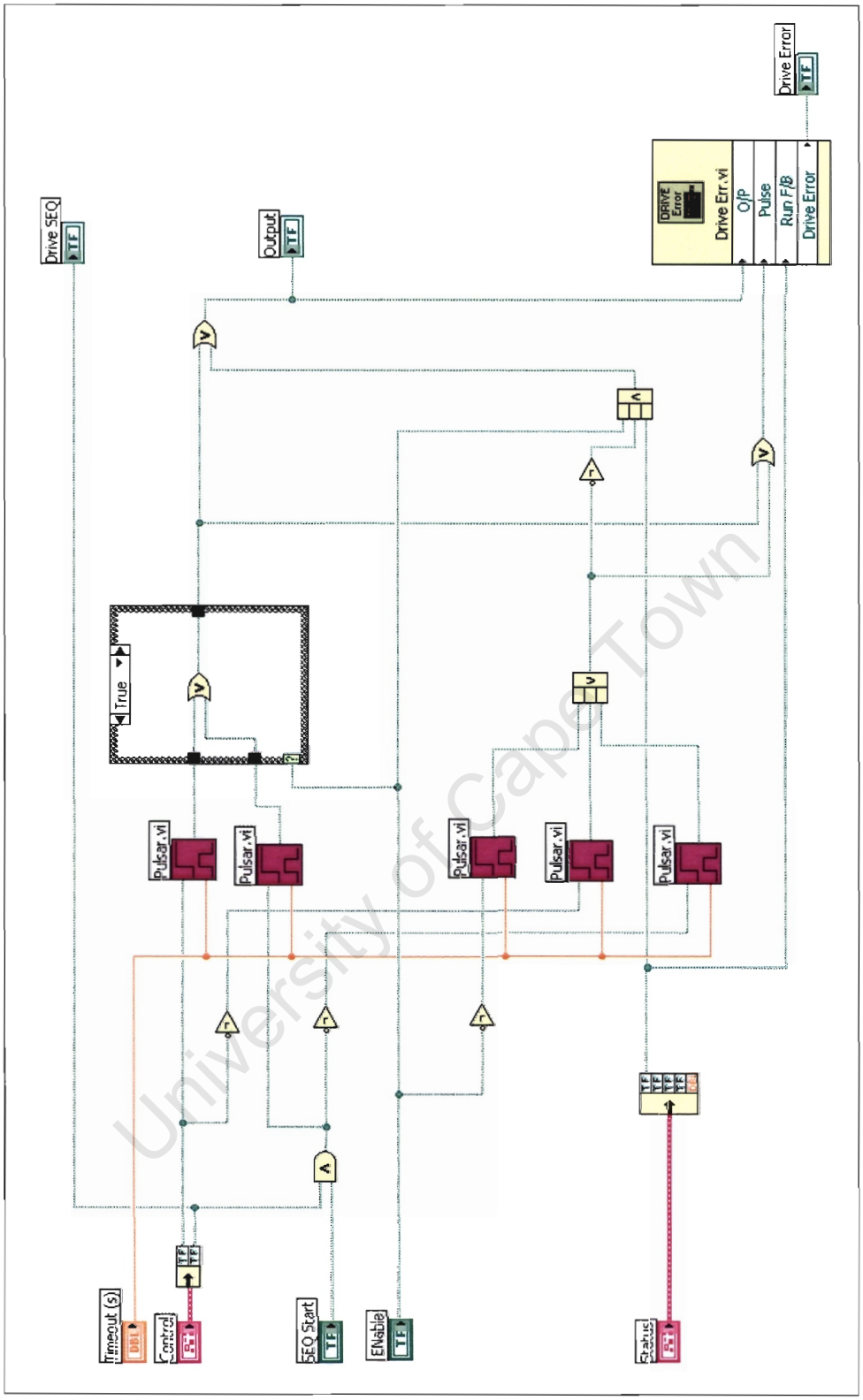

Figure 27 Drive Control VI

4.1.1.1 *Pulse Generator (Pulsar.vi)*

The Pulsar VI is once again a state engine, executed within an execute-once while loop. The while loop permits the use of shift registers that pass information from one iteration to the next. The VI is reentrant so that the shift register values are uniquely stored in memory for each instance of the pulsar VI. This VI was created due to the inadequacy of Labview's own VIs. Attempts to achieve the same functionality with Labview met only with frustration.

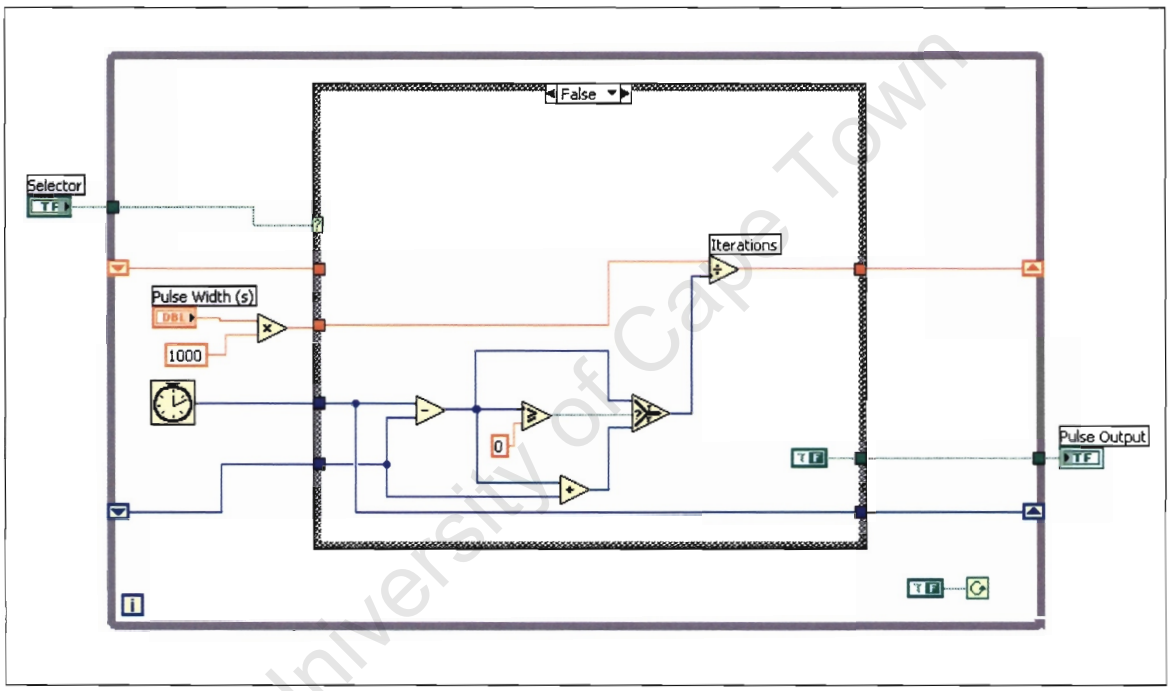

Figure 28 Pulsar VI (False Case)

The selector is the input which activates the generation of a pulse. When the selector is False, the False block of the case statement determines the duration of the pulse. The pulse width input is converted to milliseconds. At the same time the current execution interval is calculated, and from this the system works out how many iterations the output must be held high for to generate the desired pulse width. As soon as the selector goes True, the output of the *Pulsar* VI goes true. In the True case, the number of iterations is decremented by one on each cycle until it is less than or equal to zero, and the output is reset to False. The output of the VI can only go True again once the selector input has gone False to recalculate the required number of iterations. As things turn out, this is exactly the desired result, and it works very well.

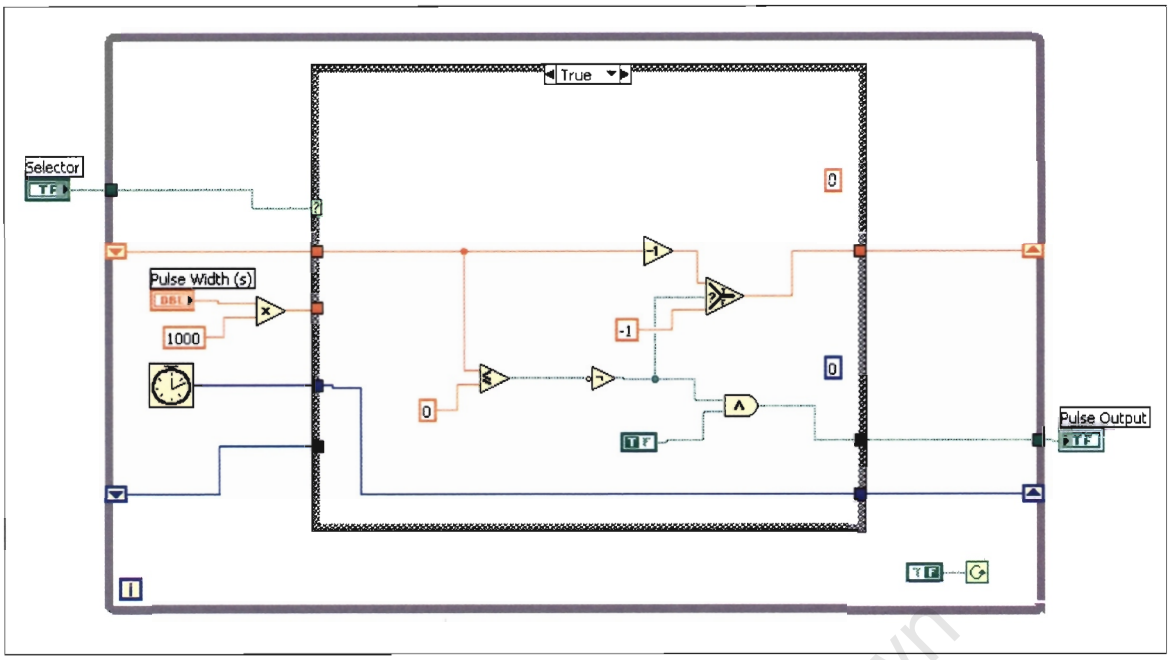

Figure 29 Pulsar VI (True Case)

4.1.1.2 Drive Error (Drive Error.vi)

The Drive Error VI shown over the page is very simple in its execution. It is disabled by the pulse input, since there are no actions in the True case of this case function. This allows the drive the opportunity to start while the pulse is held high – and avoids inconvenient error conditions that are not really valid at this point. The drive error function is also inhibited if the drive mode selector is in manual at the electrical panel.

Two basic errors are catered for by this VI, the first is where the *Drive Control* VI is generating an output, but the drive is not running (unlikely, but you never know). The second condition is where the drive is running even though no output is being generated by the *Drive Control* VI. The output from this block goes to the display VI.

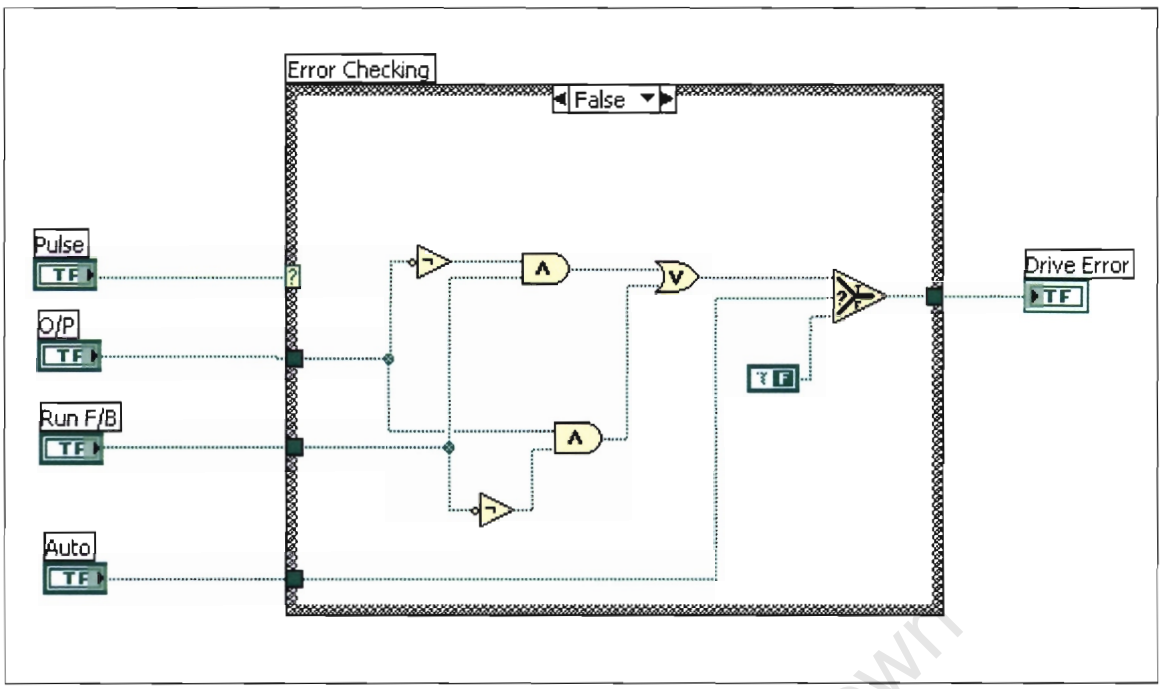

Figure 30 Drive Error VI

4.2 All Valve Control (All Valve Control.vi)

Figure 31 shows the *All Valve Control* VI. The inputs to this VI are the cluster controls from the front panel of the main VI, and the sequence controls. This VI is a container for the individual valve control VIs. The outputs go to the valve display VI, and to the digital outputs VI.

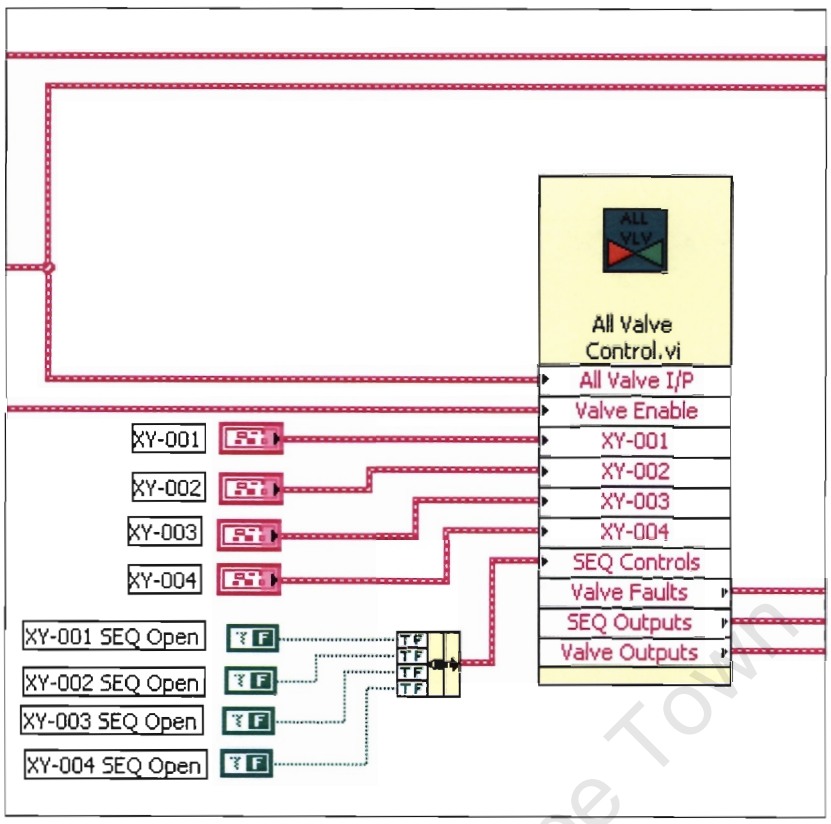

Figure 31 All Valve Control VI

Figure 32 shows a portion of the contents of this VI, showing the *Valve Control* VI.

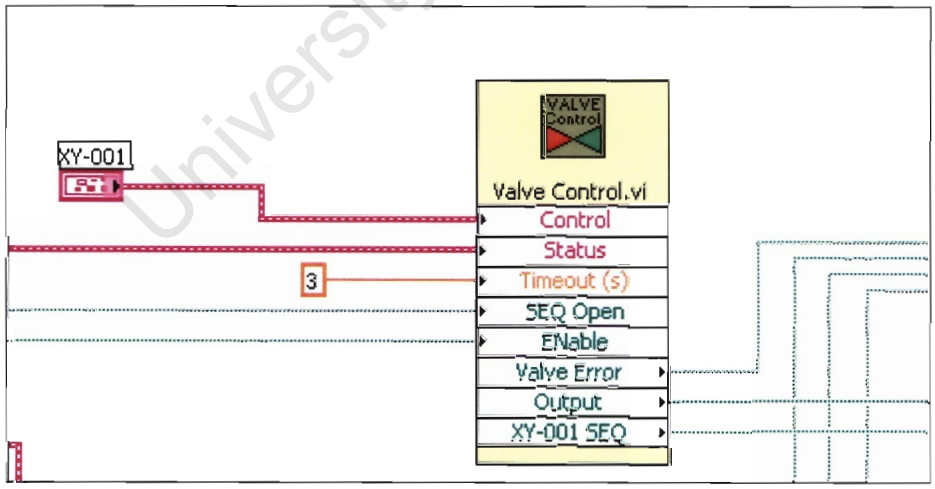

Figure 32 All Valve Control VI

4.2.1 Valve Control (Valve Control.vi)

The contents of the *Valve Control* VI are shown in Figure 33. This VI is almost identical to the drive control VI. The only noticeable difference here is that there are two feedback signals for the valve, one for the open position, and one for the closed position, where the drives only have a single feedback signal. Once again, the signals are blocked by the case statement if the enable signal is false, so that there is no way of operating the valve from the front panel, or via automatic sequence. As before, the valves are operated using pulse signals, so that they may be operated from more than one place. There is no means to operate the valve from field controls as there is with the drives. This block uses the *Pulsar* VI to generate the valve operation pulses, and the valves are held open via their feedback signals in the logic circuit. The difference with this VI, is that the pulse duration is only 3 seconds, compared with the 10 seconds of the drive VI. This is due to the lower operation time of the pneumatic valves. If a valve is installed with a longer operation time, then the timeout value is simply increased to ensure that the valve will have enough time to complete the operation.

For detail on the operation of the *Pulsar* VI, see the description in the drive control section.

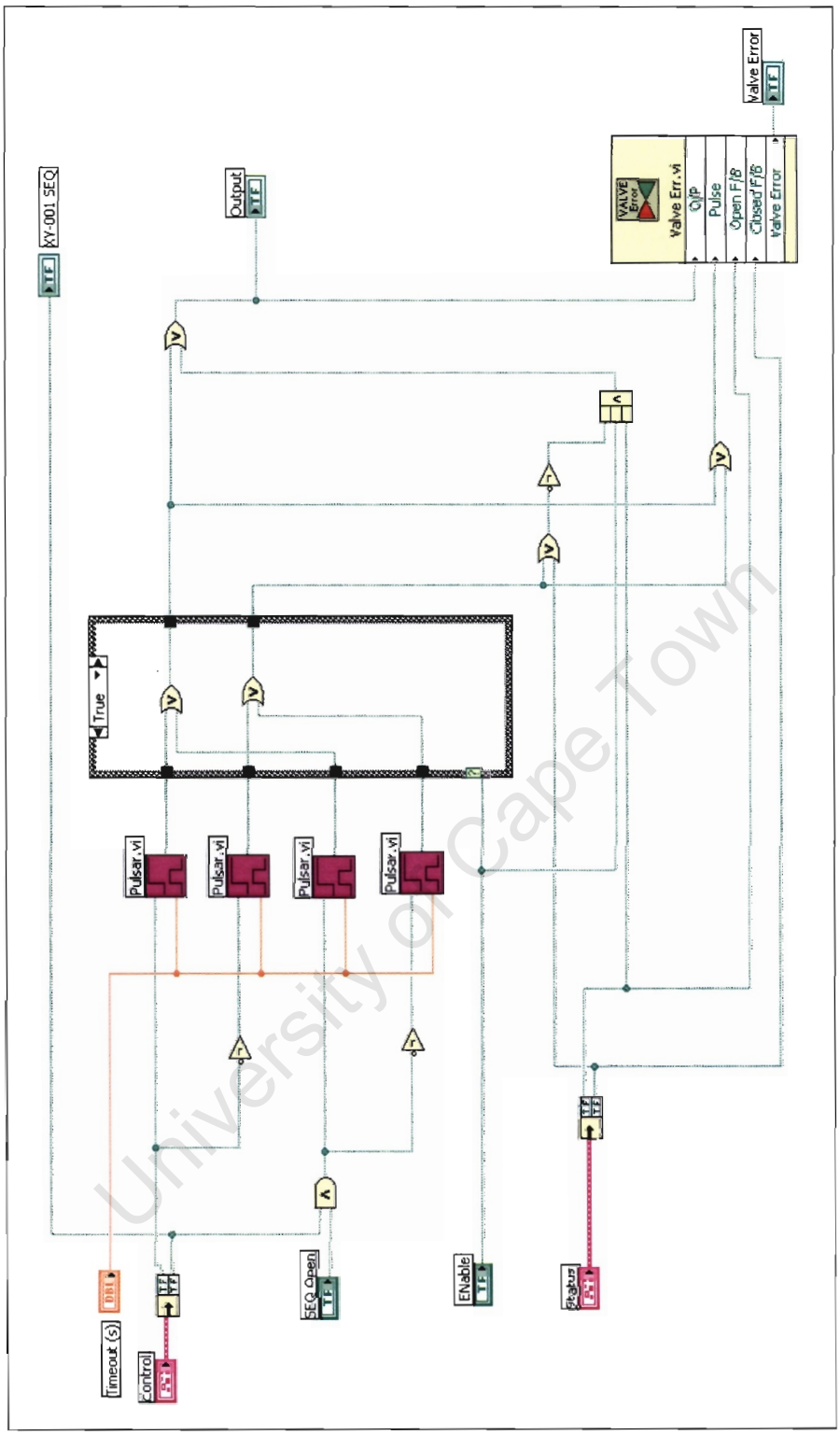

Figure 33 Valve Control VI

4.2.1.1 *Valve Error (Valve Err.vi)*

The Valve Error VI carries out very simple logic. The logic is not executed while the pulse is high, so that error conditions present during operation are ignored. Once the operation is complete, the VI checks to determine whether the output is high or low, and that the corresponding output is returned from the valve. In other words if the valve output is low, and there is either no position indication, or the valve indicates open, then an error is generated. The same is true when the valve output is high. The fault output is sent to the valve display VI, and the valve is coloured orange on an error condition. See Figure 34.

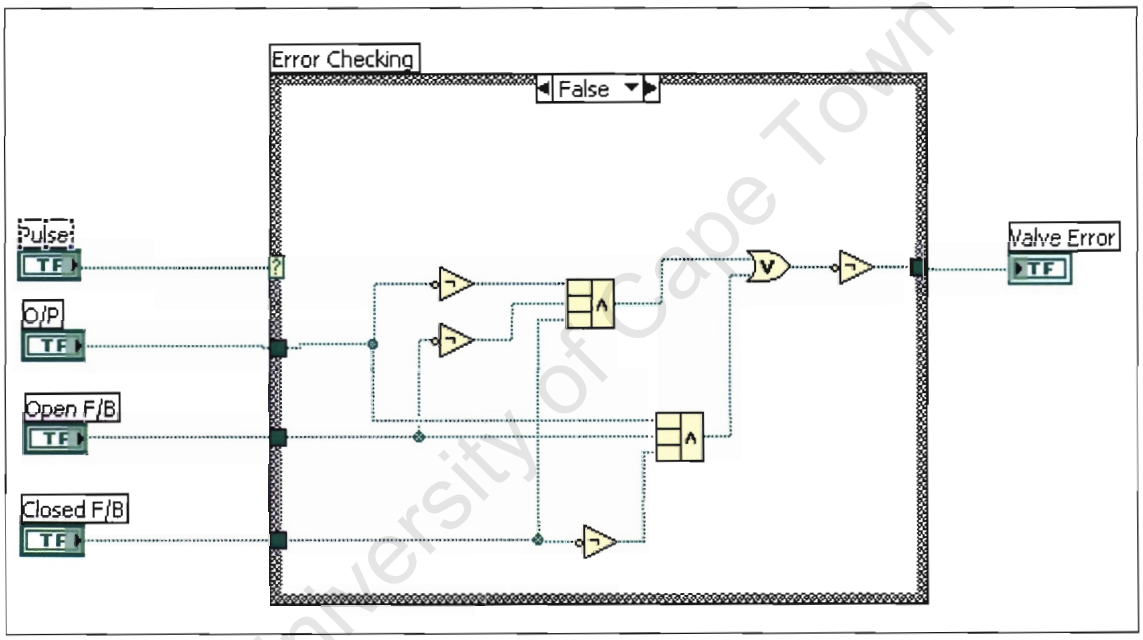

Figure 34 Valve Error VI

5. MAIN LOOP : SCREEN DISPLAY

This section discusses the VIs that format and present information for display on the front panel.

5.1 Agitator Panel Display (Ag Panel Disp.vi)

The agitator panel display VI (Figure 35) differs from the valve and pump VIs, because there is no software control of these drives. This VI simply displays the running status of the drives on the front panel, and also provides front panel display clusters containing the drive speeds in Hz and rpm. Notice that the drive healthy indications are forced high with constants here, because the relays in the electrical panel to provide the drive healthy status are not present.

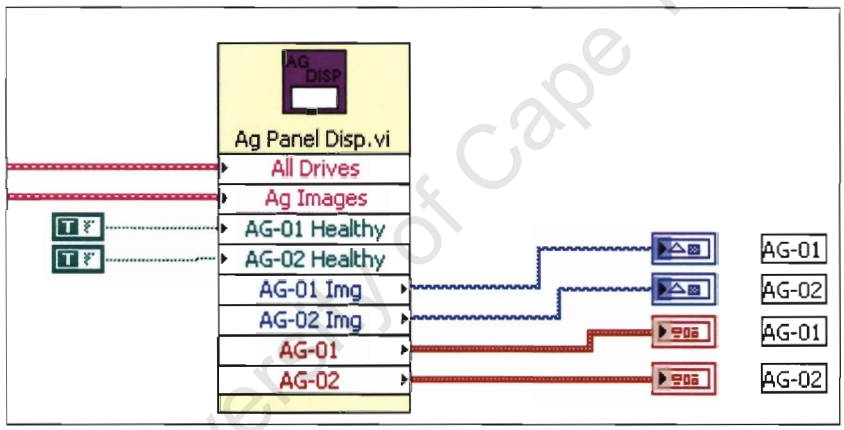

Figure 35 Agitator Panel Display

This VI contains an additional two VIs, one that handles the image selection, and a second that carries out the drive scaling. A portion is shown in Figure 36. The *Display* and *Drive Speed* VIs are present as in the *Pump Panel Display* VI. Once again there is some logic at the input to the Display VI, in order to make it re-useable throughout the program. Both of these sub-VIs are discussed in the Pump Panel Display section.

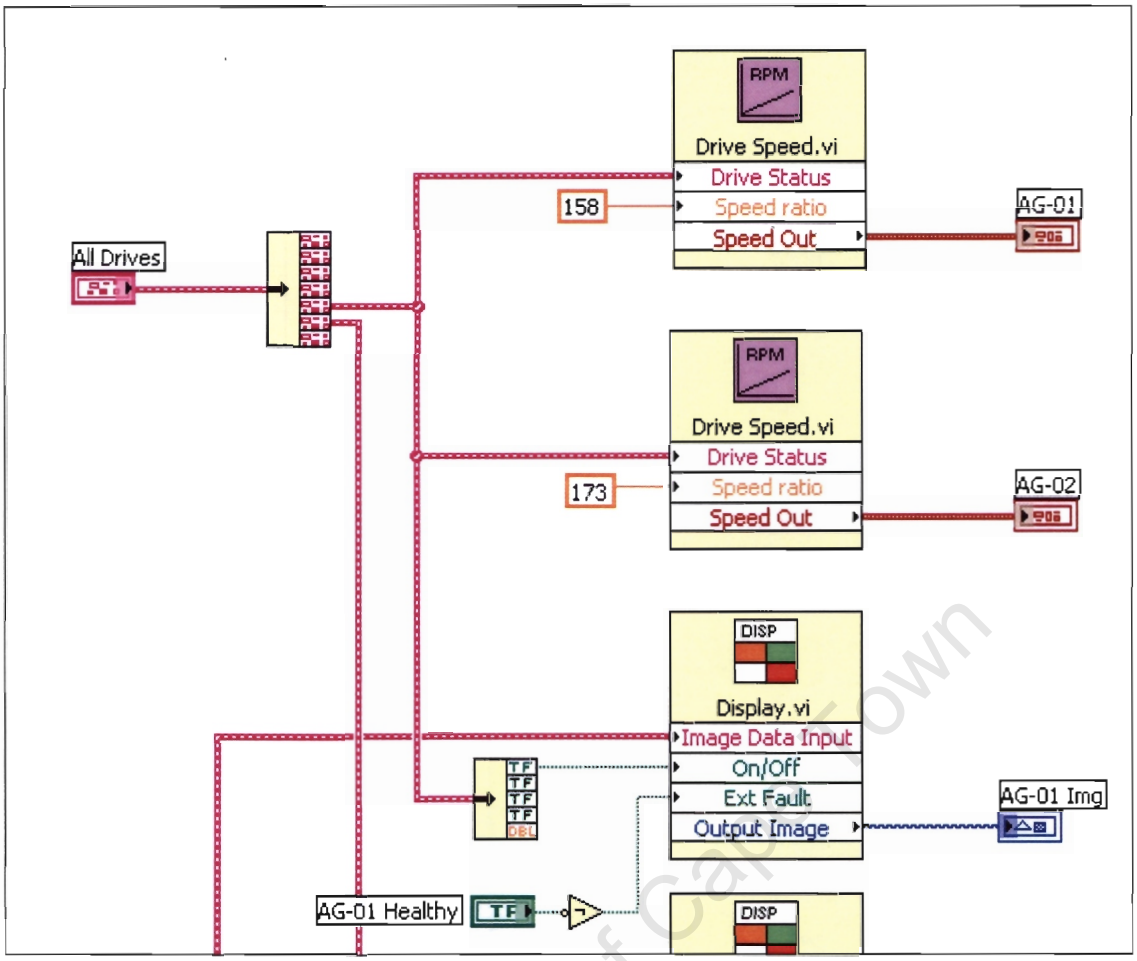

Figure 36 Agitator Panel Display VI Contents

5.1.1 Drive Speed (Drive Speed.vi)

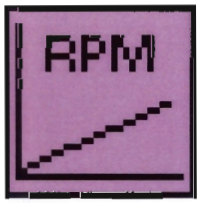

This is another simple VI (Figure 37), where the speed in Hz is converted to an rpm speed. A percentage is calculated by multiplying the speed in Hz by 0.02 so that 0 – 50 Hz becomes a value between 0 and 1, which then scales the speed multiplier. The multiplier can be adjusted external to the VI, depending on the pulley or gearbox ratio on the pump. Both the percent and rpm signals are clustered together to create the output for display on the front panel, and for use elsewhere in the program. This function also ensures that the output is forced to zero when the drive is not running. From time to time there is a small residual output even though the drive is not running.

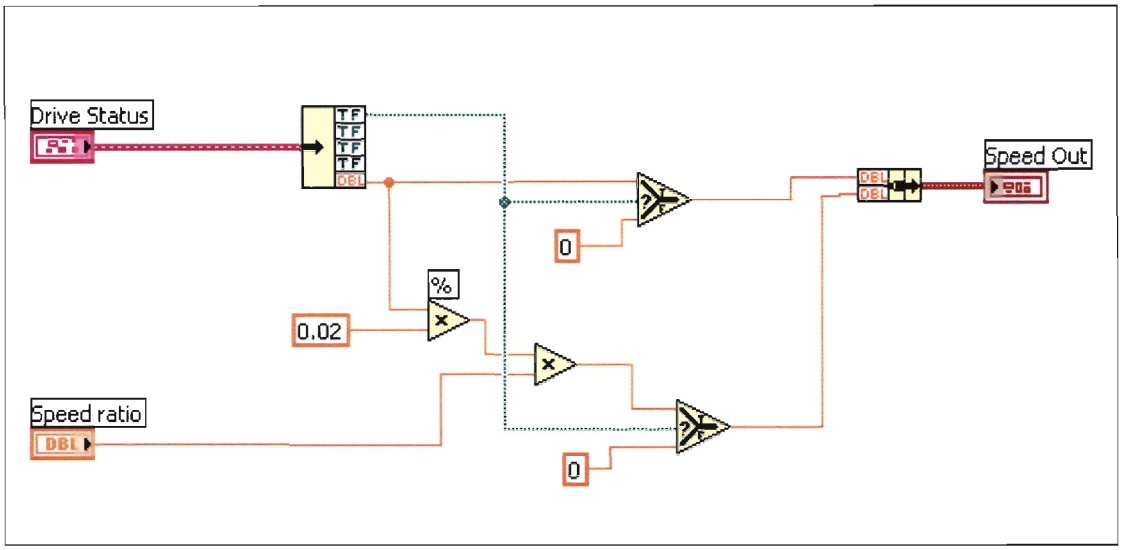

Figure 37 Drive Speed VI

5.2 Pump Panel Display (Pump Panel Disp.vi)

The pump panel display VI is shown in Figure 38. The pump and agitator display VIs are separate, since the agitators have no drive control block. The agitators are controlled manually from the electrical panel. This VI has two functions. The first is to display the pump speeds and running status on the front panel. The second function is to control the output image of the pump. As discussed earlier, there are three separate coloured images, depending on the drive status.

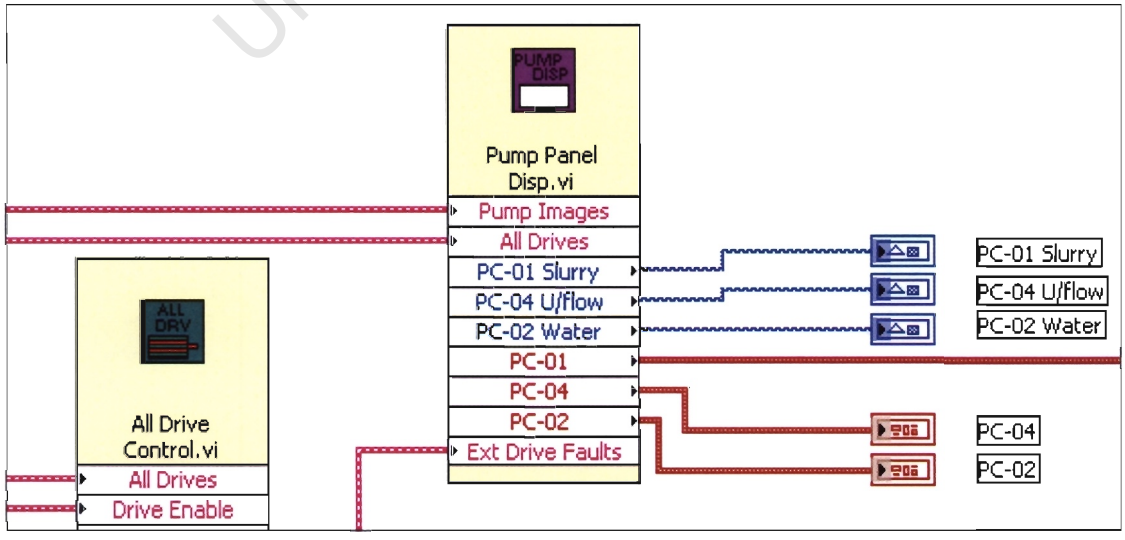

Figure 38 Pump Panel Display VI

If the drive is running, then a green image is selected, if it has stopped, then a red image is displayed. If the field stop has been activated, or a drive fault is detected (such as the output and feedback not being in agreement), then the orange image is displayed. The contents of this VI are shown in Figure 39.

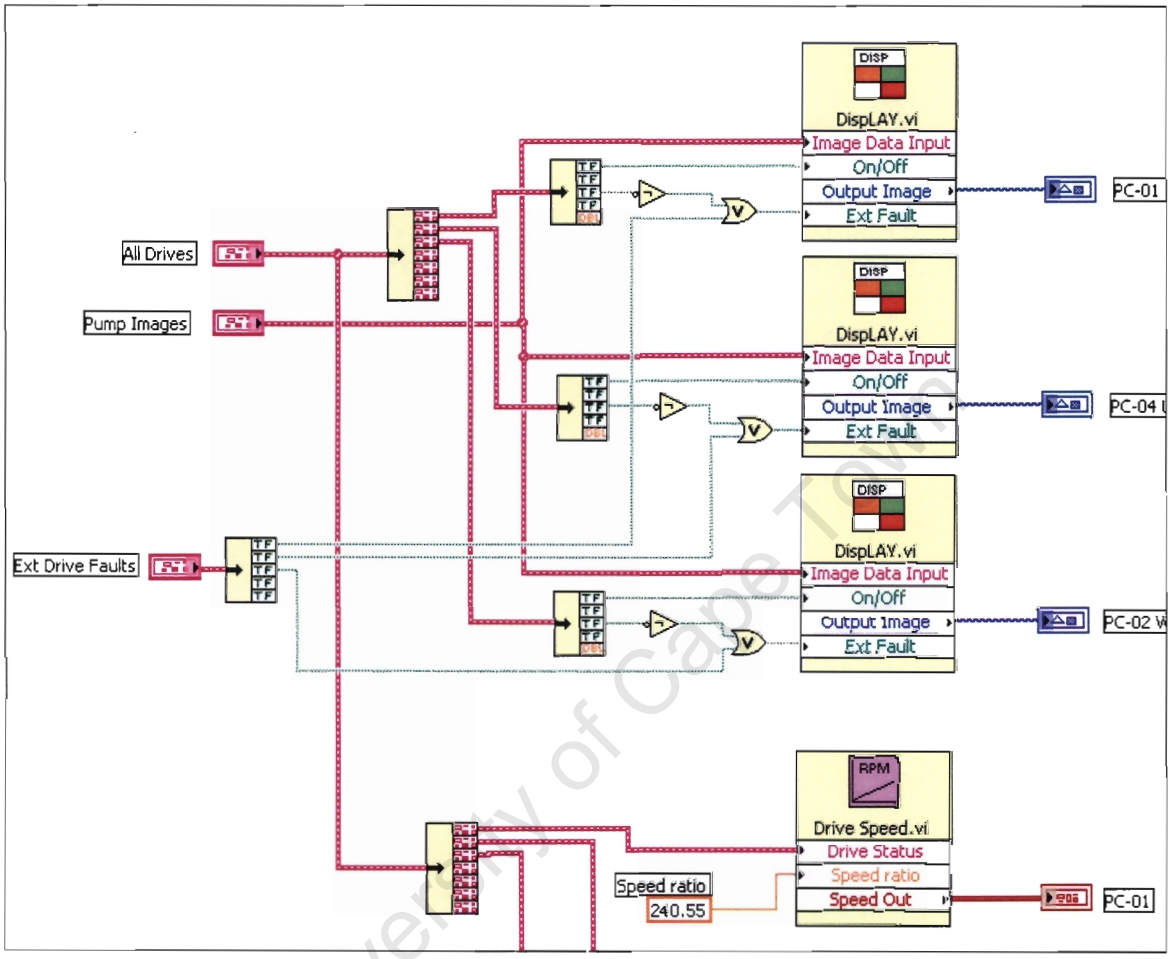

Figure 39 Pump Panel Disp. VI Contents

The pump panel display VI is a container for the individual *Pump Disp.* VI blocks to determine the image display for each drive. This block also contains the *Drive Speed* VI for each drive to convert the speed from Hz to rpm.

5.2.1 *Pump Display (Display.vi)*

This is a very simple VI, and takes the input cluster loaded at program initialization, and outputs the relevant image to the front panel image container. In Figure 39 there are a few logic gates at the input of the On/Off terminal to this VI. The reason for this is that this VI is also used in the agitator and the valve display VIs. In order to make this VI re-useable the logic must be placed outside the VI.

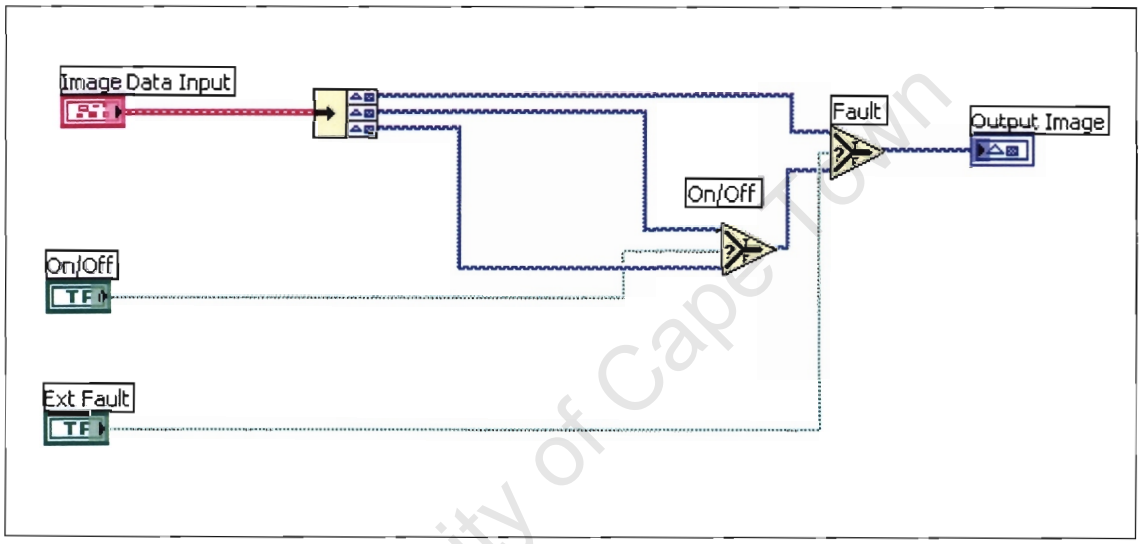

Figure 40 Display VI

5.3 Valve Panel Display (Valve Panel Disp.vi)

The Valve Panel Disp. VI takes the valve status, and the valve fault input, and determines which image to display in the image container on the front panel. Figure 41 shows the VI from the main loop.

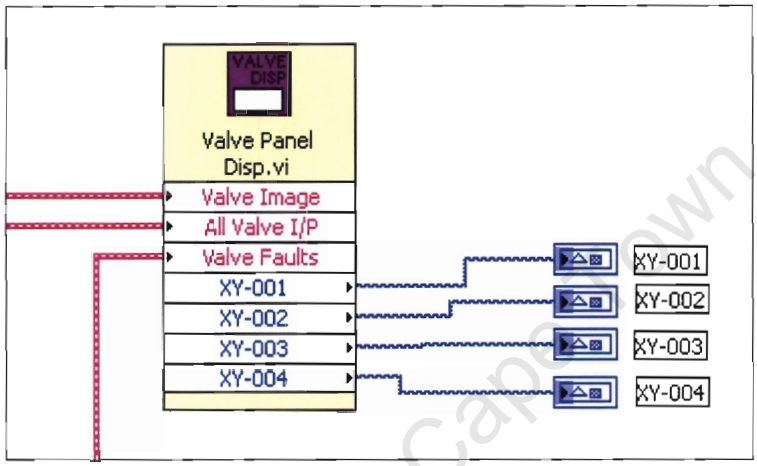

Figure 41 Valve Panel Display VI

Inside the VI, there is one display VI for each valve, and a portion is shown in Figure 42. The logic gates external to the *Display* VI are present since it is reused elsewhere. See the previous section on drive display for details of the *Display* VI.

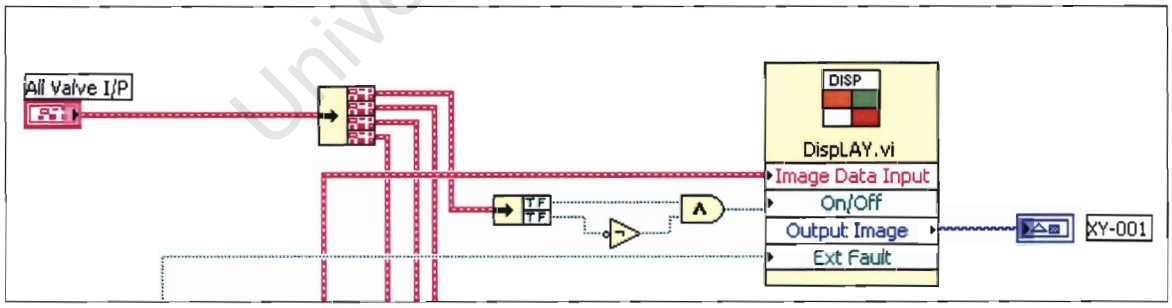

Figure 42 Valve Panel Display Contents

5.4 Analogue Displays (Analogue displays.vi)

This VI is a container for additional analogue processing for both display and control purposes, as shown in Figure 43.

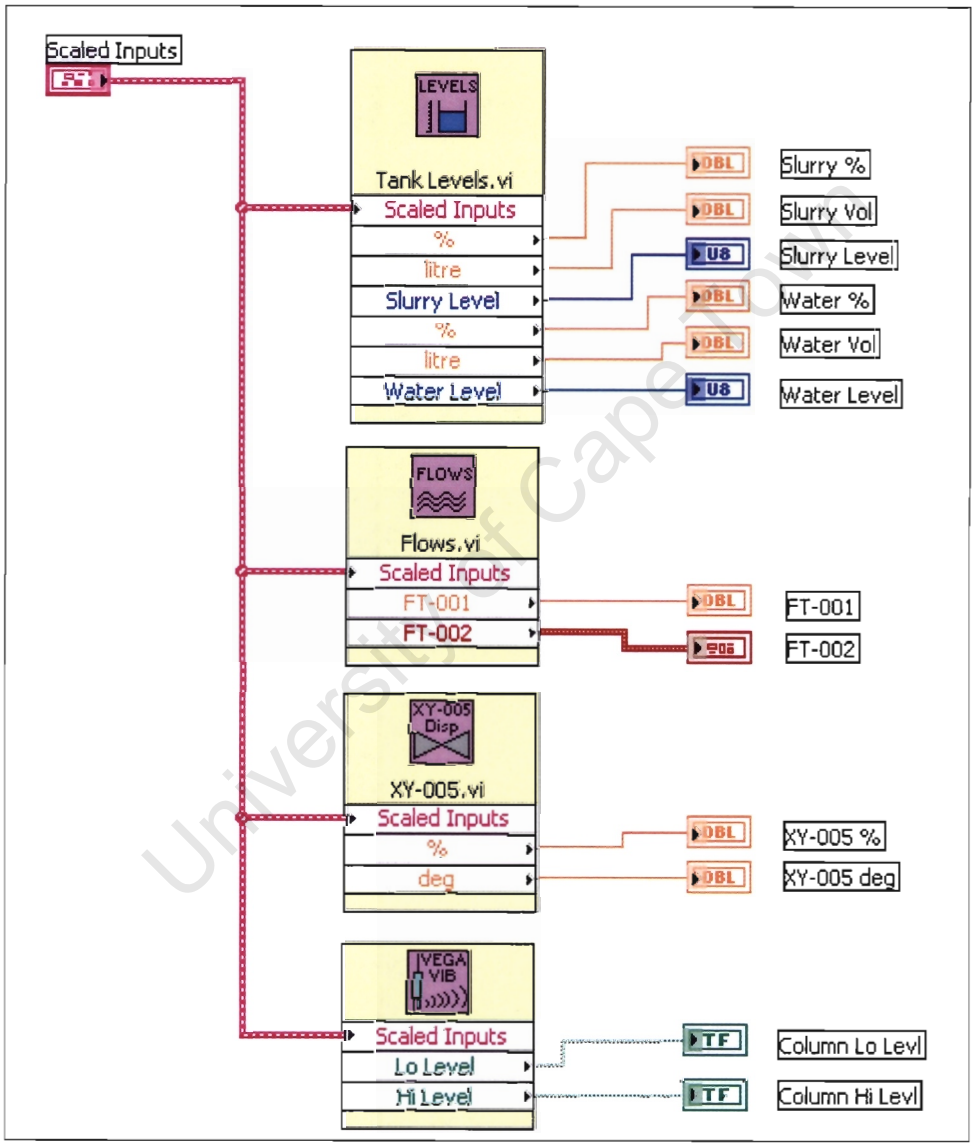

Figure 43 Analogue Display VI

5.4.1 *Tank Levels (Tank Levels.vi)*

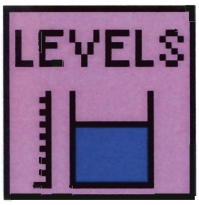

The contents of the Tank Levels VI are shown in Figure 44. This VI delivers the outputs to the front panel display for the slurry and water tanks. The % and Level outputs drive the numeric % display, and the bar graph (slider indicator – blue icon) on the front panel. A calibration from percentage output to volume in litres is also carried out on this page. For the slurry tank the calculation is:

$$V = 19.18 \times \% + 150.4$$

This calculation takes into account the fact that a 0 % reading from the Endress & Hauser level transmitter has been calibrated when the water level is just above the outlet to the pump. The calculation includes this residual volume. This is important when carrying out calculations for the slurry makeup. The bar graph output is a slider indicator.

For the water tank the volume calculation, with the result in litres, is:

$$V = 8.8 \times \% + 21.6$$

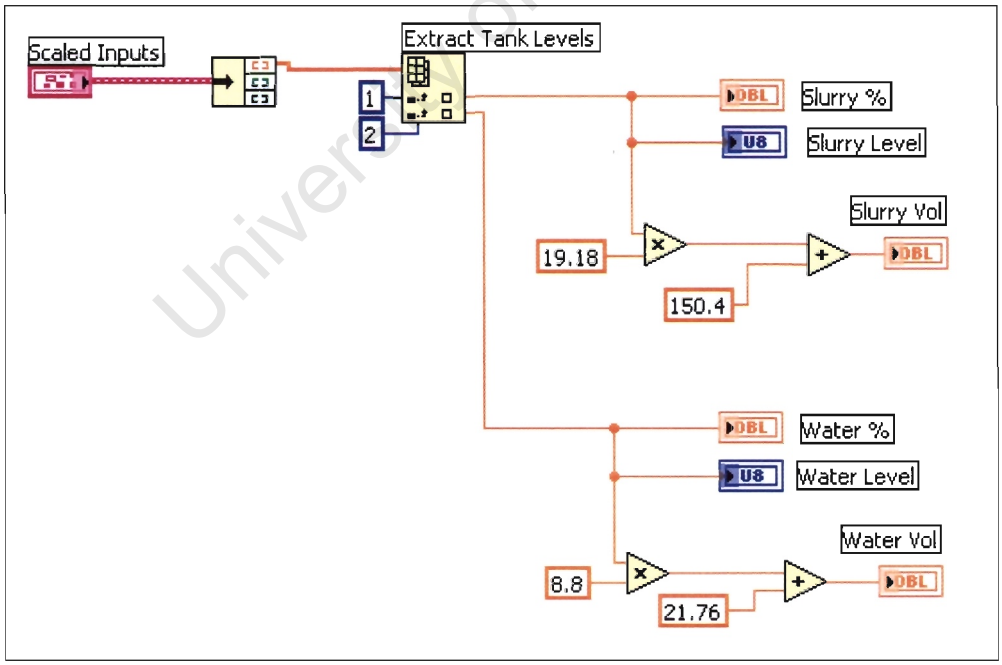

Figure 44 Tank Levels VI

It is not essential to know the exact volume of water in the clear water tank, but it has been included for completeness, and as a record of the actual volume of the tank. Figure 45 shows a portion of the front panel with the outputs from this VI.

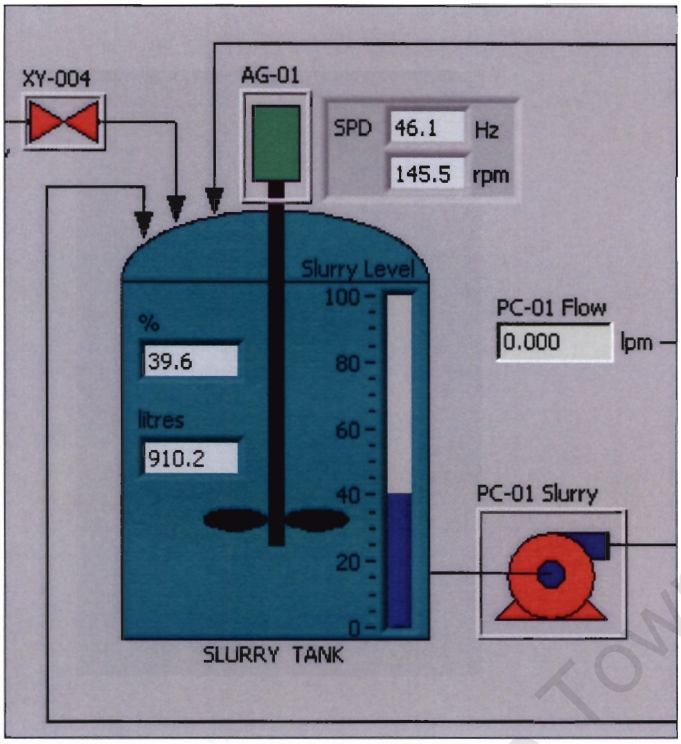

Figure 45 Tank Level Indications

In Figure 45 the picture containers for a valve, agitator, and pump can also be seen. The picture objects are contained within the raised grey borders.

5.4.2 Flows (Flows.vi)

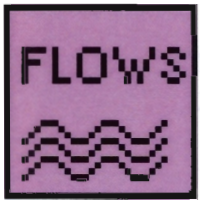

This VI extracts the inputs from the two flow meters in the plant, the dilution water flow rate (FT-001), and the underflow density and flow rate (FT-002). Figure 46 shows the contents of the VI.

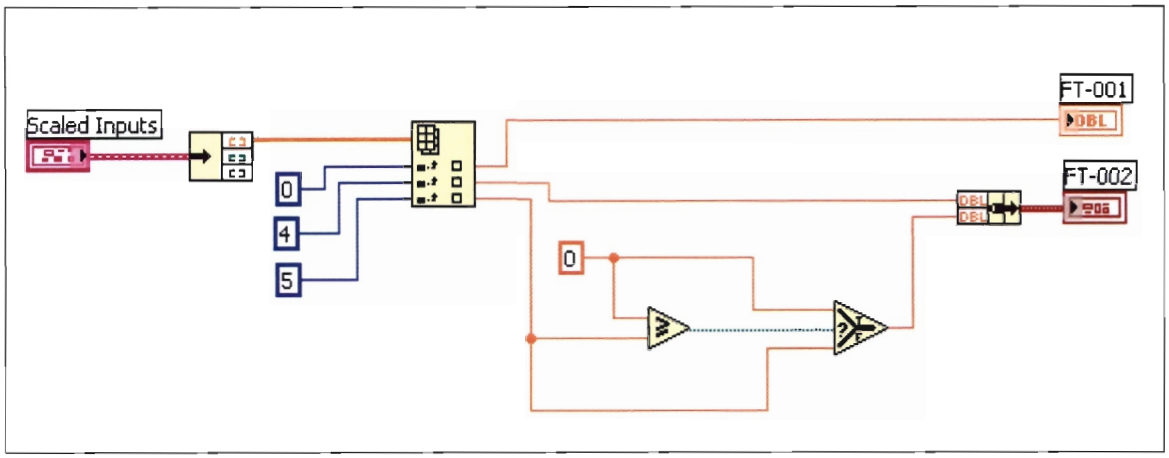

Figure 46 Flows VI

The three required values are first extracted from the Scaled Inputs array, before being processed (where necessary), and then output to the front panel. FT-001 (Yokogawa Magflow meter) is the flow from the dilution water flow meter. This value is also used by the dilution flow controller.

FT-002 (Endress & Hauser Promass 83) outputs two values since it is a mass flow meter. The first signal is the density measurement from the meter (in kg/l), and the second is the flow rate in litres per minute. The flow rate is checked to determine whether it is less than zero, and if so, a value of zero is delivered to the output. From time to time the flow meter delivers a small negative value when close to zero flow rate. The two values for the mass flow meter are then bundled together into a cluster for display on the front panel. The front panel display object is a cluster of numeric indicators.

5.4.3 XY-005 Display (XY-005.vi)

This is a very simple VI. It extracts the valve position value from the Scaled Inputs array, delivers one directly to a numeric input on the front panel (%), and delivers a second value to the front panel indicating the valve position in degrees (multiply by 0.9). The front panel display is a dial indicator that has been reconfigured to display from 0-90 over a 90 degree arc. The dial indicator includes both a graphic, and a numeric indicator for the valve position in degrees. Figure 47 shows the contents of the VI, and Figure 48 shows the front panel indicator. In this case the valve is in its default position of 45 degrees. Once the controller is in operational it attempts to maintain the valve in this position by adjusting the dilution pump speed (PC-02).

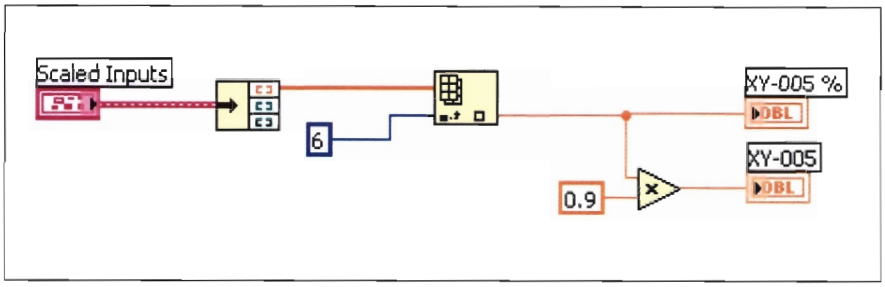

Figure 47 XY-005 VI

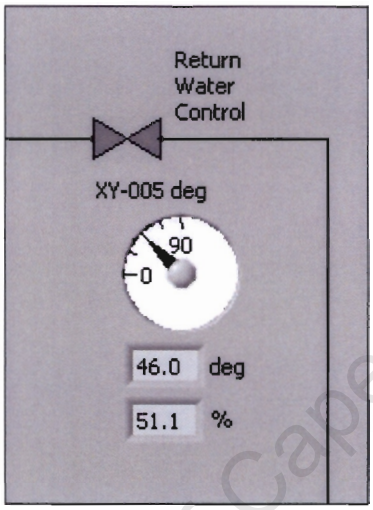

Figure 48 XY-005 Front Panel Display

5.4.4 Vega Probe Indications (Vega Ind.vi)

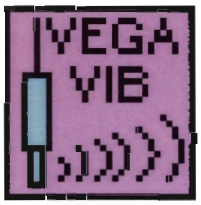

At present this VI does nothing more than extract the Column Hi and Lo level indications from the Scaled Inputs array, and presents them for display on the front panel (Figure 49). Later these outputs will be used for the mud level controller.

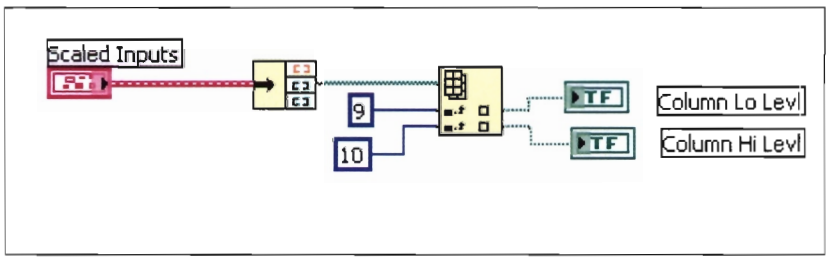

Figure 49 Vega Ind VI

6. MAIN LOOP : CONTROL BLOCKS

These blocks are responsible for control actions, and are expected to change over time. For this reason they are something of a work in progress, and will change as the nature of the test work advances. At present this consists of three VIs, based primarily on the dilution controller. In the next phase these are expected to be grouped together within a sub VI. For the present they are treated as something of a scratchpad, whilst they are modified and updated to the required functionality. The will very likely have changed beyond version 1.0 of the software. These blocks make use of some of the sequence inputs and outputs, and thus for some VIs to affect the output, the affected drives must be in sequence mode. This will be noted along the way. The previous sections, in conjunction with the output VIs, constitute the bulk of the fixed program that is not expected to change very much (with the exception of added long term functionality such as data logging, and information pages). Further details on the design and functionality of these blocks can be found in the thickener plant commissioning document [Ref 3].

6.1 Flow Estimation (Flow Est.vi)

The contents of the Flow Estimation VI are shown in Figure 50. This VI takes the slurry feed pump frequency in Hz, and converts it to a flow rate. This flow rate is calibrated by carrying out a timed fill test to determine the flow at each frequency. The relationship is linear since the pumps are all positive displacement (or progressive cavity). The underflow rate is then subtracted from the inflow rate in order to determine the overflow rate at the thickener weir. There are some other minor functions in the VI, so that the pumps cannot show a negative flow rate. Functionality has also been included so that a negative overflow rate cannot be reported. The rate is then simply forced to zero. This is important in any further flow balance calculations involving the dilution calculation, and the dilution control.

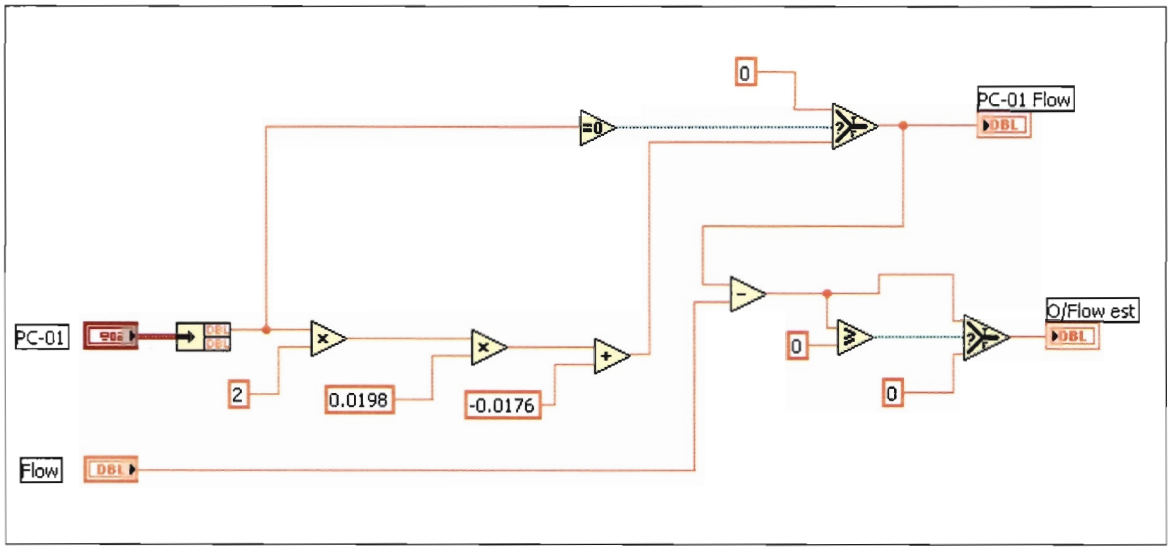

Figure 50 Flow Estimation VI

6.2 Flow Computer (Flow Computer.vi)

The Flow Computer VI is based on a state engine, and has three different modes or states in which it operates. The primary function of this VI is to keep a record of the dilution water. An additional VI (not yet completed), computes the amount of dilution water required based on the density and flow rate of the slurry being returned to the slurry tank from the underflow. The dilution computer will output a target setpoint which the dilution controller must achieve. The problem is that the accuracy of the controller is limited, but can be solved using the flow computer. Essentially it integrates the difference between the required flow setpoint (flow totaliser), and the actual flow rate so that over time the correct amount of dilution water is delivered to the slurry tank.

There are two inputs to this VI, a reset input, and an Auto input. The reset sets the flow totaliser back to zero. When the Auto input is low, the totaliser value is held, and not updated on each cycle. In Auto, the totaliser is active, and will be updated for positive or negative values of the Q Actual input. Figure 51 shows the contents of the Auto state of the state engine. The difference between the actual and required flow rates (in litres per minute) is divided by 4 (since the VI is executed four times per second), and then divided by 60 (to get to litres per second). This is then summed with the previous value of the totaliser to get a volume in litres that must either be made up over time (if positive), or reduced by dropping the dilution flow rate (if negative).

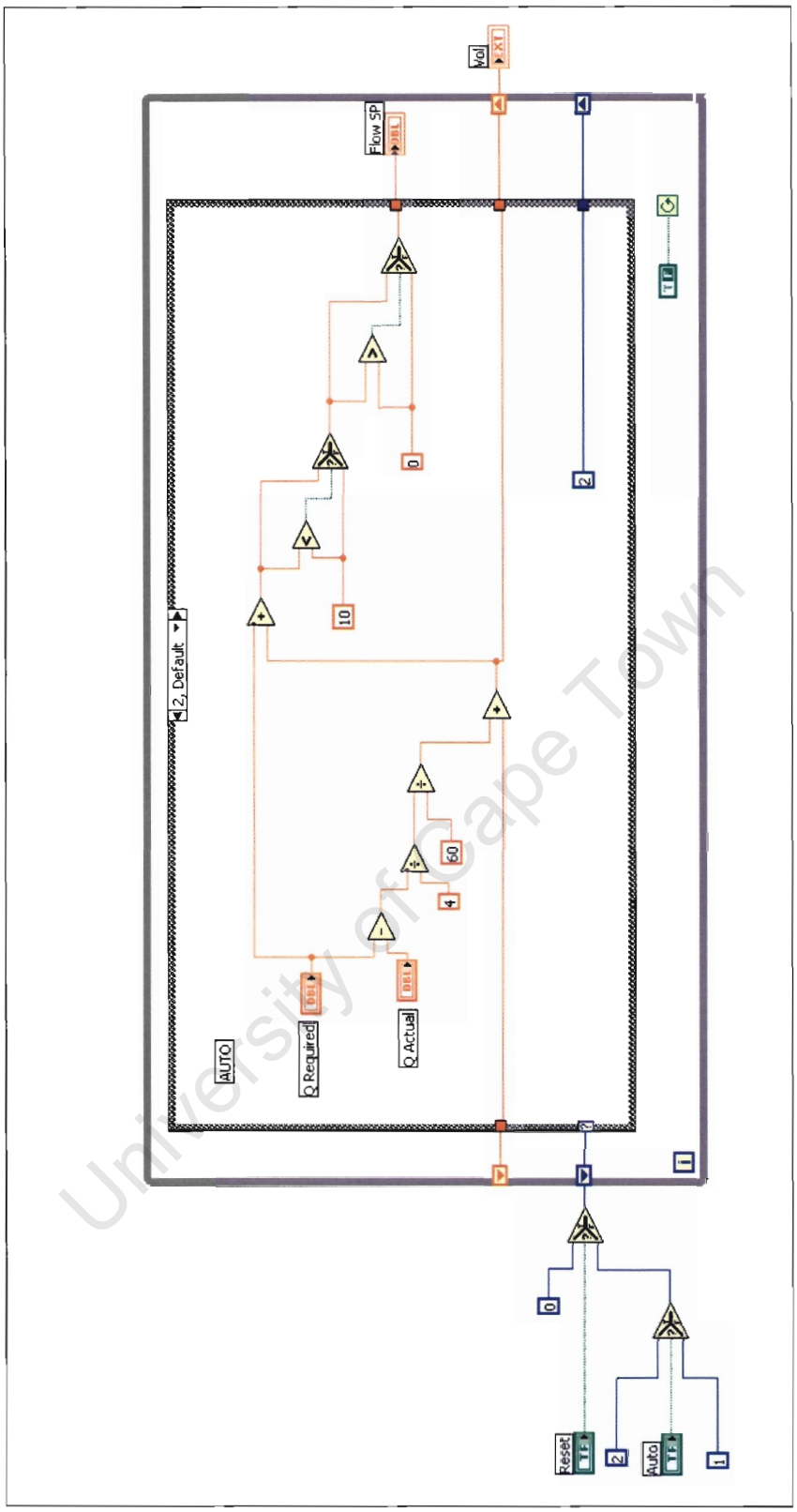

Figure 51 Flow Computer VI

The volume is then totalised from cycle to cycle, and this additional volume that is to be made up or reduced, is then included with the required flow rate. After this two simple pieces of logic are included that do not allow the flow rate setpoint to exceed 10 litres per minute, or to go below zero litres per minute. The flow setpoint from this VI is then output to the

Dilution Control VI. This VI is executed within an execute-once while loop so that shift registers can be used to totalise the volume. Attempts to make use of Labview's built in integrator met only with frustration, and the simple summation approach shown in Figure 51 was found to be far more effective. The VI has been tested, and works as advertised.

6.3 Dilution Control (Dil Control.vi)

The Dilution Control and Flow Computer VIs are shown in Figure 52.

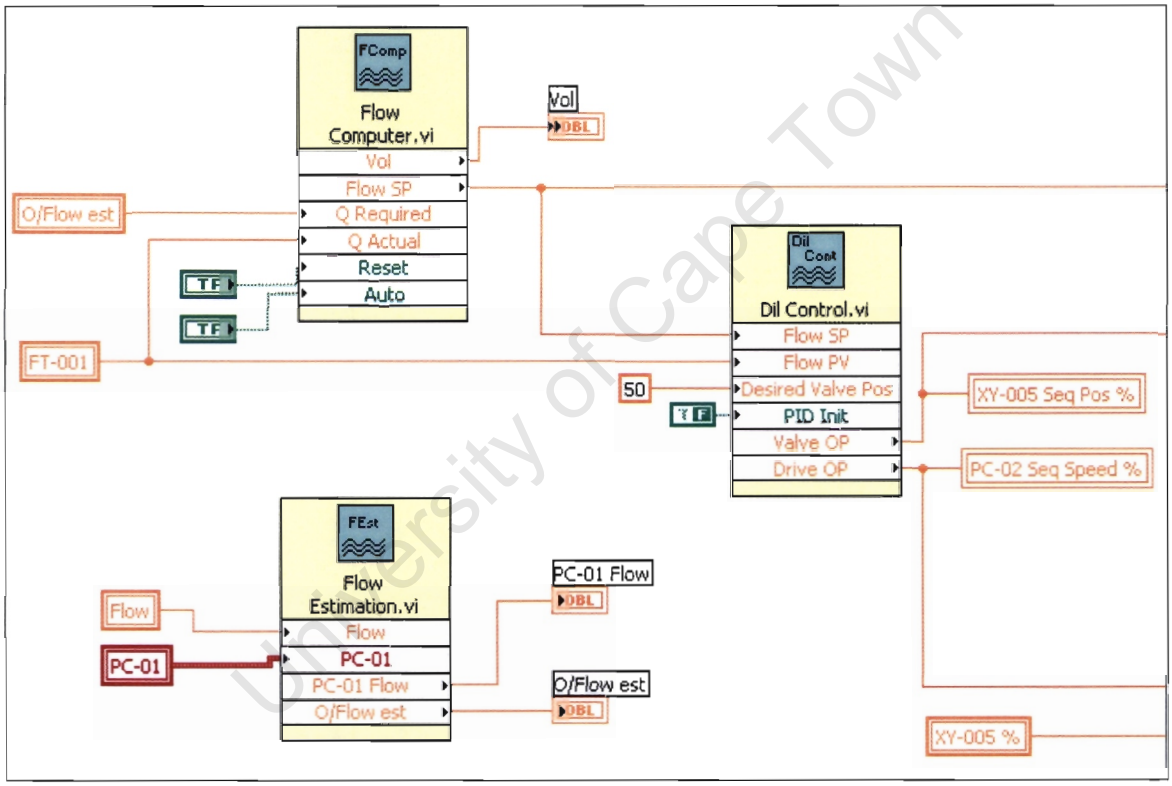

Figure 52 Control Blocks Detail

In Figure 52, all three control blocks are shown. The outputs of the dilution controller are connected to the speed and valve positions for the dilution pump (PC-02), and dilution control valve (XY-005). The outputs are connected to the sequence controls for the drives, so that they only become active once they are switched into sequence mode. When not in sequence mode, the outputs from the front panel are passed through to the drives. Figure 50 shows the cascade dilution controller (although to the author this still appears more like feedforward control than cascade – perhaps they are not that far distant from each other). The details of this controller are dealt with more specifically in the commissioning document [5], which covers the design and testing of the control system. The PID blocks are included in the

PID toolset which is included with the Developer Suite version of Labview. For more information on the configuration of these controllers see the Labview PID toolset documentation included with the software [4]

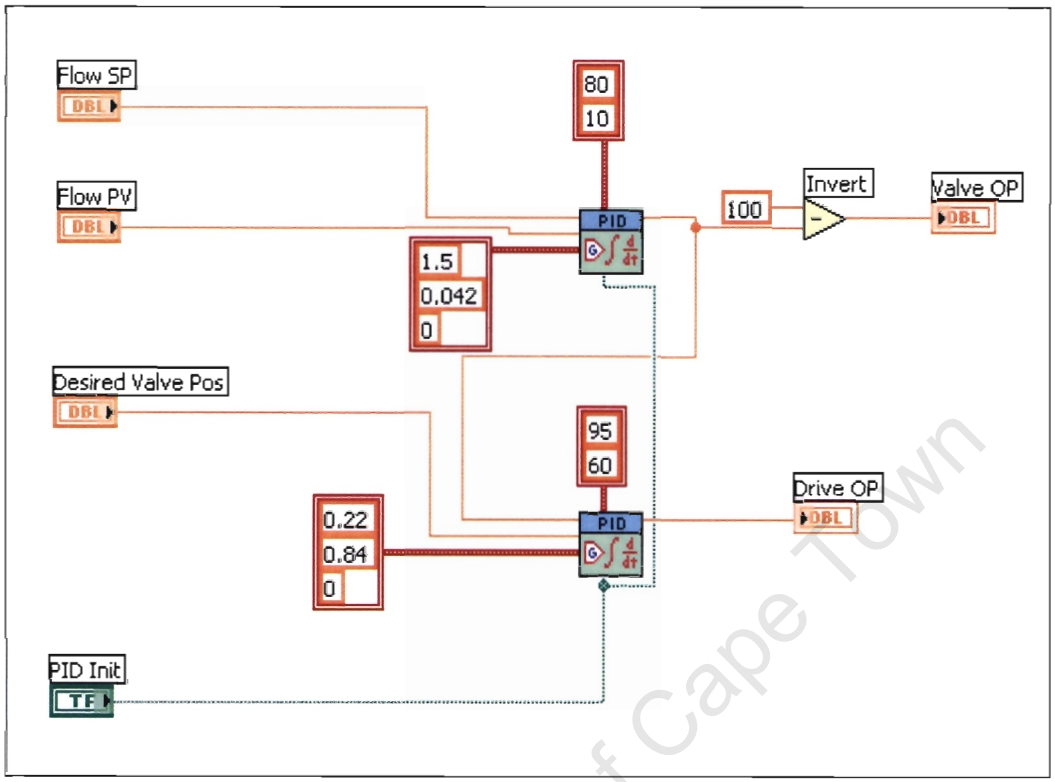

Figure 53 Cascade Dilution Controller

7. OUTPUTS

The final step in the process is to write the control outputs back to the field.

7.1 Analogue Out(Analogue Outputs.vi)

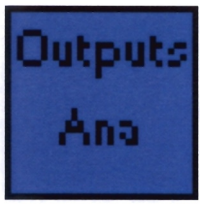

The first portion of the *Analogue Outputs* VI is shown in Figure 54. In this portion, the drive sequence inputs are used to determine whether the sequence speed value, or the speed value selected on the front panel are to be written to the field. The output values are grouped together into a one dimensional array. Any unused outputs are forced to zero, and marked as unused or spare. Not doing this results in an I/O error on the Fieldpoint module, since the status of the relevant output is uncertain.

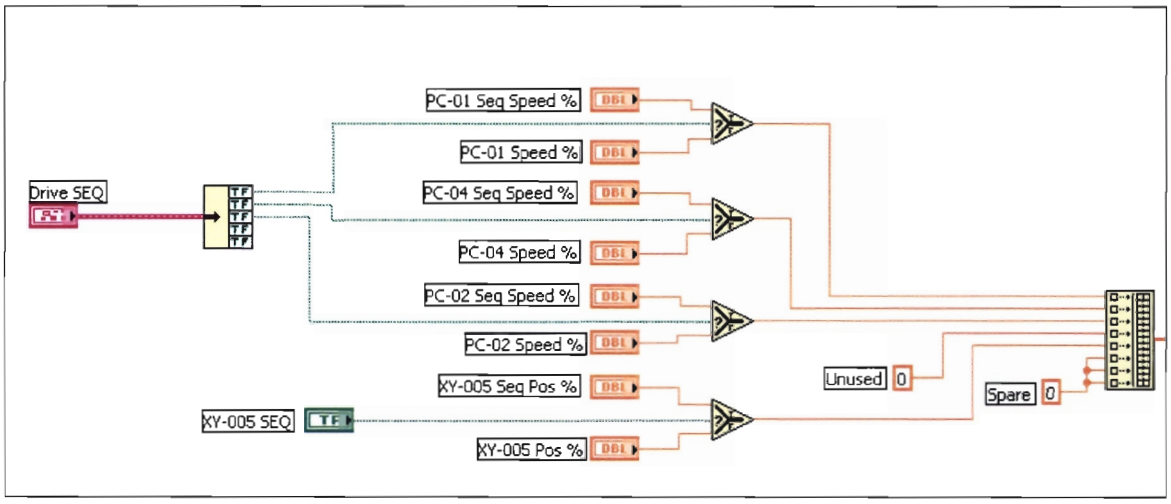

Figure 54 Analogue Output Selection

In Figure 55, the outputs are scaled from percentage values (0 – 100 %), back to a value between 0 and 1, and then scaled further to generate values in the 4 – 20 milliamp range. The unused values are forced to zero once again, since the milliamp scaling results in an offset of 4 milliamps, where no output is required from the Fieldpoint analogue output module. Since these outputs are not connected in the field they result in a loop error where the output module is unable to achieve a 4 milliamp feedback. The final stage is to convert the array to a dynamic data type, prior to being written to the field via the Fieldpoint write Express VI.

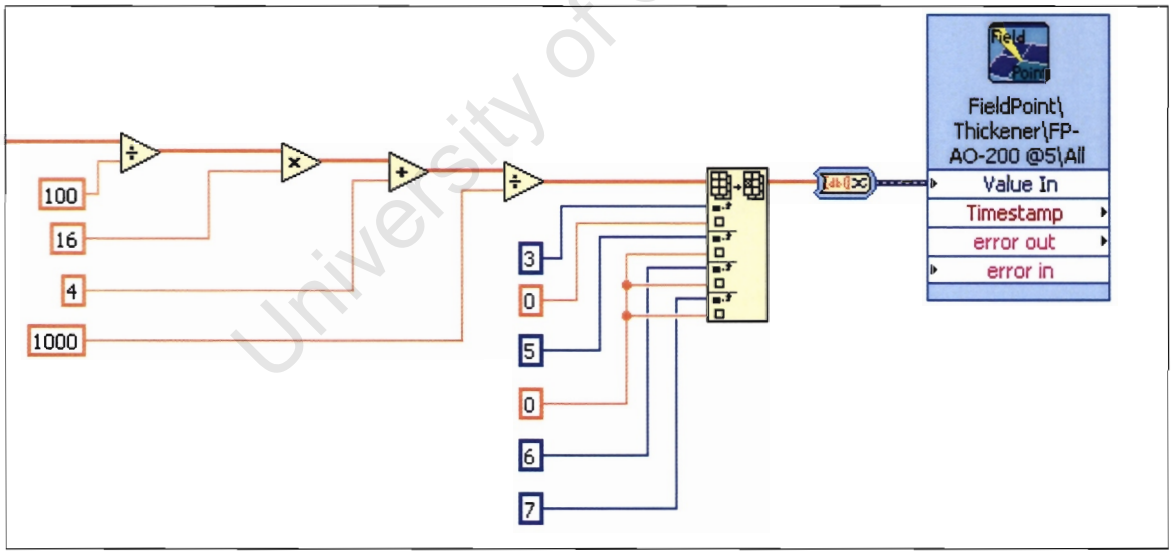

Figure 55 Analogue Output Scaling

7.2 Digital Out (Digital Outputs.vi)

This is a very simple VI, where the drive and valve digital outputs are clustered together, and all unused outputs are simply forced to a False state. The clustered Booleans are then converted to an array, and then converted to a number, before being presented to the Fieldpoint write Express VI.

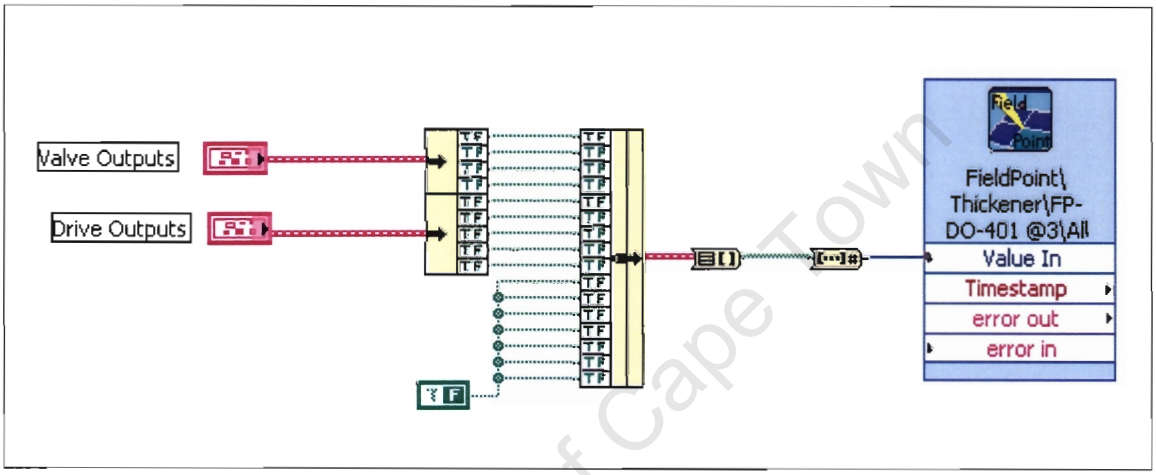

Figure 56 Digital Outputs VI

8. VI HIERARCHY

This concludes the discussion on the Scale Thickener Laboratory software. The final step is to present the VI hierarchy as shown in Figure 57. The hierarchy shows the linkages between the various Vis, and is a useful tool in navigating the software structure. The icons are as presented in the preceding sections of this document, so that the connections are easily visible.

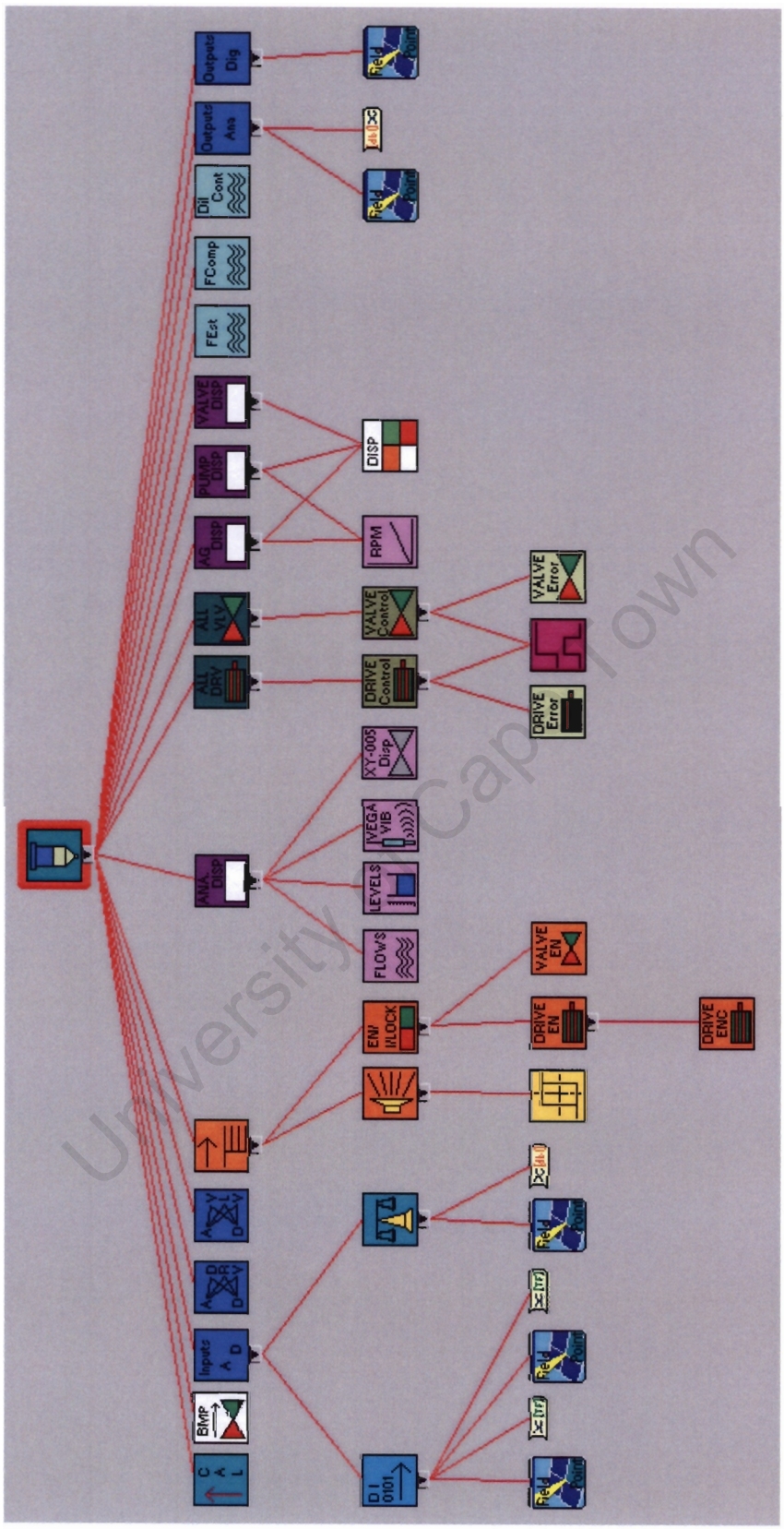

Figure 57 Scale Thickener Laboratory Software Hierarchy

9. CONCLUSIONS

This software document provides the current state of the scale thickener control laboratory software as a baseline for future modifications. There are features that have yet to be implemented, namely:

a. Interlocks page
b. Scaling update page
c. Save control values
d. Automatic sequences and controllers

The interlocks page is not essential, since the interlocking is hard coded into the interlocks VIs. It would prove useful to those not familiar with the operation of the plant, although within a short time it becomes second nature to determine the condition that is hindering the operation of a piece of equipment. Difficulties have been experienced in operating this functionality while ensuring that the remainder of the code continues to execute in the background. This becomes critical when the dilution control loop is functioning, and means (for the present) that as long as the interlocks window is open, the dilution totalisation is not being carried out. This is not a critical portion of the software, and will be included if time permits.

The scaling update page would allow the user to change instrument ranges, units and descriptions from within the executing program. Presently the same problem is experienced as with the interlocks page, where the main program does not update whilst this page is open. For the moment, instrument ranges are updated by changing the relevant entries in the text file where the data is stored. Since the code is relatively compact, and the number of instruments is small, this functionality will only be incorporated at a later stage if time permits.

Save control values is likely to become critical once automatic sequences and controllers are included in the software. This portion of the software will save critical values such as the status of the dilution controller. In the event of a software failure, or a power failure the status values will be reloaded when the software is restarted so that the state of the system is maintained.

Automatic sequences and controllers will be added and removed as the project progresses. No specific sequences or additional controllers (such as Vega probe control strategy) are included here since they are not part of the baseline software. These components will be included in the relevant test documents and will function within the structure provided by the present software and documentation.

The present software is expected to behave as a shell, within which various modules will function. These will change as the nature of the tests change over time. As it stands the software is suitable to operate the plant and to provide the interface to the user.

10. REFERENCES

1. The Design of a Scale Test Thickener for Measurement and Control Investigations, Roebl A, Technical Note 2003-10-01, 1 October 2003.
2. P&ID (data to follow)
3. Loop Diagrams (data to follow)
4. Labview PID Control Toolset User Manual, National Instruments, Part No. 322192a-01, November 2001.
5. Scale Thickener Laboratory Commissioning Document

11. APPENDIX C1: I/O SCHEDULE

Digital Inputs

DI - Module 1			**DI - Module 2**	
Channel	Signal		Channel	Signal
0	XY-001 Open		0	PC-02 Auto/Man Indication
1	XY-001 Closed		1	PC-05 RUN Indication
2	XY-002 Open		2	PC-05 Auto/Man Indication
3	XY-002 Closed		3	AG-01 RUN Indication
4	XY-003 Open		4	AG-02 RUN Indication
5	XY-003 Closed		5	PC-03 RUN Indication
6	XY-004 Open		6	PC-01 Drive Healthy
7	XY-004 Closed		7	PC-04 Drive Healthy
8	Supply Pressure OK		8	PC-02 Drive Healthy
9	Vibration Low Level Switch		9	PC-05 Drive Healthy
10	Vibration High Level Switch		10	AG-01 Drive Healthy
11	PC-01 RUN Indication		11	AG-02 Drive Healthy
12	PC-01 Auto/Man Indication		12	PC-03 Drive Healthy
13	PC-04 RUN Indication		13	Spare
14	PC-04 Auto/Man Indication		14	Spare
15	PC-02 RUN Indication		15	Spare

Digital Outputs

DO - Module 1	
Channel	Signal
0	XY-001 Open
1	XY-002 Open
2	XY-003 Open
3	XY-004 Open
4	PC-01 Start
5	PC-04 Start
6	PC-02 Start
7	PC-05 Start
8	PC-03 Start
9	Spare
10	Spare
11	Spare
12	Spare
13	Spare
14	Spare
15	Spare

Analogue Inputs

AI - Module 1	
Channel	Signal
0	FT-001 Yokogawa flow
1	LT-001
2	LT-002
3	DT-001
4	FT-002 Density
5	FT-002 Volume Flow
6	XY-005 Position Indication
7	PC-01 Speed
8	PC-04 Speed
9	PC-02 Speed
10	PC-05 Speed
11	AG-01 Speed
12	AG-02 Speed
13	PT-001
14	PT-002
15	PT-003

Analogue Outputs

AO - Module 1	
Channel	Signal
0	PC-01 Speed Set
1	PC-04 Speed Set
2	PC-02 Speed Set
3	PC-05 Speed Set
4	XY-005 Position Output
5	Spare
6	Spare
7	Spare

8.4 APPENDIX D: ORIGINAL DILUTION CONTROLLER DESIGN

The following figure shows the outline of the dilution water addition circuit strategy.

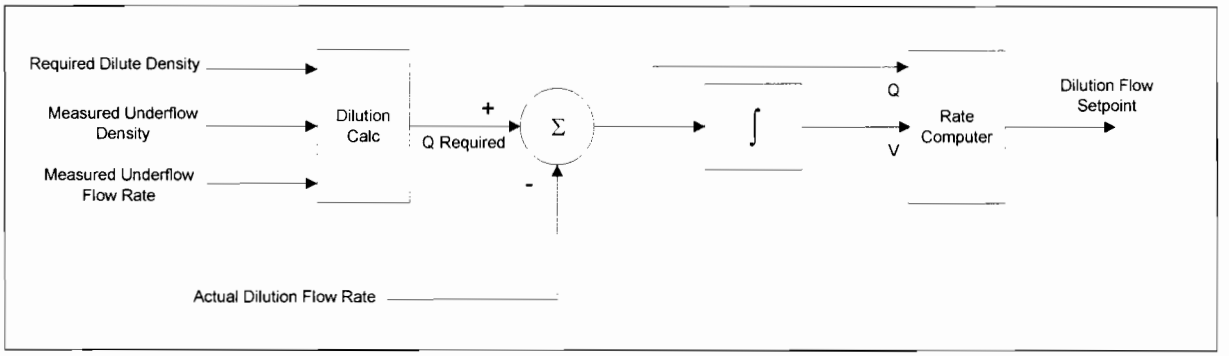

Figure 1 Dilution Control Schematic

The dilution calculation is carried out according to the calculation shown in (1). From here the required flow rate is subtracted from the existing flow rate in order to determine how much additional water is required (i.e. the error). The integrator sums the amount of required water so that some tally is maintained of the requirement should the pump/valve combination not be able to deliver the required water flow rate. This also makes it possible to sum the required amount of water should it become too low for the pump to deliver accurately, and to supply it later when the amount becomes large enough.

The rate computer is in place to convert the required volume back into a flow rate setpoint. It contains limits to prevent the dilution circuit from attempting (for example) to pump a negative amount of water into the slurry tank. In this instance the system will wait until the required dilution water flow rate is positive before adding water again. The dilution flow setpoint is passed on to the dilution controller which is dealt with in the next section.

8.4.1 Dilution Calculation

The dilution calculation is:

$$Q_{dl} = \left(\frac{C_{Musl}}{C_{Mf0.1}} - 1 \right) \frac{\rho_{sl}}{\rho_l} Q_{usl} \qquad (1)$$

$$C_{Musl} = \frac{\rho_s (\rho_{usl} - \rho_l)}{\rho_{usl} (\rho_s - \rho_l)} \qquad (2)$$

Both the flow rate and the density of the slurry are measured. The units are $l.min^{-1}$ and $kg.l^{-1}$ respectively. Since the use of these units is consistent throughout, the resulting dilution flow calculation is also in $l.min^{-1}$, and this is the input to the integrator and then converted to a flow rate again in the rate computer.

8.4.2 Rate Computer

The rate computer performs a very simple operation. It carries out the following computation:

$$Q_{sp} = Q_{req} + \frac{V}{K} \tag{4}$$

where Q_{req} is the required flow rate after the summation, and V is the integrated volume of water required. Since the output is in $l.min^{-1}$, the computer will attempt to reduce the volume V over K minutes. This reduction is intentionally slow, due to the speed of the flow controller as will become apparent in the following section.

This computation is subject to the following conditions (subject to change as test work progresses):

Maximum $Q_{sp} = 10\ l.min^{-1}$
Minimum $Q_{sp} = 0\ l.min^{-1}$
Maximum rate of change of $Q_{sp} = 1\ l.min^{-1}$

8.4.3 Flow Controller

The system is configured so that opening the control valve returns water to the clear water supply tank and reduces the amount of water delivered to the slurry tank. The first step in designing the flow controller was to carry out step tests on the valve with the pump running at fixed speeds and then doing the same to the motor with the valve in fixed positions. The first thing to note is that the valve is reverse acting, in other words, to increase the flow through the flow meter (Yokogawa ADMAG), the valve must be closed. From the step tests it was determined that stepping the system up to maximum flow (valve at 0 %, motor at 100 %) and then bringing it back to zero flow (valve at 100 %, motor at 60 %), the water did not stop flowing to the slurry tank. In other words the resistance to flow in the two lines to the slurry and water tanks was more or less the same, so that the water kept on flowing due to a siphon effect. The first step to remedy this was to introduce a ½" ball valve into the slurry tank line in order to encourage the water to return to the clear water tank rather than to the slurry tank. It was found that it was only necessary to shut the valve slightly and this was sufficient to reverse the flow. The other points of interest were that the flow began to oscillate at a motor speed of 80 % and more so at a motor speed of 100 % - more about this later. The motor range is 60 – 100 % as this is adequate to cover the required flow range. The valve range was limited to 20 – 90 %, since the areas beyond this range did not lead to any useful change in the flow due to valve non-linearity. In this range stiction was also a problem when the ball valve was close to shut or almost fully open. The maximum recorded flow rate was $10.75\ l.min^{-1}$.

From the step tests the following model was implemented in Matlab, providing a reasonable approximation to the real system. Note the presence of delays in both the valve and the pump/drive system. These delays are comparable with the system time constant. The pump delay is due, in part, to the ramp-up time programmed into the VSD and also to the VSD internal PID controller. The valve response can be increased, but this leads to oscillations around the setpoint that tend to destablise the system further.

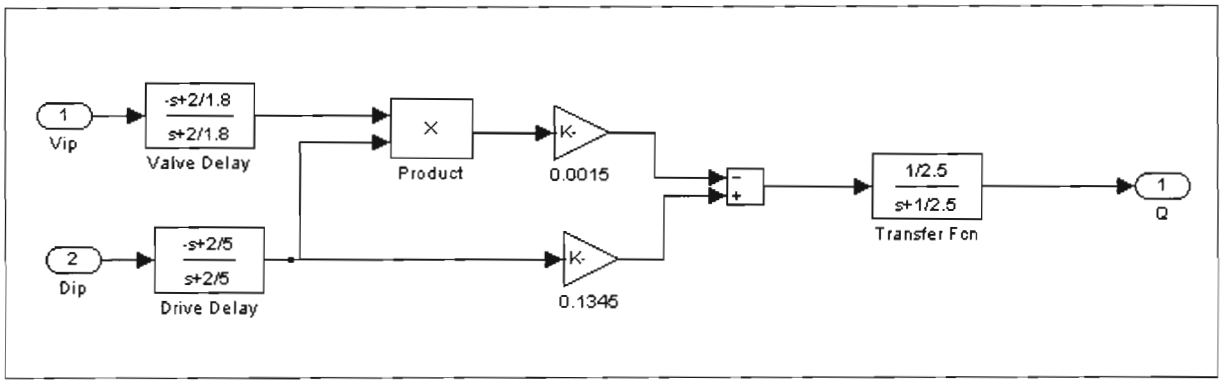

Figure 2 System Model

The system delays are estimated using the Padé approximation.

$$D(s) = \frac{-s + 2/T}{s + 2/T} \tag{5}$$

This introduces a zero in the right hand plane of the root locus, which limits the speed at which the controller can function before resulting in instability. The set of curves from which the model in figure 2 is obtained is shown in figure 3.

The topmost curve in figure 3 is for the valve at 20 % where the flow is the maximum. The change in flow is negligible below 20 % and above 90 %. For the purposes of this analysis the flow range is taken to be 0 – 10 l.min^{-1}. The pulley ratio will be adjusted later if greater flow is required. The motor % vs flow ratio is linear and, as expected, the valve % vs flow relationship is non-linear. For this reason it was decided to implement a cascade control loop, with the fast outer loop controlling the non-linear valve and the slow inner loop controlling the motor speed. The controller design is carried out using the root locus in Matlab. The controller configuration is shown in figure 4.

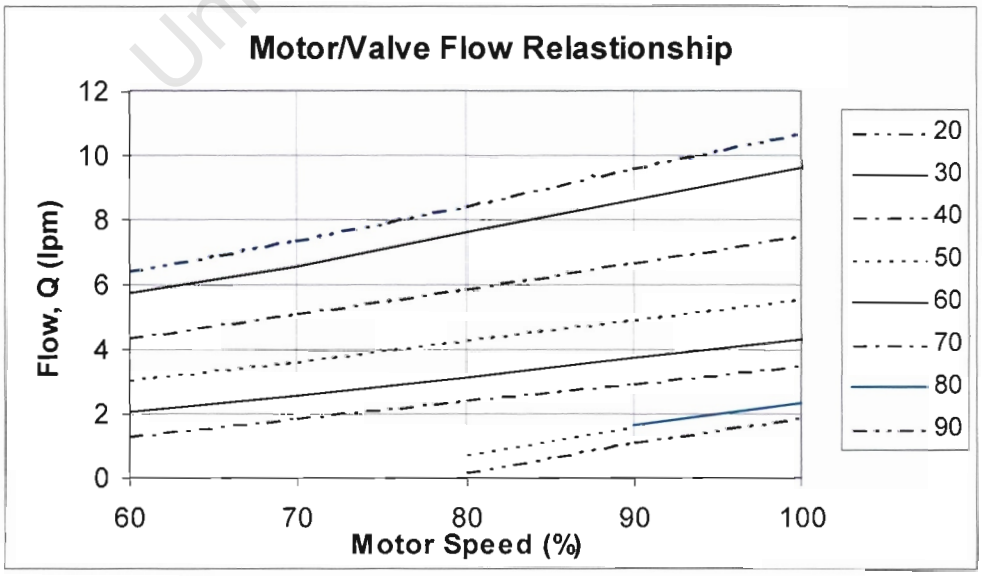

Figure 3 Motor/Valve Flow Relationship

The selected parameters for the flow control design were as follows:

- Mp < 1 % (overshoot less than 1 %), corresponding to a damping ratio $\xi \geq 0.826$.
- e_{ss} < 0.5 l.min^{-1} (steady-state error less than 0.1 l.min^{-1}, equivalent to the estimated process noise)
- System response as fast as possible whilst satisfying conditions a. and b.

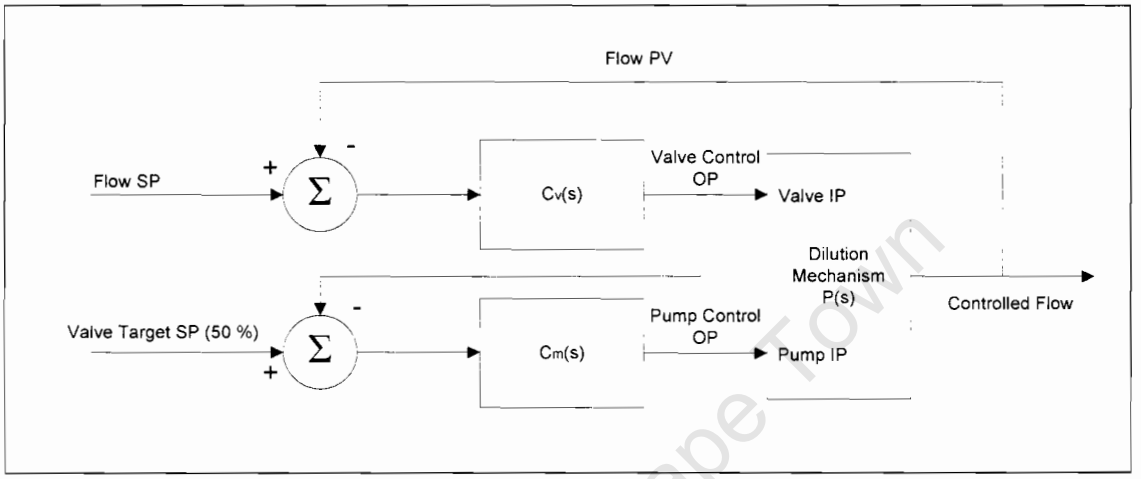

Figure 4 Auto Ranging Controller Configuration

The auto ranging control system works in such a way that the motor will adjust itself in order to attempt to maintain the valve position at a particular setpoint - in this case 50 % was selected. In this way the valve can be better adjusted so that small changes in flow can be achieved with reasonably large changes in valve position. Factors such as valve stiction have less of an impact on the system using it to make large changes. The design is carried out in such a way that the fast valve controller is first designed and then the motor controller is designed so that it is 10 – 20 times slower than the valve control. In this way a selected pump operating point can be selected, and the valve controller designed at this operating point. PI controllers were selected for implementation in both control loops. The integral component is required due to the steady state error requirement.

8.4.4 Valve Controller Design

The system is evaluated at a flow rate of 10 l.min^{-1}, where the gain is the greatest, and then tested in practice in the rest of the range. At this flow rate the system gain is 0.37 from the valve input % through to the measured flow rate (10 l.min^{-1}/27%). The pump portion of the model is ignored at this point (other than the offset it provides to the flow at 100 %).

The system transfer function is then:

$$P_{l'}(s) = 0.37\left[\frac{1/2.5}{s+1/2.5}\right]\left[\frac{-s+2/1.8}{s+2/1.8}\right] \qquad (6)$$

The zero due to the PI controller is located using the Matlab 'sisotool'. This allows the user to graphically move it around until the best response it found. The valve controller was coded into 'sisotool' as

$$C_{PI}(s) = K_c\left(1 + \frac{1}{T_i s}\right) = \frac{K_c}{T_i}\left[\frac{T_i s + 1}{s}\right] \tag{7}$$

So that the controller gain is manipulated as one parameter, and the controller zero as another. This is the labview implementation of the PI controller.

Using this approach the best location for the controller zero was found to be at s = $-^{1}/_{2.4}$ with a system gain of 1.6. This provides the fastest possible response, as either side of this the system becomes slower again. The value of T_i is then 2.4 seconds, and the resulting value of K_c is 1.6. The controller implementation is then

$$C_{PI}(s) = K_c\left(1 + \frac{1}{T_i s}\right) = 1.6\left(1 + \frac{1}{2.4s}\right) \tag{8}$$

The sisotool result is shown in figure 5, where the blocks indicate the pole locations for the selected gain. The damping constraint is shown by the greyed out region on the graph. The gain shown in figure 5 is 0.667 and when this is multiplied by 2.4, the result is 1.6 as stated above. The Labview implementation of the PI controller is as shown in equation (8) above, with the exception that the integration time is given in minutes. The value to be entered into Labview for T_i is thus $^{2.4}/_{60}$ = 0.042 minutes.

8.4.5 Pump Controller Design

Initially the pump controller was designed in the same way as the valve controller, with the zero moved to s = $-^{1}/_{24}$, but with the damping fixed at 1. In practice it was found that it needed to be slowed down further since the PV to the pump is an output that has already been integrated, so that integrating further for the pump output drove the system toward instability. Moving the controller zero to s = $-^{1}/_{50}$ proved suitable, with a system gain of 0.22. The value to be entered into Labview for T_i is thus $^{50}/_{60}$ = 0.84 minutes.

The results of two step tests to a 3 l.min^{-1}, and an 8 l.min^{-1} setpoint are shown in figure 7. The upper windows shows the valve position command (fast output), and the pump speed command (slower response), along with the actual speed of the pump drive motor. The actual speed of the motor is slightly less than the command input. The lower window shows the flow response. The second step shows that the output is not particularly stable, and somewhat outside the design limit for steady state error. This is due to valve stiction. The valve stiction was reduced by increasing the sensitivity of the valve position controller, but could not be improved beyond this point. The pump speed was also limited to 95 %, since beyond this point it seems to worsen the valve stiction problem when drive oscillation sets in. The oscillation at 100 % is too fast for the controller to compensate for (with the amount of stiction present when the valve is near to 20 %, without destabilising the rest of the system further. At a pump speed of 80 % the valve is at 50 % where stiction is almost non-existent.

This means that the maximum achievable flow rate for the system is now 9.5 $l.min^{-1}$. If a larger flow rate is required in future, the motor pulleys will be reconfigured to provide a greater pump range, and the controller reconfigured (if necessary) using the procedure described in this section. This will involve carrying out further step tests up to the maximum flow rate (at 50 Hz) of 19.5 $l.min^{-1}$. The lowest speed is governed by the pulley settings, and the maximum speed is governed by the frequency range of the VSD (20 – 650 Hz)

In figure 7 a small inset is also shown, that gives the flow response to a zero setpoint. The flow is inclined to drop off rapidly, and to flow in the reverse direction for a short while until it comes to a stop. This behaviour is inherent in the system, and will be compensated for in the dilution calculator.

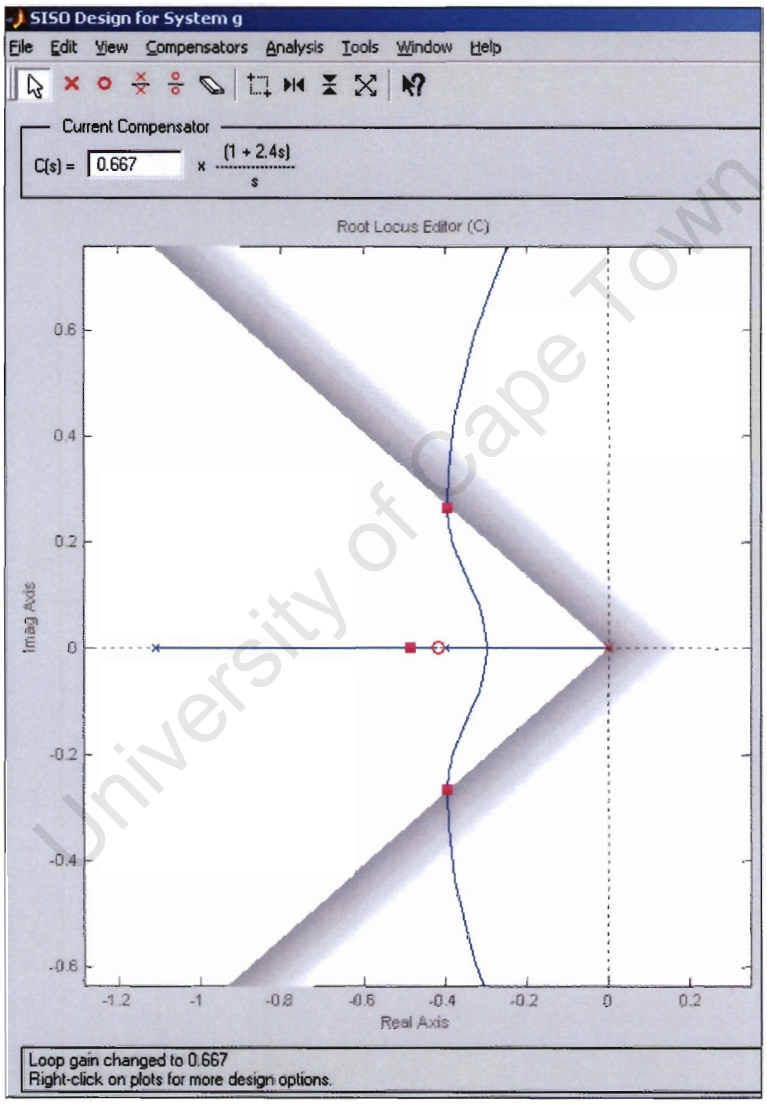

Figure 5 Final Pole Locations for Valve Control

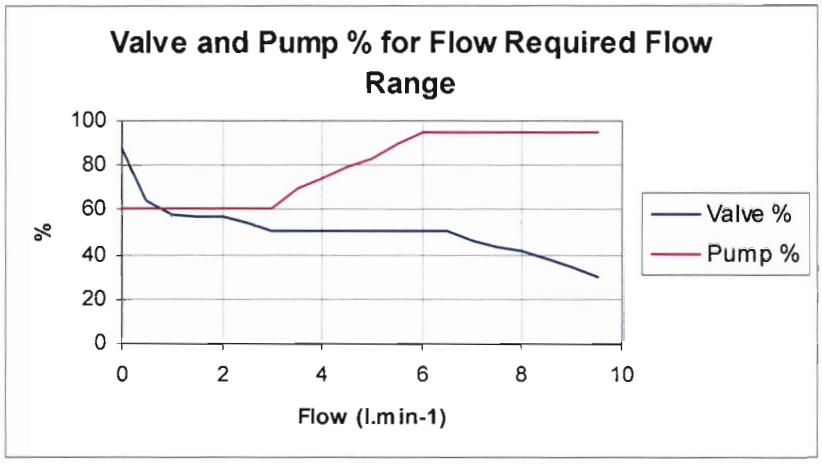

Figure 6 Valve and Pump % vs Flow Rate

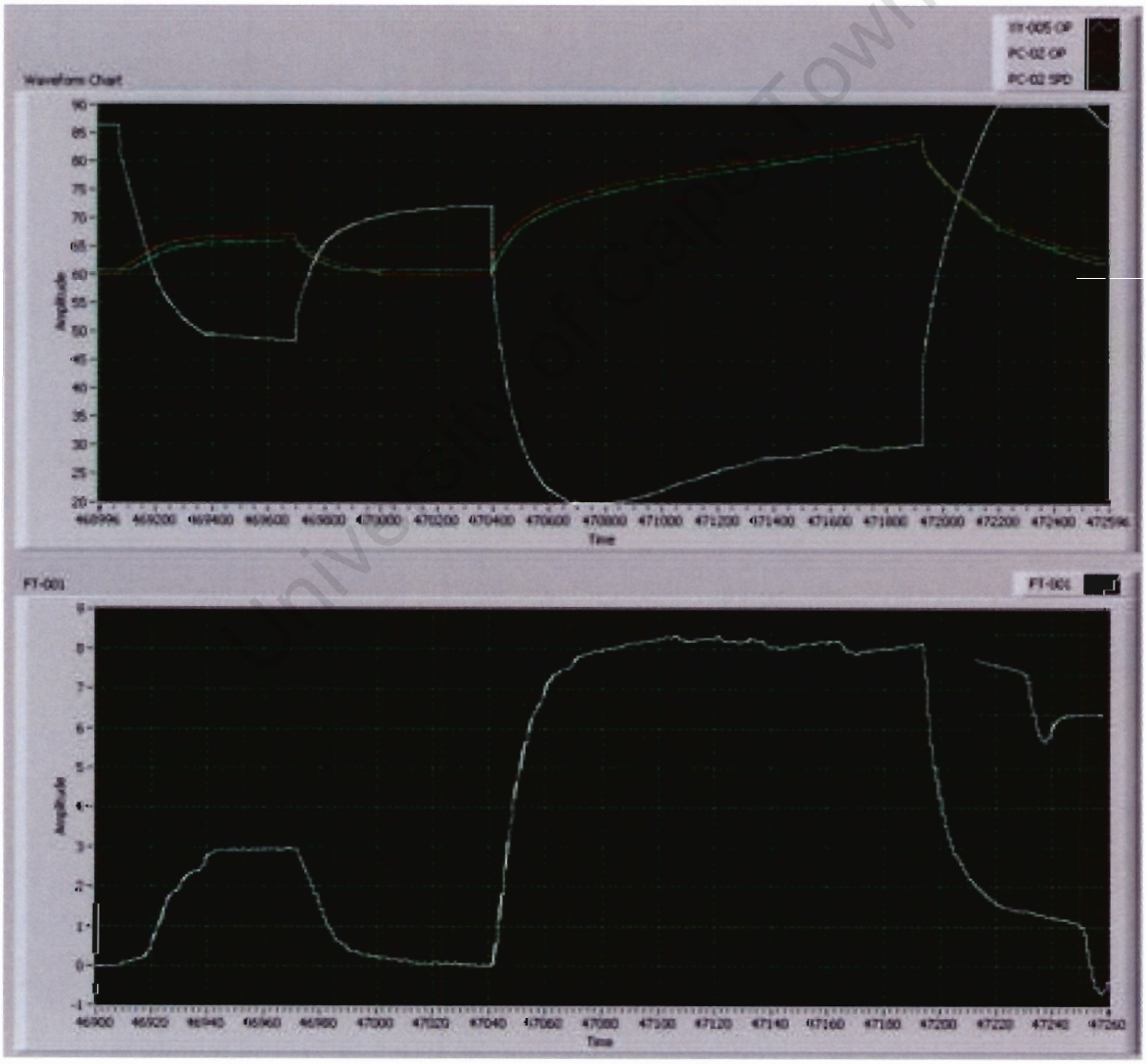

Figure 9 Dilution Control System Response

At the top and bottom ends of the range, the pump is either running at minimum or maximum speed, and the valve only is responsible for maintaining the flow setpoint. The points at which the valve and motor are in steady state are shown in the figure 6 for a range of flow rates.

It was later found that some of the observed oscillation in the dilution flowrate was due to the Siemens VSD, and it is possible to insert a damping constant that acts on the output of the built in VSD PID controller. The ramp up time of the VSD can also be significantly reduced to speed up the system. The oscillations take place at certain fixed frequencies, possibly because the VSD controller default setting is for a Siemens motor. In this case the motor is WEG. Similar oscillations have been detected on the SEW drives for the feed and underflow pumps. This has yet to be investigated further.

8.5 APPENDIX E: BAFFLE DETAILS

8.5.1 Slurry Tank

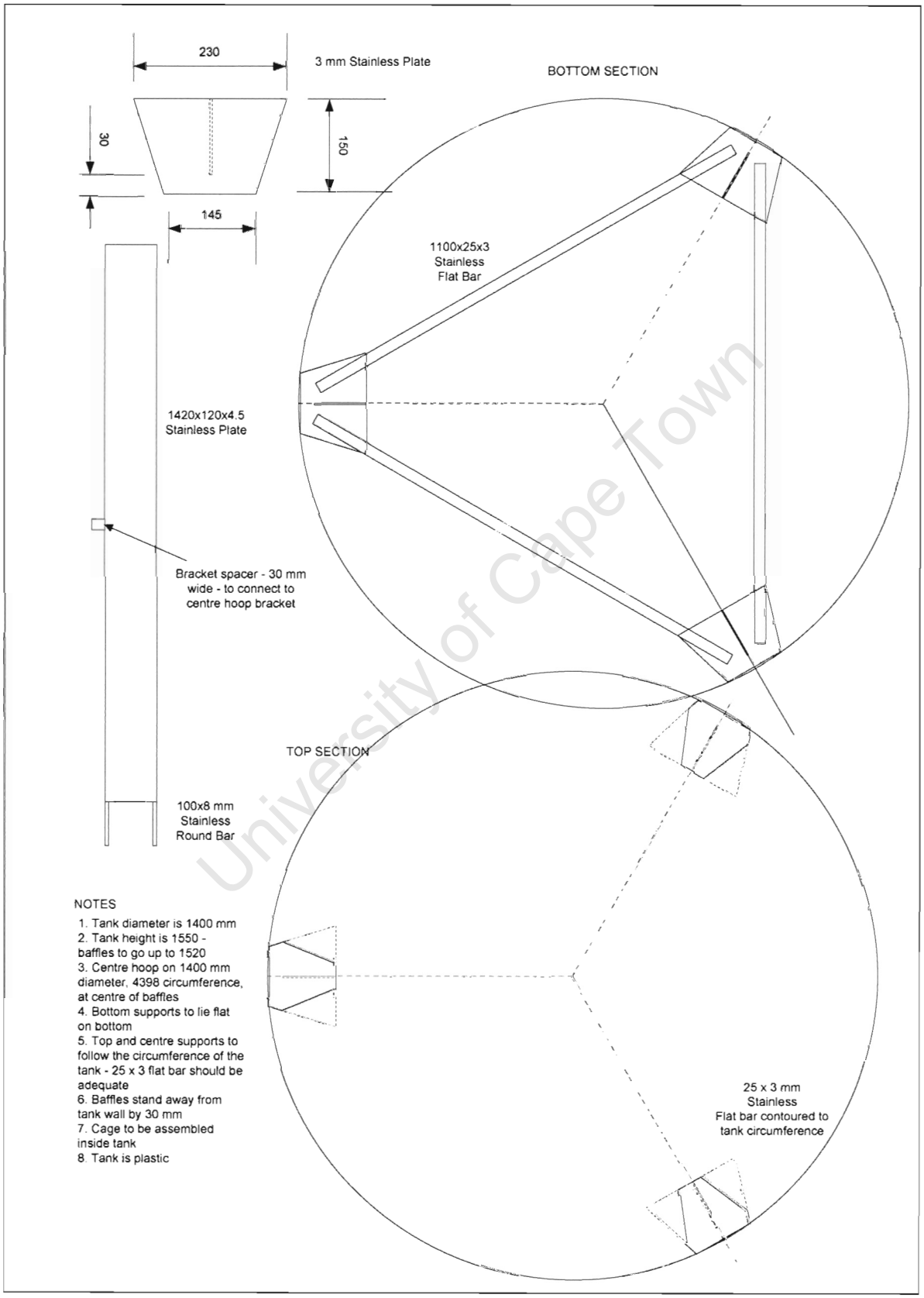

8.5.2 Clear Water Tank

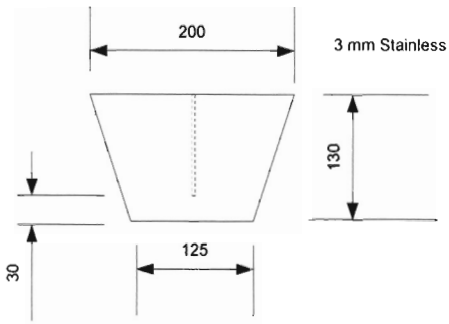

BOTTOM SECTION

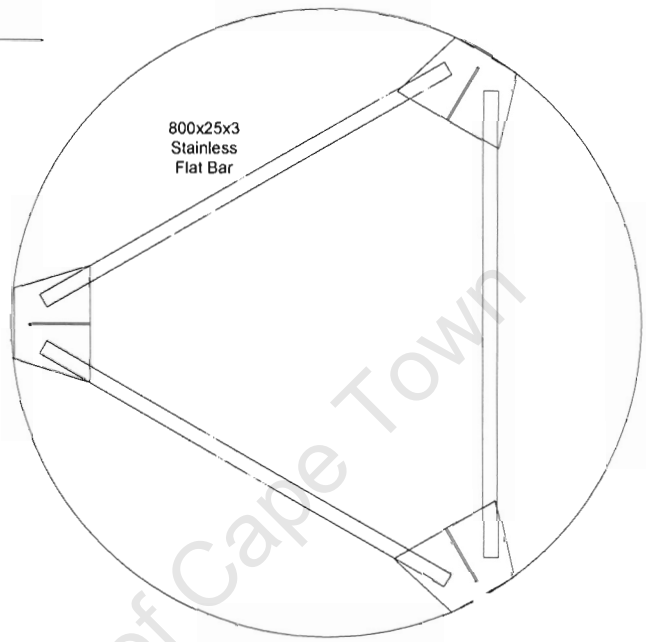

100x6 mm
Stainless
Round Bar

TOP SECTION

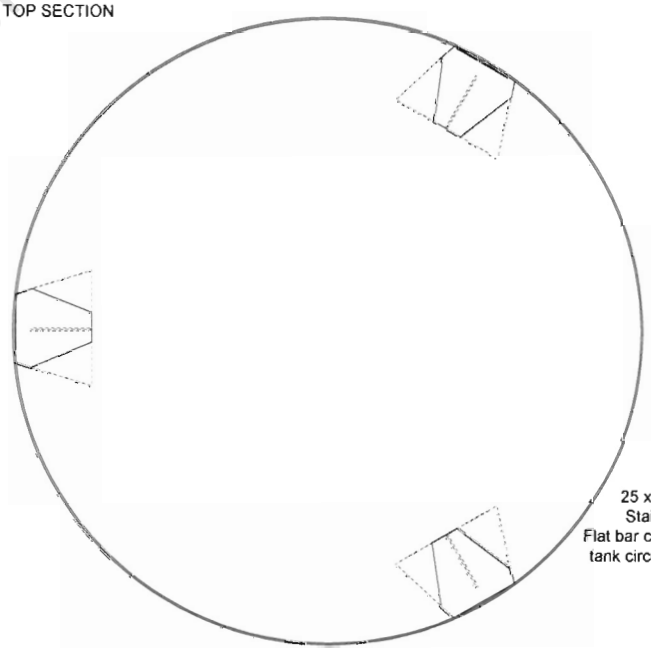

NOTES

1. Tank diameter is 1080 mm
2. Tank height is 1160 - baffles to go up to 1100
3. Bottom supports to lie flat on bottom
4. Top supports to follow the circumference of the tank - 25 x 3 flat bar should be adequate
5. Baffles stand away from tank wall by 30 mm
6. Cage to be assembled inside tank
7. Tank is plastic